

NOTE TO USERS

This reproduction is the best copy available.

UMI[®]

**The Palladium Catalyzed Multicomponent Synthesis of Münchnones:
Novel One-Pot Metal Catalyzed Routes
to Heterocycles and Peptide-Based Molecules**

*A thesis submitted to the Faculty of Graduate Studies and Research in partial
fulfillment of the requirements for the degree of Doctor of Philosophy*

By

Rajiv Dhawan

June

2004

Department of Chemistry
McGill University
Montreal, Quebec, Canada

© Rajiv Dhawan 2004



Library and
Archives Canada

Bibliothèque et
Archives Canada

Published Heritage
Branch

Direction du
Patrimoine de l'édition

395 Wellington Street
Ottawa ON K1A 0N4
Canada

395, rue Wellington
Ottawa ON K1A 0N4
Canada

Your file *Votre référence*

ISBN: 0-494-06291-6

Our file *Notre référence*

ISBN: 0-494-06291-6

NOTICE:

The author has granted a non-exclusive license allowing Library and Archives Canada to reproduce, publish, archive, preserve, conserve, communicate to the public by telecommunication or on the Internet, loan, distribute and sell theses worldwide, for commercial or non-commercial purposes, in microform, paper, electronic and/or any other formats.

The author retains copyright ownership and moral rights in this thesis. Neither the thesis nor substantial extracts from it may be printed or otherwise reproduced without the author's permission.

AVIS:

L'auteur a accordé une licence non exclusive permettant à la Bibliothèque et Archives Canada de reproduire, publier, archiver, sauvegarder, conserver, transmettre au public par télécommunication ou par l'Internet, prêter, distribuer et vendre des thèses partout dans le monde, à des fins commerciales ou autres, sur support microforme, papier, électronique et/ou autres formats.

L'auteur conserve la propriété du droit d'auteur et des droits moraux qui protègent cette thèse. Ni la thèse ni des extraits substantiels de celle-ci ne doivent être imprimés ou autrement reproduits sans son autorisation.

In compliance with the Canadian Privacy Act some supporting forms may have been removed from this thesis.

Conformément à la loi canadienne sur la protection de la vie privée, quelques formulaires secondaires ont été enlevés de cette thèse.

While these forms may be included in the document page count, their removal does not represent any loss of content from the thesis.

Bien que ces formulaires aient inclus dans la pagination, il n'y aura aucun contenu manquant.


Canada

*This thesis is dedicated to my parents and my brother
without whom, I would never have
obtained what I have*

ABSTRACT

**The Palladium Catalyzed Multicomponent Synthesis of Münchnones:
Novel One-Pot Metal Catalyzed Routes
to Heterocycles and Peptide-Based Molecules**

The purpose of this study was to develop new routes to couple commercially and/or readily available starting materials into biologically relevant structures via one-pot transition metal catalyzed multicomponent coupling reactions. More specifically, we showed that a palladium catalyst could couple imines, acid chlorides and carbon monoxide to directly generate 1,3-oxazolium-5-oxides (Münchnones).

Chapter 2 of this thesis describes a new palladium catalyzed multicomponent synthesis of β -lactams. This reaction was developed based upon previous work in this laboratory, which showed that imidazoline-carboxylates could be generated from coupling two imines, an acid chloride and CO. Mechanistic studies suggested that this product arose from a 1,3-dipolar cycloaddition of an imine-HCl molecule with Münchnone. Removal of this acid combined with adjusting reactant ratios, and the utilization of ligands generated 3-amido substituted β -lactams in moderate to good yields.

Chapter 3 discusses studies that further explain the origin of the β -lactam and imidazoline-carboxylate products obtained from catalysis. These studies demonstrate that imidazoline-carboxylates are generated either directly through a 1,3-dipolar cycloaddition reaction of imine-HCl with Münchnone, or indirectly from acid catalyzed rearrangement of an initially formed β -lactam. In addition, the potential intermediates in the catalytic cycle, including the palladium bound carbonyl complex are completely characterized.

Chapter 4 describes the first example of a metal-catalyzed synthesis of Münchnones. Reaction optimization focused on modifying the catalyst structure to $\{\text{Pd}(\text{Cl})[\eta^2\text{-CH}(\text{R}^1)\text{NR}^2\text{COR}^3]\}_2$ (formed by pre-treating $\text{Pd}_2(\text{dba})_3\cdot\text{CHCl}_3$ with imine ($\text{R}^1\text{C}(\text{H})=\text{NR}^2$) and acid chloride (R^3COCl)), increasing CO pressures and employing bromide salts to stabilize the palladium catalyst. These modifications to the reaction enabled the development of a catalytic Münchnone synthesis from imines, acid chlorides, and CO.

Chapter 5 describes the development of a highly modular one-step palladium catalyzed synthesis of pyrroles. This reaction shows that pyrroles can be thought of as being a coupling product of an imine, acid chloride and an alkyne, formed via the *in situ* trapping of Münchnones with alkynes. In addition, further improvements to the Münchnone synthesis through the utilization of sterically bulky phosphine ligands (i.e. $[\text{P}(\textit{o}\text{-Tol})_3]$) will be discussed. As well as

broadening the scope of accessible Münchnones, this ligand also increased the rate of product formation.

Chapter 6 describes some preliminary studies on the mechanism of Münchnone synthesis. Based upon kinetic data and catalyst resting state analyses, the rate determining step was suggested to possibly be *N*-acyliminium salt oxidative addition to Pd(0). In addition, crystal structures of $\{[P(o\text{-Tol})_3]Pd(\eta^2\text{-CH(Tol)N(PMB)COPh)}\}$ and its dimeric precursor $\{Pd(\eta^2\text{-CH(Tol)N(PMB)COPh)}\}_2$ were obtained.

ABSTRAIT

Synthèse catalytique des molécules hétérocycliques et peptidiques via l'in situ formation des Münchnones

Le but de cette étude vise à développer de nouvelles méthodes afin d'assembler directement plusieurs composés facilement accessibles en une étape pour fournir des structures biologiquement importantes à l'aide de catalyseurs métalliques. Plus spécifiquement, nous avons démontré qu'un catalyseur de palladium peut jumeler des imines, des chlorures d'acide et du monoxyde de carbone afin d'obtenir des 1,3-oxazolium-5-oxides (Münchnones).

Le deuxième chapitre décrit la synthèse modulaire de β -lactames. La réaction est basée sur notre synthèse modulaire des carboxylates d'imidazolines à partir d'imines, de chlorure d'acides, et de monoxyde de carbone. Suite à des développements significatifs (pour minimiser les produits non voulus), une nouvelle synthèse à multiples composantes a été réalisée. Celle-ci fournit des β -lactames à partir de deux molécules d'imines, une de chlorure d'acide et une de monoxyde de carbone. Une modification mineure des conditions de la réaction permet d'incorporer deux différentes imines dans le produit β -lactame.

Dans le troisième chapitre, nous élaborons davantage sur l'origine des produits β -lactame et des carboxylates d'imidazoline. Des études plus approfondies ont démontré qu'une réaction de cycloaddition 1,3-dipolaire entre le münchnone et l'imine·HCl ou le réarrangement du produit β -lactame par l'action catalytique

d'un acide ont été des moyens plausibles pour d'expliquer la formation du produit carboxylate imidazoline. Les intermédiaires du cycle catalytique, incluant également des complexes CO-palladium, sont entièrement caractérisées.

Le quatrième chapitre illustre le premier exemple d'une synthèse de münchnones par action catalytique d'un complexe organométallique. L'optimisation de la réaction a été accomplie par plusieurs méthodes, incluant la modification du catalyseur de $\{Pd(Cl)[\eta^2-CH(R^1)NR^2COR^3]\}_2$ (formé par traitement de $Pd_2(dba)_3$ avec une imine ($R^1C(H)=NR^2$) et un chlorure d'acide (R^3COCl)), l'augmentation de pression de CO, et l'utilisation des sels de bromure pour stabiliser le catalyseur de palladium. Ces améliorations ont permis le développement d'une réaction donnant accès aux münchnones à partir d'imines, de chlorures d'acide et de monoxyde de carbone, avec de bons rendement. D'autre part, l'addition d'alcools aux münchnones permet de convertir celles-ci en acide α -aminés déprotégés. Ainsi, la réaction catalytique peut fournir des acide α -aminés diprotégés en une étape à partir de quatre composants simples à synthétiser.

Le chapitre cinq décrit le développement d'une réaction très modulaire des pyrroles en une étape. Cette réaction démontre que les pyrroles peuvent être synthétiser à partir d'une imine, d'un chlorure d'acide et d'un alcyne. Ceci est rendu possible par la réaction de l'intermédiaire münchnone avec un alcyne. Cette méthode représente le moyen le plus facile pour former cette classe de produits. La simplicité des réactifs facilite beaucoup la synthèse de diverses familles de

pyrroles en offrant le contrôle indépendant et modulaire de chaque substituant sur l'hétérocycle. De plus, la synthèse du münchnone a été davantage améliorée avec l'utilisation de ligands encombrés. L'utilisation de tri(*o*-tolyl)phosphine accélère la réaction et de plus, augmente son rendement. L'utilité de la réaction a aussi été démontrée par la synthèse de produits tricycliques pyrroliques en une étape.

Le chapitre six décrit les résultats préliminaires du mécanisme de la synthèse des münchnones. Les résultats d'études cinétiques, d'analyse du resting state, suggèrent que c'est l'addition oxydative du sel N-acyl iminium qui limite la réaction. Les structures cristallines du complexe $\{[P(o\text{-tol})_3]Pd(\eta^2\text{-CH(Tol)N(PMB)COPh)}\}$ et de son précurseur $\{Pd(\eta^2\text{-CH(Tol)N(PMB)COPh)}\}_2$ ont par ailleurs été déterminées.

Forward

In accordance with guideline C of the “Guidelines for Thesis Preparation” (Faculty of Graduate Studies and Research), the following text is cited:

“As an alternative to the traditional thesis format, the dissertation can consist of a collection of papers of which the student is an author or co-author. These papers must have a cohesive, unitary character making them a report of a single program of research. The structure for the manuscript-based thesis must conform to the following:

Candidates have the option of including as part of the thesis, the text of one or more papers submitted, or to be submitted, for publication, or the clearly-duplicated text (not the reprints) of one or more published papers. These texts must conform to the “Guidelines for Thesis Preparation” with respect to font size, line spacing and margin sizes and must be bound together as an integral part of the thesis. (Reprints of published papers can be included in the appendices at the end of the thesis.)

The thesis must be more than a collection of manuscripts. All components must be integrated into a cohesive unit with a logical progression from one chapter to the next. In order to ensure that the thesis has continuity, connecting texts that provide logical bridges between the different papers are mandatory.

As manuscripts for publication are frequently very concise documents, where appropriate, additional material must be provided (e.g., in appendices) in sufficient detail to allow a clear and precise judgement to be made of the importance and originality of the research reported in the thesis.

In general, when co-authored papers are included in a thesis the candidate must have made a substantial contribution to all papers included in the thesis. In addition, the candidate is required to make an explicit statement in the thesis as to who contributed to such work and to what extent. This statement should appear in a single section entitled “Contributions of Authors” as a preface to the thesis. The supervisor must attest to the accuracy of this statement at the doctoral oral defense. Since the task of the examiners is made more difficult in these cases, it is in the candidate’s interest to specify the responsibilities of all the authors of the co-authored papers.

When previously published copyright material is presented in a thesis, the candidate must include signed waivers from the co-authors and publishers and submit these to the Thesis Office with the final deposition, if not submitted previously.”

This dissertation is written in the form of four papers. The papers each comprise one chapter in the main body of the thesis (Chapters 2, 3, 4, and 5), with a general

introduction to this work in the first chapter and conclusions in the seventh chapter. Following normal procedures, the papers have either been published in, submitted to, or to be submitted to scientific journals. A list of papers is given below:

- Chapter 2: Rajiv Dhawan; Daniel St. Cyr; Rania D. Dghaym and Bruce A. Arndtsen* (to be submitted)
The Use of Carbon Monoxide and Imines as α -Amino Acid Derivative Synthons: A Facile Palladium Catalyzed Synthesis of β -Lactams
- Chapter 3: Rajiv Dhawan; Rania D. Dghaym; Bruce A. Arndtsen* *Catalysis of Organic Reactions*. 2003, 89, 499-508.
The palladium catalyzed synthesis of carboxylate-substituted imidazolines: a new route using imines, acid chloride, and carbon monoxide.
- Chapter 4: Rajiv Dhawan; Rania D. Dghaym; Bruce A. Arndtsen* *Journal of the American Chemical Society*. 2003, 125, 1474.
The Development of the First Catalytic Synthesis to Münchnones: A Simple Four Component Coupling Approach to α -Amino Acid Derivatives.
- Chapter 5: Rajiv Dhawan and Bruce A. Arndtsen* *Journal of the American Chemical Society* 2004, 126, 468.
Palladium Catalyzed Multicomponent Coupling of Imines, Alkynes and Acid Chlorides: A Direct and Modular Approach to Pyrrole Synthesis.

Contributions of Authors

All of the papers in this thesis include the research director, Professor Bruce A. Arndtsen, as a co-author, since the work was done under his direction. Chapter two includes Daniel St. Cyr and Rania D. Dghaym as co-authors to acknowledge their respective contributions to the publication. Daniel synthesized and characterized one of the β -lactams in the publication, while Rania's initial work on the generation of imidazoline-carboxylates was essential in developing the synthesis of β -lactams. Chapter Three includes Rania D. Dghaym to acknowledge her significant efforts in the content of this chapter. The development and the $^1\text{H-NMR}$ and $^{13}\text{C-NMR}$ characterization of the imidazoline carboxylates was her work. Chapter four includes Rania D. Dghaym as an author to acknowledge her for her work in synthesizing one of the reaction catalysts. Other than the aforementioned contributions, all of the work presented in this dissertation was initiated and performed by the author.

I hereby give a copyright clearance for the inclusion of the following papers, of which I am co-author, in the dissertation of Rajiv Dhawan.

“The Use of Carbon Monoxide and Imines as α -Amino Acid Derivative Synthons: A Facile Palladium Catalyzed Synthesis of β -Lactams”

“The palladium catalyzed synthesis of carboxylate-substituted imidazolines: a new route using imines, acid chloride, and carbon monoxide”

“The Development of the First Catalytic Synthesis to Münchnones: A Simple Four Component Coupling Approach to α -Amino Acid Derivatives”

“Palladium Catalyzed Multicomponent Coupling of Imines, Alkynes and Acid Chlorides: A Direct and Modular Approach to Pyrrole Synthesis”

Date: _____

Bruce A. Arndtsen
McGill University
801 Sherbrooke St. West
Montreal, Quebec
H3A 2K6

Acknowledgements

I would like to thank God for all of the blessings that he has bestowed on myself and my family.

I would like to thank my parents, Vishnu and Kamlesh Dhawan and my brother Avinash. Your support and love through every part of my life has been limitless. I would not have been able to do this without you.

I thank Prof. Bruce Arndtsen for his support, guidance and his passion for this chemistry as well as his help in preparing this thesis. I would like to thank him for expecting nothing but the best from me, which has made me a better chemist. In addition, I will always remember the direction and encouragement that I received, while under his supervision.

I would also like thank my amazing friends and mentors for the first half of my tenure at McGill University: Jason Davis and David Llewellyn. Thank you for always being there to discuss chemistry with me. We have had amazing times in graduate school and I am sure that I have friends forever in these two amazing individuals. You were always there for me and I appreciate all that you have done for me.

I would also like to thank two of the finest people that one could ever dream of meeting: Debbie Mitra and Daniel Black. I have been blessed by having friends

of your quality. I never felt alone or unhappy when I was in your presence and I will never forget the great times that we had both inside and outside the Otto Maass Chemistry Building. It is an amazing feeling when one feels that they see a part of their family everyday, even when their real family is thousands of kilometers away.

I respectfully acknowledge the great educators for their support and education throughout my time in graduate school: Prof. Bruce Lennox, Prof. Scott Bohle, Prof. Patrick Farrell, Prof. James Gleason, Prof. John Harrod, Prof. Ashok Kakkar and Prof. Romas Kazlauskas.

Science is never possible without excellent support staff. Mr. Alfred Kluck, Mr. Georges Kopp, Dr. Orval Mamer, Mr. Rick Rossi, Mr. Nadim Saade and Dr. Paul Xia facilitated research by providing all of the technical assistance necessary for this thesis. I would like to also thank Dr. Francine-Belanger-Garipy and Dr. Anne-Marie Lebuis for obtaining the X-ray crystal structure data presented throughout this thesis.

In addition, I would like to thank members of Lab. 443 past and present who made it a pleasure to come to work everyday: Jason Davis, David Llewellyn, Daniel Black, Daniel St. Cyr, Yingdong Lu, Ali Siamaki, Andrew Oliver, Rania Dghaym, Janie Cabana, Anna Gril, Julie Lefebvre, David Martin, Laura Pederson, and Eoin Quinlan. I would also like to thank Daniel Black, Debbie Mitra and

Daniel St. Cyr for reading parts of this thesis and Daniel St. Cyr and Janie Cabana for translating the abstract into French.

I would like to respectfully acknowledge Ms. Renee Charron and Ms. Chantal Marrotte for all of their help from the first day that I visited McGill to my last day here. I would also like to thank Ms. Sandra Aeresen and Ms. Carol Brown for their help during my doctoral degree as well.

I would like to thank some of the amazing friends that I have made while at McGill: Elysia Pitt, Andrea Dillon, Vicki Meli, Margaret Antler, Andrew Corbett, Shane Pawsey, Victor Nassredine, James Ashenhurst, Diane Burke, Susan Burke, Ronny Priefer, Owen Terreau, Shane Pawsey, Eddie Myers, Jeff Manthorpe, Lee Fader, Stephanie Warner, and Claudia Gributs. I would like to thank Alain Ajamian and Aaron Kosar for valuable discussions during my stay at McGill.

I would like to acknowledge my past professors Prof. Roland K. Pomeroy and Prof. Saul Wolfe for their interest in me as a student and for their continued support. I would like to thank my former supervisors Mr. Yves Leblanc, Mr. Claude Dufresne, Mr. Patrick Roy, Dr. Erich Grimm, Dr. Steven Ansell, Dr. Futong Cui and Mr. Tao Sheng for their amazing mentorship during my co-op education experiences.

I would also like to thank Dr. Sleiman, Dr. Reven, Dr. Gleason and their laboratories for being so generous with their laboratory equipment and supplies.

Chapter 1

Introduction

1.0 Perspective	1
Part I: Multicomponent Coupling Reactions	6
1.1 Multicomponent Coupling Reactions: Traditional Approaches	6
1.2.1 Metal Catalyzed Multicomponent Coupling Reactions	9
1.2.2 The Pauson Khand Reaction: The Multicomponent Coupling of CO, Alkenes and Alkynes	14
1.2.2.1 Scope of the Pauson Khand Reaction	16
1.2.2.2 The Catalytic Pauson-Khand Reaction	18
1.2.2.3 The Incorporation of Heteroatoms into the Pauson Khand Reaction	23
1.2.2.4 Synthetic Applications of the Pauson Khand Reaction	26
1.2.3 Metal Mediated Cyclotrimerization of Unsaturated Compounds	28
1.2.3.1 Cyclotrimerization Reactions in Synthesis	32
1.2.3.2 Generation of Substituted Benzenes: Regioselectivity Issues	35
1.2.3.2.1 Utilization of Electronics and Sterics to Influence Chemo- and Regioselectivity	36
1.2.3.2.2 Utilization of Functionality to Influence Chemo- and Regioselectivity	39
1.2.3.4 Incorporation of Heteroatoms into the Cyclotrimerization Reaction	41
1.2.3.5 Synthetic Applications of Transition Metal Catalyzed Cyclotrimerization Reactions	45
1.2.4 The Wakamatsu Reaction: Amidocarbonylation	47
1.2.4.1 Palladium Catalyzed Amidocarbonylation	50

1.2.4.2 Generation of α -Amino Acids via Amidocarbonylation	52
1.2.4.3 Synthetic Applications of Amidocarbonylation	54
Part II: Münchnone Generation and Reactivity	56
1.3 Introduction to Münchnones	56
1.3.1.1 Münchnone Generation: Traditional Routes	57
1.3.1.2 Münchnone Generation: Utilization of Tetracarbonyl Ferrates	59
1.3.1.3 Münchnone Generation: Utilization of Chromium Carbenes	60
1.3.2 Structures of Münchnones	61
1.3.3 Nucleophilic Additions to Münchnones: Generation of Peptide-based Products	63
1.3.4 Imine Additions to Münchnones: Generation of β -Lactams	64
1.3.5 1,3-Dipolar Cycloadditions: Generation of Pyrroles	64
1.3.6 Synthetic Applications of Münchnones in Pyrrole-based Pharmaceuticals	70
1.3.7 1,3-Dipolar Cycloadditions: Generation of Imidazoles	74
1.3.8 Generation of 5-Trifluoromethyl Oxazoles: A Unique Approach from Münchnones	75
1.4 Palladium Catalyzed Synthesis of Imidazoline Carboxylates	76
1.5 Overview of the Thesis	77
1.6 References	80

Chapter 2

Palladium Catalyzed Coupling of Imine, Acid Chloride and Carbon Monoxide: A Multicomponent Coupling Approach to β -Lactams

2.0 Introduction	95
2.1 Results and Discussion	97
2.1.1 Mechanistic Considerations	97
2.1.2 Method Development	99
2.1.3 Palladium Catalyzed Synthesis of β -Lactams	101
2.2 Conclusions	106
2.3 Experimental	107
2.4 References	116

Chapter 3

The Palladium Catalyzed Synthesis of Carboxylate-Substituted Imidazolines: A New Route Using Imines, Acid Chloride and Carbon Monoxide

3.0 Introduction	123
3.1 Results and Discussion	125
3.1.1 Synthesis and Structure of Imidazole-Carboxylate 3.4	125
3.1.2 Scope of Catalytic Imidazoline Carboxylate Synthesis	127
3.1.3 Mechanistic Studies: Palladium Catalysis	129
3.1.4 Mechanistic Studies: Münchnone Reactivity	134
3.3 Conclusions	136
3.4 Experimental Section	137
3.5 References	146

Chapter 4

The Development of the First Catalytic Synthesis to Münchnones: A Simple Four Component Coupling Approach to α -Amino Acid Derivatives

4.0 Introduction	149
4.1 Results and Discussion	151
4.1.1 Palladium Catalyzed Synthesis of Münchnones: Mechanistic Considerations	151
4.1.2 Palladium Catalyzed Synthesis of Münchnones: Method Development	152
4.1.3 Palladium Catalyzed Synthesis of Diprotected α -Amino Acids	155
4.2 Conclusions	157
4.3 Experimental	157
4.4 References	168

Chapter 5

Palladium Catalyzed Multicomponent Coupling of Imines, Alkynes and Acid Chlorides: A Direct and Modular Approach to Pyrrole Synthesis

5.0 Introduction	170
5.1 Results and Discussion	172
5.3 Conclusions	178
5.4 Experimental	179
5.5 References	188

Chapter 6

Palladium Catalyzed Synthesis of Münchnones: Characterization of Intermediates and Mechanistic Analysis of the Reaction

6.0 Introduction	192
6.1 Results and Discussion	194
6.1.1 Catalyst Resting State	196
6.1.2 Preliminary Kinetic Analysis of Münchnone Formation	198
6.1.3 Probing the Oxidative Addition of <i>N</i> -Acyliminium Salts to Pd(0)	199
6.1.4 Probe for a Heterogeneous Palladium Catalyst	202
6.1.5 Triphenylphosphine in Münchnone Formation	204
6.1.6 Second Generation Münchnone Catalyst: Utilization of Sterically Hindered Phosphines	207
6.1.7 Catalyst Resting State with P(<i>o</i> -Tol) ₃	211
6.1.8 Kinetic Analysis of Münchnone Formation	212
6.1.9 Probe for a Heterogeneous Palladium Catalyst with P(<i>o</i> -Tol) ₃	214
6.1.10 Mechanistic Considerations: Probe for Radical-Based Processes	215
6.1.11 Carbonylation Studies with {[P(<i>o</i> -Tol) ₃]Pd(Cl)[η ² -CH(Tol)N(Et)COPh]}	216
6.2 Mechanistic Conclusions	218
6.3 Experimental	222
6.4 References	232

Chapter 7

Conclusions, Contributions to Original Knowledge, and Suggestions for Future Work

7.0 Conclusions and Contributions to Original Knowledge	237
7.1 Suggestions for Future Work	240
7.2 References	243

List of Figures

Figure 1.1 Biosynthetic Strategies in Organic Synthesis	3
Figure 1.2 Generation of Block-Copolymers	4
Figure 1.3 Utilization of Cascade Reactions for Increasing Molecular Complexity	5
Figure 1.4 Multi-site Bond Formation in Organic Synthesis	6
Figure 1.5 Products Potentially Available from Multicomponent Coupling Reactions	7
Figure 1.6 Examples of Classical Multicomponent Coupling Reactions	8
Figure 1.7 General Examples of Organometallic Reactions	10
Figure 1.8 The Pauson Khand Reaction	14
Figure 1.9 Schematic of the Pauson Khand Reaction	14
Figure 1.10 Mechanism of the Pauson Khand Reaction	15
Figure 1.11 First Example of an Intramolecular Pauson Khand Reaction	17
Figure 1.12 The Pauson Khand Reaction	19
Figure 1.13 Intramolecular Catalytic Pauson Khand Reaction	19
Figure 1.14 Rhodium Catalyzed Pauson Khand Reaction	22
Figure 1.15 “Disposable Tethers” in the Catalytic Pauson Khand Reaction	22
Figure 1.16 Generation of γ -Butyrolactones	24
Figure 1.17 Mechanism for γ -Butyrolactone Synthesis	25
Figure 1.18 The Pauson Khand Reaction in the Generation of Asteriscanolide 1.30	27
Figure 1.19 Pauson Khand Reactions on Solid Support	28
Figure 1.20 Pauson Khand Reaction in the Generation of Compound Libraries	28
Figure 1.21 Cycloadditions in Multicomponent Coupling Reactions	29
Figure 1.22 Cyclotrimerization of Acetylene	29
Figure 1.23 Cyclotrimerization of Alkynes	31
Figure 1.24 Generation of Multisubstituted Benzenes	33
Figure 1.25 Generation of Multisubstituted Benzenes	34
Figure 1.26 Cyclotrimerization Reactions with $\text{CpCo}(\text{CO})_2$	34

Figure 1.27 Nickel Mediated Cyclotrimerization	37
Figure 1.28 The One Pot Cyclotrimerization Reaction	37
Figure 1.29 Generation of Penta-substituted Benzenes from a Cyclotrimerization of Alkynes	38
Figure 1.30 Cyclotrimerization of Alkynes Utilizing Boron Tethers	40
Figure 1.31 Regio- and Chemoselective Cyclotrimerization of Three Different Alkynes	41
Figure 1.32 Generation of 2-Vinylpyridine	43
Figure 1.33 Mechanism for Pyridine Synthesis	43
Figure 1.34 Generation of Estrone	45
Figure 1.35 Cobalt Catalyzed Amidocarbonylation	47
Figure 1.36 Postulated Mechanism for $\text{Co}_2(\text{CO})_8$ Catalyzed Amidocarbonylation	48
Figure 1.37 Palladium Catalyzed Amidocarbonylation: Synthesis of <i>N</i> -Acetylleucine	50
Figure 1.38 Postulated Mechanism for Palladium Catalyzed Amidocarbonylation	51
Figure 1.39 Palladium Catalyzed Amidocarbonylation	53
Figure 1.40 Amidocarbonylation with Nitriles	53
Figure 1.41 Palladium Catalyzed Ureidocarbonylation	55
Figure 1.42 Examples of Mesoionic Oxazoles	56
Figure 1.43 Some of the Products Available from Münchnone Intermediates	57
Figure 1.44 Generation of Münchnones (Hüisgen)	58
Figure 1.45 Generation of <i>N</i> -Acyl Münchnones.	58
Figure 1.46 Generation of Münchnones from Acyltetracarboxylferrates	59
Figure 1.47 Proposed Mechanism for Münchnone Formation	60
Figure 1.48 Generation of Münchnones from <i>N</i> -Acylaminochromium Carbenes	61
Figure 1.49 Structures of Münchnones 1.106	62
Figure 1.50 Ketene Tautomerization of Münchnones	63
Figure 1.51 Generation of <i>N</i> -Acylamino acid (derivatives) and Dipeptides from Münchnones	63

Figure 1.52 Synthesis of β -lactams from Münchnones and Imines	64
Figure 1.53 Mechanism of Pyrrole Formation	65
Figure 1.54 Electronic Effects on 1,3-Dipolar Cycloaddition Reactions	67
Figure 1.55 Proposed Unsymmetrical Transition State for Pyrrole formation	68
Figure 1.56 Product Distribution Following Reaction with Methyl Propiolate	69
Figure 1.57 Product Distribution as a function of Dipole Sterics	69
Figure 1.58 Unexpected Behaviour in Dipolar Cycloadditions	70
Figure 1.59 Generation of Lipitor from a Münchnone Intermediate	71
Figure 1.60 Synthesis of FPL 64176	71
Figure 1.61 Generation of a HMG-CoA Reductase Inhibitors	72
Figure 1.62 Generation of Pyrroles on Solid Support	73
Figure 1.63 Generation of Multicyclic Pyrroles	73
Figure 1.64 Generation of Imidazoles from Münchnones	74
Figure 1.65 Generation of Imidazoles on Solid Support	75
Figure 1.66 Generation of Oxazoles from Münchnones and TFAA	76
Figure 1.67 Synthesis of Imidazoline-Carboxylates	78
Figure 3.1 Utility of Imidazoline-Carboxylates	124
Figure 3.2 Crystal structure of <i>N,N</i> -dimethyl-2-phenyl-4,5-(<i>p</i> -tolyl)- imidazole-4-carboxylate	127
Figure 3.3 4-Component Coupling Approach to Imidazoline-Carboxylates	130
Figure 5.1 Catalytic Cycle For Pyrrole Formation	173
Figure 6.2 Determination of the Catalyst Resting State	197
Figure 6.3 Plot of $\ln([\text{Münchnone}]_{\infty}/([\text{Münchnone}]_{\infty} - [\text{Münchnone}]_t))$ vs time	198
Figure 6.4 Formation of $\{\text{Pd}(\text{Cl})[\eta^2\text{-CH}(\text{Tol})\text{N}(\text{Bn})\text{COPh}]\}_2$ 6.6a	200
Figure 6.5 Formation of $\{\text{Pd}(\text{Cl})[\eta^2\text{-CH}(\text{Tol})\text{N}(\text{PMB})\text{COPh}]\}_2$ 6.6b	201
Figure 6.6 Crystal Structure of $\{\text{Pd}(\text{Cl})[\eta^2\text{-CH}(\text{Tol})\text{N}(\text{PMB})\text{COPh}]\}_2$ (PMB= <i>p</i> -C ₆ H ₄ OCH ₃) (6.6b)	201
Figure 6.7 Bond Lengths in Palladium Chelated Amides	202

List of Equations

Equation 2.1 Generation of β -Lactams	97
Equation 3.1 Carbonylation of Complex 3.9 to generate 3.8	133
Equation 4.1 Generation of 1,3-Oxazolium-5-oxides (Münchnones)	150
Equation 4.2 Generation of Diprotected α -Amino Acids	155
Equation 5.1 Four Component Coupling in the Generation of Pyrroles	171
Equation 5.2 Pyrrole Formation in the Presence of Weakly Coordinating Halide Salts	174
Equation 5.3 Generation of Multi-cyclic Pyrroles	177
Equation 6.1 Münchnone Generation	194

List of Schemes

Scheme 1.1 Representative Examples of Metal Mediated Multicomponent Coupling Processes	10
Scheme 1.2 Examples of Metal Catalyzed Pauson Khand Reactions	21
Scheme 1.3 Incorporation of Heteroatoms into Cyclic Molecules via [2+2+1] Processes	23
Scheme 1.4 Synthesis of Natural Products Utilizing the Pauson Khand Reaction	26
Scheme 1.5 Selected Metal Catalysts in the Cyclotrimerization Reaction	32
Scheme 1.6 Utilization of Different Metals in Cyclotrimerization Reactions	35
Scheme 1.7 Formation of Substituted Pyridines	42
Scheme 1.8 Cyclotrimerization of Other Heteroatom Containing Compounds	44
Scheme 1.9 Utilization of Cyclotrimerization Reactions in Total Synthesis	46
Scheme 1.10 Other Substrates for Amidocarbonylation	49
Scheme 1.11 Synthetic Applications of Amidocarbonylation	54
Scheme 2.1 Reaction of Münchnones with Imines	98
Scheme 2.2 Palladium Catalyzed Synthesis of β -lactams	104
Scheme 3.1 Mechanism of Imidazoline-Carboxylate Formation	131
Scheme 3.2 Reactivity of Münchnone 3.14 with Ph(H)C=NBn	135
Scheme 4.1 Mechanistic rationale for Münchnone formation	152
Scheme 6.1 Mechanistic Rationale for Münchnone Formation	195
Scheme 6.2 Mechanistic Rationale for Münchnone Formation	221

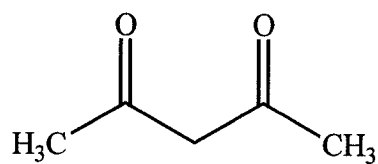
List of Tables

Table 2.1 Palladium catalyzed synthesis of β -lactams: Method Development	100
Table 2.2 Palladium Catalyzed Synthesis of β -Lactams	102
Table 2.3 Heterocoupled β -Lactam Synthesis	105
Table 3.1 Palladium Catalyzed Synthesis of Imidazoline-Carboxylates	128
Table 4.1 Catalytic Synthesis of 4.1a	154
Table 4.2 Scope of Palladium Catalyzed Münchnone Synthesis	156
Table 5.1 Ligand Influence on Münchnone Formation	175
Table 5.2 Palladium Catalyzed Pyrrole Synthesis (Eq. 5.1)	176
Table 6.1 Reaction of $\{[P(o\text{-Tol})_3]Pd(Cl)[\eta^2\text{-CH(Tol)N(Et)COPh}]\}$ with CO and $P(o\text{-Tol})_3$ (2 eq.)	217

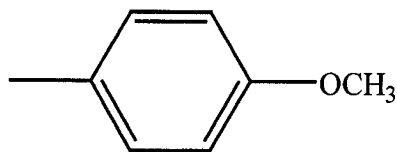
List of Abbreviations

^t Bu	-C(CH ₃) ₃
Bu	-CH ₂ CH ₂ CH ₂ CH ₃
ⁱ Pr ₂	-CH(CH ₃) ₂
Et	-CH ₂ CH ₃
Me	-CH ₃
Ph	-C ₆ H ₅
OAc	CH ₃ CO ₂ ⁻
OTf	SO ₃ CF ₃ ⁻

acac



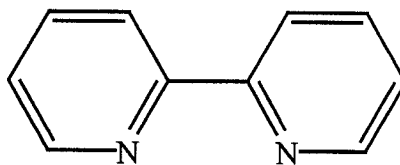
An



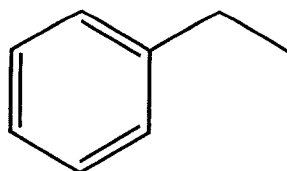
Ar-

Aryl-

bipy



Bn



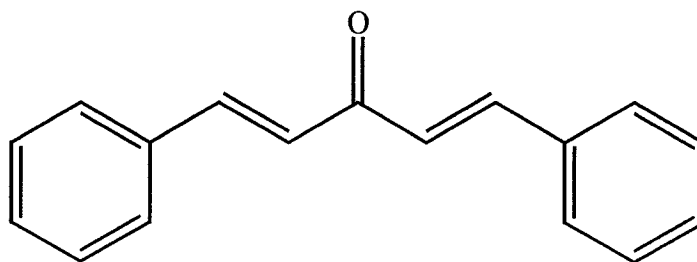
COD
COSY

1,5-cyclooctadiene
Correlation Spectroscopy

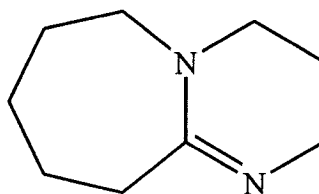
Cp



dba



DBU



DIAD

diisopropyl azodicarboxylate

DCC

dicyclohexylcarbodiimide

DIBAL

diisobutylaluminum hydride

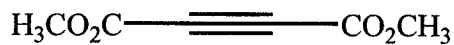
DMF

N, N - dimethylformamide

DMAc

N, N - dimethylacetamide

DMAD



dppe



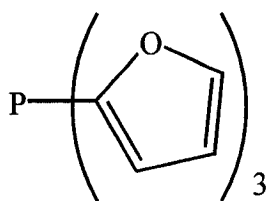
EDC

N-ethyl-*N*-dimethylaminopropyl carbodiimide

ESI

electrospray ionization

(2-furyl)₃P



HMBC

Heteronuclear Multiple Bond Coherence Spectroscopy

HMQC
spectroscopy

Heteronuclear Multiple Quantum Coherence

IR

Infrared

NMR

Nuclear Magnetic Resonance Spectroscopy

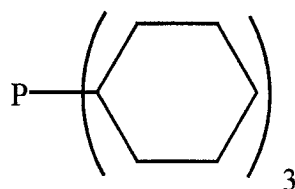
NMO

4-methylmorpholine *N*-oxide

NOESY

Nuclear Overhauser Effect Spectroscopy

PCy₃



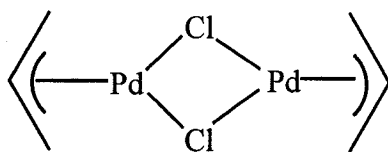
Pd/Al

Palladium on Alumina

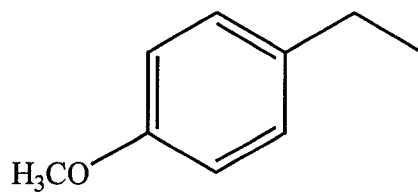
Pd/C

Palladium on Charcoal

[Pd(allyl)Cl]₂



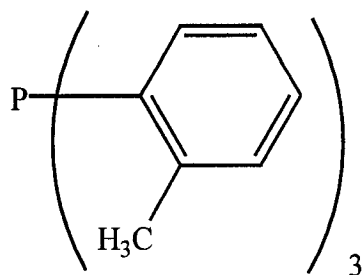
PMB



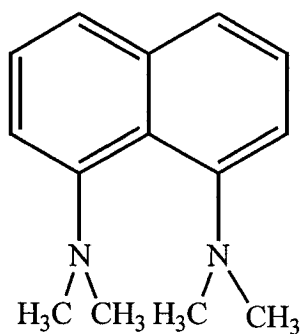
P(*o*-Tol)₃

or

P(*o*-tolyl)₃



proton sponge



RT

room temperature

THF

tetrahydrofuran

TBS

-Si(^tBu)(CH₃)₂

TMS

-Si(CH₃)₃

TMSCl

Si(CH₃)₃ Cl

TFA

trifluoroacetic acid

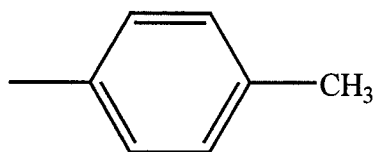
TFAA

trifluoroacetic anhydride

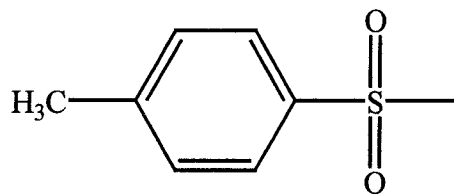
Tol

or

p-tolyl



Ts



CHAPTER ONE

Introduction

1.0 PERSPECTIVE

Chemistry, as it relates to synthesis, is powerfully displayed in our everyday lives. Plastics, pharmaceuticals, diagnostic agents and future nanotechnology endeavors all rely on synthesis for the effective generation of unique chemical structures. The science of synthesis has seen significant progress in the last century. For instance, new methods to generate specific enantiomers of a molecule from achiral precursors, which was once thought impossible, is now an everyday occurrence.¹ Many landmark total syntheses, including Kishi's synthesis of palytoxin² (115 contiguous carbon centers & 64 stereogenic centers), and the Woodward-Eschenmoser synthesis of cobyrinic acid³ (Figure 1.1a) demonstrate that almost no target molecule is unobtainable.

Despite these advances, many challenges remain in synthesis. In particular, while a tremendous variety of compounds can be synthesized, ready access to these substrates, especially those with complex structures, is often prohibitive in terms of time, resources and labour. Hence, this limits the ultimate practicality of these compounds. This has resulted in the growing prominence of strategies that can not only generate products in high yield, but do so with minimal synthetic effort, employ

simple reaction precursors, enable facile structural diversification, simple purification, and are time and resource efficient. The need to consider these features in synthesis has been addressed on numerous occasions, and include discussions of atom economy,³ environmentally benign syntheses,⁴ and the concept of ideal syntheses.⁵ The latter describes many of the features that would ideally be part of newly developed synthetic methodologies, including: a) forming products in 100% yield; b) employing readily accessible substrates; c) performing syntheses in a single step; and d) being safe and environmentally acceptable. While it is unrealistic to expect every one of these criteria to be met, reactions that embody several of these features stand as significant developments.

One approach towards fulfilling these goals of synthesis that is becoming of growing relevance involves performing multiple synthetic operations at once, which could ideally construct complex molecules in a single step reaction. These types of reactions are often more time and resource efficient compared to any linear, multistep synthetic effort. Perhaps the best illustration of the efficiency achievable by this approach is shown in recent biosynthetic efforts. For instance, Scott's⁷ conversion of the readily available building block α -aminolevulinic acid into corrin enables the formation of a significantly complex structure in a single operation (Figure 1.1b). A comparison of this reaction to the Woodward-Eschenmoser synthesis of cobyrinic acid³ puts this achievement in the proper context. These two groups employed some 100 graduate students and post-docs, and took 12 years to synthesize this complex molecule, while a biosynthetic route constructed this product in a single step.³

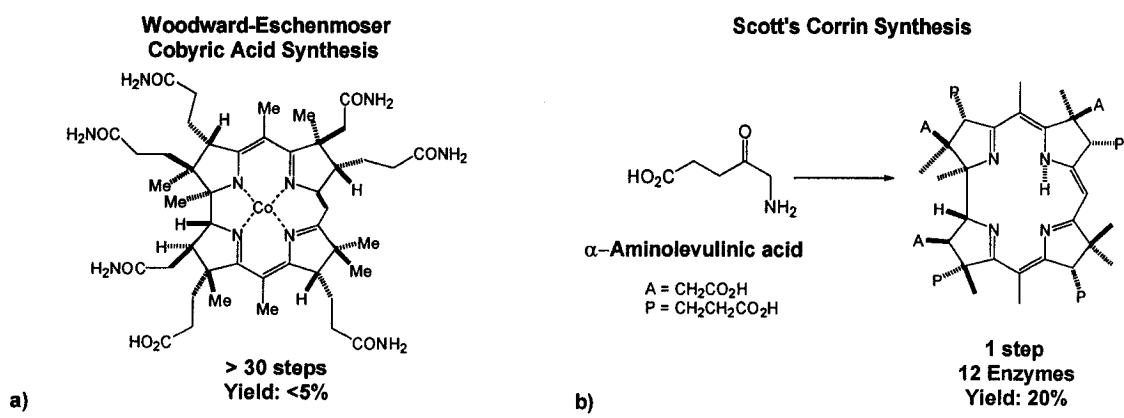
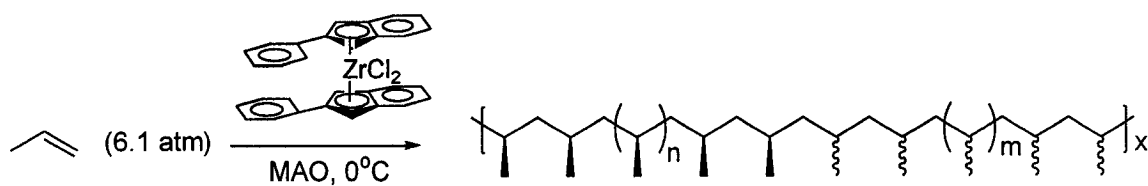


Figure 1.1 Biosynthetic Strategies in Organic Synthesis

In addition to biosynthetic approaches, another concept that is of growing relevance in the design of new reactions involves the use of metal catalysis.⁸ Considering that metal catalysts can stabilize reactive intermediates, invert normal reactivity patterns, and mediate multi-step processes, they can serve as an effective tool in synthesis.⁸ A good illustration of the potential utility of this approach is shown in Figure 1.2, where a metallocene catalyst is employed to couple propylene, into atactic-isotactic stereoblock polymers in a single step operation.⁹ The structural control in this polymerization is achieved by the slow switching of the catalyst between a chiral and an achiral form, via restricted rotation of the substituted indenyl rings, during the sequential insertion of propylene into a zirconium-carbon bond.



MAO = methylaluminoxane

Figure 1.2 Generation of Block-Copolymers

Metal catalysts can also greatly facilitate synthetic efforts with processes known as cascade reactions. In these transformations, one bond forming process leads to others, which eventually allows for the formation of complex molecules. For example, Trost's palladium catalyzed "zipper" reaction shown in Figure 1.3, which forms 5 new bonds and 4 stereocenters, generates a pentacyclic product in a single step from the acyclic precursor **1.1**.¹⁰

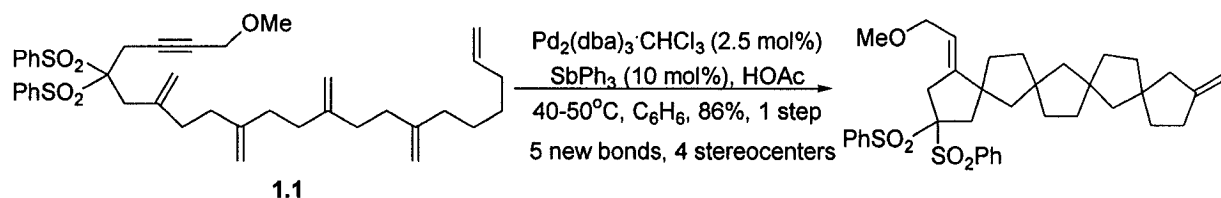


Figure 1.3 Utilization of Cascade Reactions for Increasing Molecular Complexity

The ability to conduct several functional group transformations in a single operation can also greatly facilitate access to a specific target. This type of reaction potentially enables the realization of significant levels of molecular complexity in going from starting materials to final products. An illustration of this is the Sharpless asymmetric

dihydroxylation of **1.2** (Figure 1.4), which allows the stereoselective synthesis of polyols in a process that breaks 6 bonds and forms 12 new ones in a single step.¹¹

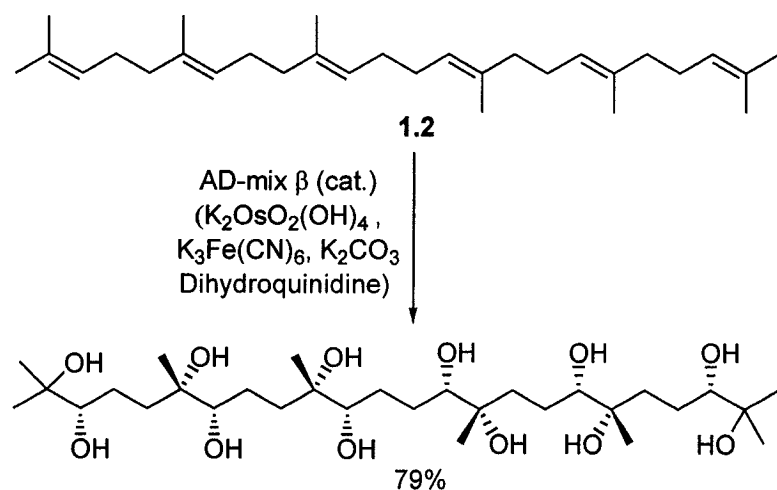


Figure 1.4 Multi-site Bond Formation in Organic Synthesis

These examples illustrate an effective concept in synthesis, where multiple bond forming steps occur in a single operation (Figure 1.3 and Figure 1.4), and where simple molecules are coupled into complex and useful products (Figure 1.1b and Figure 1.2). While these advances provide facile new routes to the specific products described, typical methods to construct most synthetic targets still rely on multistep syntheses. Considering the importance of developing methodologies that facilitate synthetic efforts, the topic of this thesis will be the generation of new methods to construct complex molecules in a single step via metal catalysis. This chapter will overview two of the major topics of this thesis: 1) metal-catalyzed multicomponent coupling reactions; and 2) the chemistry of 1,3-oxazolium-5-oxide (Münchnones), the products whose synthesis will be discussed in this thesis. The first section will aim to

highlight certain established metal-catalyzed multicomponent coupling reactions, as well as relevant stoichiometric processes. The second part of the introductory chapter will discuss the preparation of Münchnones, utilizing classical and more recent metal-based approaches. Furthermore, the use of this mesoionic heterocycle in the synthesis of pharmaceutically relevant compounds and its reactivity patterns will also be presented.

Part I: Multicomponent Coupling Reactions

1.1 Multicomponent Coupling Reactions: Traditional Approaches

As mentioned previously, one approach that could fulfill many of the features desired in synthesis is to devise methods that couple several precursors at once to generate more complex products. These types of transformations, which are commonly known as polyconvergent approaches or multicomponent coupling reactions, combine three or more components in a single reaction vessel to generate a compound that is composed of the added constituents.¹² These reactions can accomplish several operations at once, and hence hold the potential of being significantly simpler than linear synthesis. In addition, multicomponent coupling strategies allow the reaction constituents to be varied independently of each other, which can be ideal for forming families or libraries of products.¹³ In theory, in a reaction that involves four different components, the combination of 20 different reaction precursors can potentially generate 20^4 or 160,000 compounds, all through single step reactions. The number of products potentially available increases exponentially with the number of components

involved in the reaction. For instance, the coupling of five different substrates, each with the same 20-component diversity can allow for the generation of 3.2 million different compounds. The ability of this strategy to generate numerous compounds based on a set of structural building blocks is of tremendous potential importance in combinatorial chemistry (Figure 1.5).

<u>Number of Components</u>	<u>Structural Inputs/Variants</u>	<u>Number of Compounds</u>
2	20	400
3	20	8,000
4	20	160,000
5	20	3,200,000
6	20	64,000,000

Figure 1.5 Products Potentially Available from Multicomponent Coupling Reactions

A large number of multicomponent coupling processes exist and are of significant synthetic utility. Since Strecker's¹⁴ synthesis of amino acids in 1850 (Figure 1.6a), many new multicomponent coupling processes have been developed, including the Hantzsch,¹⁵ Mannich,¹⁶ Bignelli,¹⁷ Passerini,¹⁸ Bucherer-Bergs¹⁹ and the Ugi²⁰ 4-component coupling reaction (Figure 1.6b-g).

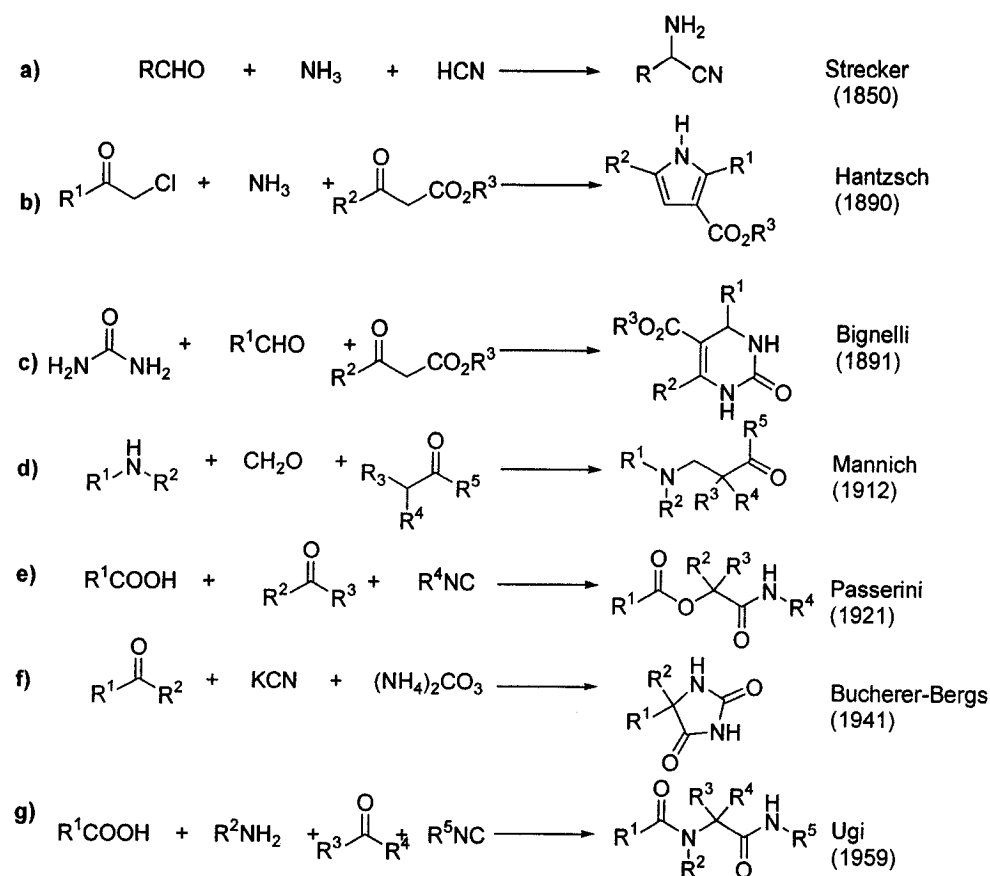


Figure 1.6 Examples of Classical Multicomponent Coupling Reactions

These reactions, which are among the most powerful multicomponent coupling methodologies known, are fully amenable for the generation of compound libraries for biological screening purposes. Of these examples, the Ugi 4 component coupling reaction (Ugi 4CC) has perhaps received the most attention. This process, which couples carboxylic acids, amines, ketones, and isocyanides, generates *N*-acyl amino amides (Figure 1.6g), can be utilized to prepare collections of diverse structures, including benzodiazepines,^{22a, 22e} pyrroles,^{22b} lactams,^{22c} and diketopiperazines.^{22d}

Multicomponent coupling strategies are not without certain limitations. For example, in the Ugi 4CC reaction, literally tens of thousands of carboxylic acids, amines and aldehydes/ketones exist; however, fewer than 30 isocyanides are commercially available, which potentially decreases the scope of the products available.²¹ More importantly, when one considers constructing more complex products from multicomponent coupling reactions, or new classes of products beyond classical routes, the requisite building blocks also increase in complexity. Considering that the required precursors in these reactions would necessitate multiple-step syntheses for their preparation, any advantage realized through accomplishing multiple bond forming steps later in the synthesis would be somewhat negated.

1.2 Metal Catalyzed Multicomponent Coupling Reactions

An approach to multicomponent coupling reactions that has been gaining significant attention involves the use of transition metal catalysts. In principle, this can allow one to work with less “programmed” or designed substrates, and instead allow the transition metal catalyst to control and mediate the coupling of the individual reaction components. In general, transition metals can serve as an excellent tool in synthesis, as they can mediate a diverse array of transformations. For instance, oxidative addition (break bonds), insertion (couple ligands), reductive elimination (form bonds), nucleophilic/electrophilic attack (modify ligands), ligand substitution (exchange ligands) and cycloaddition (combining ligands) are among the common designations of metal based reactions (Figure 1.7).²⁴ By performing multiple versions

of these bond forming, bond breaking, coupling, and ligand modification steps in sequence (i.e. a catalytic cycle), transition metal complexes can be used to mediate very complex transformations in a single synthetic protocol. This can be very powerful in designing new synthetic reactions, and in particular, new metal catalyzed multicomponent coupling reactions.

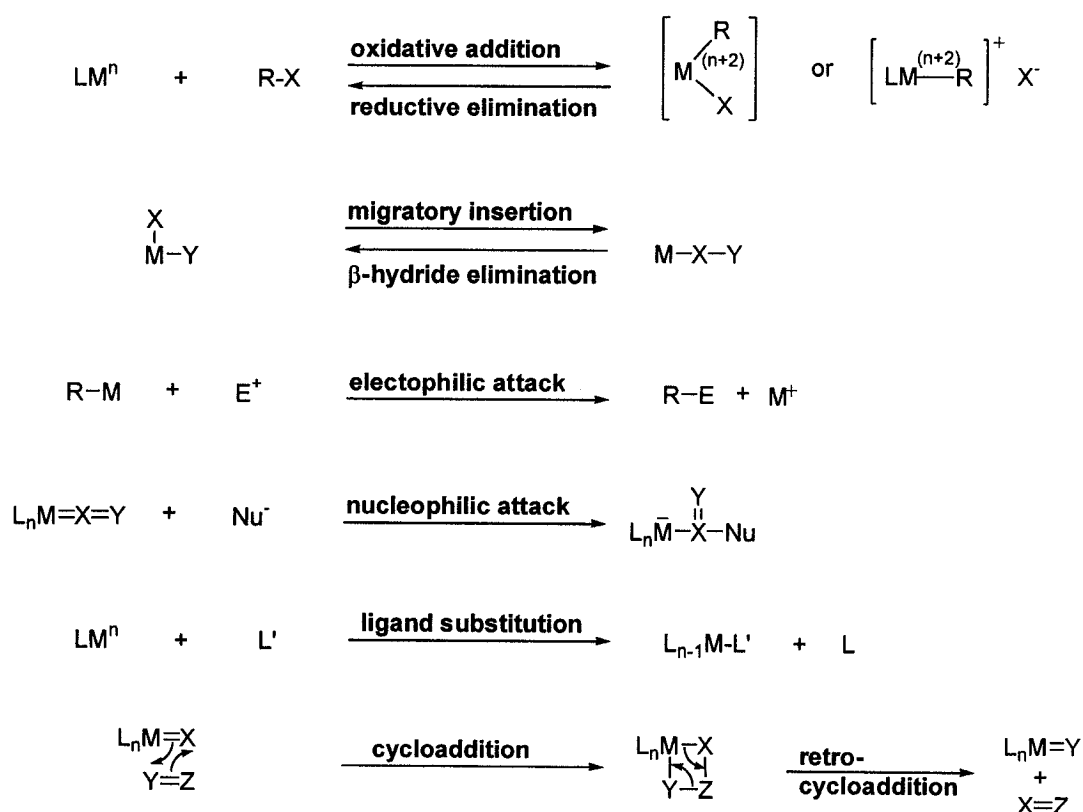
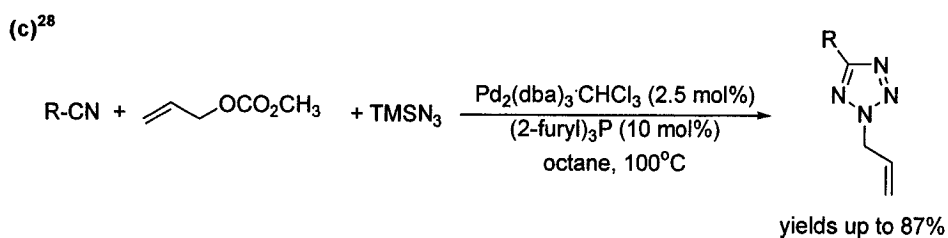
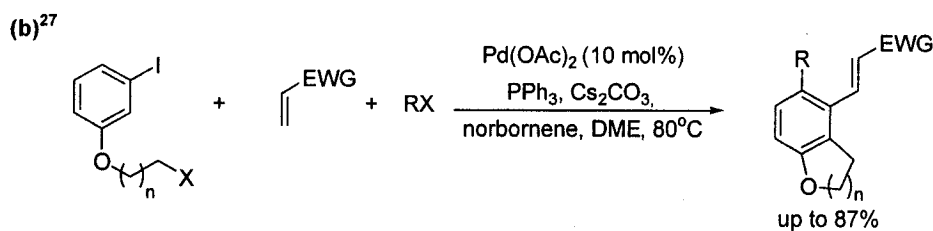
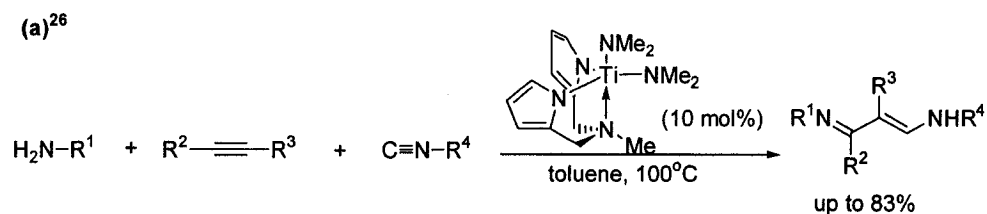
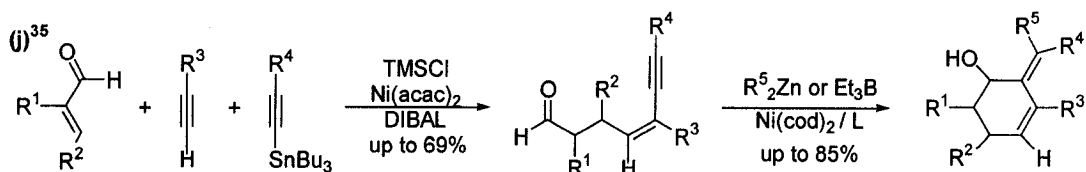
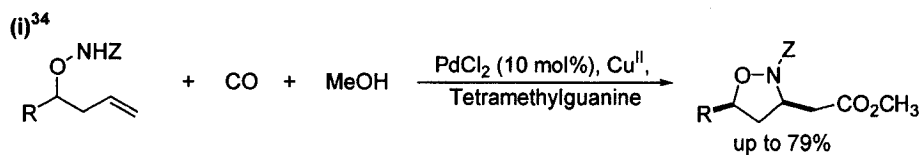
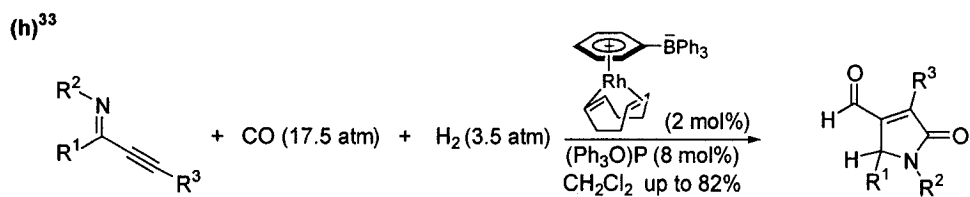
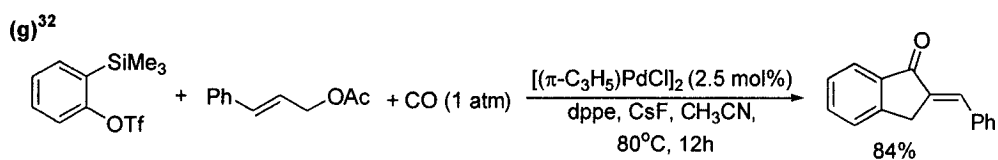
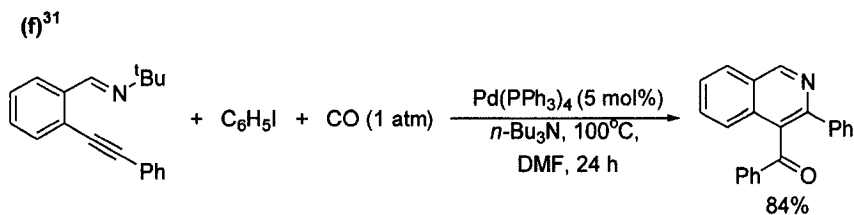
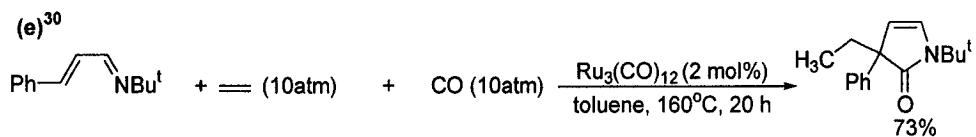
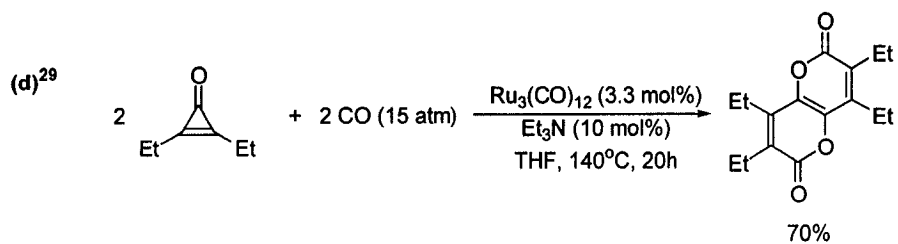


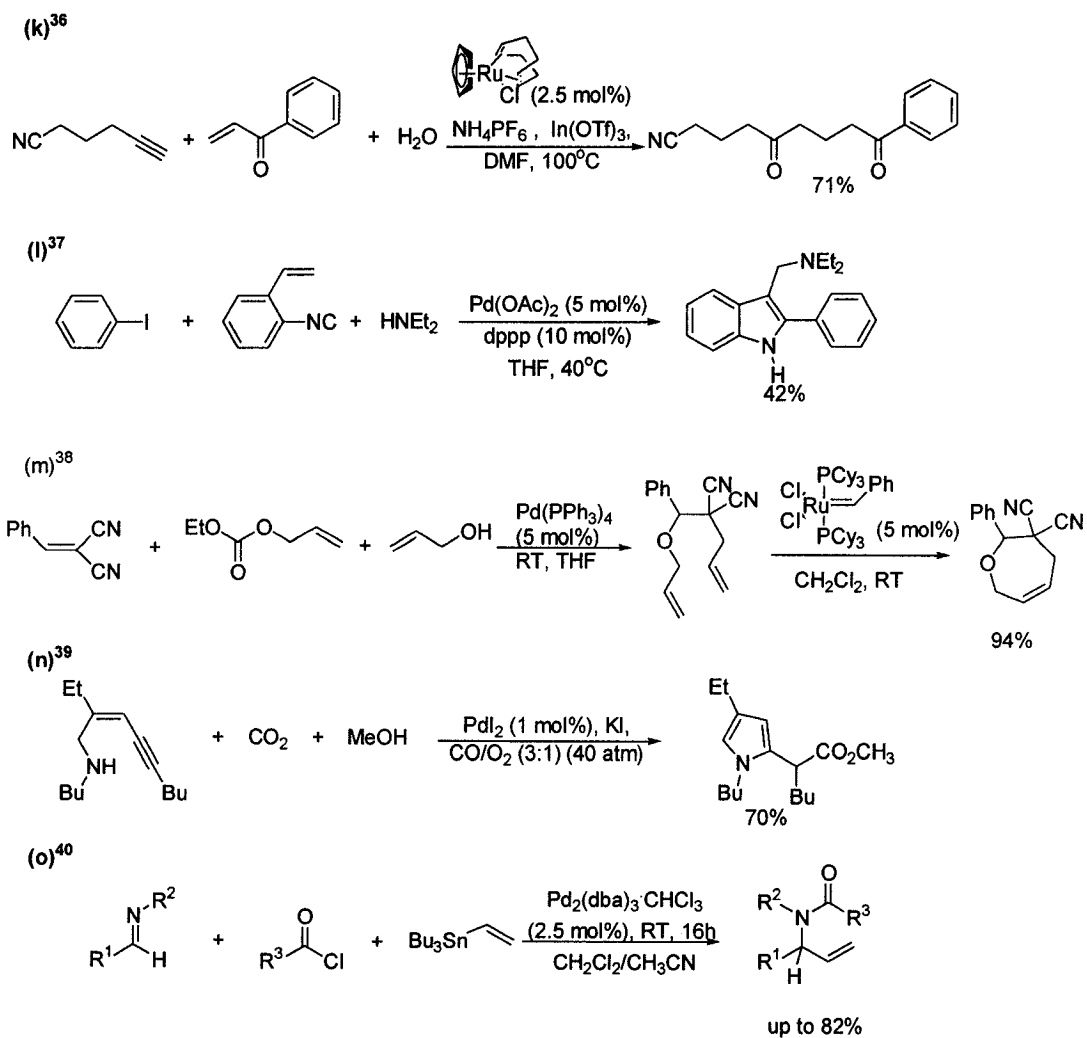
Figure 1.7 General Examples of Organometallic Reactions²⁴

The past 10 years, have seen a dramatic growth in the number of known metal catalyzed multicomponent coupling reactions.²⁵ Some representative examples of recently developed metal catalyzed multicomponent coupling reactions are shown in

Scheme 1.1.²⁶⁻⁴⁰ Considering that a plethora of metal mediated multicomponent coupling reactions exist, it is not possible to discuss all of them. However, by discussing three classic examples of these transformations (i.e. the Pauson Khand reaction,⁴¹ the cyclotrimerization of alkynes,⁴² and amidocarbonylation⁴³), we will illustrate both the challenges in designing multicomponent coupling reactions, as well as their potential utility in allowing multiple basic building blocks to be converted, in one step, into useful products.







Scheme 1.1 Representative Examples of Metal Mediated Multicomponent Coupling Processes

1.2.1 The Pauson Khand Reaction: The Multicomponent Coupling of CO, Alkenes and Alkynes

One of the earliest examples of a metal-mediated multicomponent coupling process was the Pauson Khand reaction.⁴¹ This reaction was discovered while studying the preparation and characterization of alkene and alkyne complexes derived from $\text{Co}_2(\text{CO})_8$. On heating preformed alkyne- $\text{Co}_2(\text{CO})_6$ complexes **1.3** in the presence of olefins, cyclopentenones **1.4** were generated in moderate yields.⁴⁴

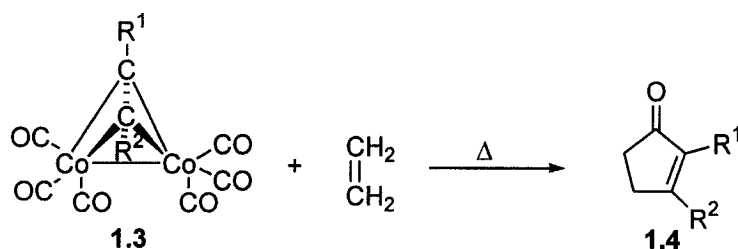


Figure 1.8 The Pauson Khand Reaction

Since its discovery, this reaction has been extensively employed as a method to construct cyclopentenones directly from alkynes, olefins, and carbon monoxide, in a formal [2+2+1] cycloaddition process. Considering that alkenes and alkynes are both readily available and easily varied, the Pauson Khand reaction provides a straightforward means for generating a diverse array of cyclopentenone structures.

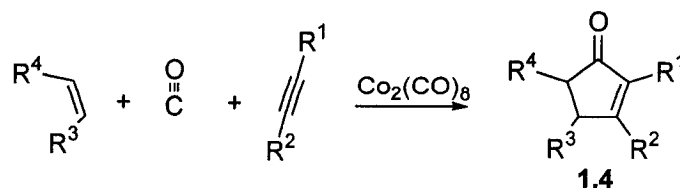


Figure 1.9 Schematic of the Pauson Khand Reaction

In order to better understand how the reaction constituents are assembled in the Pauson Khand reaction, a mechanism for this process shown below.^{45, 46} The first step involves the coordination of dicobalt hexacarbonyl to the alkyne to generate **1.6**. This is followed by alkene coordination and insertion exclusively at the carbon bearing the smaller alkynyl substituent, in the case of an unsymmetrical alkyne. Subsequent CO insertion generates **1.10**, while the loss of $[\text{Co}(\text{CO})_6]$ generates the cyclopentenone shown (**1.12**).

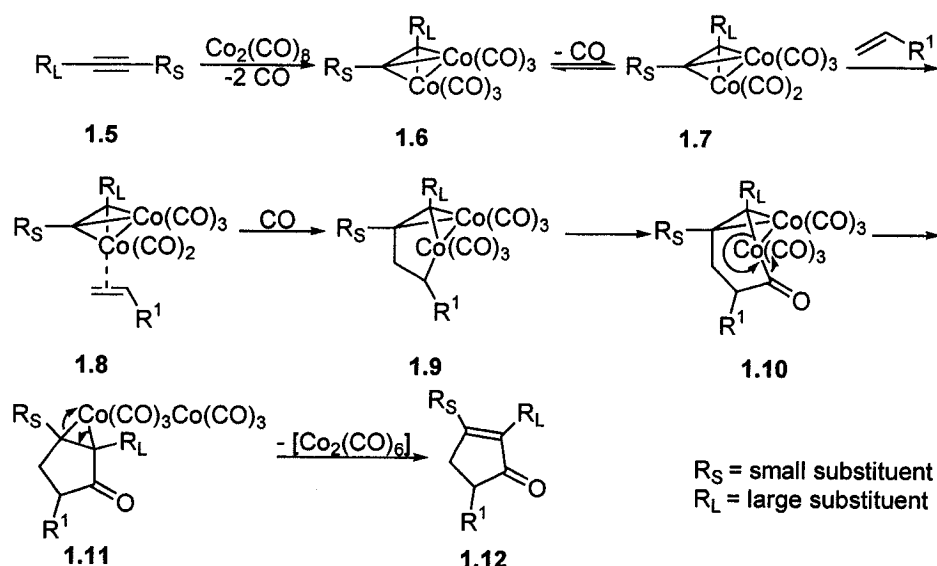


Figure 1.10 Mechanism of the Pauson Khand Reaction

This section will describe the various aspects of the Pauson Khand reaction, including its scope and limitations, as well as improvements that have been made to it over the last 30 years. Included in this discussion will be the catalytic variants of the reaction, and its application in complex molecule synthesis. Many reviews on this coupling

process exist,⁴¹ but for the purposes of this thesis, this section will mainly concentrate on intermolecular variants. The examples cited will illustrate the importance of multicomponent coupling methodologies in the synthesis of organic molecules.

1.2.2.1 Scope of the Pauson Khand Reaction

In order to appreciate the range of products available utilizing the Pauson Khand reaction, a brief discussion as to the reaction scope and limitations will be presented. This reaction is found to be tolerant of a range of remote functionalities on either the alkene or alkyne. These include alcohols, ethers, esters, thioethers, tertiary amines, ketones, ketals, nitriles, amides, sulfonamides, and heteroaromatic rings.^{41d} The reaction proceeds optimally with simple terminal alkynes, while internal alkynes typically result in lower product yields. As described in Figure 1.10, unsymmetrical alkynes yield products with the larger substituent at the 2-position of the cyclopentenone. The Pauson Khand reaction can also proceed with a range of alkenes, although strained olefins (ie. norbornene) and simple olefins (ie. ethylene and propylene) often provide the highest yields. Sterically encumbered alkenes result in low product yields, due to their significantly reduced propensity for cycloaddition. This is attributable to a decreased the ability of the olefin to compete with the alkyne for binding to the $\text{Co}_2(\text{CO})_6\text{R}\equiv\text{R}$ complex (**1.7** \rightarrow **1.8**, Figure 1.10), thereby resulting in side reactions such as alkyne trimerization.⁴² In contrast to alkynes,

unsymmetrical alkenes typically display poor regioselectivity and often yield mixtures of products.

One of the major difficulties in the intermolecular Pauson Khand reaction is the requirement for three constituents to come together at once on the cobalt center. However, this reaction can be favoured by making the coupling intramolecular, via the use of an olefin-tethered alkyne. This not only allows for unstrained olefins to be utilized, but it can also regioselectively incorporate an unsymmetrical alkene into the cyclopentenone, due to geometric restrictions.⁴⁷ This concept was demonstrated on reacting 1-hepten-6-yne with $\text{Co}_2(\text{CO})_8$ and CO, which allowed for a single step synthesis of bicyclic enone **1.13** from acyclic precursors (Figure 1.11).⁴⁷

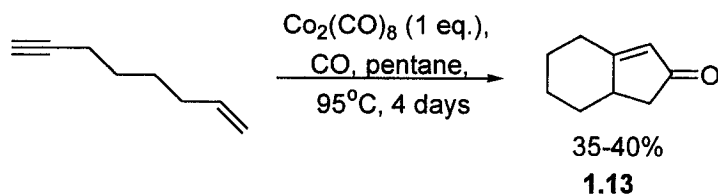


Figure 1.11 First Example of an Intramolecular Pauson Khand Reaction

As shown in the mechanism of the Pauson Khand reaction (Figure 1.10), CO loss is a prerequisite for alkyne (**1.5** \rightarrow **1.6**) and alkene (**1.7** \rightarrow **1.8**) coordination to the cobalt center (Figure 1.10). The harsh conditions utilized in early examples of the Pauson Khand reaction were required for CO labilization and subsequent insertion of the olefin, the suspected rate-determining step of the reaction. More recently, however, it has been shown that CO labilization can also be facilitated chemically, through the

use of amine *N*-oxides (ie. *N*-methylmorpholine *N*-oxide^{48a} & trimethylamine *N*-oxide^{48b}). These additives effect an oxidative removal of a CO ligand as CO₂, and enable the Pauson Khand reaction to proceed at room temperature. In addition, decreased reaction temperatures and increased reaction rates have also been achieved with the use of other promoters, including sulfides,⁴⁹ amine solvents⁵⁰ and ammonia sources.³⁴ The latter presumably labilizes a CO ligand on the cobalt center by forming weak metal-ligand complexes. Molecular sieves, which may promote ligand exchange or adsorb the enyne intermediate and stabilize the pre-transition state, have also been utilized to promote the Pauson Khand reaction.⁵¹

1.2.2.2 The Catalytic Pauson Khand Reaction

One significant limitation of the Pauson Khand reaction is that it is stoichiometric in Co₂(CO)₈. However, examination of the reaction mechanism (Figure 1.10) shows that Co₂(CO)₆ is liberated following the reaction. Considering that Co₂(CO)₆ could presumably coordinate an alkyne to re-form **1.6** (Figure 1.10), catalytic variants should be possible. Indeed, a catalytic [2+2+1] cycloaddition reaction was described in the seminal paper by Pauson and Khand. However, this reaction required specific precursors (norbornene **1.14** and a continuous flow of ethyne).⁴⁴

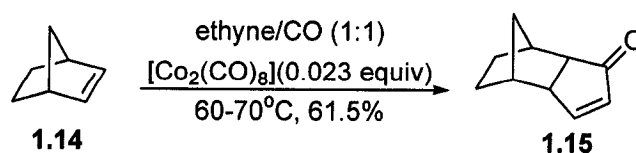


Figure 1.12 The Pauson Khand Reaction

The first example of a catalytic Pauson Khand reaction that utilized unstrained olefins at moderate temperatures and pressures is shown in Figure 1.13.⁵² The success of this reaction is in a large part attributable to it being an intramolecular process, which allows for the proper spatial orientation of the functional groups to undergo reaction.⁵³ One disadvantage of this reaction, however, was that it required highly pure $[\text{Co}(\text{CO})_8]$ to ensure reproducible results.

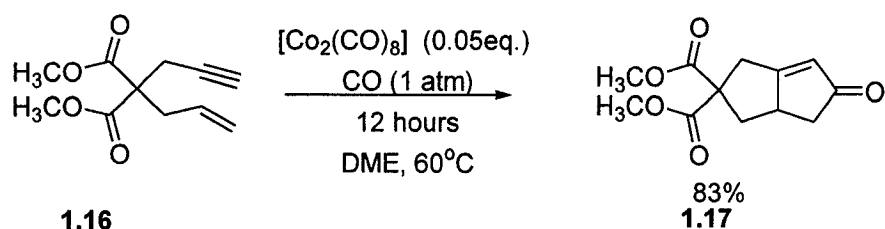
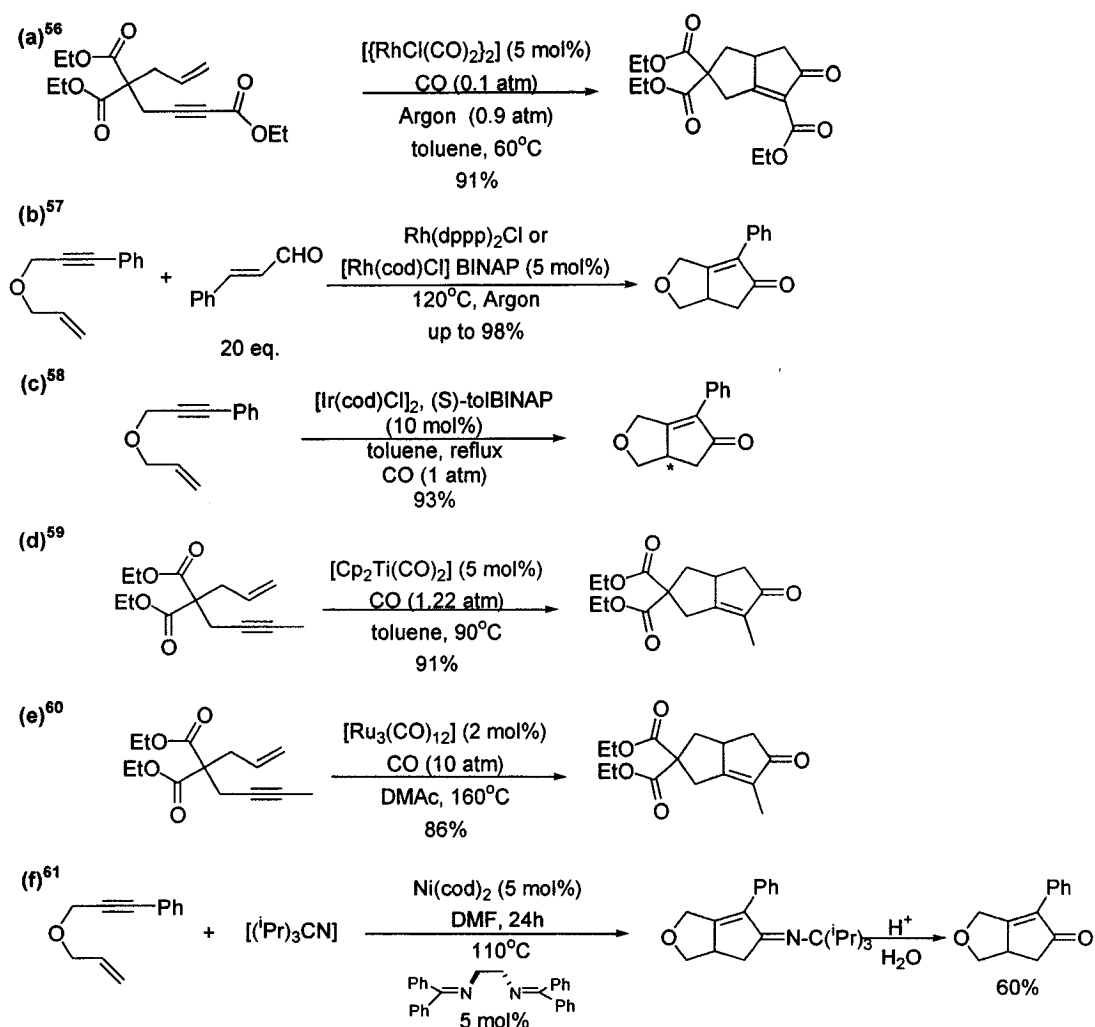


Figure 1.13 Intramolecular Catalytic Pauson Khand Reaction

In order to improve the cobalt-based catalyst, various ligands and additives have been utilized. In addition to being employed in stoichiometric processes, hard Lewis bases including 1,2-dimethoxyethane,^{41d} and cyclohexylamine⁵⁴ also promote the catalytic Pauson Khand reaction. These compounds, which are known to promote ligand labilization from low valent transition metal complexes, effectively generate products in both inter- and intramolecular catalytic Pauson Khand reactions.⁴¹ One of the major difficulties in employing cobalt complexes like $\text{Co}_2(\text{CO})_8$ as catalysts is that they are prone to forming catalytically inert cobalt clusters (e.g. $[\text{Co}_4(\text{CO})_{12}]$).⁵⁵ In order to address the issue of catalyst stability, ligands including phosphanes and phosphites have been utilized.⁴⁰ However, they are occasionally found to be detrimental to the reaction outcome.^{41c,d} Considering that ligands and additives cannot always effectively stabilize cobalt-based catalysts, other transition metal

complexes have been probed for their ability to effect the [2+2+1] cycloaddition reaction. Examples of catalysts that have been developed include $([\text{RhCl}(\text{CO})_2]_2)$, **(a)**,⁵⁶ $[\text{RhCl}(\text{CO})\text{dppp}]_2$,⁵⁷ $\text{Rh}(\text{dppp})_2\text{Cl}$ **(b)**,⁵⁷ $([\text{Ir}(\text{cod})\text{Cl}]_2)$ **(c)**,⁵⁸ $(\text{Cp}_2\text{Ti}(\text{CO})_2)$ **(d)**,⁵⁹ $(\text{Ru}_3(\text{CO})_{12})$ **(e)**,⁶⁰ $(\text{Ni}(\text{cod})_2)$ **(f)**.⁶¹ (Scheme 1.2). In general, these complexes are all considered to mediate the formation of cyclopentenones in a similar fashion to $\text{Co}_2(\text{CO})_8$: via the formation of multiple empty coordination sites for alkene and alkyne coordination followed by CO insertion and reductive elimination. Perhaps due to the lower propensity towards cluster formation, certain metal catalysts can operate at low temperatures and pressures (Scheme 1.2 a & c)^{56, 59} and at lower loadings (Scheme 1.2e).⁶⁰ In addition, aldehydes can be utilized as carbonyl sources, when certain rhodium catalysts are employed (Scheme 1.2b).⁵⁷ Furthermore, isocyanides can replace CO in the coupling process (Scheme 1.2f).⁶¹



Scheme 1.2 Examples of Metal Catalyzed Pauson Khand Reactions

As shown in Scheme 1.2, most examples of the catalytic Pauson Khand reaction are intramolecular processes; however, intermolecular variants are also known. For example, $[\text{RhCl}(\text{CO})_2]_2$ has been found to catalyze the coupling of norbornene with 1-phenyl-propyne and CO to generate enones **1.18** as a 1:1 mixture of regioisomers (Figure 1.14).⁶² Similarly, $\text{Co}_4(\text{CO})_{12}$,⁶³ $\text{Co}(\text{acac})_2$,⁶³ and $(\text{indenyl})\text{Co}(\text{cod})$,⁶⁵ have also shown activity towards catalytically coupling strained olefins, alkynes and CO to generate cyclopentenones.

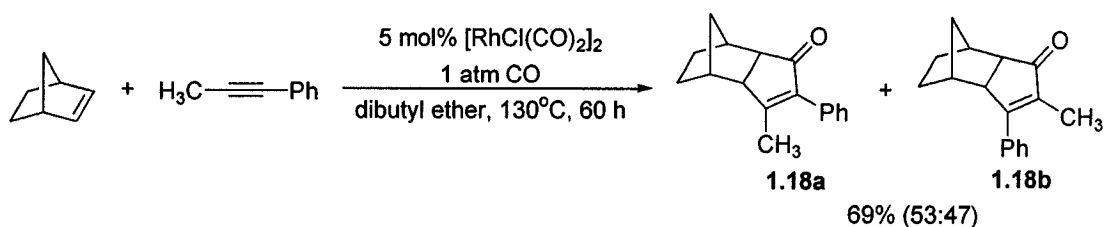


Figure 1.14 Rhodium Catalyzed Pauson Khand Reaction

Catalytic variants of the Pauson Khand reaction typically require the use of strained or simple α -olefins, likely due to less favourable coordination and cycloaddition propensity of sterically bulky alkenes with the metal center. One approach that has been utilized to address the issue of low reaction scope utilizes removable directing groups on the alkene (Figure 1.15). In this process, the alkene is tethered to a 2-pyridyldimethylsilyl moiety, which can undergo a chelation-assisted cyclization with the alkyne-metal complex to form **1.19**.⁶⁶ The presence of this pyridyl group on the silane allows for the regioselective formation of the metallacyclopentene intermediate **1.20**. Following cyclization, the silicon-based directing groups can be removed.

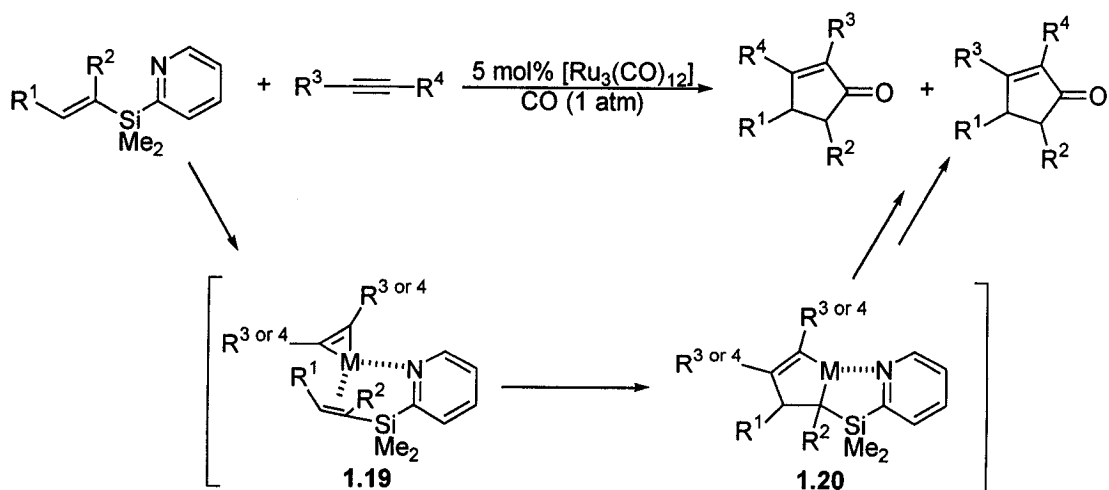
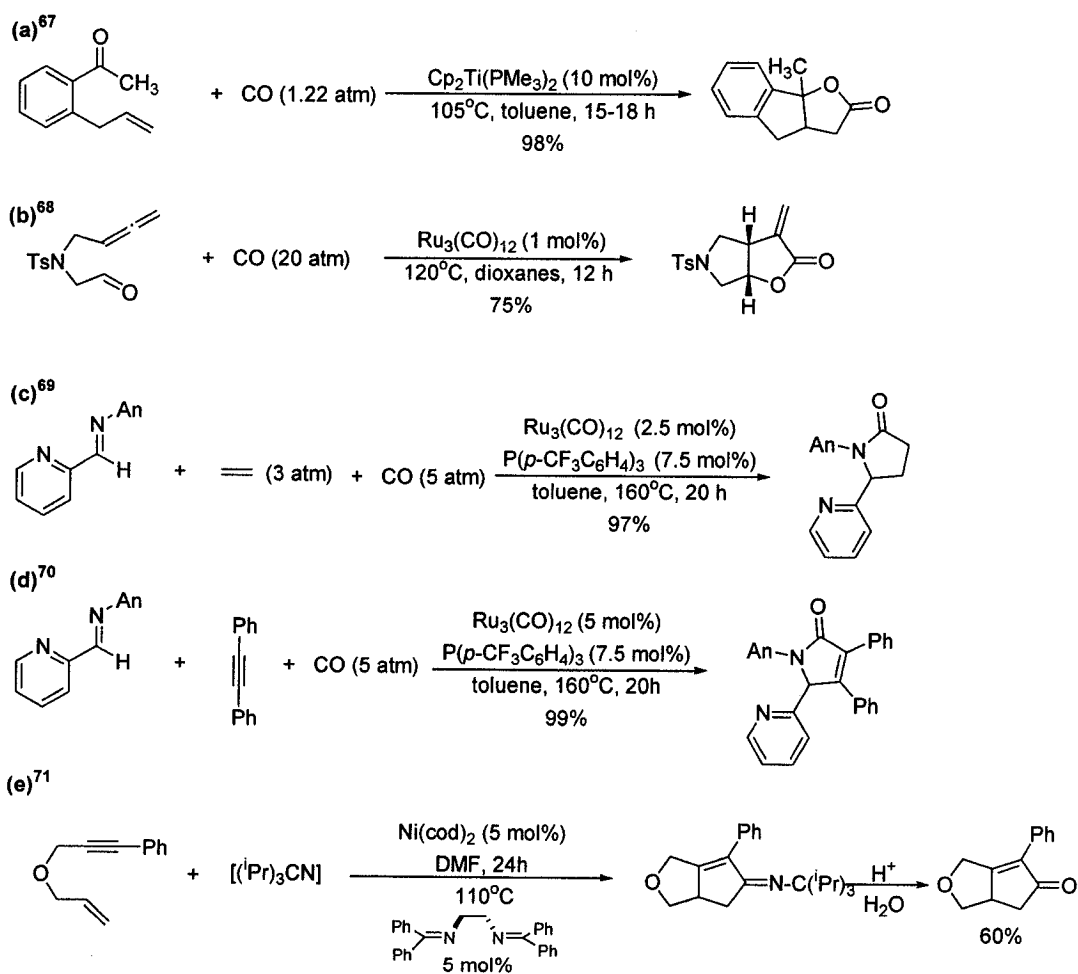


Figure 1.15 “Disposable Tethers” in the Catalytic Pauson Khand Reaction

1.2.2.3 The Incorporation of Heteroatoms into the Pauson Khand Reaction

The Pauson Khand reaction was perhaps the first example of a [2+2+1] cycloaddition process that generated cyclic molecules. Since, its discovery this methodology has been elaborated to include a variety of reaction precursors, including allenes, nitriles, isocyanides, imines, and carbonyl functionalities. In order to achieve this greater substrate diversity, new metal catalysts have also been developed (Scheme 1.3).⁶⁷⁻⁷¹



Scheme 1.3 Incorporation of Heteroatoms into Cyclic Molecules via [2+2+1] Processes

In addition to these intramolecular processes, multicomponent variants of heteroatom containing [2+2+1] cycloaddition reactions are also known. For instance, methyl benzoyl formate **1.21**, ethylene and carbon monoxide were assembled into the γ -butyrolactone methyl ester **1.22** in excellent yields through the utilization of catalytic $\text{Ru}_3(\text{CO})_{12}$ (Figure 1.16).^{72, 73} The individual reaction precursors that are integrated into this molecule are highlighted in Figure 1.16.

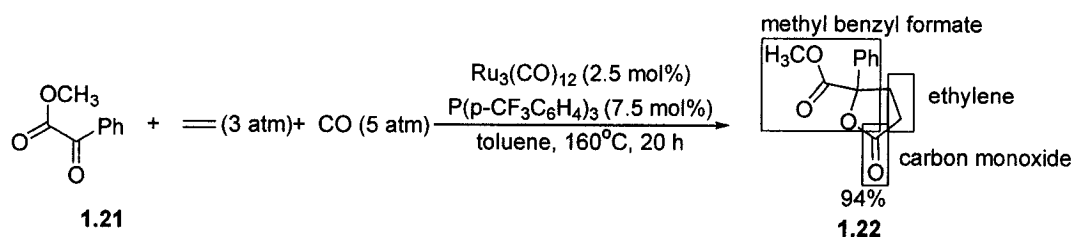


Figure 1.16 Generation of γ -Butyrolactones

The mechanism of the γ -butyrolactone formation is believed to be similar to the traditional Pauson Khand reaction, and is shown in Figure 1.17. It involves the initial coordination of a “ $\text{Ru}(\text{CO})_3$ ” species to the α -ketoester to generate **1.23**. Following coordination of the olefin **1.24** and metallacycle formation **1.25**, CO insertion into the Ru-O bond forms intermediate **1.26**. Reductive elimination then yields the final product **1.27** and regenerates the ruthenium carbonyl complex for further catalysis.

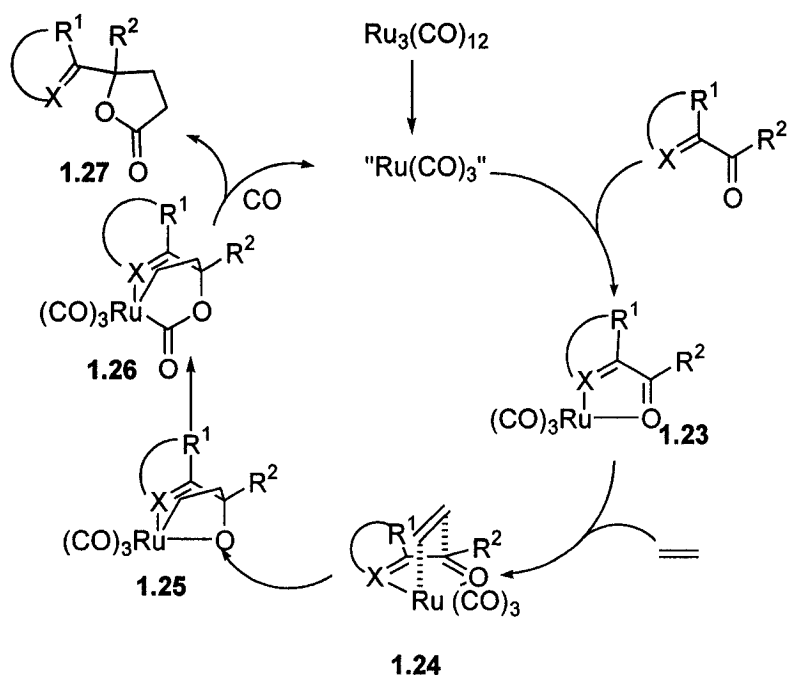
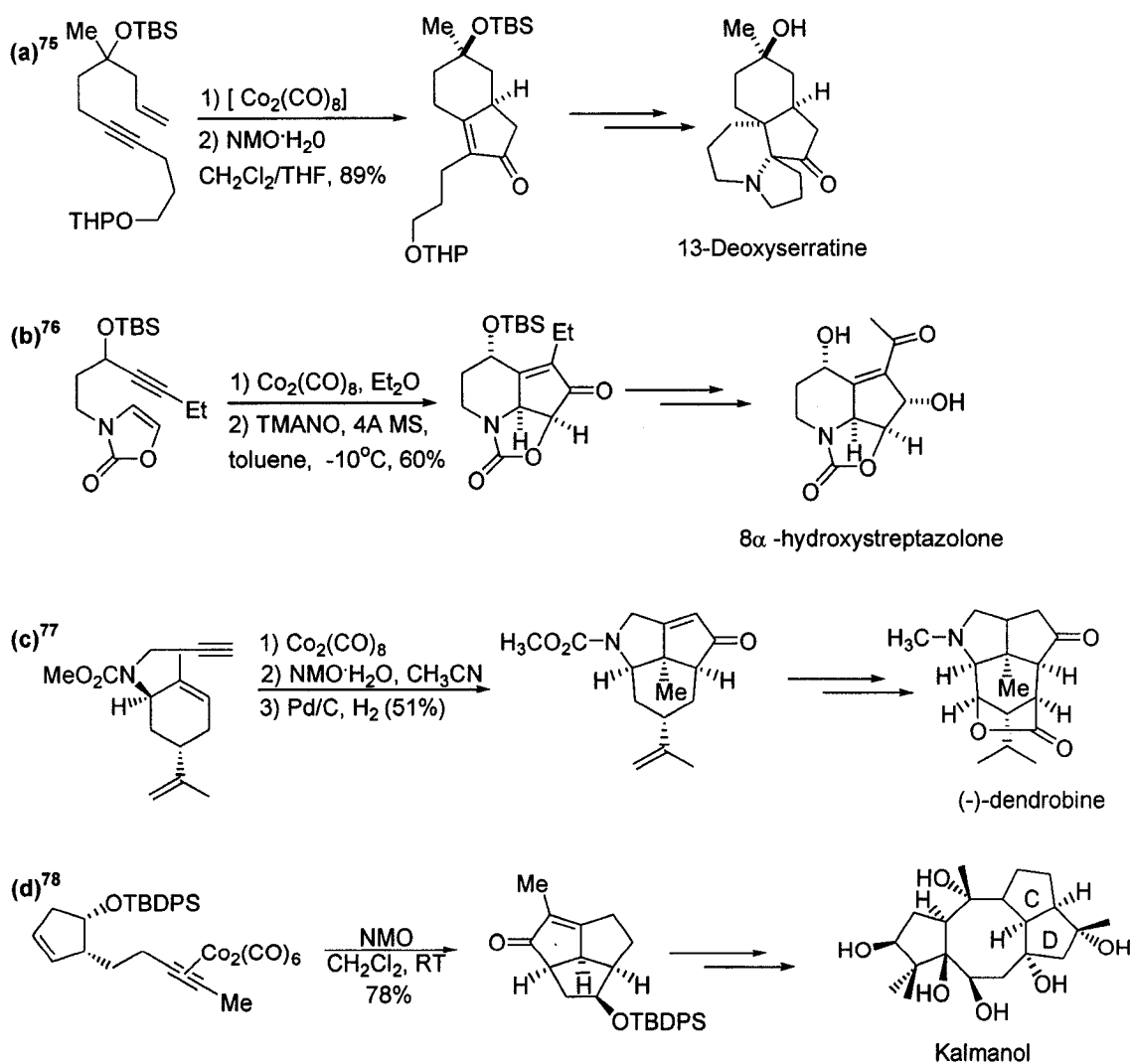


Figure 1.17 Mechanism for γ -Butyrolactone Synthesis

The examination of the catalytic cycle suggested that a substrate with a chelating atom X is required to stabilize intermediate **1.24**. Considering that 2-carbonyl substituted heterocycles generate essentially the same intermediate as **1.23**, heteroaryl ketones and aldehydes, such as 2-pyridine carboxaldehyde and 2-acetylpyridine, were also found to be viable substrates.^{72, 73} Furthermore, the alkene component is not restricted to ethylene, and can include cyclic and acyclic alkenes. In addition, alkynes are also competent reaction substrates and give rise to a hetero-Pauson Khand type reaction.^{72, 73}

1.2.2.4 Synthetic Applications of the Pauson Khand Reaction

Due to its ability to provide direct access to cyclopentenones from alkynes, alkenes, and carbon monoxide, the Pauson Khand reaction has found numerous synthetic applications. Some illustrative examples of its use in the synthesis of natural products and complex molecules are shown below.⁷⁵⁻⁷⁸



Scheme 1.4 Syntheses of Natural Products Utilizing the Pauson Khand Reaction

In addition to intramolecular cyclizations, intermolecular processes have also been utilized, as demonstrated by the preparation of asteriscanolide **1.30**.⁷⁹ This total synthesis employed the Pauson Khand reaction to generate ring A in **1.29** through the coupling of propene, CO and alkyne **1.28** in the presence of $\text{Co}_2(\text{CO})_8$ and NMO. Further elaboration of this intermediate to the final product was achieved utilizing ring closing metathesis. The Pauson Khand reaction was an obvious choice for constructing **1.29**, since the cyclopentenone structure could be generated with excellent regiocontrol utilizing readily available building blocks (propene and an alkynoate).

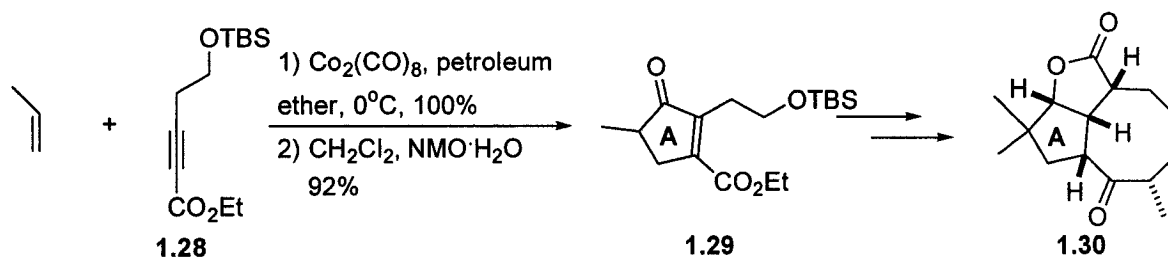


Figure 1.18 The Pauson Khand Reaction in the Generation of Asteriscanolide **1.30**

Considering that the alkenes and alkynes can be readily diversified, the Pauson Khand reaction has also found significant utility in the synthesis of compound libraries that contain the cyclopentenone core.^{80, 81} For instance, a group at Parke-Davis Research has utilized this reaction on solid support to construct hexahydro-1H-[2]pyrindinone ring systems **1.31** from supported amino acid derivatives (Figure 1.19).⁸⁰ Following a palladium catalyzed cross coupling reaction, the enyne was allowed to cyclize to form the cyclopentenone. In addition to this example, Schreiber

has utilized the Pauson Khand reaction, in part, to develop a stereoselective synthesis of 2500 tricyclic compounds (**1.32**) on solid support (Figure 1.20).⁸¹

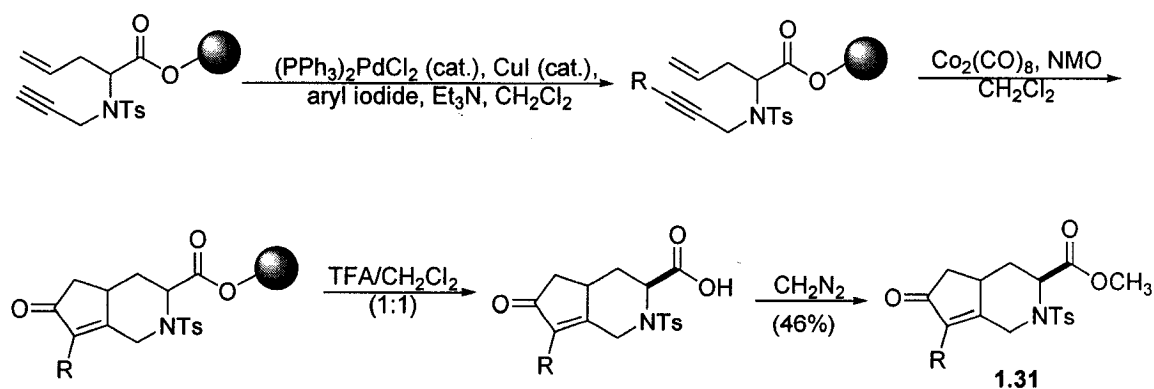


Figure 1.19 Pauson Khand Reactions on Solid Support

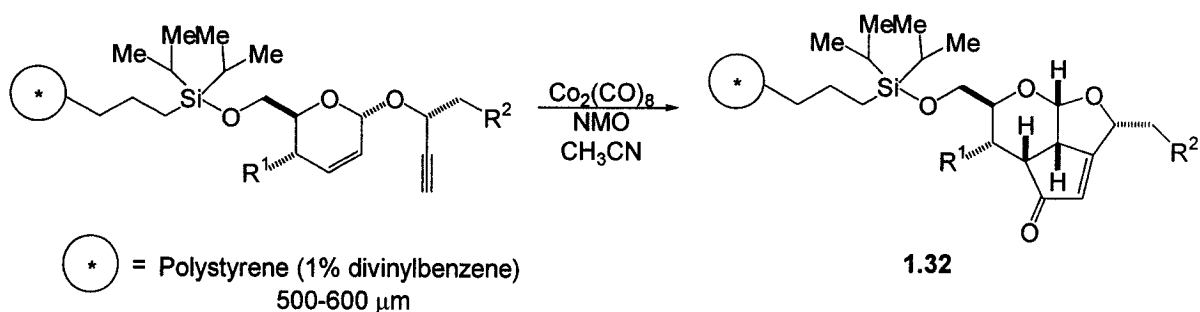


Figure 1.20 Pauson Khand Reaction in the Generation of Compound Libraries

1.2.3 Metal Mediated Cyclotrimerization of Unsaturated Compounds

Amongst the most powerful methods for constructing complex molecules from simpler precursors, include cycloaddition processes such as the Diels-Alder reaction.⁸² These reactions involve transition states consisting of $[4n+2]\pi$ electrons,

and generate six-membered ring systems from acyclic precursors. A textbook example of this type of reaction is the cyclization of 1,3-butadiene with ethylene to form cyclohexene (Figure 1.21).⁸³

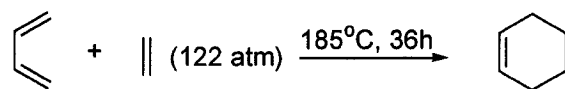


Figure 1.21 Cycloadditions in Multicomponent Coupling Reactions

The cyclization of three alkynes can also generate six-membered rings, in a process known as cyclotrimerization.⁸⁴ As in the Diels-Alder reaction, this transformation is also a symmetry allowed 6π electron cycloaddition process, the simplest example of which couples three molecules of acetylene to generate benzene (Figure 1.22a). This reaction, which was first described by Bertholet in 1866, required temperatures in excess of 400°C to generate product (Figure 1.22a).⁸⁵ This is despite the fact that this process is calculated to be highly exothermic ($\Delta H^\circ = -594 \text{ kJ/mol}$).⁸⁶ The barrier to this reaction is presumed to be a kinetic one, as it requires three reaction components to come together at once to undergo the $[2+2+2]$ cycloaddition reaction.

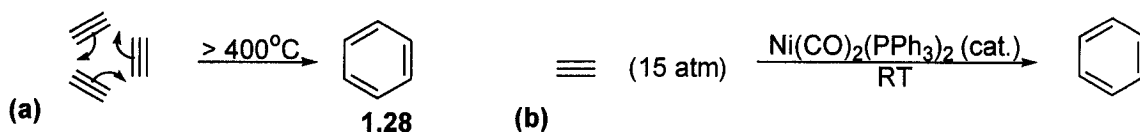


Figure 1.22 Cyclotrimerization of Acetylene

While the cyclotrimerization of acetylene is of limited utility due to its high thermal barrier, more recent results have shown that transition metal complexes can readily

catalyze this process. Eighty two years following Berthelot's report, Reppe showed that $\text{Ni}(\text{CO})_2(\text{PPh}_3)_2$ can catalyze the cyclotrimerization of alkynes at room temperature (Figure 1.22b).⁸⁷ The lower barrier to this nickel catalyzed cyclotrimerization is believed to be due the reaction mechanism, which is distinct from that of thermal cyclization, and instead involves a series of metal based reactions to construct the arene ring (Figure 1.23).⁸⁵ The reaction is thought to proceed through the initial coordination of two alkynes to the metal complex (ML_n) to form **1.33**. An oxidative coupling of these two coordinated alkynes subsequently generates metallacyclopentadiene **1.34**, which is coordinatively unsaturated. An alkyne can subsequently bind to **1.34** and undergo insertion to form the metallacycloheptatriene **1.36**. Reductive elimination yields the arene complex **1.37**, which can undergo decomplexation to regenerate the catalyst and the arene product **1.38**. All of the reaction intermediates, except for the alkyne-metallacyclopentadiene **1.35** have been isolated, hence this proposed mechanism is a realistic one.

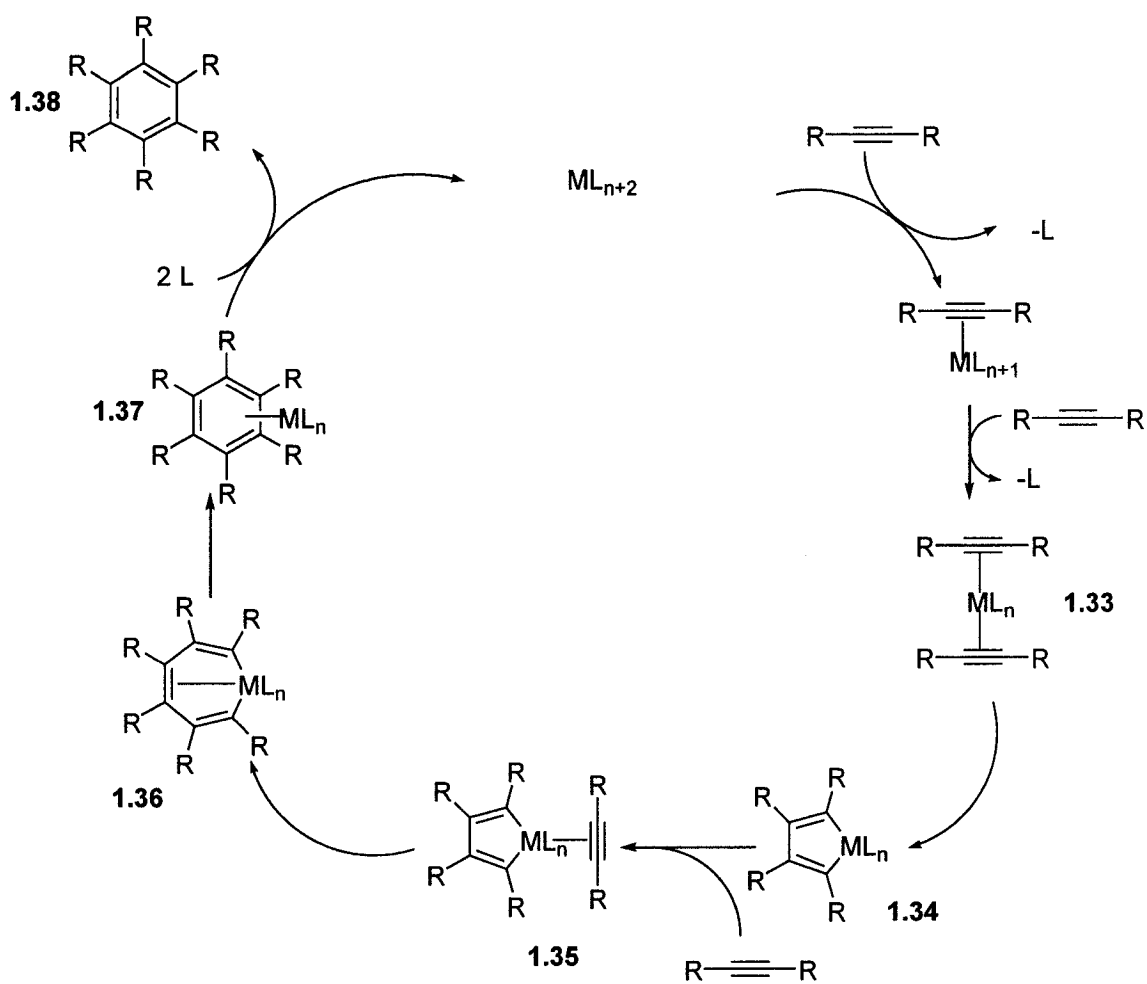
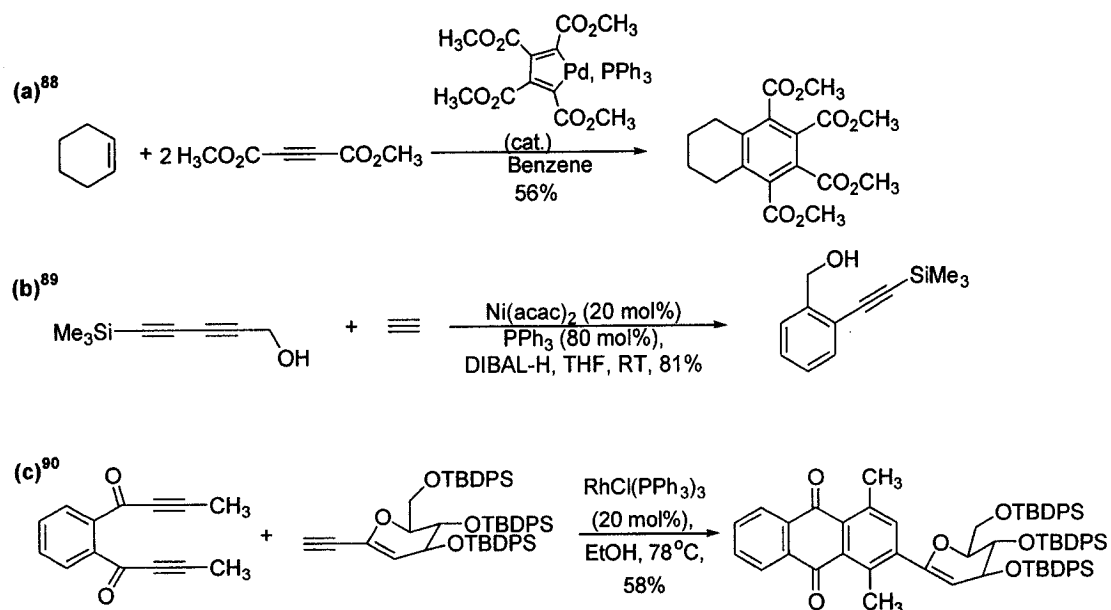


Figure 1.23 Cyclotrimerization of Alkynes

Examination of Figure 1.23 shows that the metal catalyzed cyclotrimerization of three alkynes is mechanistically similar to the previously described Pauson Khand reaction in that both require multiple transition metal coordination sites to bind unsaturated substrates, mediate cycloaddition and reductively eliminate products. As such, the catalysts that have been found to mediate cyclotrimerization processes are similar to those utilized in the Pauson Khand reaction. In addition to $\text{Ni}(\text{CO})_2(\text{PPh}_3)_2$ ⁸⁷ reported by Reppe, these include metal complexes, such as $\text{PdL}_2(\text{PPh}_3)_2$ (Scheme 1.5a),⁸⁸

([Ni(acac)₂]) (Scheme 1.5b),⁸⁹ (RhCl(PPh₃)₃) (Scheme 1.5c),⁹⁰ Pd/C & TMSCl (Figure 1.24), and CpCo(CO)₂ (Figure 1.26).



Scheme 1.5 Selected Metal Catalysts in the Cyclotrimerization Reaction

1.2.3.1 Cyclotrimerization Reactions in Synthesis

Considering the importance of multisubstituted benzenes in both industrial and pharmaceutical applications, the development of efficient means for their generation is vital. The preparation of multisubstituted arenes has been accomplished utilizing both classical and modern methods, which include directed *o*-metallation,⁹¹ nucleophilic⁹² or electrophilic⁹³ aromatic substitution, cross coupling reactions,⁹⁴ and even C-H bond activation processes.⁹⁵ These processes generally incorporate a single substituent at a time onto the arene ring or substitute in an uncontrolled manner. In contrast, cyclotrimerization potentially provides a method to assemble three different alkynes into multisubstituted arenes (Figure 1.23). Not only does this approach

facilitate access to substituted arene ring systems, but it would also enable ready diversification, simply by altering the alkyne utilized.

In cases where a symmetrical alkyne is utilized, cyclotrimerization reactions can construct a single hexasubstituted benzene. One of the most useful methods of obtaining this class of compounds employs a mixture of Pd/C with TMSCl as a catalyst to trimerize a range of symmetrical alkynes into hexasubstituted benzenes **1.39** (Figure 1.24).⁹⁶

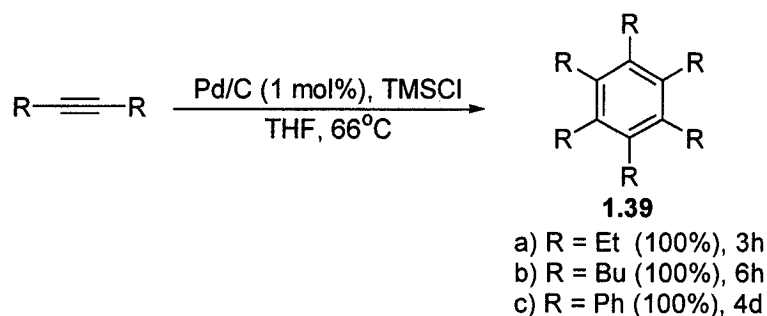


Figure 1.24 Generation of Multisubstituted Benzenes

Although this metal catalyzed cyclotrimerization is of utility in generating substituted benzenes, it is typically restricted to symmetrical alkynes. For instance, the utilization of unsymmetrical alkynes, such as *tert*-butylacetylene, generates mixtures of products (Figure 1.25).⁹⁶ Although, many approaches to address this problem have been developed, perhaps the most straightforward comes from making this process intramolecular. By employing this strategy, the reacting alkynes are effectively placed in a defined geometry that allows them to react in a predictable manner.

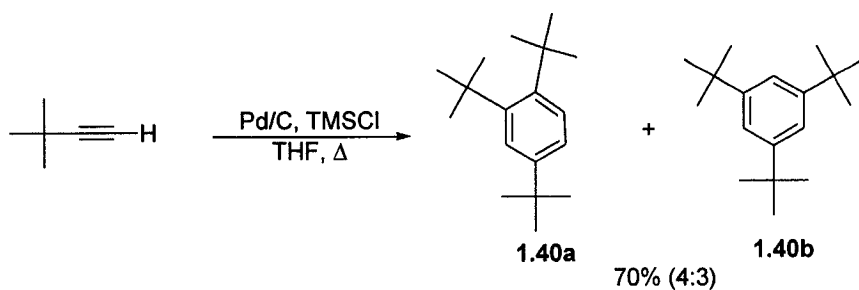


Figure 1.25 Generation of Multisubstituted Benzenes

This concept has been demonstrated through the $\text{CpCo}(\text{CO})_2$ catalyzed reaction of 1,5-hexadiyne with bis(trimethylsilyl)ethyne to generate **1.41** (Figure 1.26).⁹⁷ This study showed that the bulk of the bis(trimethylsilyl)ethyne prevents its self-condensation, and allows it to react with the *in situ* generated metallacyclopentadiene **1.42** to yield the final product. The high temperatures in this reaction are necessary for vacant site generation through CO loss and subsequent alkyne coordination (ie. generation of **1.33** in Figure 1.23).

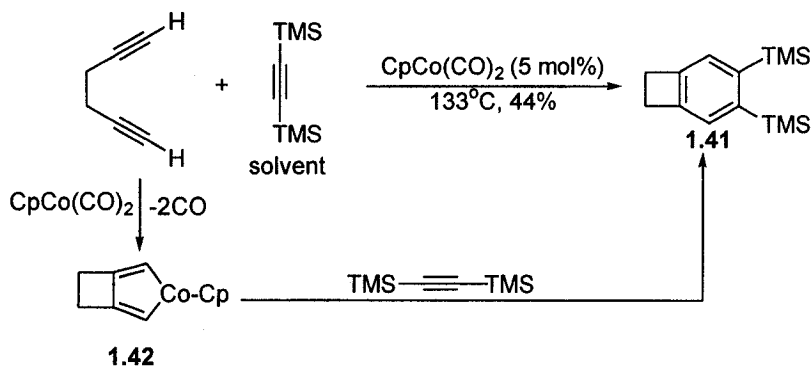
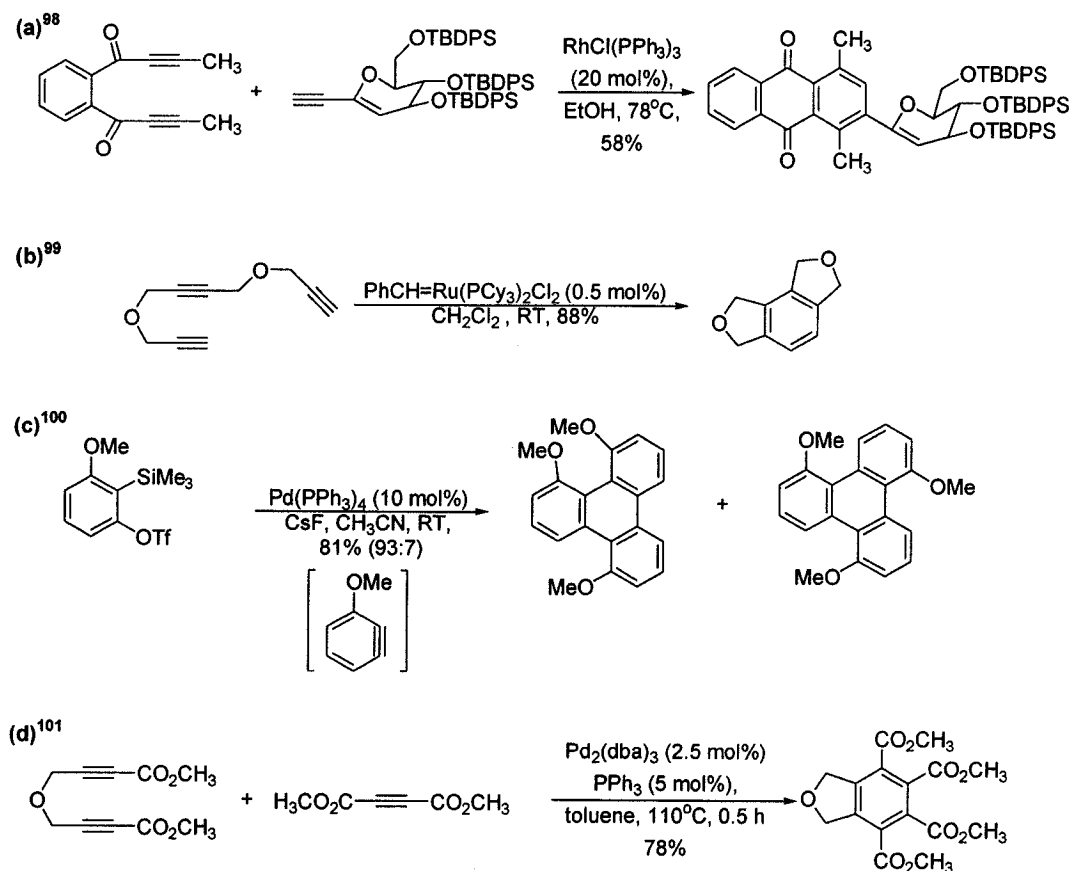


Figure 1.26 Cyclotrimerization Reactions with $\text{CpCo}(\text{CO})_2$

A large number of other examples of intramolecular cyclotrimerization reactions have been reported to construct polycyclic arenes. Several representative examples are shown in Scheme 1.6.⁹⁸⁻¹⁰¹



Scheme 1.6 Utilization of Different Metals in Cyclotrimerization Reactions

1.2.3.2 Generation of Substituted Benzenes: Regioselectivity Issues

In contrast to intramolecular processes, intermolecular variants of cyclotrimerization are far more challenging in obtaining chemo- and regioselectivity. For instance, the combination of three non-symmetrical alkynes can potentially generate 38 different

benzene derivatives.¹⁰² As previously shown, the utilization of a partially or completely intramolecular processes can greatly aid in achieving selectivity in multicomponent cyclotrimerization reactions. Two major approaches for obtaining chemo- and regioselectivity in intermolecular processes have been developed. These include coupling alkyne substrates that have unique electronic or steric properties and therefore react in a specific manner. In addition, through employing directing functionality on the alkynyl precursors, reactions can also be induced to occur regioselectively.

1.2.3.2.1 Utilization of Electronics and Sterics to Influence Chemo- and Regioselectivity

One method to facilitate the generation of multisubstituted benzenes from three different alkynes involves sequentially coupling the alkynes at a metal center. This subsequently enables selective generation of a metallacyclopentadiene intermediate. The regioselective formation of this cyclic metal species is a direct consequence of the steric and electronic properties of the alkynes utilized. The subsequent addition of the third alkyne can generate the substituted benzene by the mechanism shown in Figure 1.27 (**1.43** → **1.44**). The effectiveness of this concept was demonstrated by utilizing a zirconium complex as a template for generation of a zirconacyclopentadiene **1.43**. This was followed by a nickel mediated cyclotrimerization to generate the hexasubstituted benzene as a single product in 50% yield.¹⁰³

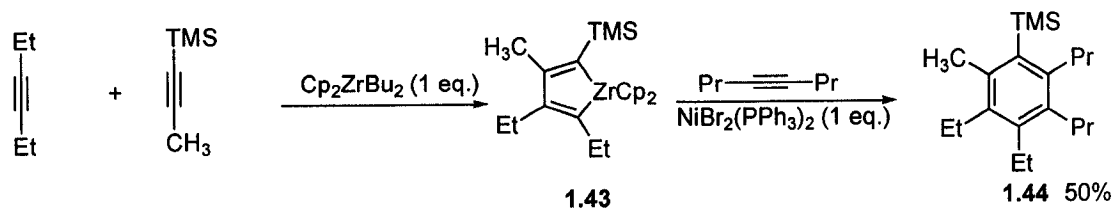


Figure 1.27 Nickel Mediated Cyclotrimerization

In addition to this example, a titanium variant that utilized three distinct alkynes has also recently been described (Figure 1.28).¹⁰⁴ In this reaction, two unsymmetrical alkynes are initially combined to construct a dialkoxytitanacyclopentadiene **1.45**. This is followed by the addition of a third alkyne, which generates aryltitanium compound **1.46**, which can subsequently react with a range of electrophiles to yield the final product **1.47**. The selectivity obtained in the reaction comes from the exclusive formation of a single titanacycle from two different alkynes.

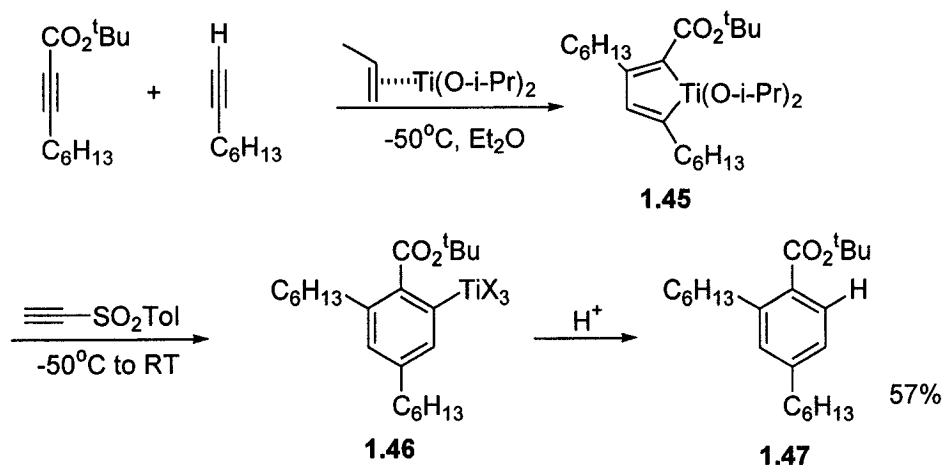


Figure 1.28 The One Pot Cyclotrimerization Reaction

In addition to these stoichiometric processes, catalysis can also be employed to construct multisubstituted benzenes. For instance, Gevorgyan and Yamamoto have

recently reported a formal [2+2+2] cyclotrimerization of alkynes, that couples three structurally and electronically distinct alkynes to generate tetra- and penta-substituted benzenes (Figure 1.29).¹⁰⁵ The complete regioselectivity obtained in this transformation is the result of the reaction not proceeding via a traditional cyclotrimerization mechanism, which often entails the non-selective formation of a metallacyclopentadiene intermediate. Instead, the initial step involves the precedented palladium catalyzed coupling of an electron rich and electron poor alkyne to form an eneyne intermediate **1.48**.¹⁰⁶ This intermediate subsequently undergoes a [4+2] benzannulation process with 5,7-dodecadiyne to generate the penta-substituted benzene **1.49** (Figure 1.29). By utilizing three structurally and electronically distinct alkynes that react in a predictable manner, regio- and chemoselectivity is realized in this multicomponent coupling reaction.

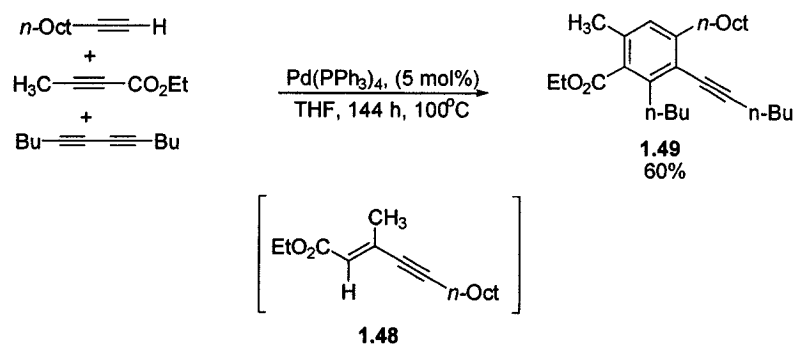


Figure 1.29 Generation of Penta-substituted Benzenes from a Cyclotrimerization of Alkynes

1.2.3.2.2 Utilization of Functionality to Influence Chemo- and Regioselectivity

Structurally and electronically distinct alkynes can also be employed to generate multisubstituted benzenes in a regio- and chemoselective manner. One complementary method involves the utilization of chemical functionality to orient the alkyne precursors in a specific manner to obtain generation of a specific isomer. For instance, a Ru(II) catalyst has recently been found to effect a three-component, one-pot coupling reaction to generate tetra-substituted benzene derivatives (Figure 1.30).¹⁰⁷ This reaction proceeds through an initial chemo- and regioselective Ru (II) catalyzed cyclization of two alkynes to generate a ruthenacycle intermediate **1.50**. This selectivity is believed to be due to the condensation of the propargyl alcohol with **1.51** to form **1.52**, which then undergoes an intramolecular cyclotrimerization. This is followed by the subsequent insertion of the third alkyne to generate the temporary tethered-boron arene **1.53**. Suzuki coupling between this complex and an aryl halide subsequently generates the final product **1.54**.

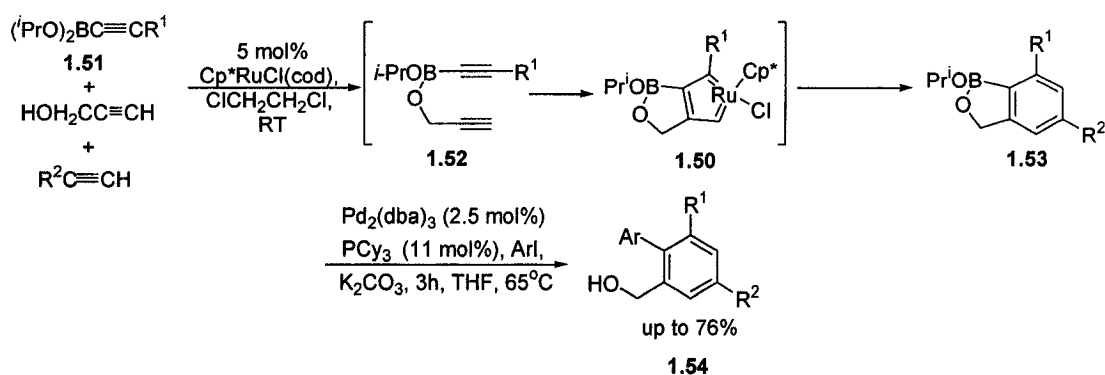


Figure 1.30 Cyclotrimerization of Alkynes Utilizing Boron Tethers

Considering the level of chemo- and regioselectivity that is obtainable by utilizing intramolecular processes, tethers that permit a pseudo-intramolecular reaction have also been employed. In this type of transformation, the tri-yne **1.55** is initially assembled from three different alkynes.¹⁰⁸ This intermediate can subsequently be cyclized in the presence of catalytic $\text{CpCo}(\text{CO})_2$ to generate **1.56** in 78% yield. Following the cyclization, the silyl tethers can be removed to generate a polysubstituted arene ring system **1.57**. The high temperatures and irradiation required in this reaction are presumably for labilization of the carbonyl ligands in the catalyst.

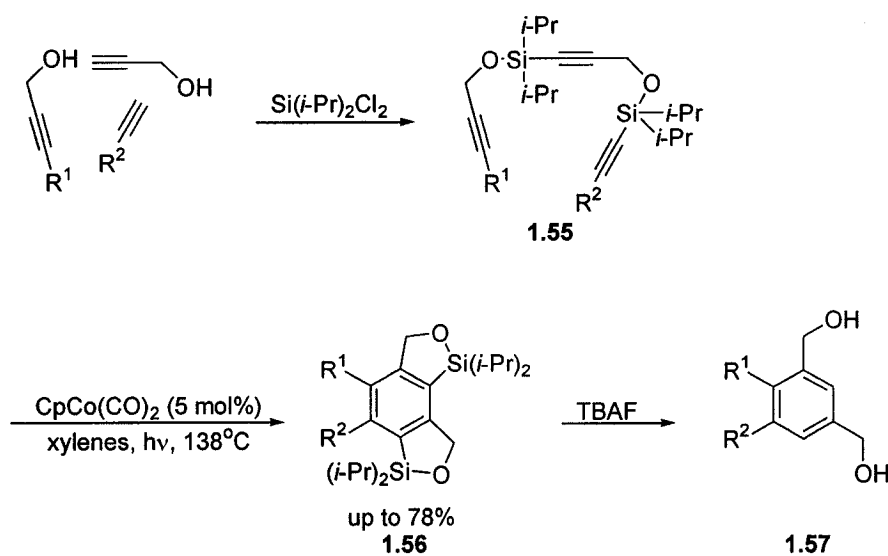
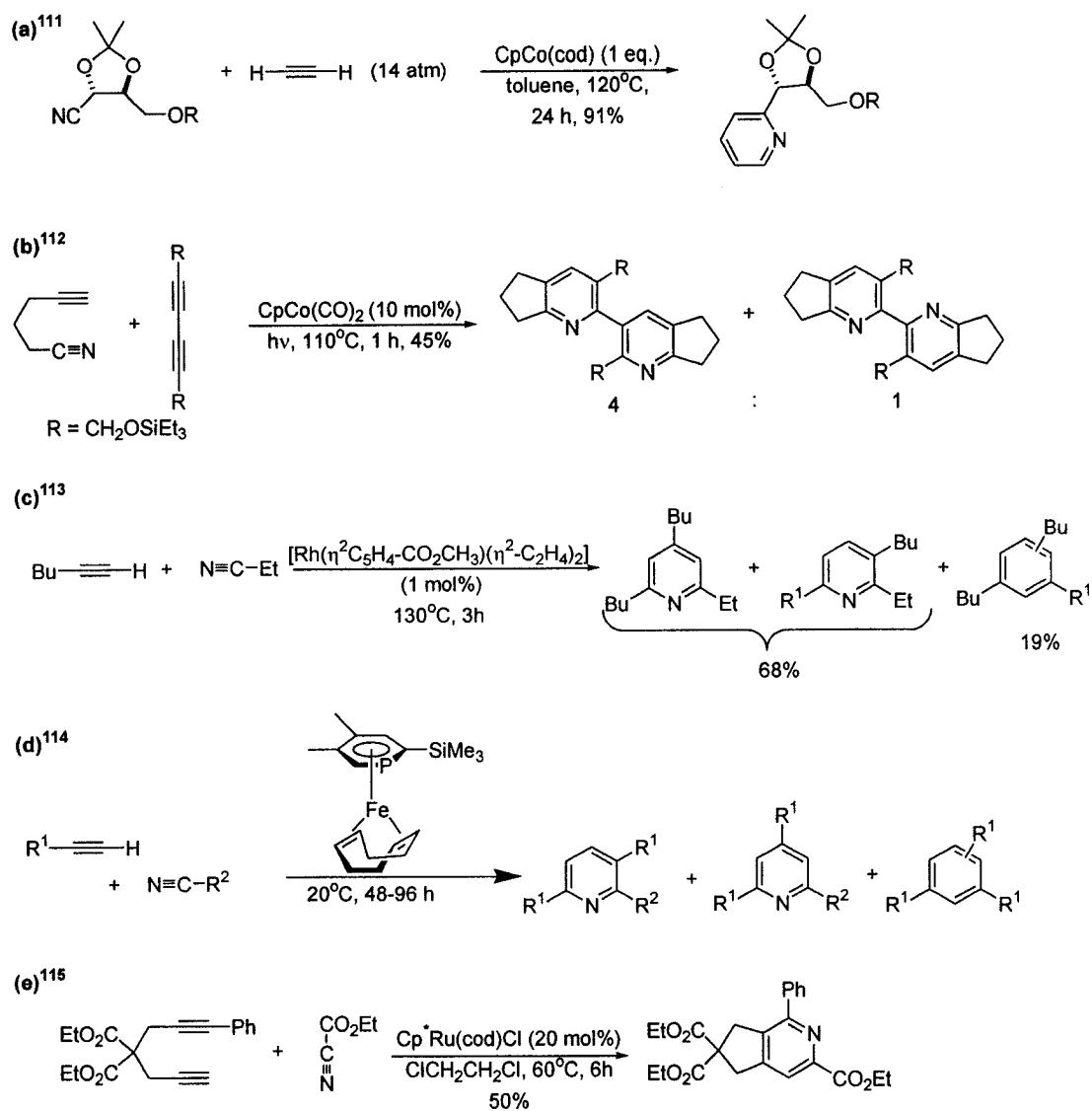


Figure 1.31 Regio- and Chemoselective Cyclotrimerization of Three Different Alkynes

1.2.3.4 Incorporation of Heteroatoms into the Cyclotrimerization Reaction

In addition to forming multisubstituted benzenes, cyclotrimerization reactions can also generate heteroaromatic compounds.¹⁰⁹ For example, pyridines can be prepared via a metal catalyzed [2+2+2] cycloaddition reaction of two alkynes and a nitrile.¹¹⁰ It is generally found that most catalysts capable of facilitating the cyclotrimerization of alkynes are also competent in promoting the formation of pyridines. Considering this, a large number of metal catalysts are able to effect this [2+2+2] cycloaddition reaction. Some examples of these are shown in Scheme 1.7.¹¹¹⁻¹¹⁵



Scheme 1.7 Formation of Substituted Pyridines

In addition to the examples cited above, a cobalt catalyst has also been employed to effect a [2+2+2] cycloaddition between acetylene and acrylonitrile to generate 2-vinylpyridine **1.58** (62% yield) on an industrial scale (Figure 1.32).¹¹⁶

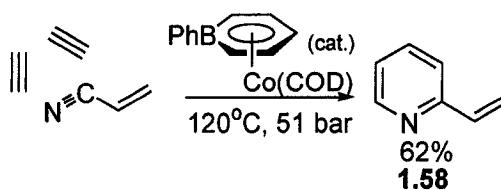


Figure 1.32 Generation of 2-Vinylpyridine

The formation of pyridines from alkynes and a nitrile is mechanistically similar to the cyclotrimerization of three alkynes (Figure 1.23). The reaction generally requires a 2:1 alkyne to nitrile ratio; however, considering that nitriles do not readily undergo cyclotrimerization, the lesser amount of this reactant in comparison to the alkyne is not a serious impediment.¹¹⁰ The initial reaction step involves metallacyclopentadiene **1.60** formation, which increases the metal oxidation state by two and favours nitrile binding over alkyne coordination. This presumably accounts for the selectivity seen for pyridine formation over substituted benzene generation. Following nitrile insertion, the intermediate metallacycloheptatriene **1.61** is formed, which can undergo reductive elimination to yield the pyridine **1.62**.

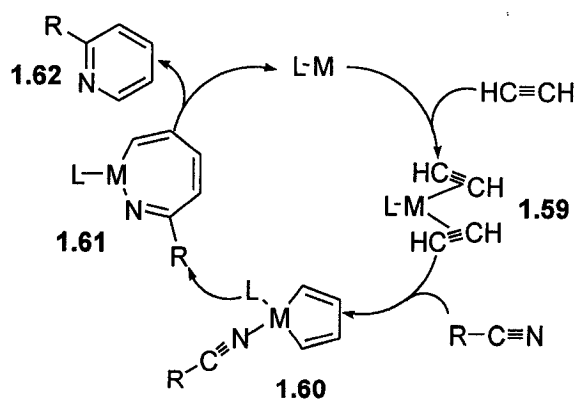
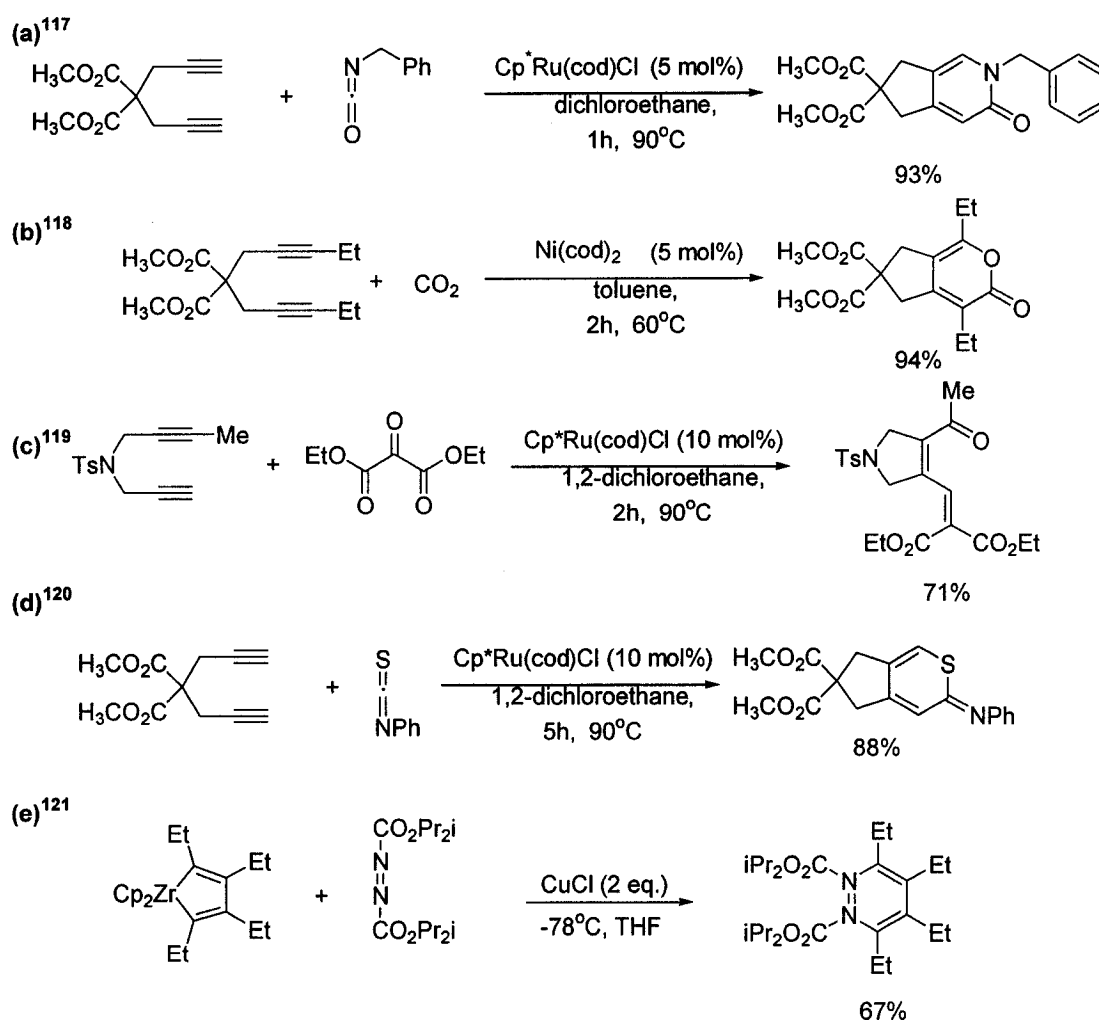


Figure 1.33 Mechanism for Pyridine Synthesis

In addition to constructing multisubstituted pyridines, the cyclotrimerization reaction has also enabled the incorporation of other heteroatomic monomers in the cyclotrimerization process, including isocyanates,¹¹⁷ carbon dioxide,¹¹⁸ ketomalonates,¹¹⁹ isothiocyanates,¹²⁰ and carbodiimides (Scheme 1.8).¹²¹ This has further cemented the importance of [2+2+2] cyclotrimerization processes in the preparation of heteroaromatic molecules.



Scheme 1.8 Cyclotrimerization of Other Heteroatom Containing Compounds

1.2.3.5 Synthetic Applications of Transition Metal Catalyzed Cyclotrimerization Reactions

Considering the utility of cyclotrimerization reactions in facilitating generation of multisubstituted benzenes, this methodology has been exploited to prepare many complex molecules and natural products. Several reviews on this topic have been written and are very comprehensive.¹²² One example that illustrates the significant utility of [2+2+2] cycloadditions involves the preparation of the steroidal derivative, estrone (Figure 1.34).¹²³ This reaction initially forms benzocyclobutane **1.63**, which can be cleaved thermally to generate a diene, that can subsequently undergo a Diels-Alder reaction to provide the steroid **1.64**. Further elaboration enabled the preparation of estrone (Figure 1.34).

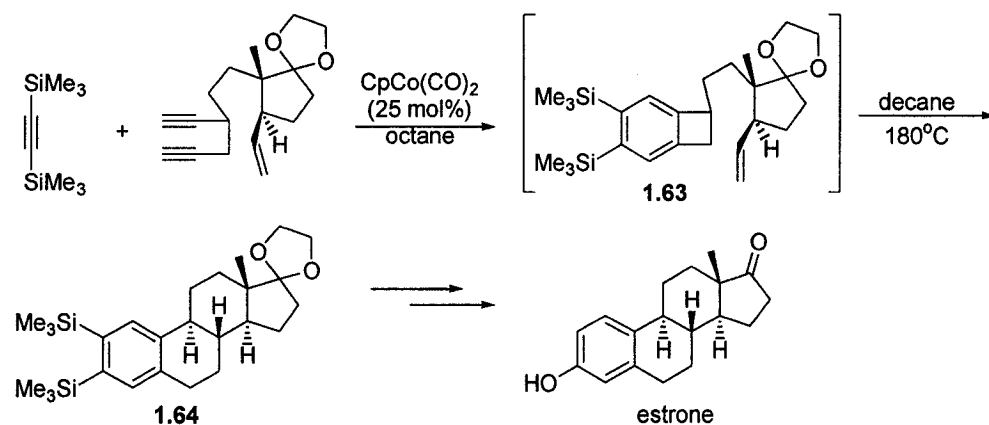
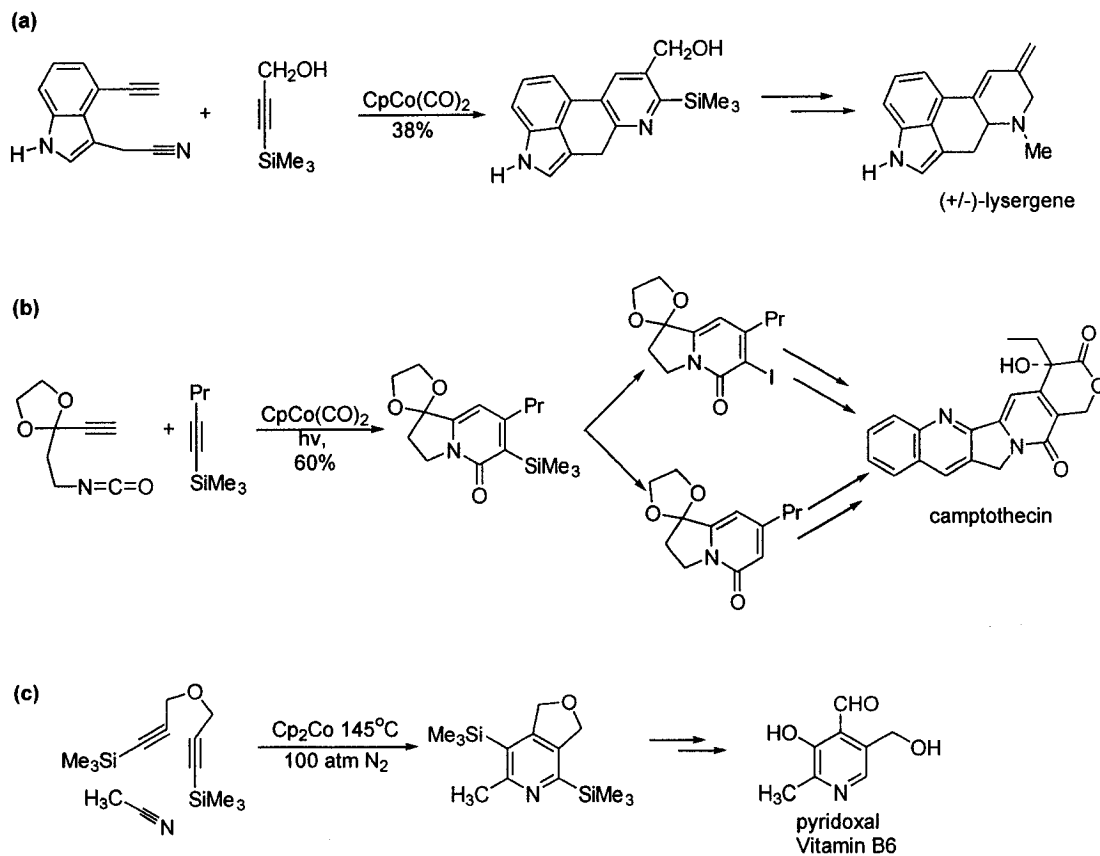


Figure 1.34 Generation of Estrone

In addition to the cyclotrimerization processes that generate arene rings, this reaction has also been employed to prepare various natural products that contain

heteroaromatic functionality. Some illustrative examples include (\pm)-lysergine (Scheme 1.9a),¹²⁴ and camptothecin (Scheme 1.9b),¹²⁵ and pyridoxal (Vitamin B6) (Scheme 1.9c).¹²⁶



Scheme 1.9 Utilization of Cyclotrimerization Reactions in Total Synthesis

1.2.4 The Wakamatsu Reaction: Amidocarbonylation

One of the more important products from an industrial and pharmaceutical perspective are α -amino acids.¹²⁷ These products are not only extensively utilized in the preparation of detergents, lubricating agents, and chelating agents, but are also constituents of peptides and proteins.¹²⁷ Many α -amino acid syntheses exist, including the Strecker reaction, which generates these compounds from HCN, NH₃ and aldehydes.¹⁴ Considering the acute toxicity of HCN, other approaches to form these products on an industrial scale have been developed. Perhaps the best known of these is amidocarbonylation.¹²⁸ This multicomponent coupling process, which utilizes catalytic Co₂(CO)₈, couples aldehydes **1.65**, amides **1.66**, and CO to form *N*-acyl- α -amino acids **1.67** (Figure 1.35).¹²⁹

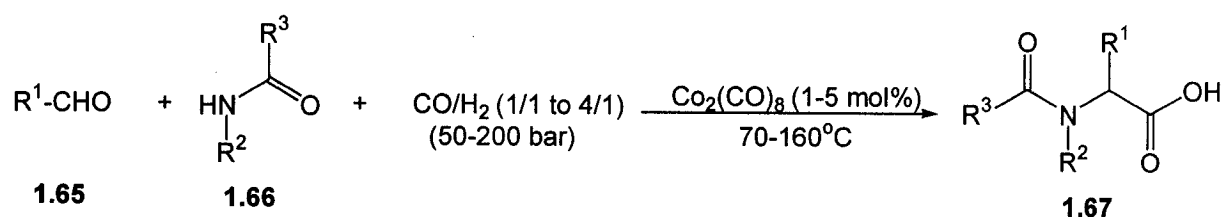


Figure 1.35 Cobalt Catalyzed Amidocarbonylation

In order to better understand how the various reaction components are assembled, mechanistic postulates have been developed. The reaction is thought to proceed through the initial nucleophilic attack of an amide on the aldehyde to form an *N*-acyl- α -hydroxyalkyl amide **1.68** (Figure 1.36).¹³⁰ When protonated, the hydroxyamide **1.69** reacts with the *in situ* generated tetracobaltate anion to form **1.70**. Subsequent

CO insertion furnishes intermediate **1.71**, which can undergo hydrolytic cleavage to form *N*-acyl amino acid **1.72**. The reaction is generally conducted under high pressures of H₂ and CO (50-200 bar) and at temperatures between 70-160°C.

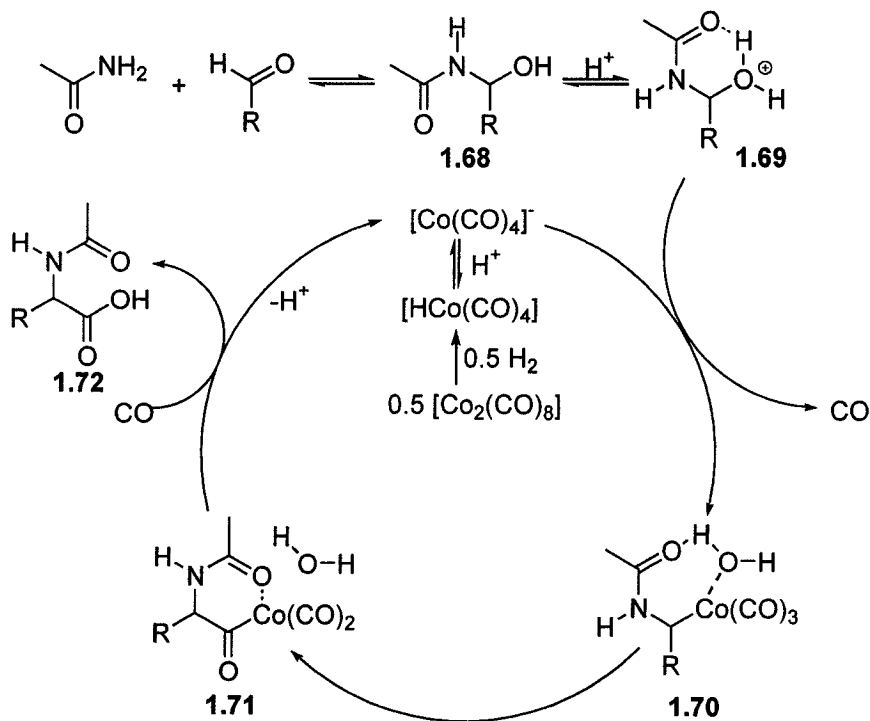
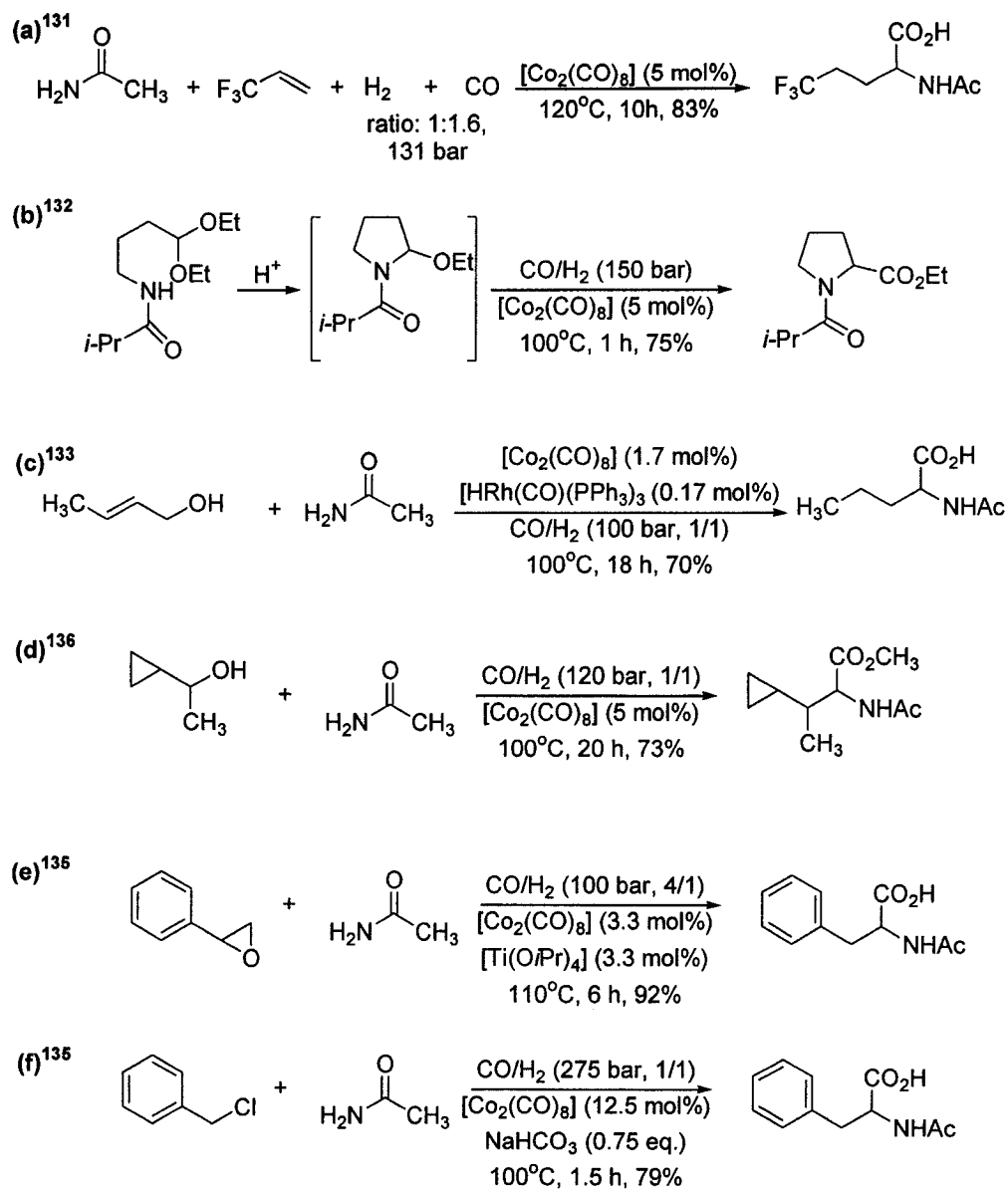


Figure 1.36 Postulated Mechanism for Co₂(CO)₈ Catalyzed Amidocarbonylation

In addition to aldehydes, olefins,¹³¹ acetals,¹³² allyl alcohols,¹³³ alcohols,¹³⁴ epoxides,¹³⁵ and benzyl chloride¹³⁶ are also competent substrates for the Co₂(CO)₈ catalyzed amidocarbonylation reaction (Scheme 1.10). Although some success has been obtained with these precursors, aldehydes remain the starting material of choice. Competent aldehyde substrates for cobalt catalysis are formaldehyde and those aldehydes with at least a single α -hydrogen atom.



Scheme 1.10 Other Substrates for Amidocarbonylation

1.2.4.1 Palladium Catalyzed Amidocarbonylation

Considering the requisite harsh conditions, poor selectivity, and limited catalyst activity of the cobalt catalyzed amidocarbonylation, new metal catalysts have been developed.^{43a} Of these, palladium complexes are found to be the best alternative to the originally developed $\text{Co}_2(\text{CO})_8$.^{43a} In addition to being 10-100 times more reactive than the cobalt system, the palladium catalyzed processes are found to have a greater reaction scope. Furthermore, palladium catalyzed reactions require much milder conditions (70-130°C and CO (10-60 bar)) when compared to cobalt catalyzed processes (70-160°C and H_2/CO (50-200 bar)). Moreover, optimal catalyst turnover numbers of up to 60,000 can be realized, as demonstrated in the synthesis of *N*-acetylleucine **1.75** (Figure 1.37).^{137c}

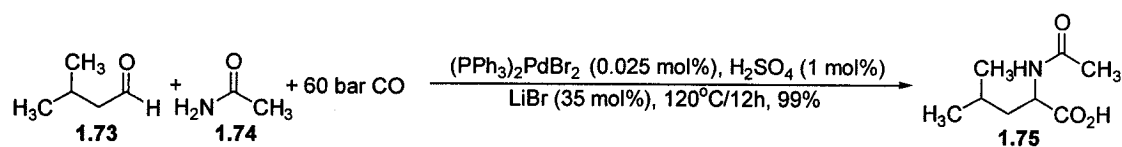


Figure 1.37 Palladium Catalyzed Amidocarbonylation: Synthesis of *N*-Acetylleucine

The mechanism of amidocarbonylation with a palladium catalyst is similar to that of the cobalt variant; however, a few key differences exist. In addition to utilizing different metals, the palladium catalyzed reaction requires halide additives (LiBr or Bu_4NBr) as well as catalytic amounts of H_2SO_4 . In fact, without these halide co-catalysts, the starting materials are not converted to final product.^{137b} It is postulated that in the presence of halide salts and a strong acid, *N*- α -hydroxyamide **1.76** can

exist as α -haloamide **1.77**, or as the corresponding ion pair **1.78** (Figure 1.38). The latter two species are thought to be the active oxidative addition substrates. Acceptable catalyst precursors for the oxidative addition include both Pd (0) sources (ie. $[\text{Pd}_2(\text{dba})_3]$ and $[\text{Pd}(\text{PPh}_3)_4]$ and Pd (II) sources (eg. PdBr_2 and $[\text{Pd}(\text{OAc})_2]$); however, the catalytically active species is Pd(0). This complex can oxidatively add to the C-Br bond to form **1.79**, which can subsequently coordinate and presumably insert CO to generate **1.80**. Hydrolysis of this intermediate finally yields the *N*-acyl amino acid **1.82**. The possible intermediacy of an oxazolone species **1.81** in this reaction, however, cannot be ruled out (Figure 1.38).^{43a} The presence of phosphine ligands in catalysis is thought to stabilize the palladium (0) center, and is not believed to be vital in the oxidative addition step. In addition, the high pressures utilized in this reaction are thought to be necessary to ensure rapid CO insertion.^{43a}

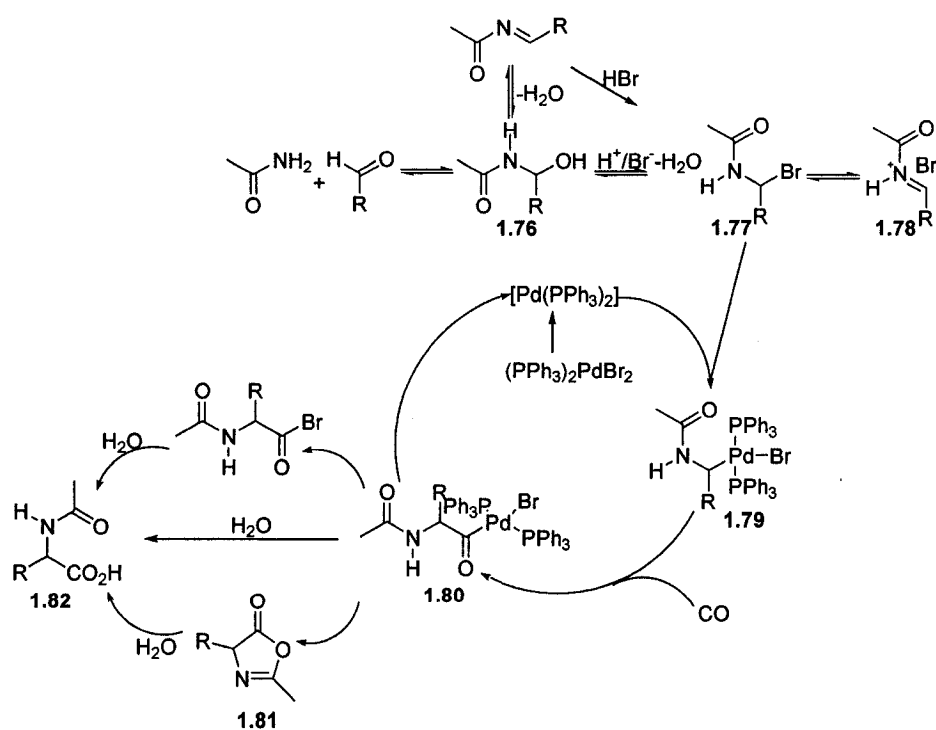


Figure 1.38 Postulated Mechanism for Palladium Catalyzed Amidocarbonylation

In addition to the Pd(0) and Pd(II) catalysts described previously, this reaction has also been developed utilizing a heterogeneous source: palladium on charcoal. This palladium source is considered to be the method of choice to effect this transformation, as product isolation is greatly facilitated in the absence of phosphine ligands.^{137g} In addition, amidocarbonylation has also been achieved utilizing a range of other metal catalysts including those of platinum (K_2PtCl_4/PPh_3)¹³⁸ rhodium ($[Rh(OAc)_2]_2$),¹³⁹ iridium ($[IrCl(COD)]_2$ and $[Ir(CO)Cl(PPh_3)_2]$) and ruthenium ($[RuCl_2(PPh_3)_3]$ and $[RuCl_3]$),¹³⁹ although product yields for these processes are typically low.

1.2.4.2 Generation of α -Amino Acids via Amidocarbonylation

Considering the prevalence of *N*-acyl- α -aryl glycines in a range of biologically active compounds, methods for their generation are of significant interest.¹²⁷ As mentioned previously, aldehydes devoid of α -hydrogens are not viable substrates for cobalt catalyzed amidocarbonylation. These include carbohydrate aldehydes, indole aldehydes, certain arylacetaldehydes and iodo- or bromo-substituted aldehydes. In addition, neither cobalt nor palladium based catalysts can effectively prepare α -quaternary amino acids, which could be accomplished by utilizing ketones as amidocarbonylation substrates. However, palladium catalysts can readily convert amides, CO, and aldehydes, with and without α -hydrogens, into α -amino acid derivatives in excellent yields (Figure 1.39). Furthermore, optically active

arylglycines can be generated from the products of amidocarbonylation through enantioselective enzymatic hydrolysis, by utilizing acylases.^{137d}

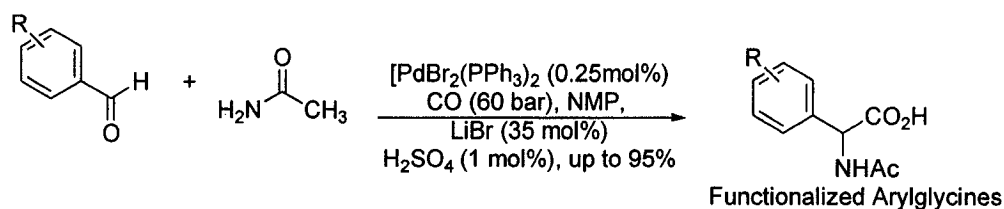


Figure 1.39 Palladium Catalyzed Amidocarbonylation

Considering that aldehydes and carbon monoxide are both inexpensive and readily available, amidocarbonylation is potentially of great utility in industrial processes. However, the significant impediment towards greater industrial utilization of this process is the expense of the amide component: acetamide. This issue is being addressed through the *in situ* generation of amides from nitriles and subsequent amidocarbonylation in the same reaction vessel.¹³⁶ Although this methodology is not completely developed, certain *N*-acyl amino acids can be prepared in good yields.

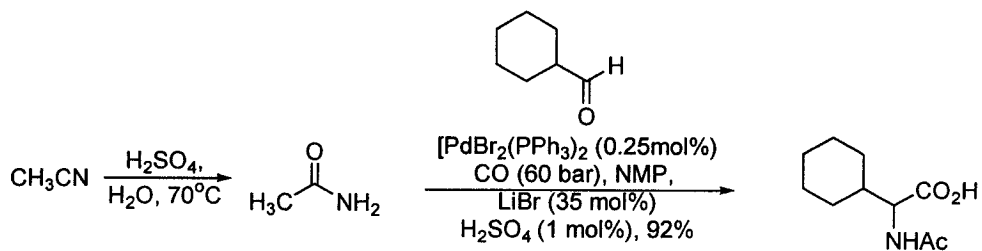
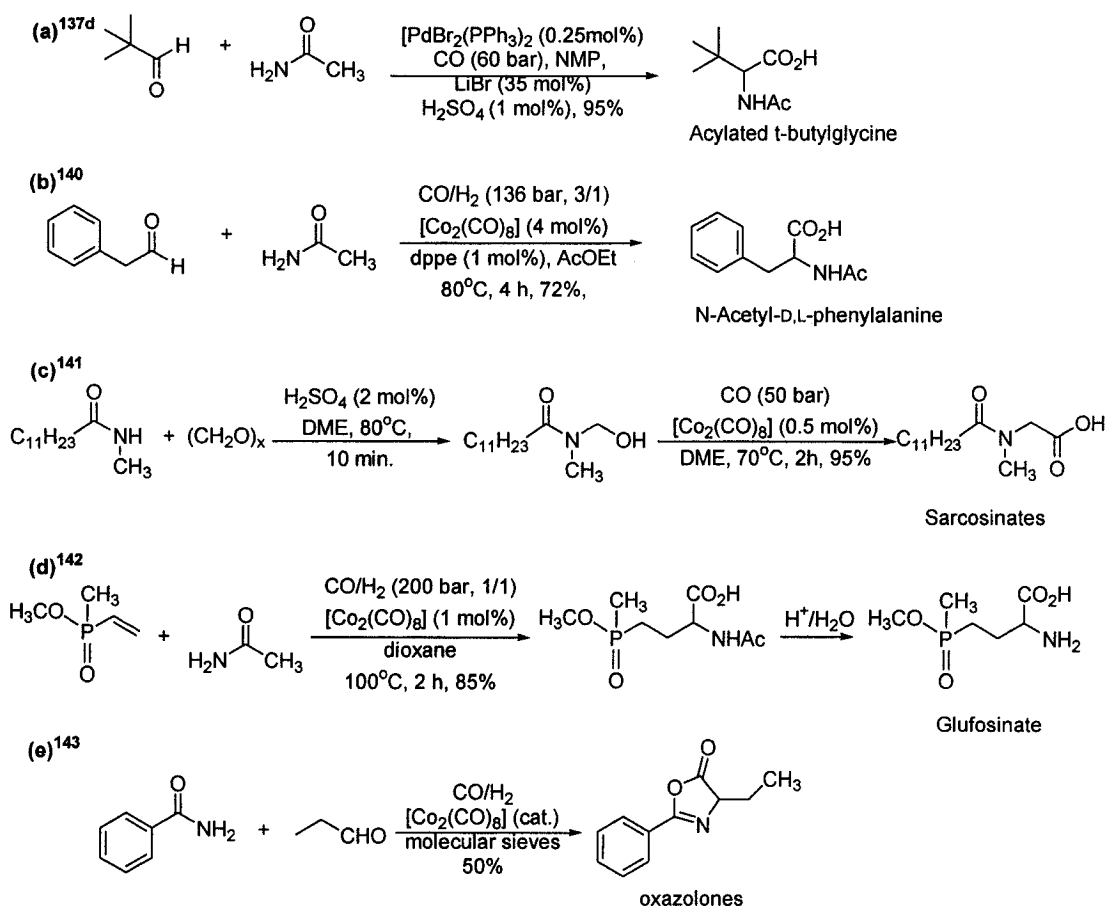


Figure 1.40 Amidocarbonylation with Nitriles

1.2.4.3 Synthetic Applications of Amidocarbonylation

Amidocarbonylation has been used to prepare a range of useful α -amino acid derivatives. These include *N*-acetyl-D,L-phenylalanine, which is a key intermediate in the synthesis of aspartame (Scheme 1.11b).¹⁴⁰ In addition, sarcosinates, which are used as component of emulsifiers, soaps, and surfactants, can be constructed through the use of amidocarbonylation (Scheme 1.11c)¹⁴¹ as can glufosinate, a naturally occurring herbicide (Scheme 1.11d).¹⁴² Furthermore, and of special significance to this thesis, is the generation of oxazolones, which can be prepared by conducting amidocarbonylation in the presence of molecular sieves (Scheme 1.11e).¹⁴³



Scheme 1.11 Synthetic Applications of Amidocarbonylation

In addition to the preparation of *N*-acyl α -amino acids,^{137d} and other industrially relevant compounds, amidocarbonylation has also been extended to multicomponent coupling reactions that generate hydantoins **1.83** (Figure 1.41).^{137b} These products, which are generally prepared through the Bucherer-Bergs reaction,¹⁹ are formed by a mechanism similar to that shown in Figure 1.38.¹⁴⁴ The utilization of amidocarbonylation chemistry to develop routes to other important pharmaceutically and industrially important molecules is an area with significant potential.

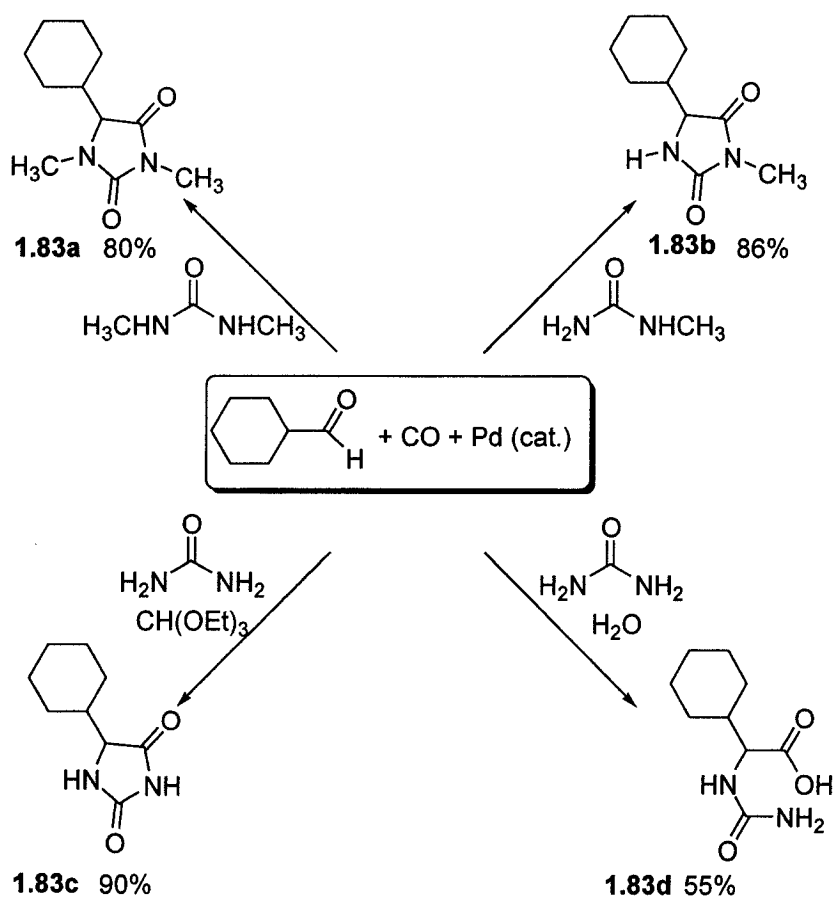


Figure 1.41 Palladium Catalyzed Ureidocarbonylation

Part II: Münchnone Generation and Reactivity

1.3 Introduction to Münchnones

Mesoionic heterocycles are among the more useful and versatile synthetic intermediates known.¹⁴⁵ This family of compounds includes 1,3-oxazolium-5-oxides (Münchnones) **1.84**, 1,3-oxazolium-4-oxides (isomünchnones) **1.85**, 1,2,3-oxadiazolium-5-oxides (Sydnones) **1.86**, 1,3-oxathiolium-5-oxides (thiomünchnones) **1.87** and 1,3-thiazolium-4-oxides (thioisomünchnones) **1.88** (Figure 1.42). Of these, Münchnones are perhaps the most synthetically useful as they enable the generation of a broad range of compounds including pyrroles, imidazoles, oxazoles, amino acids, imidazoles and β -lactams.¹⁴⁵

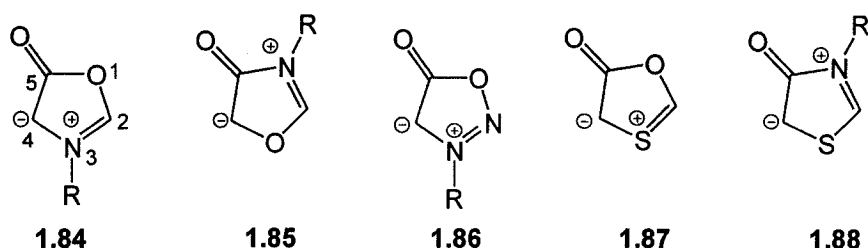


Figure 1.42 Examples of Mesoionic Oxazoles

The broader understanding of Münchnone reactivity and utility in synthesis is primarily due to the extensive studies conducted by Rolf Hüisgen during the late 1960's and early 1970's.¹⁴⁶ Hüisgen was the first to show that Münchnones have cyclic and acyclic valence tautomeric forms. In their cyclic form, they undergo 1,3-dipolar cycloaddition reactions with certain unsaturated species to construct 5-

membered nitrogen containing heterocycles, while in their acyclic form they react with ketenophiles to generate β -lactams and amino acid-based products (Figure 1.43).¹⁴⁶ Interestingly, 1,3-oxazolium-5-oxides were named Münchnones in honour of Munich, Germany. This was a witty retort to scientists in Sydney, Australia, who named a similar class of molecules “Sydnones.”

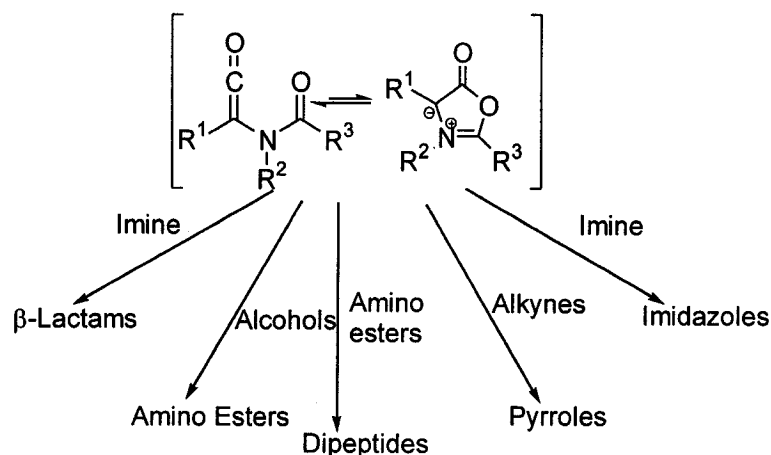


Figure 1.43 Some of the Products Available from Münchnone Intermediates

This brief review will address several aspects of Münchnone chemistry, including routes for their preparation, their reactivity, and their utility in pharmaceutical development. In addition, a theoretical basis for the regioselectivity obtained in 1,3-dipolar cycloadditions of Münchnones with alkynes in pyrrole synthesis will also be discussed.

1.3.1.1 Münchnone Generation: Traditional Routes

Münchnones **1.90** are typically prepared by acetic anhydride mediated dehydration of *N*-acylamino acids **1.89**. This method was extensively employed by Hüisgen in his

development of 1,3-dipolar cycloaddition chemistry, and is still considered the method of choice for generating these mesoionic heterocycles.¹⁴⁶

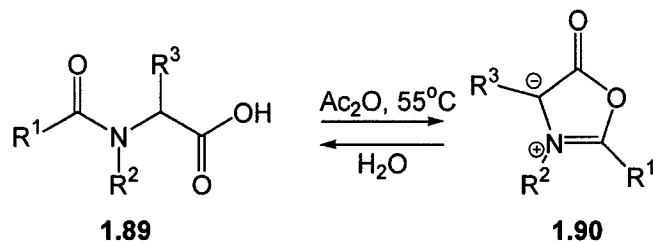


Figure 1.44 Generation of Münchnones (Hüisgen)

Other methods of generating these compounds utilize dehydrating agents such as, SiCl_4 ,¹⁴⁷ dicyclohexylcarbodiimide (DCC),¹⁴⁸ and 1-(3-dimethylaminopropyl)-3-ethylcarbodiimide (EDC).¹⁴⁷ The latter two reagents form urea byproducts following dehydration, which in the case of DCC is very difficult to remove. In addition to the preparation of *N*-alkyl or *N*-aryl Münchnones, *N*-acyl variants **1.92** can also be generated by the simultaneous acylation-desilylation sequence of 5-silyloxyoxazoles **1.91**. The addition of acid chloride initially forms *N*-acyloxazoles, which are readily converted to Münchnones under basic conditions (Figure 1.45).¹⁴⁹

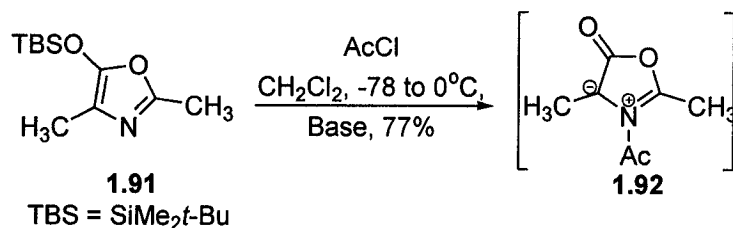


Figure 1.45 Generation of *N*-Acyl Münchnones

In general, Münchnones are not isolated; instead, they are generated and trapped *in situ* with nucleophiles and dipolarophiles.¹⁵⁰ These mesoionic heterocycles are also hydrolytically unstable and rapidly revert to the parent *N*-acylamino acid in the presence of water **1.90** → **1.89** (Figure 1.44).¹⁵¹

1.3.1.2 Münchnone Generation: Utilization of Tetracarbonyl Ferrates

Metal-mediated processes for Münchnone generation have also been developed. Through reacting sodium acyltetracarbonylferrate **1.93** with imidoyl chlorides **1.94**, Münchnones **1.95** were prepared in moderate to good yields.¹⁵²

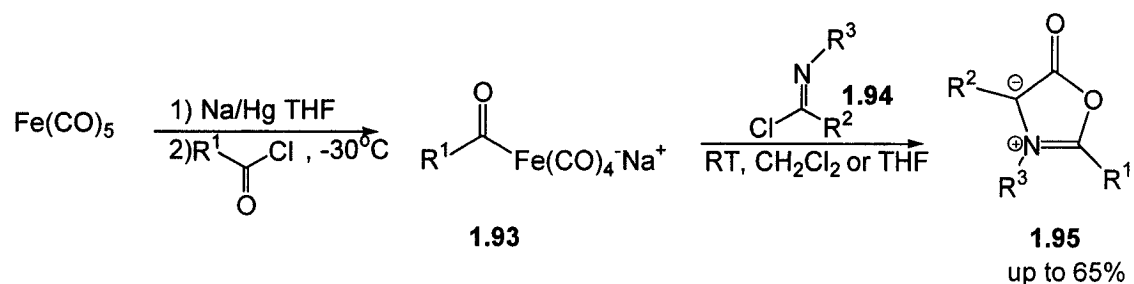


Figure 1.46 Generation of Münchnones from Acyltetracarbonylferrates

The mechanism of this reaction is believed to involve the initial displacement of the chloride from the imidoyl chloride **1.94** to generate **1.96** (Figure 1.47). This is followed by acyl migration from the iron center to the imidoyl chloride nitrogen, which forms “Fischer” carbene complex **1.97**. CO insertion, followed by amidoketene formation, finally yields the 1,3-oxazolium-5-oxide **1.95**. Although a range of different Münchnones can be generated utilizing this methodology, the substituents R^1 and R^2 are restricted to being aryl, while R^3 may be aryl or alkyl.

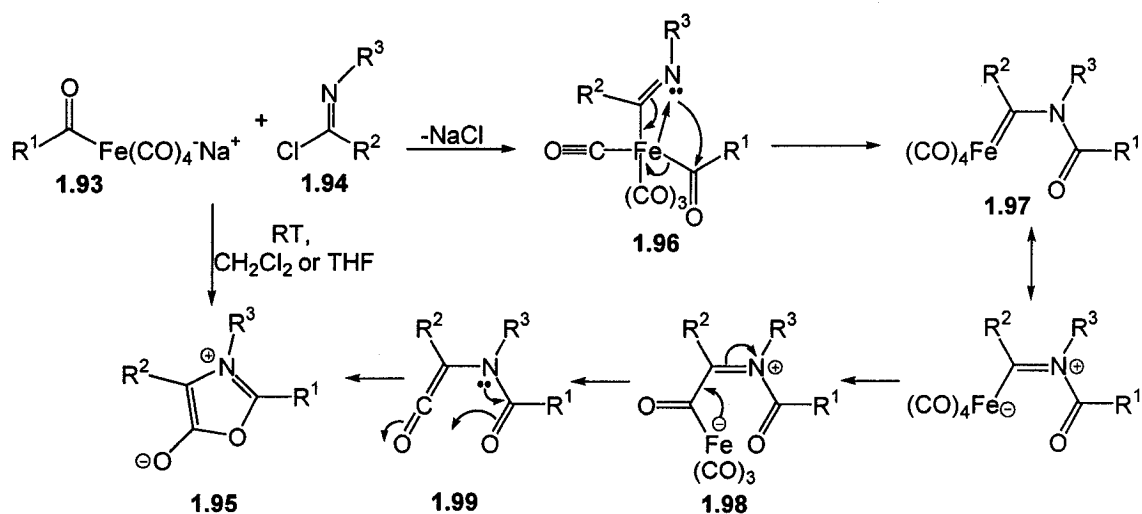


Figure 1.47 Proposed Mechanism for Münchnone Formation

1.3.1.2 Münchnone Generation: Utilization of Chromium Carbenes

As shown by the acyltetracarbonyl ferrate mediated generation of Münchnones, metal carbonyl complexes can readily incorporate carbonyl functionality into molecules. Another class of reagents that facilitate carbonylation are the “Fischer” chromium-carbene complexes (i.e. $(\text{CO})_5\text{Cr}=\text{C}(\text{R})(\text{R}')$, where $\text{R} = \text{OR}''$, NR_2).¹⁵³ These complexes have been utilized to prepare a large number of biologically active molecules, including Münchnones (Figure 1.48).^{153, 154} The chromium carbene mediated synthesis of Münchnones is postulated to proceed through CO insertion into the metal-carbon double bond of an *N*-acylaminochromium carbene complex **1.100** to generate ketene complex **1.101**. Subsequent cyclization results in the intermediate formation of Münchnone **1.104**, which can be trapped *in situ* to produce pyrroles **1.105** (see Section 1.3.5 for the formation of pyrroles).¹⁵⁴ Interestingly, thermal CO

insertions with heteroatom stabilized chromium carbene complexes are relatively unprecedented.¹⁵⁵ It is likely that the presence of an electron withdrawing acyl group on the carbene nitrogen sufficiently decreases the electron density at the carbene carbon and thus favours carbonyl insertion.¹⁵⁴ This communication reported the synthesis of only two Münchnones, so a true measure of the reaction scope is not known.

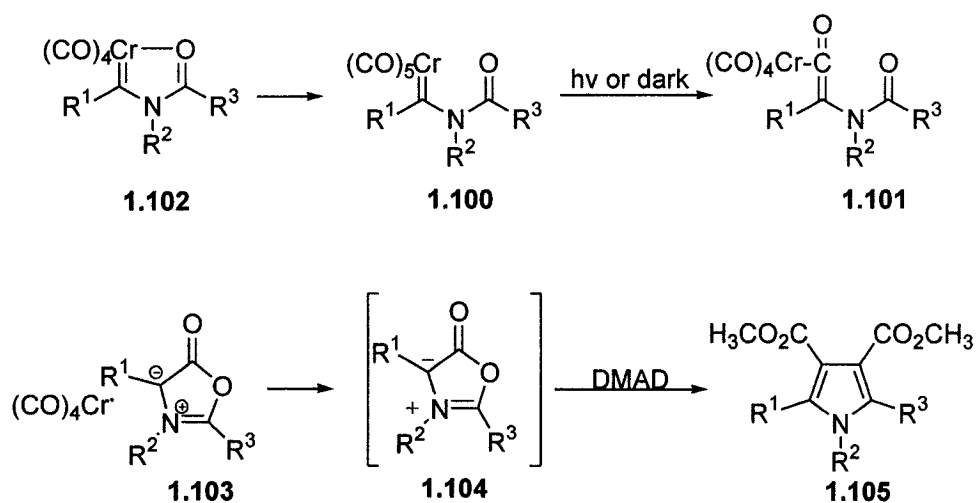


Figure 1.48 Generation of Münchnones from *N*-Acylaminochromium Carbenes

1.3.2 Structures of Münchnones

X-ray diffraction data determined that the true Münchnone structure was intermediate between resonance forms **1.106a** and **1.106b**, based on the intermediacy of the various bond lengths about this compound (Figure 1.49). This study unequivocally established the Münchnone as being a mesoionic in character.¹⁵⁶ This fact was also confirmed utilizing infrared spectroscopy, which showed the presence of a carbonyl

stretch between 1690-1700 cm^{-1} (KBr). This value is significantly different from that seen with the non-mesoionic azlactones **1.107**, which typically show a band at 1800-1820 cm^{-1} (Figure 1.49).¹⁵⁷

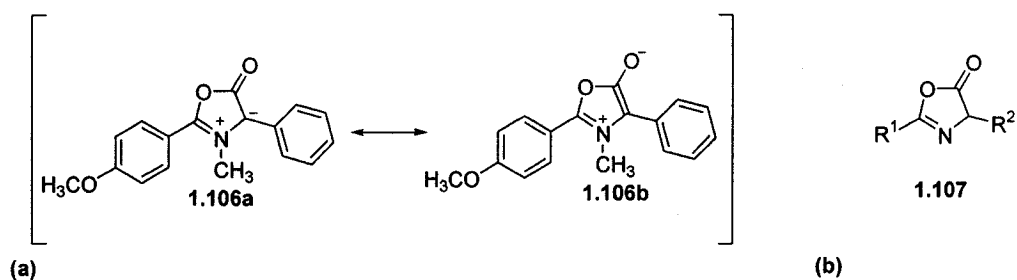


Figure 1.49 Structures of Münchnones **1.106**

As mentioned previously, Münchnones have both acyclic and cyclic tautomeric forms; however, they exist predominantly as the latter in solution.¹⁵⁸ Evidence for this unseen equilibrium was obtained by reactivity studies on the *N*-acyl Münchnone **1.109a**, formed through the addition of benzoyl chloride to 5-siloxyoxazoles **1.108**.¹⁵⁹ DMAD was subsequently added to this mixture, which enabled isolation of two different pyrrole products, **1.111** and **1.112** (See Section 1.3.5). This reaction outcome was attributed to *N*-acyl Münchnone **1.109a** tautomerizing through Münchnone **1.110**, presumably through ketene intermediate **1.109b**.¹⁵⁹

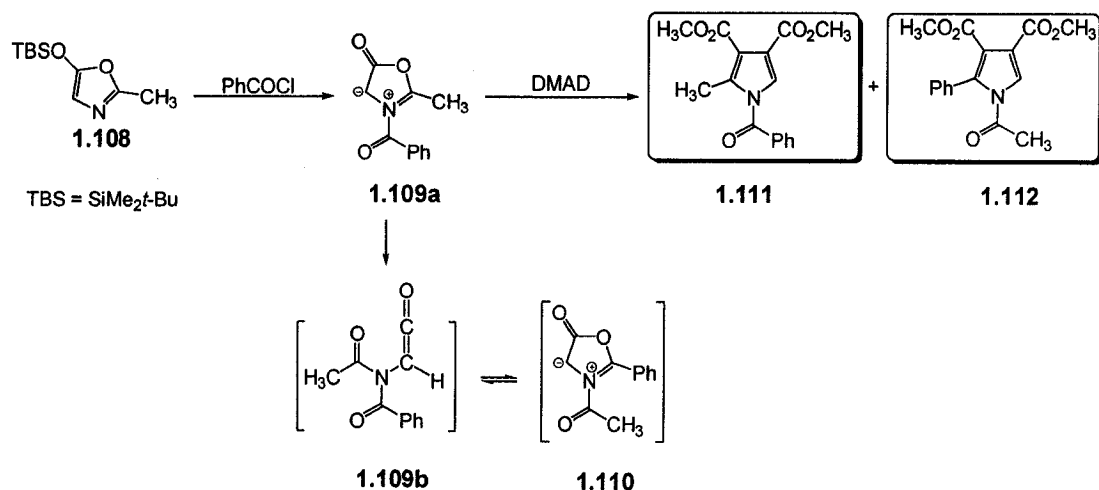


Figure 1.50 Ketene Tautomerization of Münchnones

1.3.3 Nucleophilic Additions to Münchnones: Generation of Peptide-based Products

Münchnones are known to readily react with nucleophiles such as water or alcohols to construct α -amino acid derivatives.¹⁴⁶ Considering that amino acids are also nucleophilic reagents, Münchnones can react with α -amino esters to generate dipeptides (Figure 1.51).¹⁴⁵ However, these products are racemic and asymmetric variants of this reaction have not as of yet been reported.

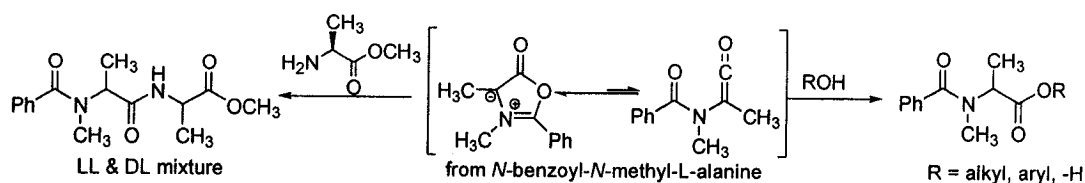


Figure 1.51 Generation of *N*-Acylamino Acid (derivatives) and Dipeptides from Münchnones

1.3.4 Imine Additions to Münchnones: Generation of β -Lactams

β -lactams are a useful class of molecules as they comprise the core structure of a range of antibiotics, including penicillin.¹⁶⁰ This class of molecules is traditionally prepared by reacting imines and ketenes, in a formal [2+2] cycloaddition reaction.¹⁶¹ Considering that Münchnones have a valence tautomeric ketene form, they are also competent precursors for β -lactam generation.¹⁶¹ In fact, β -lactams can be prepared by reacting imines with Münchnones in yields of up to 80%.^{146a,162}

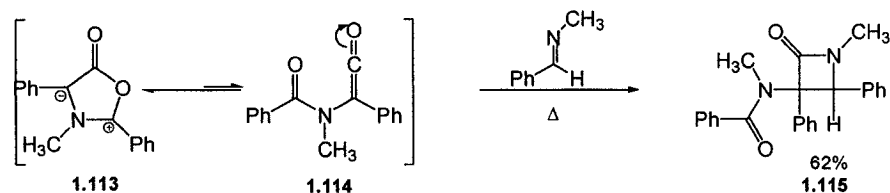


Figure 1.52 Synthesis of β -lactams from Münchnones and Imines^{146a}

1.3.5 1,3-Dipolar Cycloadditions: Generation of Pyrroles

The nucleophilic reactivity of Münchnones is useful; however, the greatest value of these synthetic intermediates stems from their propensity to undergo 1,3-dipolar cycloaddition reactions to generate nitrogen-based heterocycles. The most commonly utilized reaction of this type constructs pyrroles via the initial [3+2] cyclization of the mesoionic oxazole **1.116** with an alkyne dipolarophile (Figure 1.53) to form adduct **1.117**. This intermediate, which is isolable in only specific cases,¹⁶³ undergoes a cycloreversion to eliminate CO₂ and can subsequently aromatize to furnish pyrroles

1.118 and **1.119**. These products are generated in yields dependent upon the steric and electronic properties of the dipole and dipolarophile.

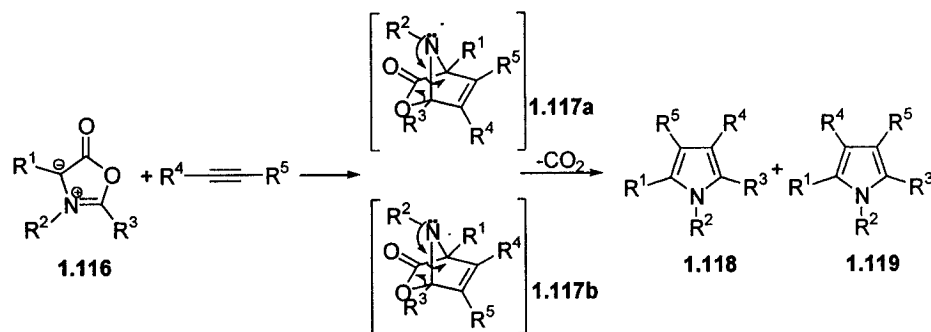


Figure 1.53 Mechanism of Pyrrole Formation

The electronic nature of the alkyne is critical for the rate of 1,3-dipolar cycloaddition reaction. Münchnones are found to react most readily with alkynes bearing electron-withdrawing substituents directly bound to the acetylenic carbon. These so-called strong dipolarophiles (e.g. dimethylacetylene dicarboxylate (DMAD), methyl propiolate and arylsulfonyl alkynes) typically react with Münchnones at room temperature. Unactivated alkynes, such as phenylacetylene, diphenylacetylene, 1-octyne, and 1-hexyne, react much more slowly at elevated temperatures and typically give poorer yields. The acetylenic dipolarophiles can generally be employed in excess in order to trap the Münchnone, provided that the initial product generated is not capable of reacting with further equivalents of the alkyne.^{145b}

As shown in Figure 1.53, the reaction of Münchnones with alkynes can generate two isomeric pyrrole structures when R¹ ≠ R³ and R⁴ ≠ R⁵. In such cases, mixtures of pyrroles are often obtained. One of the most thorough mechanistic studies on this

process was described by Coppola and co-workers.¹⁶⁴ These authors found that the regioselectivity of cyclization is complex, and the final product outcome involves several competing factors, both steric and electronic. In fact, a recent review on the selectivity of 1,3-dipolar cycloaddition reactions stated that: “No single criterion can successfully be used to correlate the experimental observations regarding regioselectivity in Münchnone cycloaddition reactions.”¹⁶⁴ As with other cycloaddition reactions, molecular orbital theory has been utilized to rationalize the product distributions that are obtained. The propensity of alkynes to undergo 1,3-dipolar cycloadditions can be understood by considering the frontier molecular orbitals (FMO) of the two reacting species. The orbitals suspected of being involved in the reaction are the HOMO (highest occupied molecular orbital) on the dipole (Münchnone) and the LUMO (lowest unoccupied molecular orbital) on the alkyne dipolarophile. Sufficient overlap of the orbitals in question permits the formation of the primary adduct, which can subsequently eliminate CO₂ to form the pyrrole.¹⁶⁵ However, non-covalent interactions (steric) may potentially be of greater importance in determining the regiochemistry of the cycloaddition process.¹⁶⁴

Factors influencing the regiochemical outcome of 1,3-dipolar cycloaddition reactions can be somewhat complex; however, certain trends exist. Several examples will best illustrate the potential outcomes of the reaction. In order to demonstrate the electronic effect of substituents on the 2 and 4 positions of this mesoionic heterocycle, the reactivity of two regioisomeric Münchnones has been examined (**1.121** and **1.123**) (Figure 1.54). This study showed that the same ratio of pyrrole

regioisomers (**1.124** and **1.125**) is obtained regardless of the Münchnones used (**1.121** and **1.123**). In addition, the most crowded product **1.124** was formed in higher yields. Typically, when one of the substituents at the 2 or 4 positions on the Münchnone is a hydrogen, the pyrrole distribution favours the more crowded regioisomer in a 3-4.1 : 1 ratio. This is postulated to occur due to the presence of an unsymmetrical transition state in the approach of the alkyne to the 1,3-dipole (Figure 1.55). This favoured approach results in bond formation between the β -carbon of the alkyne with the least sterically encumbered position of the Münchnone, thereby generating the more sterically hindered compound.¹⁶⁴

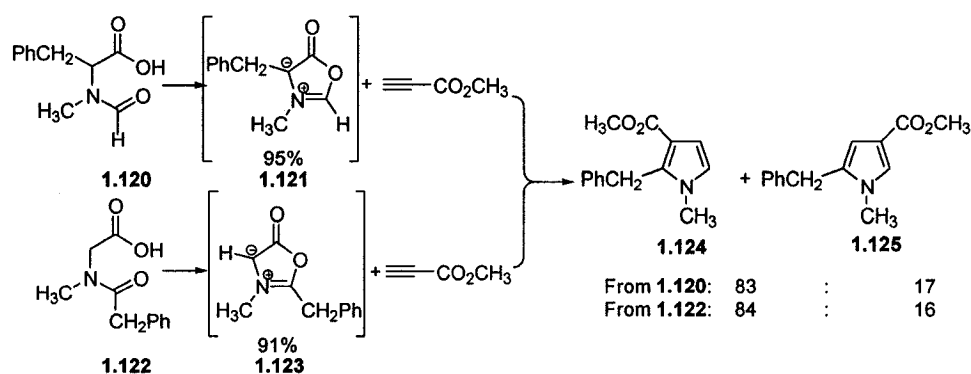


Figure 1.54 Electronic Effects on 1,3-Dipolar Cycloaddition Reactions

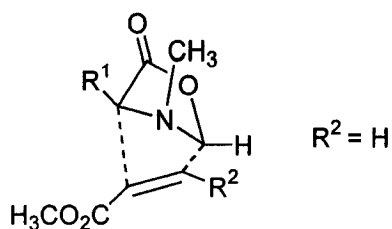


Figure 1.55 Proposed Unsymmetrical Transition State for Pyrrole Formation

In order to establish the potential existence of an inherent electronic bias in 1,3-oxazolium-5-oxides, many studies have been conducted. However, most of these studies have not employed substituents at the 2 and 4 positions of the Münchnone that are assumed to be electronically equivalent. Coppola and co-workers were the first to observe the absence of an inherent electronic bias by utilizing labeling experiments.¹⁶⁴ In order to completely eliminate the possibility of a substitution-induced electronic bias, a symmetrical Münchnone with methyl groups on the 2 and 4 positions was prepared. However, one of the methyl groups was ¹³C-labeled, while the other was not. Considering that these two substituents on the Münchnone are essentially electronically equivalent, differential pyrrole product formation ratios would be directly attributable to the electronic properties of the dipole. The experiment resulted in the formation of nearly 1:1 product mixtures, which suggests that only a small intrinsic bias exists in the 1,3-dipole of Münchnones.¹⁶⁴

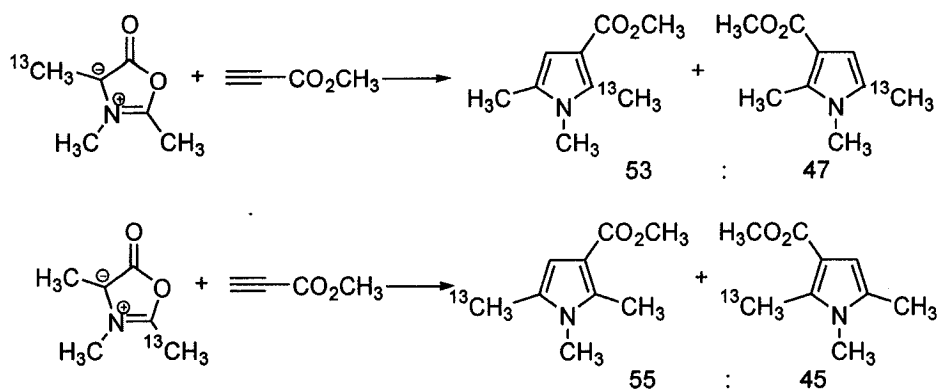


Figure 1.56 Product Compositions Following Reaction with Methyl Propiolate

In order to determine the role of steric interactions in effecting product distribution, a series of phenylthio/hydrogen-substituted Münchnones were prepared and reacted with dipolarophiles of differing steric bulk. Eclipsing interactions between the dipole and the approaching dipolarophile, as seen in Figure 1.55 ($R^2 = \text{H}, \text{CH}_3,$ or Ph), were found to be of paramount importance in the reaction outcome. These studies determined that the approach of the alkyne to the 1,3-dipole favours joining the two least sterically encumbered positions with methyl propiolate, but this bias decreases dramatically as the substituent on the 3-position of the alkyne increases in size (Figure 1.57).¹⁶⁴

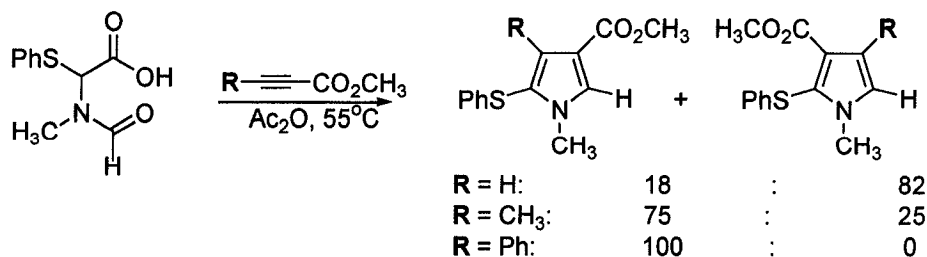


Figure 1.57 Product Distribution as a Function of Dipole Sterics

When alkyl groups are on both the 2 and 4 positions, the trend favours product formation that results in the least crowded isomer. No patterns concerning the level of regiochemistry obtainable with unsymmetrical alkyl/aryl substituted Münchnones (i.e. **1.127**, Figure 1.58) at the 2 and 4 positions have been established; however, several examples suggest that this result is relatively unpredictable. This uncertainty in product ratios is best exemplified by a report which showed that different regioisomeric ratios are realized for two, arguably electronically similar alkynes (**1.128** and **1.129**) (Figure 1.58).¹⁶⁶

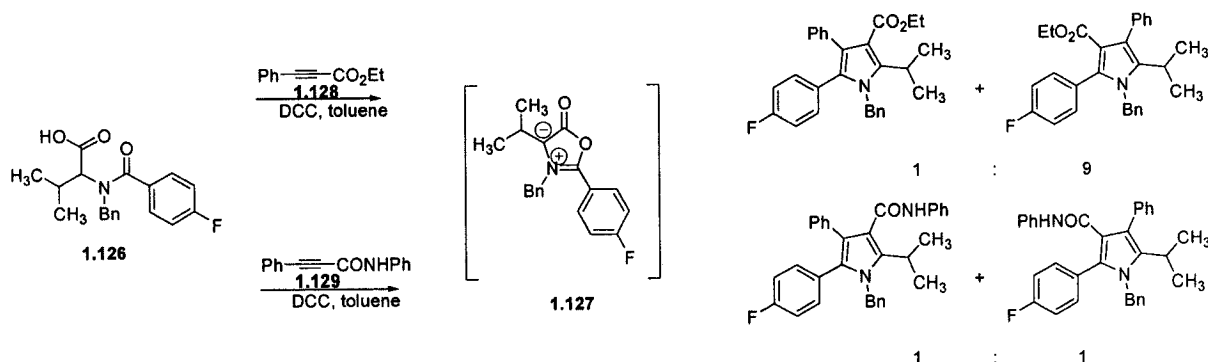


Figure 1.58 Unexpected Behaviour in Dipolar Cycloadditions

1.3.6 Synthetic Applications of Münchnones in Pyrrole-based Pharmaceuticals

The pyrrole core is present in a variety of biologically active molecules, including Atorvastatin Calcium (Lipitor[®] **1.132**),¹⁶⁷ a multibillion dollar statin based inhibitor marketed by Pfizer[®]. In examining potential routes to generate this molecule, one method employed acetic anhydride to dehydrate the *N*-acylamino acid **1.130** (Figure

1.59). This resulted in the *in situ* generation and subsequent trapping of the Münchnone to generate **1.131**, as the sole regioisomer. This intermediate was further elaborated to generate Lipitor[®].

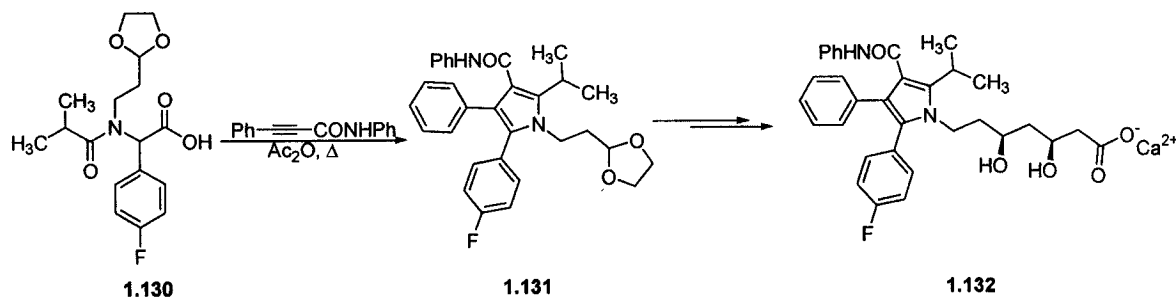


Figure 1.59 Generation of Lipitor from a Münchnone Intermediate.

In addition, Marion Merrell Dow Research utilized Münchnone chemistry to prepare the calcium channel activator FPL 64176, **1.135** (Figure 1.60).¹⁶⁸ Acetic anhydride was utilized as the dehydrating agent in the presence of alkyne **1.133**, to generate the pyrrole **1.134** in 49% yield. The protecting group on the pyrrole nitrogen was subsequently removed utilizing DBU.

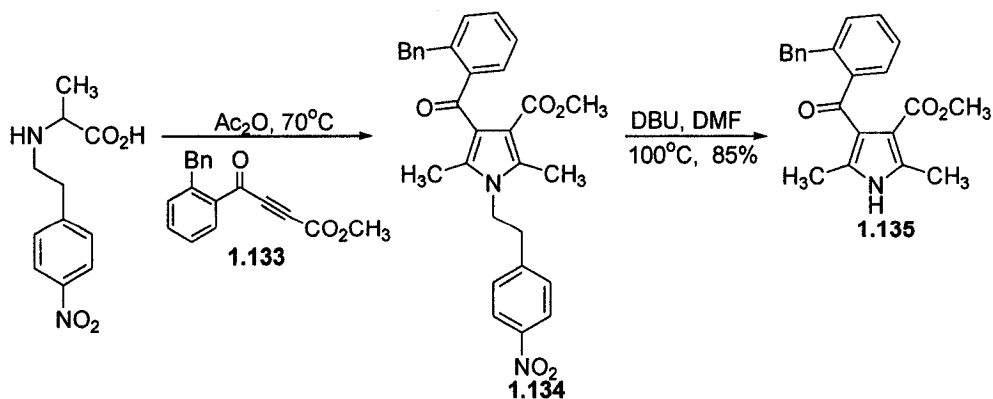


Figure 1.60 Synthesis of FPL 64176

GlaxoSmithKline has also employed Münchnone intermediates to generate a new family of HMG-CoA reductase inhibitors with antifungal properties.¹⁶⁹ The reaction of the *N*-acylamino acid **1.136** with acetic anhydride formed the Münchnone, which was subsequently trapped *in situ* with a range of different alkynes to yield several different pyrroles **1.138** in moderate to excellent yields (Figure 1.61). Furthermore, Münchnone intermediates were also employed by Warner Lambert to generate a range of non-nucleoside HIV-1 reverse transcriptase inhibitors.¹⁷⁰

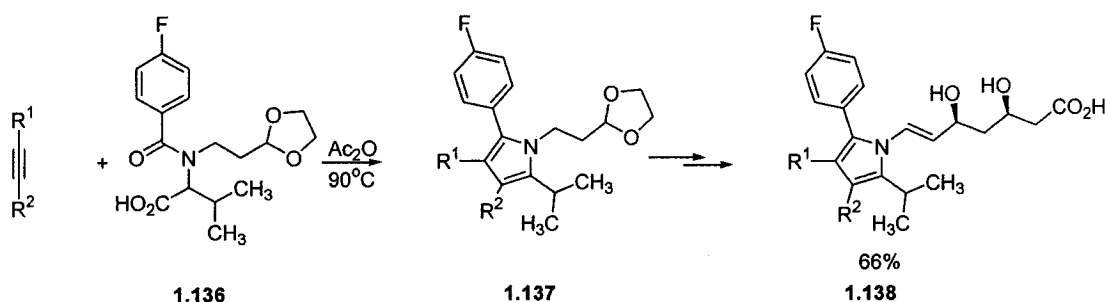


Figure 1.61 Generation of HMG-CoA Reductase Inhibitors

As the pyrrole nucleus is known to be a key pharmacophore, pyrroles have been generated on solid support for their inclusion into pyrrole-based combinatorial libraries.¹⁷¹ The coupling of a carboxylic acid, amine, aldehyde and isocyanocyclohexene (a Ugi 4CC reaction) on solid support generated the α -aminoacylamide **1.140** (Figure 1.62). The subsequent addition of HCl to the reaction mixture results in the cycloelimination of the protonated cyclohexenamide and generates the Münchnone *in situ*. This intermediate can react with DMAD to form pyrrole **1.141**, which can be cleaved from the solid-support with trifluoroacetic acid

to generate the final product **1.142** in 15-20% yield. Mjalli has also reported a similar reaction where the yields range from 32-72%.¹⁷²

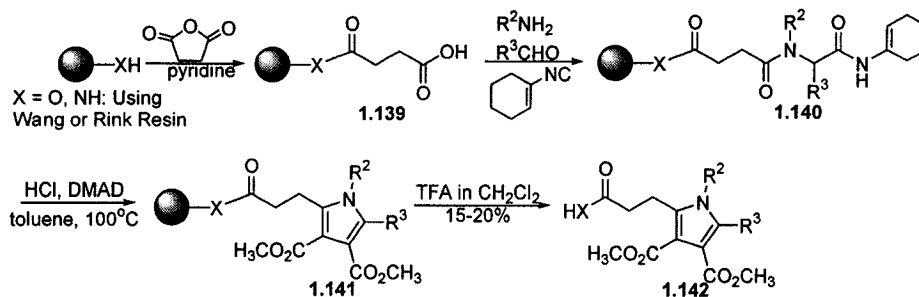


Figure 1.62 Generation of Pyrroles on Solid Support

Münchnone chemistry can also be utilized to yield significant levels of molecular complexity by appending a dipolarophile to the Münchnone precursor (Figure 1.63). Subsequent formation of the Münchnone and intramolecular trapping can generate multicyclic pyrroles **1.143**, regardless of the dipolarophile reactivity. Even unactivated alkynes, such as a tethered ethynyl group are competent partners in this type of reaction, presumably due to the entropic favourability of the process.¹⁷³

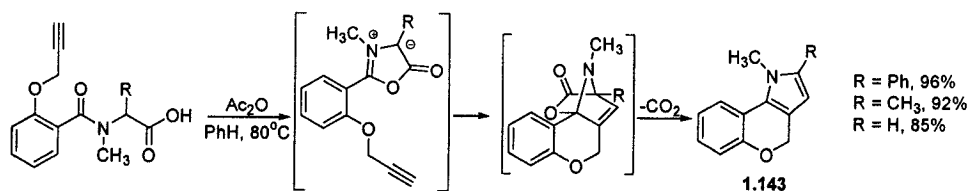


Figure 1.63 Generation of Multicyclic Pyrroles

1.3.7 1,3-Dipolar Cycloadditions: Generation of Imidazoles

Another important class of heterocyclic molecules available through 1,3-dipolar cycloaddition chemistry are multisubstituted imidazoles. Dalla Croce and co-workers have constructed these compounds in moderate to good yields through the reaction of *N*-tosyl imines **1.145** with Münchnones (Figure 1.64).¹⁷⁴ As *N*-tosyl imines are non-nucleophilic at the imine nitrogen, they do not form β -lactams; instead, they undergo a 1,3-dipolar cycloaddition with the Münchnone to form **1.146**. Subsequent CO₂ cycloreversion, sulfonic acid elimination, and aromatization generates imidazoles **1.147** in moderate to good yields. The reaction scope was shown to be somewhat limited, as R¹, R³, and R⁴ are restricted to aryl groups, while R² may be aryl or alkyl.

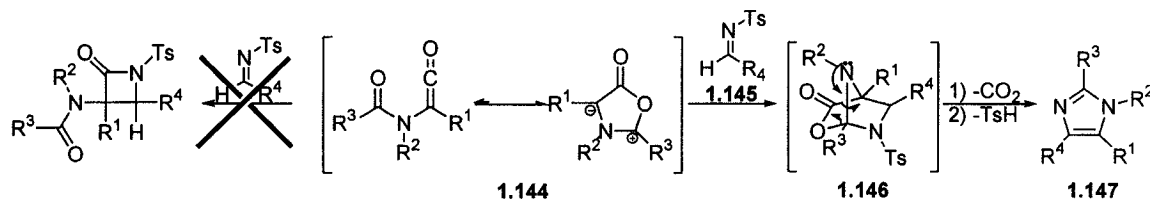


Figure 1.64 Generation of Imidazoles from Münchnones

The importance of this reaction was further exemplified by Bilodeau at Merck Research Laboratories, who generated a library of triarylimidazoles **1.148** utilizing this methodology.¹⁷⁵ After the synthesis of *N*-acylamino acids on a polystyrene-poly(ethyleneglycol) graft copolymer resin, *N*-ethyl-*N,N*-dimethylaminopropyl carbodiimide (EDC) was added to prepare the Münchnone **1.149**.¹⁷⁵ Subsequent

cyclization with *N*-tosylimine gave the imidazole, which could be cleaved from the resin on treatment with glacial acetic acid at 100°C (Figure 1.65).

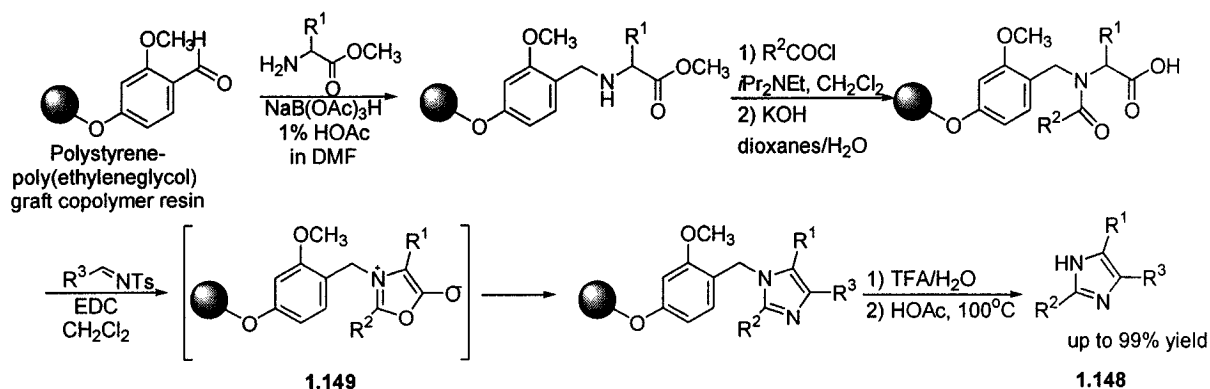


Figure 1.65 Generation of Imidazoles on Solid Support

1.3.8 Generation of 5-Trifluoromethyl Oxazoles: A Unique Approach from Münchnones

Another class of heterocyclic compounds available from Münchnones are oxazoles. For instance, Kawase and co-workers have described the synthesis of this class of heterocycles from the addition of trifluoroacetic anhydride (TFAA) to Münchnones.¹⁷⁶ The mechanism of the reaction involves a series of nucleophilic additions and rearrangements, which eventually generate the oxazole in excellent yields.

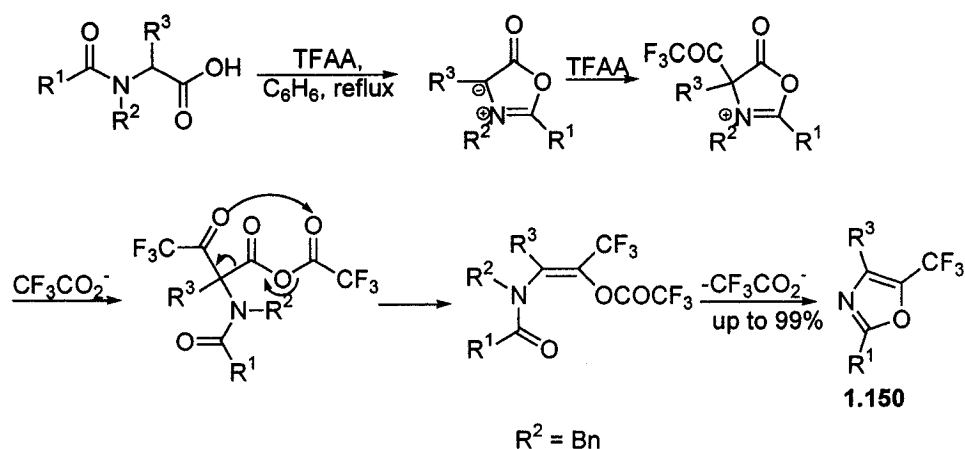


Figure 1.66 Generation of Oxazoles from Münchnones and TFAA

1.4 Palladium Catalyzed Synthesis of Imidazoline-Carboxylates

As shown in this section, a wide range of products are potentially available from Münchnone intermediates. In addition to these examples, we have recently demonstrated that imidazoline-carboxylates **1.153** can be accessed through coupling Münchnones and imines. This reaction was developed as part of a research program into metal catalyzed multicomponent coupling processes that combine imines and carbon monoxide to generate peptide-based derivatives (Figure 1.67).¹⁷⁷ The palladium catalyzed ($\text{Pd}_2(\text{dba})_3 \cdot \text{CHCl}_3$) reaction of imine **1.151**, acid chloride **1.152** and CO was found to generate imidazoline-carboxylates **1.153**.¹⁷⁸ This transformation was postulated to proceed via an initially formed Münchnone **1.154**, which subsequently undergoes 1,3-dipolar cycloaddition with *in situ* generated imine-HCl to form **1.153**. Due to the nature of the building blocks employed in this methodology, a range of imidazoline products were constructed by simple modification of the imine or acid chloride substrates.

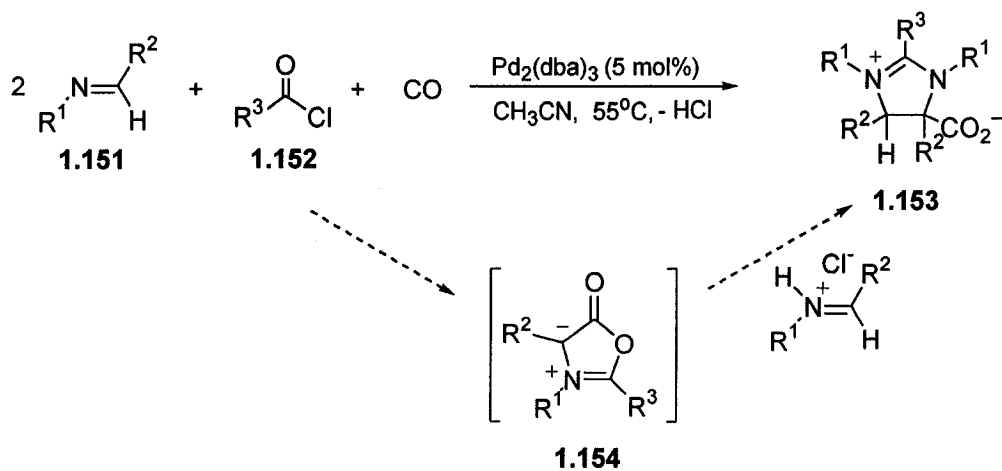


Figure 1.67 Synthesis of Imidazoline-Carboxylates

1.5 Overview of the Thesis

Multicomponent coupling reactions have been demonstrated to be valuable tools in synthesis. As shown by the large number of examples cited in this introduction, when combined with the reactivity of transition metal complexes, these processes can be used to effectively combine multiple precursors and assemble them into complex products, generally in a single operation. Reactions of this type not only enable product generation, but do so simply and in a time and resource efficient manner. In addition, Münchnones are exceedingly useful synthetic intermediates that have been utilized to construct a range of different heterocycles and peptide-based molecules. This thesis will describe a palladium catalyzed multicomponent coupling route to

generate these molecules from simple, inexpensive and readily available precursors (i.e. imines, acid chlorides and carbon monoxide). Furthermore, through these intermediates, the development of new efficient methodologies for the modular construction of α -amino acid derivatives, β -lactams and pyrroles will be presented.

Chapter 2 of this thesis will describe an extension of the previously developed imidazoline-carboxylate synthesis to prepare 3-amide substituted β -lactams. Chapter 3 of this thesis will describe mechanistic studies that further explain the origin of the β -lactams and imidazoline-carboxylate products in this palladium catalyzed chemistry. The mechanistic rationale for the formation of these products, and more complete characterization of the catalytic intermediates, will also be described. Chapter 4 discusses a new palladium catalyzed synthesis of Münchnones directly from imines, acid chlorides and carbon monoxide. These products were reacted with alcohols to develop a one pot, four component coupling route to diprotected α -amino acids. In addition, a range of different reactants can be added to this intermediate to generate a range of different heterocyclic and peptide-based products (eg. β -lactams in Chapter 2). Chapter 5 will describe improvements made to the catalytic preparation of Münchnones through the use of the bulky $P(o\text{-Tol})_3$ ligand. This chapter will also discuss the development of a one-step pyrrole synthesis, utilizing imines, acid chlorides, carbon monoxide and alkynes. The efficacy of this process will be demonstrated through the synthesis of a multicyclic pyrrole ring system in a single step. In Chapter 6 we will present a mechanistic discussion of the Münchnone synthesis, with a greater analysis of the presumed catalytic intermediates. In addition,

attempts to address the rate controlling steps in Münchnone generation, as well as comparisons of the various reaction conditions, will be presented.

1.6 References

- 1) For a review on asymmetric catalysis, see: *Comprehensive Asymmetric Synthesis* (Comprehensive Overviews in Chemistry) Eds. Jacobsen, E.; Pfaltz, A.; Yamamoto, H.; **1999**, Springer-Verlag.
- 2) Armstrong, R.W.; Beau, J.-M.; Cheon, S.H.; Christ, W.J.; Fujioka, H.; Ham, W.-H.; Hawkins, L.D.; Jin, H.; Kang, S.H.; Kishi, Y.; Martinelli, M.J.; McWhorter, W.W. , Jr.; Mizuno, M.; Nakata, M.; Stutz, A.E.; Talamas, F.X.; Taniguchi, M.; Tino, J.A.; Ueda, K.; Uenishi, J.-i.; White, J.B.; Yonaga, M. *J. Am. Chem. Soc.*, **1989**, *111*, 7530.
- 3 a) Woodward, R.B. *Pure Appl. Chem.* **1973**, *33*, 145 b) Eschenmoser, A.; Wintner, C. *Science* **1977**, *196*, 1410. c) Eschenmoser, A. *Angew. Chem. Int. Ed.* **1988**, *27*, 5.d) Riether, D.; Mulzer, J. *Eur. J. Org. Chem.* **2003**, 30.
- 4 a) Trost, B.M. *Science* **1991**, *254*, 1471. b) Trost, B.M. *Acc. Chem. Res.* **2002**, *35*, 695.
- 5 a) Anastas, P.T.; Warner, J.C. *Green Chemistry: Theory and Practice*, Oxford University Press, New York, **1998**. b) Clark, J.H. *Green Chemistry.* **1999**, 1. c) Ritter, S.K. *Chem. & Eng. News* **2002**, *80*, 38. d) Li, C.-J. *Acc. Chem. Res.* **2002**, *35*, 533.
- 6) Wender, P.; Handy, S.T.; Wright, D.L. *Chemistry & Industry.* **1997**, 765
- 7) Roessner, C.A.; Scott, A.I. *Chemistry & Biology* **1996**, *3*, 325.

- 8) Collman, J.P.; Hegedus, L.S.; Norton, J.R.; Finke, R.G. *Principles and Applications of Organotransition Metal Chemistry*, 2nd Edition. University Science Books, **1987**, 235-458.
- 9 a) Coates, G.W.; Waymouth, R.M. *J. Am. Chem. Soc.*, **1991**, *113*, 6270 b) Coates, G.W.; Waymouth, R.M. *Science*, **1995**, *267*, 217.
- 10) Trost, B.M.; Shi, Y. *J. Am. Chem. Soc.* **1991**, *113*, 701.
- 11) Crispino, G.A.; Ho, P.T.; Sharpless, K.B. *Science* **1993**, *259*, 64.
- 12 a) Capdevilla, E.; Rayó, J.; Carrión, F.; Jové, I.; Borrel, J.I.; Teixidó, J. *Afinidad*, **2003**, *60*, 317. b) Bienaymé, H.; Hulme, C.; Oddon, G.; Schmitt, P. *Chem. Eur. J.* **2000**, *6*, 3321. c) Tietze, L.F.; Modi, A. *Med. Res. Rev.* **2000**, *20*, 304. d) Posner, G.H. *Chem. Rev.* **1986**, *86*, 831.
- 13) Armstrong, R.W.; Combs, A.P.; Tempest, P.A.; Brown, S.D.; Keating, T.A. *Acc. Chem. Res.* **1996**, *29*, 123.
- 14 a) Strecker, A. *Justus Liebigs Ann. Chem.* **1850**, *75*, 27. b) Strecker, A. *Justus Liebigs Ann. Chem.* **1854**, *91*, 349.
- 15) Hantzsch, A. *Ber. Dtsch. Chem. Ges.* **1890**, *23*, 1474.
- 16) Mannich, C.; Krosche, W. *Arch. Pharm. (Weinheim. Ger.)* **1912**, *250*, 647
- 17 a) Bignelli, P. *Ber. Dtsch. Chem. Ges.* **1891**, *24*, 2962. b) Bignelli, P. *Ber. Dtsch. Chem. Ges.* **1893**, *26*, 447.
- 18) Passerini, M. *Gazz. Chim. Ital.* **1921**, *51*, 181.
- 19 a) Bucherer, H.T. Fischbeck, H.T. *J. Prakt. Chem.* **1934**, *140*, 69. b) Bucherer, H.T. Steiner, W. *J. Prakt. Chem.* **1934**, *140*, 24. c) Bergs, H. *Ger. Patent* 566,094., **1929**.

- 20) Ugi, I. *Angew. Chem. Int. Ed.* **1962**, *1*, 8.
- 21) For Reviews: a) Ugi, I.; Lohberger, S.; Karl, R. In *Comprehensive Organic Synthesis*; Trost, B.M.; Fleming, I., Eds.; Pergamon: New York, **1991**: vol. 2, pg. 1083-1109. b) Ugi, I.; Dömling, A.; Hörl, W. *Endeavour* **1994**, *18*, 115.
- 22) a) Keating, T.A.; Armstrong, R.W. *J. Org. Chem.* **1996**, *61*, 8935. b) Mjalli, A.M.M.; Sarshar, S.; Baiga, T.J.; *Tetrahedron Lett.* **1996**, *37*, 2943. c) Hanusch-Kompa, C.; Ugi, I. *Tetrahedron Lett.* **1998** *39*, 2725. d) Hulme, C.; Morrissette, M.W.; Volz, F.A.; Burns, C.J. *Tetrahedron Lett.* **1998**, *39*, 1113.
- 23) Keating, T.A.; Armstrong, R.W. *J. Am. Chem. Soc.*, **1995**, *117*, 7842.
- 24) Collman, J.P.; Hegedus, L.S.; Norton, J.R.; Finke, R.G. *Principles and Applications of Organotransition Metal Chemistry*, 2nd Edition. University Science Books, **1987**, 235-458.
- 25) For Reviews on Transition Metal Catalyzed Multicomponent Coupling Reactions, see: a) Balme, G.; Bossharth, E.; Monteiro, N. *Eur. J. Org. Chem.* **2003**, 4101. b) Montgomery, J. *Acc. Chem. Res.* **2000**, *33*, 467.
- 26) Cao, C.; Shi, Y.; Odom, A.L. *J. Am. Chem. Soc.* **2003**, *125*, 2880.
- 27) Pache, S.; Lautens, M. *Org. Lett.* **2003**, *5*, 4827.
- 28) Kamijo, S.; Jin, T.; Yamamoto, Y. *J. Org. Chem.* **2002**, *67*, 7413.
- 29) Kondo, T.; Kaneko, Y.; Taguchi, Y.; Nakamura, A.; Okada, T.; Shiotsuki, M.; Ura, Y.; Wada, K.; Mitsudo, T. *J. Am. Chem. Soc.* **2002**, *124*, 6824.
- 30) Chatani, N.; Kamitani, A.; Murai, S. *J. Org. Chem.* **2002**, *67*, 7014.
- 31) Dai, G.; Larock, R.C. *Org. Lett.* **2002**, *4*, 193.

- 32) Chatani, N.; Kamitani, A.; Oshita, M.; Fukumoto, Y.; Murai, S. *J. Am. Chem. Soc.* **2001**, *123*, 12686.
- 33) Van den Hoven, B.; Alper, H. *J. Am. Chem. Soc.* **2001**, *123*, 10214.
- 34) Bates, R.W.; Sa-Ei, K. *Org. Lett.* **2002**, *4*, 4225.
- 35) Lozanov, M.; Montgomery, J. *J. Am. Chem. Soc.* **2002**, *124*, 2106.
- 36) Trost, B.M.; Portnoy, M.; Kurihara, H. *J. Am. Chem. Soc.* **1997**, *119*, 836.
- 37) Onitsuka, K.; Suzuki, S.; Takahashi, S. *Tetrahedron Lett.* **2002**, *43*, 6197.
- 38) Xie, R.L.; Hauske, J.R. *Tetrahedron Lett.* **2000**, *41*, 10167.
- 39) Gabriele, B.; Salerno, G.; Fazio, A.; Campana, F.B. *Chem. Commun.* **2002**, 1408.
- 40) Davis, J.L.; Dhawan, R.; Arndtsen, B.A. *Angew. Chem. Int. Ed.* **2004**, *43*, 590.
- 41) For Reviews on the Pauson Khand Reaction, see: a) Chung, Y.K. *Coord. Chem. Rev.* **1999**, *188*, 297. b) Frühauf, H.-W. *Chem. Rev.* **1997**, *97*, 523. c) Geis, O.; Schmalz, H.-G. *Angew. Chem. Int. Ed.* **1998**, *37*, 911. d) Brummond, K.M.; Kent, J.L. *Tetrahedron*, **2000**, *56*, 3263. e) Schore, N.E. *Organic Reactions* vol. 40. **1991**, Wiley New York. f) Gibson, S.E.; Stevenazzi, A. *Angew. Chem. Int. Ed.* **2003**, *42*, 1800.
- 42) For Reviews on Cyclotrimerization, see: a) Saito, S.; Yamamoto, Y.; *Chem. Rev.* **2000**, *100*, 2901. b) Frühauf, H.-W.; *Chem. Rev.* **1997**, *97*, 523. c) Ojima, I.; Tzamarioudaki, M.; Zhaoyang, L.; Donovan, R.J.; *Chem. Rev.* **1996**, *96*, 635. d) Lautens, M.L.; Klute, W.; Tam, W. *Chem. Rev.* **1996**, *96*, 49. e) Schore, N.E. *Chem. Rev.* **1988**, *88*, 1081. f) Vollhardt, K.P.C. *Angew. Chem. Int. Ed.* **1984**, *23*, 536. g) Grotjahn, D.B. In *Comprehensive Organometallic Chemistry II*; Ed. Abel,

- Stone, Wilkinson, Hegedus. Pergamon Press: Oxford, **1995**; vol. 12, pp 741-770. h) Litvinov, V.P. *Russ. Chem. Rev.* **2003**, *72*, 69.
- 43) For Reviews on Amidocarbonylation, see: a) Beller, M. and Eckert, M. *Angew. Chem. Int. Ed.* **2000**, *39*, 1010. b) Knifton, J.F. Amidocarbonylation. In *Applied Homogeneous Catalysis with Organometallic Compounds*. 2nd Ed. **2002**, 156-164.
- 44) Khand, I.U.; Knox, G.R.; Pauson, P.L.; Watts, W.E.; Foreman, M.I. *J. Chem. Soc. Perkin I.* **1973**, 977
- 45) Schore, N.E. "Transition Metal Alkyne Complexes: Pauson Khand Reactions" In *Comprehensive Organometallic Chemistry II*. Eds.: Abel, Stone, Wilkinson. Elsevier, Oxford, **1995**, vol. 12 pp. 703-741.
- 46) Imhof, W.; Anders, E.; Gobel, A.; Gorus, H. *Chem. Eur. J.* **2003**, *9*, 1166.
- 47) Schore, N.E.; Croudace, M.C. *J. Org. Chem.* **1981**, *46*, 5436.
- 48 a) Shambayati, S.; Crowe, W.E.; Schreiber, S.L. *Tetrahedron Lett.* **1990**, *31*, 5289.
b) Jeong, N.; Chung, Y.K.; Lee, B.Y.; Lee, S.H.; Yoo, S.-E.; *Synlett*, **1991**, 204.
- 49) Sugihara, T.; Yamada, M.; Yamaguchi, M.; Nishizawa, M. *Synlett*, **1999**, 771
- 50) Sugihara, T.; Yamada, M.; Ban, H.; Yamaguchi, M.; Kaneko, C. *Angew. Chem. Int. Ed.*, **1997**, *36*, 2801.
- 51) Perez-Serrano, L; Casarrubios, L.; Dominguez, G.; Perez-Castells, J. *Org. Lett.* **1999**, *1*, 1187.
- 52) Belanger, D.B.; O'Mahoney, D.J.R.; Livinghouse, T. *Tetrahedron Lett.* **1998**, *39*, 7637.
- 53) March, J. *Advanced Organic Chemistry: Reactions, Mechanism and Structure*. 4th Ed. Wiley: New York. **1992**

- 54) Krafft, M.E.; Bonaga, L.V.R.; Hirosawa *Tetrahedron Lett.* **1999**, *40*, 9171.
- 55) Magnus, P.; Principe, L.M.; Slater, M.J. *J. Org. Chem.* **1987**, *52*, 1483.
- 56) Jeong, N.; Sung, B.K.; Kim, J.S.; Park, S.B.; Seo, S.D.; Shin, J.Y.; In, K.Y.; Choi, Y.K. *Pure Appl. Chem.* **2002**, *74*, 85.
- 57) Morimoto, T.; Fuji, K.; Tsutsumi, K.; Kakiuchi, K.; *J. Am. Chem. Soc.* **2002**, *124*, 3806. b) Shibata, T.; Toshida, N.; Takagi, K. *J. Org. Chem.* **2002**, *67*, 7446.
- 58) Shibata, T.; Takagi, *J. Am. Chem. Soc.* **2000**, *122*, 9852
- 59) Hicks, F.A.; Kablaoui, N.M.; Buchwald, S.L. *J. Am. Chem. Soc.* **1999**, *121*, 5881.
- 60 a) Morimoto, T.; Chatani, N.; Fukumoto, Y.; Murai, S. *J. Org. Chem.* **1997**, *62*, 3762. b) Kondo, T.; Suzuki, N.; Okada, T.; Mitsudo, T.-A. *J. Am. Chem. Soc.* **1997**, *119*, 6187.
- 61) Zhang, M.; Buchwald, S.L. *J. Org. Chem.* **1996**, *61*, 4498.
- 62) Kobayashi, T.; Koga, Y.; Naraska, K. *J. Organomet. Chem.* **2001**, *624*, 73.
- 63) Chung, Y.K. *Coord. Chem. Rev.* **1999**, *188*, 297.
- 64) Lee, B.Y.; Chung, Y.K.; Jeong, N.; Lee, Y.; Hwang, S.H.; *J. Am. Chem. Soc.* **1994**, *116*, 8793.
- 65) See Ref. 63.
- 66) Itami, K.; Mitsudo, K.; Yoshida, J. *Angew. Chem. Int. Ed.* **2002**, *41*, 3481.
- 67) Kablaoui, N. M.; Hicks, F.A.; Buchwald, S.L. *J. Am. Chem. Soc.* **1996**, *118*, 5818.
- 68) Kang, S.-K.; Kim, K.-J.; Hong, Y.-T.; *Angew. Chem. Int. Ed.* **2002**, *41*, 1584.
- 69) Chatani, N.; Tobisu, M.; Asaumi, T.; Murai, S. *Synthesis* **2000**, 925.
- 70) Chatani, N.; Tobisu, M.; Asaumi, T.; Murai, S. *Synthesis* **2000**, 925.

- 71) Zhang, M.; Buchwald, S.L. *J. Org. Chem.* **1996**, *61*, 4498
- 72) Chatani, N.; Tobisu, M.; Asaumi, T.; Fukumoto, Y.; Murai, S. *J. Am. Chem. Soc.* **1999**, *121*, 7160.
- 73) Tobisu, M.; Chatani, N.; Asaumi, T.; Amako, K.; Ie, Y.; Fukumoto, Y.; Murai, S. *J. Am. Chem. Soc.* **2000**, *122*, 12663.
- 74) For Reviews on Natural Product Synthesis utilizing the Pauson Khand Reaction, see: Ref. 41.
- 75) Cassayre, J.; Gagosz, F.; Zard, S.Z. *Angew. Chem. Int. Ed.* **2002**, *41*, 1783.
- 76) Nomura, I.; Mukai, C. *Org. Lett.* **2002**, *4*, 4301.
- 77) Cassayre, J.; Zard, S.Z. *J. Am. Chem. Soc.* **1999**, *121*, 6072.
- 78) Paquette, L.A.; Borrelly, S. *J. Org. Chem.* **1995**, *60*, 6912.
- 79) Krafft, M.E.; Cheung, Y.Y.; Abboud, K.A. *J. Org. Chem.* **2001**, *66*, 7443.
- 80) Bolton, G.L.; Hodges, J.C.; Rubin, J.R. *Tetrahedron.* **1997**, *53*, 6611.
- 81a) Schreiber, S. *Science* **2000**, *287*, 1964 b) Kubota, H. Lim, J; Depew, K.M. and Schreiber, S.L. *Chemistry & Biology* **2002**, *9*, 265.
- 82) Fleming, I. *Pericyclic Reactions Oxford Press*, New York. **1999**.
- 83) Conditions reported for 1,1,4,4-dideuterio-1,3-butadiene: Houk, K.N.; Lin, Y.-T.; Brown, F.T. . *J. Am. Chem. Soc.* **1986**, *108*, 554. For general review, see: March, J. *Advanced Organic Chemistry: Reactions, Mechanism, and Structure.* 4th Ed. Wiley: New York, **1992**, 839-852.
- 84) See Ref. 42.
- 85) See Ref. 42g
- 86) Bertholet, M. C. R. *Held. Seances Acad. Sci.* **1866**, 905.

- 87) Reppe, W.; Schlichting, O.; Klager, K.; Toepel, T. *Justus Liebigs Ann. Chem.* **1948**, 560, 1
- 88 a) Moseley, K.; Maitlis, P.M. *J. Chem. Soc. Dalton Trans.* **1974**, 169, 1974. b)
Brown, L.D.; Itoh, K.; Suzuki, K.; Hirai, K.; Ibers, J.A. *J. Am. Chem. Soc.* **1978**,
100, 8232.
- 89) Sato, Y.; Ohashi, K.; Mori, M. *Tetrahedron Lett.* **1999**, 40, 5231.
- 90) McDonald, F.E.; Zhu, H.Y.H.; Holmquist, C.R. *J. Am. Chem. Soc.* **1995**, 117,
6605
- 91) Snieckus, V. *Chem. Rev.* **1990**, 90, 879.
- 92) March, J. *Advanced Organic Chemistry: Reactions, Mechanism, and Structure.*
4th Ed. Wiley: New York, **1992**, 641-676.
- 93) March, J. *Advanced Organic Chemistry: Reactions, Mechanism, and Structure.*
4th Ed. Wiley: New York, **1992**, 501-568.
- 94) Diedrich, F.; Stang, P. *Metal-Catalyzed Cross Coupling Reactions.* VCH
Publishers. **1998**, Wiley. New York
- 95) Jia, C.; Kitamura, T.; Fujiwara, Y. *Acc. Chem. Res.* **2002**, 34, 633.
- 96) Jhingan, A.K.; Maier, W.F. *J. Org. Chem.* **1987**, 52, 1161.
- 97) Vollhardt, K.P.C. *Acc. Chem. Res.* **1977**, 10, 1.
- 98) See Ref. 90.
- 99) Blechert, S.; Peters, J.-U. *Chem. Comm.* **1997**, 1983.
- 100) Peña, D.; Escudero, S.; Pérez, D.; Guitián, E.; Castedo, L. *Angew. Chem. Int.*
Ed. **1998**, 37, 2659.
- 101) Yamamoto, Y.; Nagata, A.; Itoh, K. *Tetrahedron. Lett.* **1999**, 40, 5035

- 102) Vollhardt, K.P.C. *Angew. Chem. Int. Ed.* **1984**, *23*, 536.
- 103) Takahashi, T.; Tsai, F.-U.; Li, Y.; Nakajima, K.; Kotori, M. *J. Am. Chem. Soc.* **1999**, *121*, 11093
- 104) Suzuki, D.; Urabe, H.; Sato, F. *J. Am. Chem. Soc.* **2001**, *123*, 7925.
- 105) Gevorgyan, V.; Radhakrishnan, U.; Takeda, A.; Rubina, M.; Rubin, M.; Yamamoto, Y. *J. Org. Chem.* **2001**, *66*, 2835.
- 106) Trost, B.M.; Sorum, M.T.; Chan, C.; Harms, A.E.; Rühler, G. *J. Am. Chem. Soc.* **1997**, *119*, 698.
- 107) Yamamoto, Y.; Ishii, J.-I.; Nishiyama, H.; Itoh, K.; *J. Am. Chem. Soc.* **2004**, *126*, 3712
- 108) Chouraqui, G.; Petit, M.; Aubert, C.; Malacria, M. *Org. Lett.* **2004**, *6*, 1519.
- 109) For reviews on generating heterocyclic molecules with [2+2+2] cyclization reactions, see: Varela, J.A.; Saá, C. *Chem. Rev.* **2003**, *103*, 3787
- 110) Varela, J.A.; Saá, C. *Chem. Rev.* **2003**, *103*, 3787
- 111) Chelucci, G.; Cabras, M.A.; Botteghi, C.; Marchetti, M. *Tetrahedron Asymm.* **1994**, *5*, 299.
- 112) Varela, J.A.; Castedo, L.; Saá, C. *J. Am. Chem. Soc.* **1998**, *120*, 12147.
- 113) Diversi, P.; Ermini, L.; Ingrosso, G.; Lucherini, A. *J. Organomet. Chem.* **1993**, *447*, 291.
- 114) Knoch, F.; Kremer, F.; Schmidt, U.; Zenneck, U. *Organometallics*, **1996**, *15*, 2713.
- 115) Yamamoto, Y.; Okuda, S.; Itoh, K. *Chem. Comm.* **2001**, 1102.
- 116) Bonnemann, H.; Brijoux, W. *Bull. Soc. Chim. Belg.* **1985**, *94*, 635.

- 117) Yamamoto, Y.; Takagishi, H.; Itoh, K. *Org. Lett.* **2001**, *3*, 2117.
- 118) Louie, J.; Gibby, J.E.; Farnworth, M.V.; Tekavec, T.N. *J. Am. Chem. Soc.* **2002**, *124*, 15188.
- 119) Yamamoto, Y.; Takagishi, H.; Itoh, K. *J. Am. Chem. Soc.* **2002**, *124*, 6844.
- 120) Yamamoto, Y.; Takagishi, H.; Itoh, K. *J. Am. Chem. Soc.* **2002**, *124*, 28.
- 121) Takahashi, T.; Li, Y.; Ito, T.; Xu, F.; Nakajima, K.; Liu, Y. *J. Am. Chem. Soc.* **2002**, *124*, 1144.
- 122) See Ref. 42.
- 123) Funk, R.L.; Vollhardt, K.P.C. *J. Am. Chem. Soc.* **1980**, *102*, 5253.
- 124) Saá, C.; Crotts, D.D.; Hsu, G.; Vollhardt, K.P.C. *Synlett* **1994**, 487.
- 125) Earl, R.A.; Vollhardt, K.P.C. *J. Org. Chem.* **1984**, *49*, 4786.
- 126) Geiger, R.E.; Lalonde, M.; Stoller, H.; Schleich, K. *Helv. Chim. Acta.* **1984**, *67*, 1274.
- 127) Williams, R.W.; Hendrix, J.A. *Chem. Rev.* **1992**, *92*, 889.
- 128) See Ref. 43.
- 129) Wakamatsu, H.; Uda, J.; Yamakami, N. *J. Chem. Soc. Chem. Commun.* **1971**, 1540.
- 130) Ojima, I.; Zhang, Z. *Organometallics* **1990**, *9*, 3122.
- 131) Ojima, I.; Okabe, M.; Kato, K.; Kwon, H.B.; Horvath, I.T. *J. Am. Chem. Soc.* **1988**, *110*, 150.
- 132) Iwaza, K. *Yuki Gosei Kagaku Kyokaiishi* **1988**, *46*, 218. See: Beller, M. and Eckert, M. *Angew. Chem. Int. Ed.* **2000**, *39*, 1010.
- 133) Amino, Y.; Izawa, K. *Bull. Chem. Soc. Jpn.* **1991**, *23*, 2491.

- 134) Hirai, K.; Takahashi, Y.; Ojima, I. *Tetrahedron Lett.* **1982**, *64*, 1040
- 135) de Vries, J.G.; de Boer, R.P.; Hogeweg, M.; Gielens, E.E.C.G. *J. Org. Chem.* **1996**, *61*, 1842.
- 136) Beller, M.; Eckert, M.; Moradi, W.A. *Synlett*, **1999**, 108.
- 137 a) Beller, M.; Eckert, M. *Angew. Chem. Int. Ed.* **2000**, *39*, 1011. b) Beller, M.; Eckert, M.; Moradi, W.A.; Neumann, H. *Angew. Chem. Int. Ed.* **1999**, *38*, 1454. c) Gördes, D.; Neumann, H.; Jacobi von Wangelin, A.; Fischer, C.; Drauz, K.; Krimmer, H.-P.; Beller, M. *Adv. Synth. Cat.* **2003**, *345*, 510 d) Beller, M.; Eckert, M.; Geissler, H.; Napierski, B.; Rebenstock, H.-P.; Holla, E.W.; *Chem. Eur. J.* **1998**, *4*, 935. e) Beller, M. and Eckert, M.; Holla, E.W. *J. Org. Chem.* **1998**, *63*, 5658. g) Beller, M.; Morad, W.A.; Eckert, M.; Neumann, M. *Tetrahedron Lett.* **1999**, *40*, 4523. h) Beller, M.; Eckert, M.; Vollmüller, F.; Bogdanovic, S.; Geissler, H. *Angew. Chem. Int. Ed.* **1997**, *36*, 1494.
- 138 a) Sagae, T.; Sugihara, M.; Hagio, H.; Kobayashi, S. *Chem. Lett.* **2003**, *23*, 160. b) Jacobi von Wangelin, A.; Neumann, H.; Gördes, D.; Klaus, S; Strübing, D.; Beller, M. *Chem. Eur. J.* **2003**, *9*, 4286.
- 139) Drauz, K.; Burkhardt, O.; Beller, M.; Eckert, M. United States Patent: 6,294,681 (8pp.)
- 140) Ojima, I.; Hirai, K.; Fujita, M.; Fuchikami, T. *J. Organomet. Chem.* **1985**, *279*, 203.
- 141) Beller, M.; Fischer, H.; Gross, P.; Gerdau, T.; Geissler, H.; Bogdanovic, (Hoeschst AG), DE-B 4415712, **1995** [*Chem. Abstr.* **1996**, *124*, 149264a]

- 142 a) Takigawa, S.; Shinke, S.; Tanaka, M. *Chem. Lett.* **1990**, 1415. b) Sakakura, T.; Huang, X.-Y.; Tanaka, M. *Bull. Chem. Soc. Jpn.* **1991**, *64*, 1707.
- 143) Iwaza, K. *Yuki Gosei Kagaku Kyokaiishi* **1988**, *46*, 218.
- 144 a) Xiao, X.; Ngu, K.; Chao, C.; Patel, D.V. *J. Org. Chem.* **1997**, *62*, 6968. b) Drauz, K.; Waldmann, H. *Enzyme Catalysis in Organic Synthesis* VCH, Weinheim, **1995**.
- 145 a) *Mesoionic Ring Systems* by K.T. Potts in *1,3 Dipolarcycloaddition Chemistry* A. Padwa Ed. pg. 1-81. **1983** John Wiley & Sons Inc. New York b) *Mesoionic Oxazoles* by H.L. Gingrich and J.S. Baum in *Oxazoles*. I.J. Turchi Ed. 731-958. **1984** John Wiley & Sons Inc. New York c) *Synthetic Applications of 1,3-Dipolar Cycloaddition Chemistry Toward Heterocycles and Natural Products* in *Mesoionic Ring Systems* by G.W. Gribble. **2002** John Wiley & Sons Inc. New York . A. Padwa Ed. pg. 681-753. d) *Mesoionic Oxazoles* by G.W. Gribble in *Oxazoles: Synthesis, Reactions, and Spectroscopy Part. A.* Ed. D.C. Palmer **2003**, John Wiley & Sons. New York.
- 146 a) Bayer, H.O.; Hüisgen, R.; Knorr, R.; Schaefer, F.C. *Chem. Ber.* **1970**, *103*, 2581 b) Hüisgen, R.; Gotthardt, H.; Bayer, H.O.; Schaefer, F.C. *Angew. Chem. Int. Ed.* **1964**, *3*, 136. c) Hüisgen, R.; Gotthardt, H.; Bayer, H.O.; Schaefer, F.C. *Chem. Ber.* **1970**, *103*, 2611 d) Knorr, R.; Hüisgen, R.; Staudinger, G.K. *Chem. Ber.* **1970**, *103*, 2639 e) Hüisgen, R.; Funke, E.; Schaefer, F.C.; Knorr, R. *Angew. Chem. Int. Ed.* **1967**, *6*, 367.
- 147) Anderson, W.K.; Heider, A.R. *Synth. Comm.* **1986**, *16*, 357.
- 148) Potts, K.T.; Yao, S. *J. Org. Chem.* **1979**, *44*, 977.

- 149) Wilde, R.G. *Tetrahedron Lett.* **1988**, 29, 2027
- 150) See Ref. 145a and 145b
- 151) See Ref. 146
- 152) Alper, H.; Tanaka, M. *J. Am. Chem. Soc.* **1979**, 101, 4245.
- 153 a) Hegedus, L.S. *Acc. Chem. Res.* **1995**, 28, 299. b) Hegedus, L.S. *Tetrahedron* **1997**, 53, 4105 c) Imwinkelried, R.; Hegedus, L.S. *Organometallics* **1988**, 7, 702.
d) Schwindt, M.A.; Lejon, T.; Hegedus, L.S. *Organometallics* **1990**, 9, 2814.
- 154) Merlic, C.A.; Baur, A.; Aldrich, C.C. *J. Am. Chem. Soc.* **2000**, 122, 7398.
- 155) See Ref. 154.
- 156) Toupet, L.; Texier, F.; Carrié, R. *Acta Crystallogr. Sect. C Cryst. Struct. Commun.* **1991**, C47, 328.
- 157) See Ref. 145b
- 158) See Ref. 145
- 159) Wilde, R.G. *Tetrahedron Lett.* **1988**, 29, 2027.
- 160) For reviews on the synthesis of β -lactams: (a) Ratcliffe, R. W.; Albers-Schonberg, G. *Chemistry and Biology of β -Lactam Antibiotics*; Morin, R. B., Gorman, M., Eds.; Academic Press; N. Y., 1982, Vol. 2. (b) Carruthers, W. in *Cycloaddition Reactions in Organic Synthesis*, Pergammon Press: Oxford, 1990. (c) Hart, D. J.; Ha, D.-C. *Chem. Rev.* **1989**, 89, 1447. (d) Southgate, R.; Branch, C.; Coulton, S.; Hunt, E. in *Recent Progress in the Chemical Synthesis of Antibiotics and Related Microbial Products*, vol. 2 (Ed: G. Lukacs.) Springer-Verlag, Berlin e) Palomo, C.; Aizpurua, J. M.; Ganboa, I.; Oiarbide, M. *Eur. J. Org. Chem.* **1999**, 3223. f) Singh, G.S. *Tetrahedron* **2003**, 59, 7631. g) *The*

Organic Chemistry of β -lactams, Georg, G.I. Ed., VCH Publishers, New York, **1993**.

- 161 a) Tidwell, T., "Ketenes" Wiley, New York. **1995**. b) Hegedus, L. *Tetrahedron* **1997**, *53*, 4105. c) Cossio F.P.; Arrieta, A.; Lecea, B.; Ugalde, J.M. *J. Am. Chem. Soc.* **1994**, *116*, 2085.
- 162) Sain, B.; Sandhu, J.S. *Heterocycles* **1985**, *23*, 1611.
- 163) Uchida, T.; Tsubokawa, S.; Harihara, K.; Matsumoto, K. *J. Heterocyclic Chem.* **1978**, *15*, 1303.
- 164) Coppola, B.P.; Noe, M.C.; Schwartz, D.J.; Abdon, R.L. II, Trost, B.M. *Tetrahedron*, **1994**, *50*, 93.
- 165) Padwa, A.; Burgess, E.M.; Gingrich, M.L.; Roush, D.M. *J. Org. Chem.* **1982**, *47*, 786.
- 166) Pandey, P.S.; Rao, T.S. *Biorg. Med. Chem. Lett.* **2004**, *14*, 129.
- 167 a) Roth, B.D. U.S. Patent 4,681,893 **1987** b) Graul, A.; Castaner, J. *Drugs of the Future* **1997**, *22*, 956.
- 168) Santiago, B.; Dalton, C.R.; Huber, E.W.; Kane, J.M. *J. Org. Chem.* **1995**, *60*, 4947.
- 169) Castro, J.; Coteron, J.M.; Fraile, M.T.; Garcia-Ochoa, S.; Gomez de las Heras, F.; Martin-Cuesta, A. *Tetrahedron Lett.* **2002**, *43*, 1851.
- 170) Antonucci, T.; Warmus, J.S.; Hodges, J.C.; Nickell, D.G. *Antiviral Chem. Chemo.* **1995**, *6*, 98.
- 171 a) Keating, T.A.; Armstrong, R.W. *J. Am. Chem. Soc* **1995**, *117*, 7842. b) Keating, T.A.; Armstrong, R.W. *J. Am. Chem. Soc* **1996**, *118*, 2574. c) Keating,

- T.A.; Armstrong, R.W. *J. Org. Chem.* **1996**, *61*, 8935. d) Strocker, A.M.; Keating, T.J.; Tempest, P.A.; Armstrong, R.W. *Tetrahedron Lett.*, **1996**, *37*, 1149.
- 172) Mjalli, A.M.M.; Sarshar, S.; Baiga, T.J. *Tetrahedron Lett.* **1996**, 2943.
- 173) Kato, H.; Wang, S.-Z.; Nakano, H. *J. Chem. Soc. Perkin Trans. I.* **1989**, 361.
- 174) Consonni, R.; Dalla Croce, P.; Ferraccioli, R.; La Rosa, C. *J. Chem. Res. Synop.* **1991**, 188.
- 175) Bilodeau, M.T.; Cunningham, A.M. *J. Org. Chem.* **1998**, *63*, 2800.
- 176) Kawase, M. *Heterocycles* **1993**, *36*, 2441.
- 177 a) Dghaym, R.D.; Yaccato, K.J.; Arndtsen, B.A. *Organometallics*, **1998**, *17*, 4.
b) Davis, J.L.; Arndtsen, B.A. *Organometallics*, **2000**, *19*, 4657 c) Lafrance, D.; Davis, J.L.; Dhawan, R.; Arndtsen, B.A.. *Organometallics*, **2001**, *20*, 1128.
- 178) Dghaym, R.D.; Dhawan, R.; Arndtsen, B.A. *Angew. Chem. Int. Ed.* **2001**, *40*, 3228.

CHAPTER TWO

Palladium Catalyzed Coupling of Imine, Acid Chloride and Carbon Monoxide: A Multicomponent Coupling Approach to β -Lactams

Preface

As mentioned in the introduction, previous work in this laboratory has shown that the palladium catalyzed coupling of imine, acid chloride and carbon monoxide generates imidazoline-carboxylates. This reaction is postulated to proceed through a 1,3-oxazolium-5-oxide (Münchnone) intermediate. In Chapter 2, we discuss the development of a new four-component palladium catalyzed coupling of imines, acid chloride and carbon monoxide to form β -lactams. This reaction is postulated to proceed via the generation of the same Münchnone intermediate.

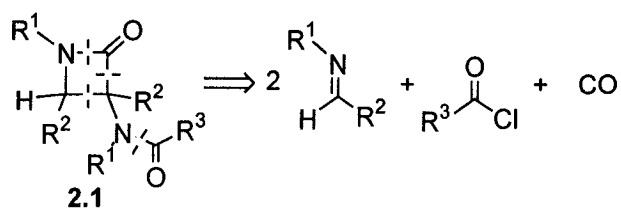
2.0 Introduction

The synthesis of β -lactams has garnered significant attention over the past seventy years.^{1a} This has been driven in large part to the importance of these molecules as constituents of antibiotics, ranging from penicillin^{2b} to other structurally diverse classes of β -lactams, including penems,^{2c} cepheids,^{2c} monobactams,^{2d,e} carbapenems,^{2d} and trinems.^{2f} In addition to their biological activity, β -lactams have significant utility as intermediates in organic synthesis,³ as well as monomers in the

generation of polymers such as poly(β -peptides).⁴ To further complement the classical synthetic routes to these molecules (i.e. from imines and acid chlorides),¹ a number of efficient metal based methodologies have been reported to construct these compounds.⁵⁻¹⁶ These include the metal catalyzed carbonylative ring expansion of aziridines,⁵ as well as the palladium catalyzed carbonylative coupling of imines with allyl phosphates,⁶ and allyl halides.⁷ Furthermore, the carbonylation of bromoallylamine derivatives,⁸ Lewis acid catalyzed processes^{11, 13} and the cycloaddition of imines with ketenes, generated from a rhodium catalyzed decomposition of diazo compounds¹⁵ are known to form β -lactams. In addition, the stoichiometric reaction of imines with chromium-carbene¹⁶ and acyl-ironcarbonyl¹⁷ precursors have also been shown to be viable routes for the preparation of the β -lactam core.

While each of the approaches above is effective, they all require the initial construction of precursors prior to β -lactam formation. This not only complicates the synthesis, but also limits the number of possible structures readily available, by requiring the construction of each precursor before ultimate product formation. A more attractive approach would be to consider relatively complex molecules as simply arising through the coupling of basic and readily available building blocks. Transition metal catalysts could serve as an excellent tool for mediating these transformations by employing the diverse reactivity of metal complexes in mediating the coupling of traditionally unreactive precursors into more complex molecules.¹⁸ We describe below our application of just such an approach to the synthesis of β -

lactams. This involves the palladium catalyzed coupling of two imines, acid chloride, and carbon monoxide to generate a β -lactam of the form **2.1** (Equation 2.1). In addition to providing one of the more facile routes to constructing the β -lactam core, this approach also allows the first catalytic construction of α -amino acid based 3-amide substituted β -lactams, which represents the core active structure of many bio-relevant β -lactams (i.e. penicillin, nocardicins, and cephalosporins).¹⁹



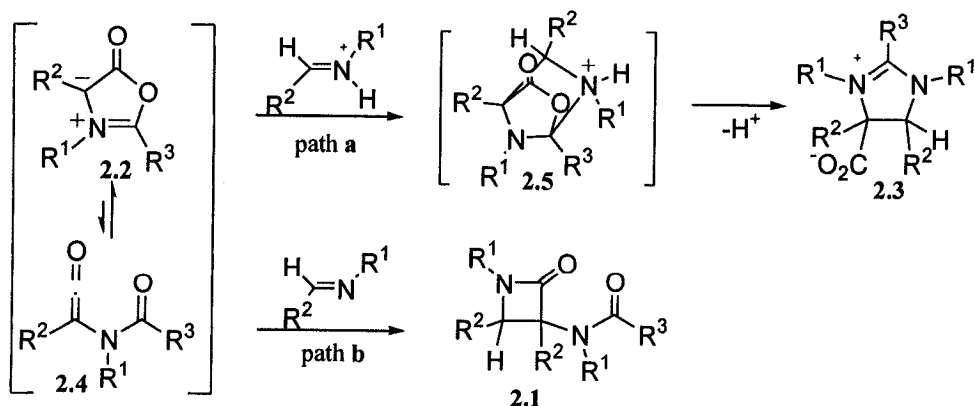
Equation 2.1 Generation of β -Lactams

2.1 Results and Discussion

2.1.1 Mechanistic Considerations

Our approach to a β -lactam synthesis is based on our previously reported palladium catalyzed synthesis of imidazolines.²⁰ This reaction is suspected to proceed through the formation of a mesoionic 1,3-oxazolium-5-oxide (i.e. Münchnone) intermediate **2.2**, which undergoes a 1,3-dipolar cycloaddition with imine·HCl to generate **2.3** (path a) (Scheme 2.1).²¹⁻²² Considering that Münchnones are known to be in equilibrium with their ketene isomer **2.4**,²³ we postulated that this catalytic coupling could be employed to provide access to 3-amido substituted β -lactams **2.1**. In principle, this can be accomplished by inducing the second equivalent of imine to

undergo a formal [2 + 2] cycloaddition with the *in situ* generated ketene isomer **2.4**, rather than 1,3-dipolar addition to **2.2**. Indeed, previous reports have demonstrated that *N*-alkyl substituted imines react with Münchnones via their ketene isomer to generate β -lactams,²³ suggesting the formation of **2.3** in this catalytic process is the result of our specific reaction conditions. In order to explore this phenomenon, the reactivity of independently generated Münchnone **2.2** (R^1 =Bn; R^2 =Ph; R^3 =Ph) has been examined (Scheme 2.1).^{21, 24} On reacting Münchnone **2.2** with Ph(H)C=NBn, β -lactam product is generated in a 79% NMR yield (path b).^{21, 22} However, the reaction of **2.2** with Ph(H)C=NBn in the presence of HCl, which is present in our catalytic reaction, completely inhibits β -lactam formation, and instead results in the clean formation of an imidazoline-carboxylate in a 99% NMR yield. The role of acid in influencing this cyclization is not presently known, but may be related to increasing the electrophilicity of the imine via protonation of nitrogen.^{22a} This data suggests that eliminating any HCl generated during the catalytic coupling of imine, acid chloride and carbon monoxide may allow this methodology to be applied to the catalytic synthesis of β -lactams.



Scheme 2.1 Reaction of Münchnones with Imines

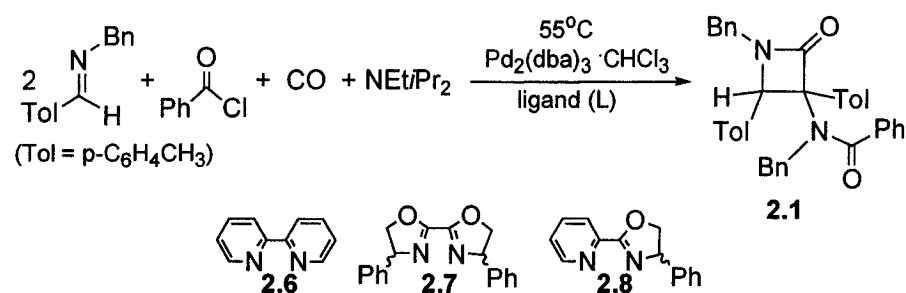
The ability of this chemistry to access β -lactams was first probed in the stoichiometric reaction of 0.5 equiv. $\text{Pd}_2(\text{dba})_3 \cdot \text{CHCl}_3$ with 2 equiv. of $\text{Ph}(\text{H})\text{C}=\text{NBn}$, PhCOCl , and 1 atm CO and base in acetonitrile. Various inorganic (Cs_2CO_3 and NaOAc) and organic bases (NEt_3 , proton sponge and DBU) were examined; however, no identifiable products were produced. In contrast, changing the base to the more sterically hindered *N,N*-diisopropylethylamine (NEt^iPr_2), and monitoring this reaction at 55°C for 24 h by ^1H NMR reveals the quantitative formation of $\text{Et}^i\text{Pr}_2\text{NH}^+ \text{Cl}^-$. More importantly, closer examination of the final reaction mixture reveals the formation of the desired 3-amido substituted β -lactam **2.1** (Table 2.1, entry 1). However, **2.1** is formed in only ca. 5% NMR yield, and almost 1 equivalent of free imine is recovered.²⁵

2.1.2 Method Development

In contrast to the stoichiometric coupling, performing this reaction under catalytic conditions provides a synthetically useful method to combine imines, carbon monoxide and acid chloride into β -lactams. As shown in Table 2.1, this same reaction with a 5% catalyst loading results in the formation of β -lactam **2.1** in 45% yield (entry 3). Interestingly, increasing the palladium loading actually inhibits the formation of **2.1** (entries 1-3, *vide infra*). The efficiency of this catalysis can be further improved by the addition of a chelating ligand (entries 4-6). The optimal results are obtained by using ligand **2.7** in a 1:1 THF/acetonitrile solvent mixture,

which leads to the clean coupling of the imine, acid chloride and carbon monoxide fragments into a single β -lactam product in up to 76% yield (Table 2.2). To our knowledge, this represents the first metal catalyzed synthesis of 3-amido substituted β -lactams.

Table 2.1. Palladium Catalyzed Synthesis of β -lactams: Method Development



#	L	[Pd] ^b	%Yield ^c
1 ^d	-	100	5
2 ^d	-	20	8.5
3 ^d	-	5	30
4 ^a	2.6	5	45
5 ^a	2.7	5	55
6 ^a	2.8	5	58
7 ^a	2.8	2.8	64 (50)

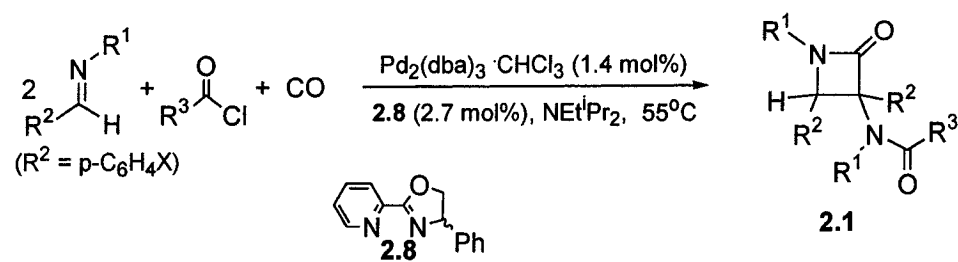
^a 1.2 mmol imine, 0.54 mmol acid chloride, 1 atm CO, 0.54 mmol NEt^tPr₂ and 2.7 mol% L for 96 h at 55°C in 1:1 CH₃CN/THF.

^bmol%. ^cNMR (isolated). ^dIn CD₃CN.

2.1.3 Palladium Catalyzed Synthesis of β -Lactams

Particularly attractive about this process is that it provides a one step method to convert four readily available substrates into the β -lactam core. Indeed, previous syntheses of these amide-substituted β -lactams **2.1** involve up to a five-step synthesis.²⁶ This type of multicomponent coupling reaction (MCR) has become of growing interest due to their ability to provide simple, environmentally friendly syntheses of complex molecules.²⁷ In addition, this general class of reaction can be adapted to provide a one step synthesis of families of products, as illustrated in Table 2.2. This coupling process proceeds cleanly with a number of imines and acid chlorides, all generating β -lactams in good yields. Importantly, functionalities such as aromatic ethers **2.1e**, thioethers **2.1b** and heteroaromatics **2.1f** and **2.1g** do not appear to inhibit the reaction. In addition, both aryl and alkyl acid chlorides can be employed. However, the yields of β -lactams are lower with electron withdrawing substituents on the imine **2.1c** and **2.1h**. The latter is likely a consequence of the lower nucleophilicity of these imines, which inhibits their interaction with the acid chloride (*vide infra*). Considering that this reaction involves the simultaneous coupling of 4 reagents with the formation of 4 new bonds, these all represent efficient β -lactam syntheses.

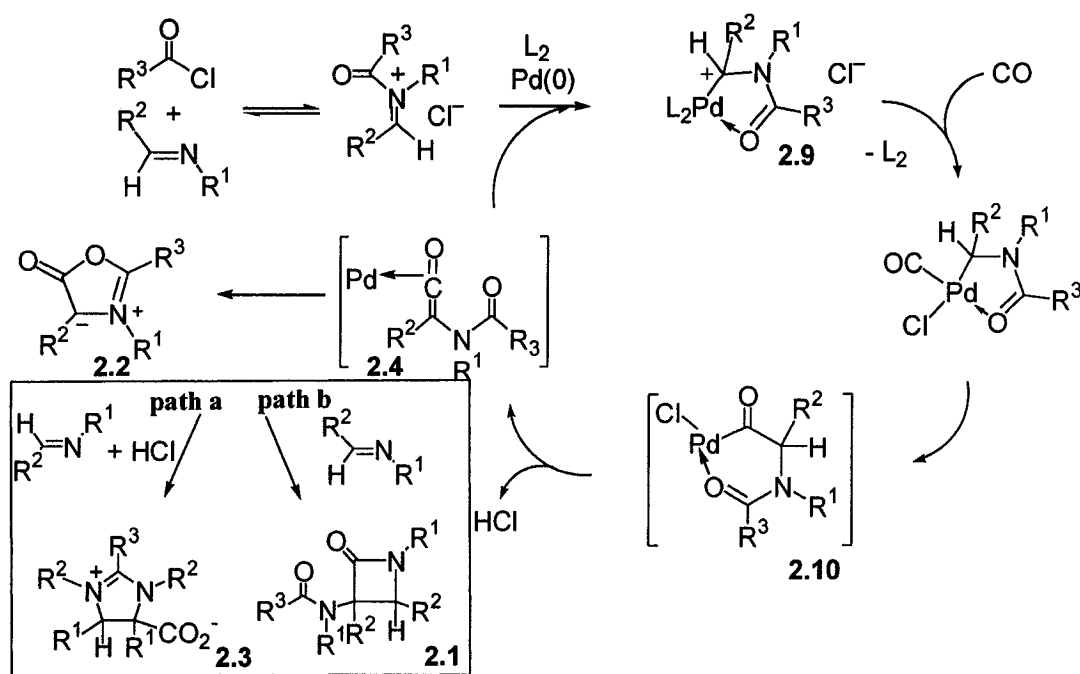
Table 2.2 Palladium Catalyzed Synthesis of β -Lactams^a



#	R ¹	X	R ³	%Yield ^b
2.1a	Bn	H	Ph	64 (50)
2.1b	Bn	CH ₃	Ph	68 (55)
2.1c	Bn	SCH ₃	Ph	60 (45)
2.1d	Bn	CF ₃	Ph	38 (32)
2.1e	Bn	H	<i>i</i> -Pr	50 (45)
2.1f		H	Ph	67 (53)
2.1g		H	Ph	68 (60)
2.1h		H	Ph	76 (60)
2.1i		H	Ph	37 (30)
2.1j	-hexyl	H	Ph	60 (55)
2.1k	-ethyl	H	Ph	63 (50)

^a 1.2 mmol imine, 0.54 mmol acid chloride, 1 atm CO, 0.54 mmol NEtⁱPr₂, 1.4 mol% Pd₂(dba)₃·CHCl₃, and 2.7 mol% L for 96 h at 55°C in 1:1 CH₃CN/THF. ^bNMR (isolated).

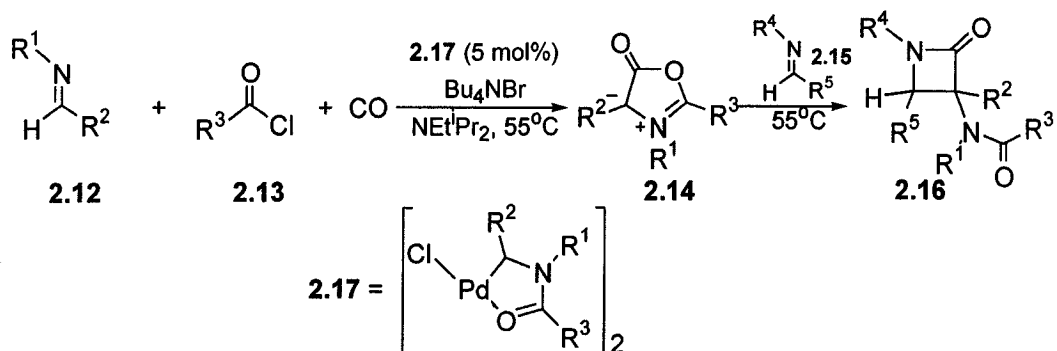
The mechanism of this coupling (Scheme 2.2) is believed to be similar to that reported for the synthesis of imidazolines.²⁰ The oxidative addition of the *in situ* generated *N*-acyl iminium salt to Pd(0) would generate complex **2.9**, as has been previously characterized.^{20, 21} Following CO insertion, the loss of HCl from the palladium-bound α -amino acid complex **2.10** would form the Münchnone/ketene intermediate and regenerate Pd(0) for further catalysis. In the presence of EtNⁱPr₂ to remove HCl from the reaction mixture, imine cyclization occurs with the ketene isomer **2.4**, rather than Münchnone **2.2**, resulting in the generation of β -lactam **2.1**. Thus, by simply modifying the acid content in the catalytic mixture, the same palladium catalyzed coupling of imine, carbon monoxide and acid chloride can provide facile access to two separate classes of heterocyclic products: carboxylate-substituted imidazolines²⁰ and β -lactams (Scheme 2.2). The source of lower β -lactam yields under high palladium loading conditions (Table 2.1, entries 1-3) is suggested by control experiments, which show that Pd₂(dba)₃·CHCl₃ mediates the decomposition of **2.2**, albeit at a slower rate than its formation.^{29, 30}



Scheme 2.2 Palladium Catalyzed Synthesis of β -Lactams

As suggested by the mechanism of β -lactam formation, this coupling requires the incorporation of two identical imines. Employing two distinct imines in this reaction results in poor control, and the formation of a statistical mixture of β -lactam products (Scheme 2.2).³¹ However, we have previously shown (described in Chapter 4) that Münchnones can be generated from imine, acid chloride and CO in the absence of an imine trap.³² Thus, performing this catalytic coupling with one equivalent of imine, acid chloride and carbon monoxide allows for the generation of **2.14** (Table 2.3).³³ Subsequent addition of imine (1.5 eq.) and heating at $55^\circ C$ for 24 hours generates β -lactam products in good yields (Table 2.3). This latter approach provides a method to construct the β -lactam in a single pot with independent control of 5 separate substituents on the heterocyclic core.

Table 2.3 Heterocoupled β -Lactam Synthesis^a



#	Imine 2.12	Acid Chloride 2.13	Imine 2.15	β -Lactam 2.16 (% yield)
2.16a		PhCOCl		
2.16b		PhCOCl		
2.16c		PhCOCl		

^a 0.54 mmol imine **2.12** , 0.54 mmol Bu₄NBr , 0.76 mmol acid chloride, 0.84 mmol base, 5 mol% **2.17** and CO (4 atm) for 24-30 h at 55°C. Addition of Imine **2.15** and heating at 55°C for 24 h. **2.17** is preformed from imine **2.12**, acid chloride **2.13** and Pd₂(dba)₃·CHCl₃. (See ref. 20, 21, 32)

2.3 Conclusions

In conclusion, 3-amido substituted β -lactams can be readily prepared by the palladium catalyzed coupling of imine, carbon monoxide and acid chloride in the presence of amine base. Considering the mild conditions (1 atm CO, 55°C) and simple building blocks employed, this represents one of the most facile routes to access the β -lactam core. In addition, this coupling occurs to generate the 3-amido substituted β -lactams, providing ready access to non-natural versions of those β -lactams found to be of bio-relevance.³⁴ The utilization of this process to catalytically generate other α -amino acid derived products and/or heterocycles from imine and carbon monoxide, and the complete elucidation of the reaction mechanism, are currently the subject of research in our laboratories.

2.4 Experimental

General Procedures

Unless otherwise noted, all manipulations were performed under an inert atmosphere in a vacuum atmosphere 553-2 dry box or by using standard Schlenk or vacuum line techniques. Tris(dibenzylideneacetone) dipalladium chloroform adduct was obtained from Strem Chemical Co. (Catalog No.46-3010) and was used without further purification. Carbon monoxide (99.99%) was purchased from Matheson and used as received. Imines,³⁵ (benzoyl-benzyl-amino)-phenylacetic acid³⁶ and 3-Benzyl-2,4-

diphenyl-oxazolium-5-oxide **2.2**³⁷ were prepared using literature procedures. All other reagents were purchased from Aldrich and used as received. Tetrahydrofuran (THF) was distilled from sodium/benzophenone ketyl under nitrogen. Acetonitrile and methylene chloride were distilled from CaH₂ under nitrogen. Deuterated solvents were dried as their protonated analogues, but were transferred under vacuum from the drying agent, and stored over 3Å molecular sieves.

¹H, and ¹³C NMR spectra were recorded on Varian 300 and Varian 400 Spectrometers. Infrared spectra were recorded on a Nicolet Avatar 320 FT-IR. Elemental analyses were performed at Guelph Chemical Laboratories. HRMS was obtained from McGill University Mass Spectral Facility by Mr. Nadim Saade and from the McGill University Biomedical Mass Spectrometry Unit by Dr. Orval Mamer.

General Procedure for Catalytic Formation of β-Lactams

Imine (1.2 mmol) and acid chloride (0.54 mmol) were dissolved in 10 mL of CH₃CN/THF (1:1) solution and stirred for 15 min in a 50mL reaction bomb. To this solution was added (4S)-4-phenyl-(2-pyridinyl)-2-oxazoline (3.3 mg, 2.7 mol%), Pd₂(dba)₃.CHCl₃ ((C₆H₅CH=CHCOCH=CHC₆H₅)₃Pd₂.CHCl₃) (7.7 mg, 1.4 mol%), and diisopropylethylamine (77 mg, 0.59 mmol). The reaction bomb was evacuated once and pressurized with CO (g) (1 atm). The reaction mixture was stirred at 55°C for 5 days. The β-lactam product was isolated by chromatography on Silica Gel 60

using hexanes/ethyl acetate as eluent. The relative stereochemistry of the β -lactam was determined by NOESY1D. The structure was assigned based upon 2D-NMR spectroscopy (see Appendix B)

N-Benzyl-N-(1-benzyl-2-oxo-3,4-diphenyl-azetidin-3-yl)-benzamide (2.1a)

Yield: 58% isolated, white solid

$^1\text{H-NMR}$ (400 MHz, CDCl_3): δ 7.52 (d, 2H, 8Hz), 7.40-7.35 (3H, m), 7.28-7.67 (18H, m), 6.65 (d, 2H, 8Hz), 5.53(s, 1H), 4.98 (d, 1H, 15Hz), 4.92 (d, 1H, 17 Hz), 4.84 (d, 1H, 17Hz), 3.84 (d, 1H, 15Hz). $^{13}\text{C NMR}$ (101 MHz, CDCl_3): δ 174.0, 165.6, 138.3, 137.0, 135.6, 135.1, 134.3, 134.3, 130.0, 129.9, 129.6, 129.2, 128.1, 128.4, 128.3, 128.2, 128.1, 126.8, 126.8, 126.7, 81.2, 66.3, 52.3, 44.4. **IR** (KBr): ν_{CO} : 1753 cm^{-1} , 1639 cm^{-1} Elemental analysis calcd. for $\text{C}_{36}\text{H}_{30}\text{N}_2\text{O}_2$: C, 82.73; H, 5.79; N, 5.36; found: C, 82.57; H, 6.13; N, 5.32

N-Benzyl-N-(1-benzyl-2-oxo-3,4-di-p-tolyl-azetidin-3-yl)-benzamide (2.1b)

Yield: 61% isolated, white solid

$^1\text{H-NMR}$ (400 MHz, CDCl_3): δ 7.38 (d, 2H, 8Hz), 7.36-7.01 (17H, m), 6.98 (d, 2H, 8Hz), 6.63 (d, 2H, 8Hz), 5.44(s, 1H), 4.90 (d, 1H, 15Hz), 4.86 (d, 1H, 17 Hz), 4.72 (d, 1H, 17Hz), 3.88(d, 1H, 15Hz), 2.27(s, 3H), 2.23 (s, 3H) $^{13}\text{C NMR}$ (101 MHz, CDCl_3): δ 173.8, 165.8, 138.6, 138.0, 137.9, 137.1, 135.2, 132.5, 131.2, 129.8, 129.7, 129.5, 129.2, 129.1, 128.8, 128.8, 128.3, 128.2, 128.2, 128.1, 126.7,

126.6, 80.7, 66.2, 52.1, 44.2, 21.5, 21.4. IR (KBr): ν_{CO} : 1751 cm^{-1} , 1638 cm^{-1}

Elemental analysis calcd. for $\text{C}_{38}\text{H}_{34}\text{N}_2\text{O}_2$: C, 82.88; H, 6.22; N, 5.09; found: C, 82.57; H, 6.54; N, 5.11

N-Benzyl-N-[1-benzyl-2,3-bis-(4-methylsulfanyl-phenyl)-4-oxo-azetidin-3-yl]-

benzamide (2.1c)

Yield: 45% isolated, white solid

$^1\text{H-NMR}$ (400 MHz, CD_3CN): δ 7.44-7.33 (m, 6H), 7.28-7.15 (m, 8H), 7.11-7.00 (m, 7H), 6.80 (d, 2H, 8Hz), 5.47(s, 1H), 4.82(d, 1H, 15Hz), 4.82 (d, 1H, 17 Hz), 4.71(d, 1H, 17Hz), 3.97(d, 1H, 15Hz), 2.44(s, 3H), 2.41(s, 3H) $^{13}\text{C NMR}$ (75.5 MHz, CD_3CN): δ 173.6, 165.4, 139.2, 138.9, 138.6, 137.2, 135.6, 131.9, 131.2, 130.2, 129.7, 129.1, 129.0, 128.4, 128.2, 128.1, 126.8, 126.6, 126.6, 125.2, 125.2, 80.8, 66.6, 51.6, 44.5, 14.5, 14.5. IR (KBr): ν_{CO} : 1752 cm^{-1} , 1638 cm^{-1}

Elemental analysis calcd. for $\text{C}_{38}\text{H}_{34}\text{N}_2\text{O}_2\text{S}_2$: C, 74.23; H, 5.57; N, 4.56; found: C, 74.22; H, 5.20; N, 4.49

N-Benzyl-N-[1-benzyl-2-oxo-3,4-bis-(4-trifluoromethyl-phenyl)-azetidin-3-yl]-

benzamide (2.1d)

Yield: 32% isolated, white solid

$^1\text{H-NMR}$ (400 MHz, CD_3CN): δ 7.55 (d, 2H, 8Hz), 7.48-7.32 (m, 12H), 7.24 (d, 2H, 8Hz), 7.05(m, 5H), 6.81 (d, 2H, 8Hz), 5.59 (s, 1H), 4.90(d, 1H, 15Hz), 4.87 (d,

1H, 17 Hz), 4.83(d, 1H, 17Hz), 4.06 (d, 1H, 15Hz) ¹³C NMR (75.5 MHz, CD₃CN): 173.8, 164.8, 139.7, 139.1, 137.9, 136.7, 135.2, 130.4, 130.2, 130.1, 129.9, 129.8, 129.5, 129.3, 129.1, 129.1, 128.6, 128.2, 126.9, 126.9, 126.3, 126.1, 124.8, 124.8, 124.7, 122.5, 81.0, 66.3, 51.9, 45.0 IR (KBr): ν_{CO}: 1759 cm⁻¹, 1643 cm⁻¹ Elemental analysis calcd. for C₃₈H₂₈F₆N₂O₂: C, 69.30; H, 4.28; N, 4.25; found: C, 69.25; H, 3.93; N, 4.05

N-Benzyl-N-(1-benzyl-2-oxo-3,4-di-p-tolyl-azetidin-3-yl)-isobutyramide (2.1e)

Yield: 45% isolated, white solid

¹H-NMR (400 MHz, CDCl₃): δ 7.31 (d, 2H, 8Hz), 7.31-6.98 (10H, m), 6.97 (d, 2H, 8Hz), 6.88 (d, 2H, 8Hz), 6.56 (d, 2H, 8Hz), 5.40(s, 1H), 5.07 (d, 1H, 18Hz), 4.85 (d, 1H, 15 Hz), 4.54 (d, 1H, 18Hz), 3.69 (d, 1H, 15Hz), 2.48(m, 1H), 2.26(s, 3H), 2.21(s, 3H), 0.97(d, 3H), 0.91(s, 3H) ¹³C NMR (101 MHz, CDCl₃): δ 179.5, 165.5, 138.8, 137.9, 137.7, 135.3, 133.0, 131.3, 129.4, 129.2, 129.0, 128.9, 128.8, 128.1, 127.0, 125.6, 80.4, 66.1, 49.8, 44.0, 43.4, 31.7, 21.4, 21.3, 19.5, 19.4 IR (KBr): ν_{CO}: 1755 cm⁻¹, 1652 cm⁻¹ Elemental analysis calcd. for C₃₅H₃₆N₂O₂: C, 81.36; H, 7.02; N, 5.42; found: C, 81.58; H, 6.73; N, 5.26

N-(4-Methoxy-benzyl)-N-[1-(4-methoxy-benzyl)-2-oxo-3,4-diphenyl-azetidin-3-yl]-benzamide (2.1f)

Yield: 53% isolated, white solid

¹H-NMR (400 MHz, CD₃CN): δ 7.42 (d, 2H, 8Hz), 7.35-7.09 (15H, m), 6.94 (d, 2H, 8Hz), 6.62 (d, 2H, 8Hz), 6.56 (d, 2H, 8Hz), 5.48(s, 1H), 4.80 (d, 1H, 15Hz), 4.76 (d, 1H, 17 Hz), 4.66 (d, 1H, 17Hz), 3.91(d, 1H, 15Hz), 3.81(s, 3H), 3.70(s, 3H) ¹³C NMR (101 MHz, CD₃CN): δ173.5, 165.5, 159.6, 158.5, 137.5, 135.9, 135.7, 134.8, 130.5, 130.4, 129.7, 129.6, 129.5, 128.4, 128.2, 128.1, 128.0, 127.9, 127.6, 126.6, 114.3, 113.5, 81.3, 66.7, 55.2, 55.0, 51.1, 43.9. IR (KBr): ν_{CO}: 1754 cm⁻¹, 1640 cm⁻¹ Elemental analysis calcd. for C₃₈H₃₄N₂O₄: C, 78.33; H, 5.88; N, 4.81; found: C, 78.14; H, 6.14; N, 4.81

N-Furan-2-ylmethyl-N-(1-furan-2-ylmethyl-2-oxo-3,4-diphenyl-azetidin-3-yl)-benzamide (2.1g)

Yield: 60% isolated, white solid

¹H-NMR (400 MHz, CDCl₃): δ 7.40-6.95 (m, 17H), 6.31 (m, 1H), 6.16 (m, 1H), 5.93 (m, 1H), 5.60 (m, 1H), 5.46(s, 1H), 4.90 (d, 1H, 15Hz), 4.89 (d, 1H, 17 Hz), 4.80 (d, 1H, 17Hz), 4.01(d, 1H, 15Hz) ¹³C NMR (75.5 MHz, CD₃CN): δ173.6, 165.9, 151.2, 149.1, 143.2, 141.7, 137.1, 135.0, 134.8, 130.0, 129.4, 129.3, 128.6, 128.3, 128.1, 128.1, 127.8, 127.0, 126.8, 117.6, 110.8, 110.4, 109.3,

107.9, 81.6, 67.5, 45.5, 37.5 IR (KBr): ν_{CO} : 1758 cm^{-1} , 1644 cm^{-1} Elemental analysis calcd. for $\text{C}_{32}\text{H}_{26}\text{N}_2\text{O}_4$: C, 76.48; H, 5.21; N, 5.57 ; found: C, 76.83; H, 5.59; N, 5.60

N-(2-Oxo-3,4-diphenyl-1-thiophen-2-ylmethyl-azetidin-3-yl)-N-thiophen-2-ylmethyl-benzamide (2.1h)

Yield: 60% isolated, white solid

$^1\text{H-NMR}$ (400 MHz, CDCl_3): δ 7.47-7.03 (m, 15H), 6.94 (m, 1H), 6.88 (m, 1H), 6.81 (m, 1H), 6.51 (m, 2H), 6.08 (m, 1H), 5.48(s, 1H), 5.15 (d, 1H, 17Hz), 5.13 (d, 1H, 15 Hz), 5.00 (d, 1H, 17Hz), 4.11(d, 1H, 15Hz) $^{13}\text{C NMR}$ (75.5 MHz, CDCl_3) : δ 173.8, 165.9, 141.1, 136.9, 136.9, 135.2, 134.2, 130.2, 130.0, 129.4, 128.6, 128.4, 128.3, 128.1, 128.1, 127.9, 127.4, 127.1, 126.5, 126.3, 125.0, 81.3, 66.3, 47.7, 38.7 IR (KBr): ν_{CO} : 1754 cm^{-1} , 1641 cm^{-1} Elemental analysis calcd. for $\text{C}_{32}\text{H}_{26}\text{N}_2\text{O}_2\text{S}_2$: C, 71.88; H, 4.90; N, 5.24 ; found: C, 71.76; H, 5.10; N, 5.28

N-(4-Methoxy-phenyl)-N-[1-(4-methoxy-phenyl)-2-oxo-3,4-di-p-tolyl-azetidin-3-yl]-benzamide (2.1i)

Yield: 30% isolated, white solid

$^1\text{H-NMR}$ (400 MHz, CDCl_3): δ 7.36-7.30 (8H, m), 7.24 (d, 2H, 9Hz), 7.23-7.11 (m, 3H, 8Hz), 6.97 (d, 2H, 8Hz), 6.86 (d, 2H, 9Hz), 6.79 (d, 2H, 8Hz), 6.60-6.50(m, 2H), 6.17(s, 1H), 3.73(s, 3H), 3.66(s, 3H), 2.25(s, 3H), 2.21(s, 3H) $^{13}\text{C NMR}$

(101.1 MHz, CDCl₃): δ 172.7, 162.7, 159.0, 156.4, 137.9, 137.8, 137.0, 133.1, 132.4, 131.9, 131.9, 131.0, 130.2, 129.6, 129.1, 129.0, 128.6, 128.5, 128.4, 127.9, 119.5, 114.5, 113.5, 81.6, 67.4, 55.7, 55.3, 21.5, 21.4 **IR** (KBr): ν_{CO} : 1751 cm⁻¹, 1650 cm⁻¹ Elemental analysis calcd.: C, 78.33; H, 5.88; N, 4.81 ; found: C, 78.18; H, 5.88; N, 4.51

N-Hexyl-N-(1-hexyl-2-oxo-3,4-diphenyl-azetidin-3-yl)-benzamide (2.1j)

Yield: 55% isolated, oil

¹H-NMR (400 MHz, CD₃CN): δ 7.48-7.42 (m, 7H), 7.34-7.31 (m, 2H), 7.17-7.12(m, 6H), 5.56 (s, 1H), 3.68-3.50 (m,2H), 3.50-3.35 (m, 1H), 2.95-2.84 (m, 1H), 1.58-0.68 (m, 22H) **¹³C NMR** (75.5 MHz, CD₃CN): δ 173.1, 166.1 , 138.0, 136.5, 135.2, 129.7, 129.5, 129.4, 128.7, 128.1, 128.0, 127.9, 127.8, 126.8, 81.2, 67.0, 48.9, 40.1, 31.2, 30.8, 29.9, 27.0, 26.7, 26.0, 22.6, 22.1, 13.6, 13.4. **IR** (KBr): ν_{CO} : 1754 cm⁻¹, 1639 cm⁻¹ Elemental analysis calcd. for C₃₄H₄₂N₂O₂ : C, 79.96; H, 8.29; N, 5.49; found: C, 79.69; H, 8.63; N, 5.44

N-Ethyl-N-(1-ethyl-2-oxo-3,4-diphenyl-azetidin-3-yl)-benzamide (2.1k)

Yield: 50% isolated, white solid

¹H-NMR (300 MHz, CD₃CN): δ 7.54-7.43 (m, 6H), 7.36-7.20 (m,3H), 7.19-7.13 (m, 6H), 5.60 (s, 1H), 3.69 (m, 1H), 3.66 (m, 1H), 3.56 (m, 1H), 3.02 (m, 1H), 1.19(t, 3H, 7Hz), 0.71 (t, 3H, 7Hz) **¹³C NMR** (300 MHz, CD₃CN): δ 173.1, 165.9,

138.0, 136.6, 135.4, 130.0, 129.4, 129.4, 129.0, 128.7, 128.1, 128.0, 127.7, 126.8, 80.9, 66.6, 43.4, 35.5, 15.4, 12.0 IR (KBr): ν_{CO} : 1753 cm^{-1} , 1639 cm^{-1}
Elemental analysis calcd. for $\text{C}_{26}\text{H}_{26}\text{N}_2\text{O}_2$: C, 78.36; H, 6.58; N, 7.03; found: C, 78.89; H, 6.33; N, 7.10 HRMS calcd.: 399.2073; found; 399.2073

N-Benzyl-N-(1-ethyl-2-oxo-3,4-di-p-tolyl-azetidin-3-yl)-4-methyl-benzamide

(2.16a)

Yield: 65%, white solid

^1H NMR (30 MHz, CDCl_3): δ 7.37 (d, 2H, 8.20 Hz), 7.31 (m, 2H), 7.26-7.22 (m, 2H), 7.22-7.14 (m, 4H), 7.06 (d, 2H, 8.20 Hz), 6.96-6.88(m, 4H), 5.26 (s, 1H), 5.01 (d, 1H, 14.70 Hz), 3.81 (d, 1H, 14.70 Hz), 3.81 (d, 1H, 14.70 Hz), 3.81-3.45 (m, 2H), 2.37 (s, 3H), 2.25 (s, 3H), 2.23 (s, 3H), 0.67 (t, 3H). ^{13}C NMR (75.5 MHz, CD_3CN): δ 173.7, 166.6, 139.9, 137.8, 137.6, 135.4, 134.7, 133.3, 131.3, 129.5, 129.3, 129.0, 128.8, 128.7, 128.9, 128.1, 126.9, 81.2, 66.3, 44.4, 43.9, 21.9, 21.7, 21.6, 16.3. IR (CH_2Cl_2): ν_{CO} : 1750 cm^{-1} , 1633 cm^{-1} HRMS. Calculated for $\text{C}_{34}\text{H}_{34}\text{N}_2\text{O}_2$: 502.26203; found 502.22256 + $[\text{K}]^+$.

N-Benzyl-N-(1-benzyl-2-furan-2-yl-4-oxo-3-phenyl-azetidin-3-yl)-benzamide

(2.16b)

Yield: 49%, white solid.

¹H NMR (300 MHz, CDCl₃): δ 7.56 (d, 2H, 7.90 Hz); 7.42-7.32 (m, 4H), 7.26-7.12 (m, 11H), 7.12-7.00 (m, 4H), 6.75 (d, 2H, 7.91Hz), 7.04-6.96 (m, 2H), 6.33(m, 1H), 6.24 (m, 1H), 5.54 (s, 1H), 4.96-4.72 (m, 3H), 3.97 (d, 2H, 14.66 Hz) ¹³C NMR (75.5 MHz, CDCl₃): δ 173.8, 165.0, 148.3, 142.9, 142.7, 138.3, 136.6, 135.4, 135.0, 129.9, 129.1, 128.9, 128.3, 128.1, 126.7, 111.8, 111.6, 110.9, 110.7, 80.4, 61.0, 52.2, 45.3. IR (CH₂Cl₂): ν_{CO}: 1759 cm⁻¹, 1640 cm⁻¹ Calculated for C₃₄H₂₈N₂O₃: 512.20999; found 512.20999 + [H⁺]

N-Ethyl-N-(2-oxo-1-p-tolyl-1,4,5,9b-tetrahydro-2H-azeto[2,1-a]isoquinolin-1-yl)-benzamide (2.16c)

Yield: 48%, white solid

¹H NMR (300 MHz, CDCl₃): δ 7.73 (d, 1H, 7.62 Hz), 7.62-7.54 (m, 2H), 7.52-7.43 (m, 3H), 7.10-6.87 (m, 7H), 5.40 (s, 1H), 4.25 (m, 1H), 3.68 (q, 2H, 7.33 Hz), 3.20 (2H, 2H, 7.33 Hz), 3.20 (m, 2H), 2.80 (m, 1H), 2.20 (s, 3H), 1.07 (t, 3H, 7.33 Hz). ¹³C NMR (100 MHz, CDCl₃): δ 172.7, 167.1, 137.6, 137.4, 133.9, 132.0, 130.7, 129.9, 129.6, 128.9, 128.8, 128.7, 127.5, 127.3, 126.7, 81.3, 62.6, 45.0, 37.6, 29.4, 21.5, 16.5 IR (CH₂Cl₂): ν_{CO}: 1755 cm⁻¹, 1633 cm⁻¹ HRMS. Calculated for C₂₇H₂₆N₂O₂: 410.19943; found: 410.20071.

Reaction of 3-Benzyl-2,4-diphenyl-oxazolium-5-oxide³⁰ (2.2) with Ph(H)C=NBn and HCl

(Benzoyl-benzyl-amino)-phenylacetic acid³⁰ (12.5 mg, 0.036 mmol) was added to a CD₃CN (1 mL) solution of *N,N*-dicyclohexylcarbodiimide (8.9 mg, 0.043 mmol). To this, now intense yellow solution of 3-benzyl-2,4-diphenyl-oxazolium-5-oxide **2.2**, was added *N*-benzyl benzaldimine hydrochloride salt (12.5 mg, 0.054 mmol). The solution was heated for 1 hour at 55°C. This results in the formation of a colorless solution. ¹H-NMR analysis reveals the formation of 1,3-Dibenzyl-2,4,5-triphenyl-4,5-dihydro-1H-imidazole-4-carboxylate **2.3** (R¹= -CH₂Ph, R²=Ph and R³=Ph) in 99% NMR yield (vs. Internal standard: (CH₃)₃SiPh).

¹H-NMR (400 MHz, CDCl₃): δ 7.73-7.27 (16H, m), 7.04-6.89 (5H, m), 6.34 (d, 2H, 8Hz), 5.56 (s, 1H), 4.97 (d, 1H, 16Hz), 4.54 (d, 1H, 16Hz), 4.35 (d, 1H, 15Hz), 3.99(d, 1H, 15Hz), ¹³C NMR (400 MHz, CDCl₃): δ 166.3, 165.7, 135.6, 132.5, 132.3, 130.2, 129.9, 129.7, 129.5, 129.2, δ 129.1, 128.8, 128.5, 128.4, 128.2, 128.6, 127.6, 123.8, 84.3, 51.6, 49.5 IR (KBr): ν_{CO}: 1638 cm⁻¹

Reaction of 3-benzyl-2,4-diphenyl-oxazolium-5-oxide 2.2 with Ph(H)C=NBn

(Benzoyl-benzyl-amino)-phenylacetic acid (20 mg, 0.043 mmol) was added to a CD₃CN (1 mL) solution of dicyclohexylcarbodiimide (13.1mg, 0.047 mmol). To this, now intense yellow solution of 3-benzyl-2,4-diphenyl-oxazolium-5-oxide, was added

N-benzyl benzaldimine (11.2mg, 0.057mmol). The solution was heated over 54 hours at 60°C. ¹H-NMR analysis reveals the formation of **2.1** in 79% yield.

Reaction of 3-benzyl-2,4-diphenyl-oxazolium-5-oxide 2.2 with Pd₂(dba)₃·CHCl₃

(Benzoyl-benzyl-amino)-phenylacetic acid (12.5mg, 0.036 mmol) was added to a CD₃CN (1 mL) solution of *N,N*-dicyclohexylcarbodiimide (8.9mg, 0.043 mmol). To this, now intense yellow solution of 3-benzyl-2,4-diphenyl-oxazolium-5-oxide, was added Pd₂(dba)₃·CHCl₃ (1.9 mg, 5 mol%). The solution was heated for 18 hours at 57°C. ¹H-NMR analysis reveals the decomposition of 3-benzyl-2,4-diphenyl-oxazolium-5-oxide of 31%: (vs. Internal standard: (CH₃)₃SiPh). This reaction was compared to a reaction mixture that did not contain Pd₂(dba)₃·CHCl₃, which was heated to 57°C, for 18 hours. The latter shows no decomposition of 3-benzyl-2,4-diphenyl-oxazolium-5-oxide.

2.5 References

- 1) For reviews on the synthesis of β-lactams: a) Ratcliffe, R. W.; Albers-Schonberg, G. *Chemistry and Biology of β-Lactam Antibiotics*; Morin, R. B., Gorman, M., Eds.; Academic Press; N. Y., 1982, Vol. 2. b) Carruthers, W. in *Cycloaddition Reactions in Organic Synthesis*, Pergamon Press: Oxford, 1990. c) Hart, D. J.; Ha, D.-C. *Chem. Rev.* **1989**, *89*, 1447. d) Southgate, R.; Branch, C.; Coulton, S.; Hunt, E. in *Recent Progress in the Chemical Synthesis of Antibiotics and Related Microbial Products*, vol. 2 (Ed: G. Lukacs.) Springer-Verlag, Berlin e) Palomo, C.; Aizpurua,

- J. M.; Ganboa, I.; Oiarbide, M. *Eur. J. Org. Chem.* **1999**, 3223. f) Singh, G.S. *Tetrahedron* **2003**, *59*, 7631.
- 2) a) *Recent Advances in the Chemistry of β -Lactam Antibiotics*, Brown, A.G.; Roberts, S. M., Eds. The Royal Society of Chemistry, London, **1985** b) *Cephalosporins and penicillins: chemistry and biology*. Flynn, E.H. Academic Press. **1972**. c) Singh, G.S. *Mini-Rev. Med. Chem.* **2004**, *4*, 93. d) Singh, G.S. *Mini-Rev. Med. Chem.* **2004**, *4*, 69. e) Hwu, J.; Ethiraj, K.; Hakimelahi, G.H. *Mini-Rev. Med. Chem.* **2003**, *3*, 305. f) Sader, H.; Gales, A.C. *Drugs* **2001**, *61*, 553.
- 3) For an example of the utilization of β -lactams in organic synthesis, see: a) Ojima, I.; Delalogue, F. *Chem. Soc. Rev.* **1997**, *26*, 377. b) Alcaide, B.; Almendros, P. *Chem. Soc. Rev.* **2001**, *30*, 226. c) Alcaide, B.; Almendros, P.; Aragoncillo, C.; *Chem. Eur. J.* **2002**, *8*, 3646. d) Klapars, A.; Parris, S.; Anderson, K.W.; Buchwald, S.L. *J. Am. Chem. Soc.* **2004**, *126*, 3529.
- 4) a) Cheng, J.; Deming, T.J. *J. Am. Chem. Soc.* **2001**, *123*, 9457. b) Cheng, R.P.; Gellman, S.H.; DeGrado, W.F. *Chem. Rev.* **2001**, *101*, 3219.
- 5) For the carbonylative ring-expansion of aziridines: a) Khumtaveeporn, K.; Alper, H. *Acc. Chem. Res.* **1995**, *28*, 414. b) Piotti, M. E.; Alper, H. *J. Am. Chem. Soc.* **1996**, *118*, 111. c) Davoli, P.; Moretti, I.; Prati, F.; Alper, H. *J. Org. Chem.*, **1999**, *64*, 518. d) Magriotis, P.A. *Angew. Chem. Int. Ed.* **2001**, *40*, 4377. e) Mahadevan, V.; Geltzer, Y.D.Y.L.; Coates, G.W. *Angew. Chem. Int. Ed.* **2001**, *41*, 2781. f) Lu, S.-M.; Alper, H. *J. Org. Chem.* **2004**, *69*, 3558.

- 6) For the carbonylation of allyl phosphates: a) Zhou, Z.; Alper, H. *J. Org. Chem.*, **1996**, *61*, 1256. b) Tanaka, H.; Abdul Hai, A. K. M.; Sadakane, M.; Okumoto, H.; Torii, S. *J. Org. Chem.*, **1994**, *59*, 3040.
- 7) For the carbonylation of allyl halides: a) Kim, T.-J.; Shim, S.- C.; Kim, M.- C. *Bull. Kor. Chem. Soc.* **2000**, *21*, 541. b) Troisi, L.; De Vitis, L.; Granito, C.; Epifani, E. *Eur. J. Org. Chem.*, **2004**, 1357.
- 8) For the carbonylation of bromoallylamine derivatives: a) Mori, M.; Chiba, K.; Okita, M.; Ban, Y. *Tetrahedron* **1985**, *41*, 375. b) Chiba, K.; Mori, M.; Ban, Y. *J. Chem. Soc., Chem. Commun.* **1980**, 770. c) Mori, M.; Chiba, K.; Okita, M.; Ban, Y. *J. Chem. Soc., Chem. Commun.* **1979**, 698.
- 9) Fujieda, H.; Kanai, M.; Kmbara, T.; Iida, A.; Tomioka, K. *J. Am. Chem. Soc.* **1997**, *119*, 2060 and references therein.
- 10) Ojima, I.; Park, Y. H.; Sun, C. M.; Brigaud, T.; Zhao, M. *Tetrahedron Lett.* **1992**, *33*, 5737.
- 11) Annunziata, R.; Ciquini, M.; Cozzi, F.; Molteni, V.; Schupp, O. *J. Org. Chem.* **1996**, *61*, 8293.
- 12) Doyle, M. P.; Kalinin, A. V. *Synlett*, **1995**, 1075.
- 13) Shintani, R.; Fu, G.C. *Angew. Chem., Int. Ed. Engl.* **2003**, *42*, 4082.
- 14) Townes, J.A.; Evans, M.A.; Queffelec, J.; Taylor, S.J.; Morken, J.P. *Org. Lett.* **2002**, *4*, 2537
- 15) Lawlor, M.D.; Lee, T.W.; Danheiser, R.L. *J. Org. Chem.* **2000**, *65*, 4375

- 16 a) Hegedus, L. S.; Montgomery, J.; Narukawa, Y.; Snustad, D. C. *J. Am. Chem. Soc.* **1991**, *113*, 5784. b) Hegedus, L. S., McGuire, J. *J. Am. Chem. Soc.* **1982**, *104*, 5538.
- 17 a) Annis, G.D.; Hebblethwaite, E.M.; Hodgson, S.T.; Hollingshead, D.M.; Ley, S.V. *J. Chem. Soc. Perkin Trans. I* **1983**, 2851. b) Berryhill, S.R.; Price, T.; Rosenblum, M. *J. Org. Chem.* **1983**, *48*, 158. c) Ley, S. V.; Cox, L. R.; Meek, G. *Chem Rev*, **1996**, *96*, 423.
- 18) Collman, J.P.; Hegedus, L.S.; Norton, J.R.; Finke, R.G. *Principles and Applications of Organotransition Metal Chemistry*, 2nd Edition. University Science Books, **1987**, 235-458.
- 19) See Ref. 2
- 20) Dghaym, R.D.; Dhawan, R.; Arndtsen, B.A. *Angew. Chem. Int. Ed.* **2001**, *40*, 3228.
- 21) Dhawan, R.; Dghaym, R.D.; Arndtsen, B.A. *Cat. Org. React.* **2003**, *89*, 499.
- 22 a) Dalla Croce, P.; Ferraccioli, R.; La Rosa, C. *Tetrahedron Lett.* **1995**, *51*, 9385.
b) Huisgen, R.; Funke, E.; Schaefer, F. C.; Knorr, R. *Angew. Chem. Int. Ed.* **1967**, *6*, 367
- 23 a) Mesoionic Ring Systems by K.T. Potts in *1,3 Dipolarcycloaddition Chemistry* A. Padwa Ed. pg. 1-81. **1983** John Wiley & Sons Inc. New York b) Mesoionic Oxazoles by H.L. Gingrich and J.S. Baum in *Oxazoles*. I.J. Turchi Ed. 731-958. **1984** John Wiley & Sons Inc. New York c) Mesoionic Ring Systems by G.W. Gribble in *Synthetic Applications of 1,3-Dipolar Cycloaddition Chemistry Toward Heterocycles and Natural Products*. **2002** John Wiley & Sons Inc. New York . A.

- Padwa Ed. pg. 681-753. d) Mesoionic Oxazoles by G.W. Gribble in *Oxazoles: Synthesis, Reactions, and Spectroscopy Part. A.* Ed. D.C. Palmer **2003**, John Wiley & Sons. New York.
- 24) For synthesis of **2.2**, see: Gribble, G.W.; Sponholtz, W.R.; Switzer, F.L.; D'Amato, F.J.; Byrn, M.P. *Chem. Comm.* **1997**, 993.
- 25) ¹H NMR of this reaction mixture shows a complex mixture of decomposition products in addition to **2.2**. See footnote 28.
- 26) see ref. 23.
- 27) Armstrong, R. W.; Combs, A. P.; Tempest, P. A.; Brown, S. D.; Keating, T. A. *Acc. Chem. Res.* **1996**, *29*, 123.
- 28) The role of the bidentate ligand in this process appears to be through inhibition of the formation of 2-benzyl-3-phenyl-1-isoindolinone. The latter, which is formed in ca. 15-20% in the absence of ligand, likely arises from the C-H bond activation of the aromatic R³ in intermediate **2.8**. The discussion of this process will be the subject of a future report.
- 29) The generation of **2.2** in the presence of 5 mol% Pd₂(dba)₃·CHCl₃ in CD₃CN, followed by heating to 55°C for 24 h, results in the decomposition of ca. 30% of **2.2** (determined by ¹H NMR vs. an internal standard) to an unidentifiable mixture of products. A similar reaction without Pd₂(dba)₃·CHCl₃ present shows no appreciable loss of **2.2** after heating to 55°C for 24 h.
- 30) For an example of the inhibiting effect of dba on palladium catalysis with azlactones, see: Liu, X.; Hartwig, J.F. *Org. Lett.* **2003**, *5*, 1915.

- 31) Reaction of PhC(H)=NBn (10 mg, 0.051mmol), PhC(H)=NPMB (12.3 mg, 0.051mmol) (PMB = $-(\text{CH}_2)_p\text{-C}_6\text{H}_4\text{OCH}_3$), PhCOCl (7.2 mg, 0.051mmol), Pd₂(dba)₃·CHCl₃ (1.3 mg, 5 mol%), NEt^tPr₂ (6.6 mg, 0.051mmol) and CO (1 atm.) in CD₃CN (1 mL) at 55°C for 48 hours.
- 32) See Chapter 4 for full discussion on Münchnone formation. Also see: Dhawan, R.; Dghaym, R.D.; Arndtsen, B.A. *J. Am. Chem. Soc.* **2003**, *125*, 1474.
- 33) For other metal-based routes to Münchnones, see: a) Merlic, C. A.; Baur, A.; Aldrich, C. C. *J. Am. Chem. Soc.* **2000**, *122*, 7398; b) Alper, H.; Tanaka, M. *J. Am. Chem. Soc.* **1979**, *101*, 4345.
- 34) see Ref. 2
- 35) Layer, R. W. *Chem. Ber.* **1963**, *63*, 489.
- 36) Gribble, G.W., Sponholtz III, W.R., Switzer, F.L, D'Amato, F.J. and Byrn, M.P. *Chem. Comm.* **1997**, 993.
- 37) Consonni, R., Dalla Croce, P., Ferraccioli, R., La Rosa, C. *J. Chem. Res.*, **1991**, 188.

CHAPTER THREE

The Palladium Catalyzed Synthesis of Carboxylate-Substituted Imidazolines: A New Route Using Imines, Acid Chloride and Carbon Monoxide*

Preface

In Chapter 2, we discussed the palladium catalyzed four component coupling of imines, acid chloride, and carbon monoxide towards the generation of β -lactams. The generation of these four membered heterocycles was considered to proceed through the initial formation of Münchnones, which are also a common intermediate in the synthesis of the previously described imidazoline-carboxylates. In Chapter 3, attempts are made to completely characterize the various catalytic intermediates in the generation of β -lactams and imidazoline-carboxylates. In addition, we discuss the possible mechanistic pathways for imidazoline-carboxylate formation.

3.0 Introduction

The design of new methods to prepare peptide analogues, i.e. peptidomimetics, is an area of growing importance in pharmaceutical design.^{1, 2} The incorporation of peptidomimetics into peptides can lead to a number of beneficial features, including

* Previously Published: Dhawan, R.; Dghaym, R.D.; Arndtsen, B.A. *Catalysis of Organic Reactions*, **2003**, 89, 499.

increased proteolytic stability, improved bioavailability, decreased side-effects and higher selectivity and potency compared to the parent peptide sequence.¹ One such class of peptidomimetics are carboxylate-substituted imidazoline derivatives **3.1** (Figure 3.1). Compounds such as **3.1** have been shown to be suitable as peptidic amide bond replacements, as illustrated in **3.1a**.² This not only modifies the structural properties of the amino acid residue, but also stabilizes it towards degradation, thereby potentially enhancing its therapeutic utility.² Imidazoline-carboxylates can also be considered as non-naturally occurring proline derivatives (**3.1b**), and have been used as synthetic intermediates towards the synthesis of non-proteinogenic 1,2-diamino acids.³ The latter are useful building blocks for a variety of antibiotics, enzyme inhibitors and other biologically active peptide-based molecules.

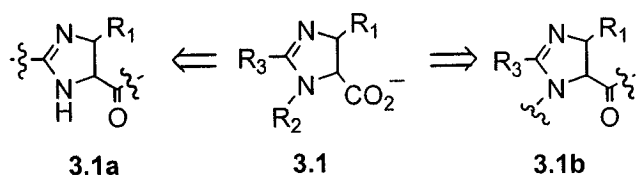


Figure 3.1 Utility of Imidazoline-Carboxylates

The synthesis of carboxylate-substituted imidazoline derivatives has previously been accomplished by the condensation of presynthesized 1,2-diamines with amides, or through the transition metal catalyzed aldol-type reaction between isocyanates and imines.^{4, 5} We have recently communicated an alternative palladium catalyzed route to synthesize a new class of imidazoline carboxylates, utilizing acid chloride, imines and carbon monoxide as starting materials (see Table 3.1).⁶ This work was the first demonstration of a goal in our laboratory of developing metal-mediated routes to

peptide-based molecules, using CO and imines as α -amino acid residue synthons. Notably, this process has the advantage of allowing for the synthesis of these heterocycles from readily available imine, acid chloride and carbon monoxide precursors, via a four component coupling methodology. As imines are derived from a large pool of commercially available aldehydes and amines, this methodology could lend itself to the synthesis of a number of new and structurally diverse imidazoline derivatives. In this report, we explore the scope and limitations of this catalytic process as a route to prepare imidazoline carboxylates. In addition, the mechanism by which the four separate components (imines, carbon monoxide and acid chloride) are coupled into the imidazoline product is also examined.⁷

3.1 Results and Discussion

3.1.1 Synthesis and Structure of Imidazole-Carboxylate 3.4

The reaction of a 1:1 mixture of Tol(H)C=NBn (**3.2**) (Tol= *p*-C₆H₄CH₃, Bn= CH₂C₆H₅) and PhCOCl (**3.3**) with 1 atm CO in the presence of 5 mol% Pd₂(dba)₃·CHCl₃ (dba= *trans, trans*-dibenzylideneacetone) and 2,2'-bipyridine (10 mol%) in CH₃CN leads to the slow disappearance of starting materials over the course of 4 days at 55°C. Filtration of the reaction mixture, followed by acid and base washing and recrystallization, yields the imidazoline derivative **3.4** as a white solid (82% yield; Table 3.1, entry 1). To our knowledge, N,N-disubstituted, imidazoline-carboxylates such as **3.4** have not been reported prior to this work. In addition, the mechanism by which they might be formed from imine, carbon

monoxide and acid chloride is not readily obvious (*vide infra*). Both of these features made the structural assignment of **3.4** challenging. Notably, both ^1H and ^{13}C NMR show two inequivalent imine units and one acid chloride phenyl ring incorporated into **3.4**. This is despite the presence of an equimolar amount of imine and acid chloride in the initial reaction mixture.⁸ The ^{13}C NMR shows the resonances for the imidazoline ring carbons (166.4, 81.4, and 72.2 ppm), along with an additional downfield peak for the carboxylate group (165.2 ppm). HMBC, HMQC and NOESY experiments are all consistent with the connectivity about the five-membered ring, with the substituents, as shown.

The structure of **3.4** has been definitively assigned by x-ray crystallography on the related N,N-dimethyl substituted imidazoline derivative (Table 3.1, entry 2). As illustrated in Figure 3.2, this clearly shows the incorporation of two imines, an acid chloride and carbon monoxide into the product, with an overall transoid orientation of the aromatic groups. The two imines are coupled through their carbons in the heterocyclic core, with one imine unit having its methine hydrogen replaced with the carboxylate group. In addition, the “CPh” unit of the benzoyl chloride bridges the two imine nitrogens, while the former acid chloride oxygen is coupled with CO into the carboxylate unit in the 4-position.

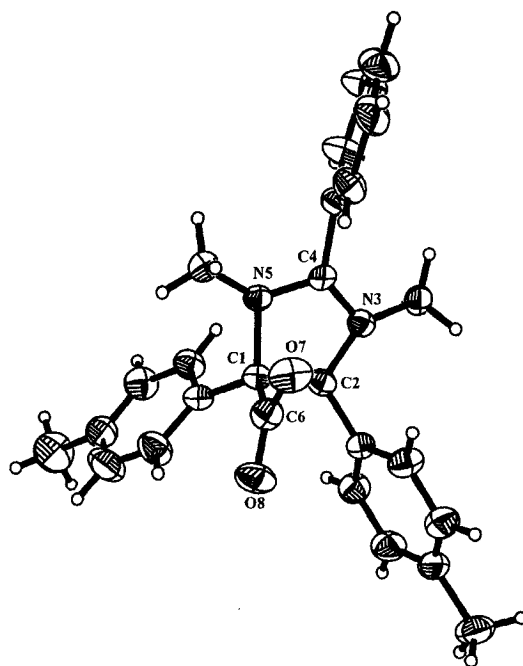


Figure 3.2 Crystal structure of N,N-dimethyl-2-phenyl-4,5-(p-tolyl)-imidazole-4-carboxylate (only one structure from unit cell shown). Selected bond lengths: C4-N5, 1.338 (8); C4-N3, 1.302 (8); C2-N3, 1.475 (7); C1-N5, 1.527 (7).

3.1.2 Scope of Catalytic Imidazoline-Carboxylate Synthesis

The overall scope of this catalytic transformation is summarized in Table 3.1. In general, this palladium catalyzed process proceeds in high yield with a range of imines of aromatic aldehydes. In particular, functionality within the imine fragment is tolerated, including ethers (entry c) and thioethers (entry d) and aromatic halides (entry e). More complex rings systems can also be generated via this process, including products such as the furfuryl- (entry i) and piperonal-based imidazolines (entry j). In addition, both aryl and alkyl acid chlorides can be utilized.

Table 3.1. Palladium Catalyzed Synthesis of Imidazoline-Carboxylates

#	Ligand	R ₁	R ₂	R ₃	% Yield ^b
a	bipy	PhCH ₂	p-tolyl	Ph	82
b	bipy	CH ₃	p-tolyl	Ph	92
c	bipy	CH ₃ OCH ₂ CH ₂	p-tolyl	Ph	78
d	bipy	PhCH ₂	p-CH ₃ SC ₆ H ₄	Ph	73
e	bipy	PhCH ₂	p-ClC ₆ H ₄	Ph	62
f	bipy	PhCH ₂	p-tolyl	CH ₃	70
g	bipy	PhCH ₂	p-NO ₂ C ₆ H ₄	CH ₃	-
h	bipy	Ph	p-tolyl	Ph	-
i ^d	-	2-furfuryl	p-tolyl	Ph	67
j ^d	-	PhCH ₂	2-piperonyl	Ph	50
k	-	PhCH ₂	<i>i</i> -butyl	Ph	-
l	-	PhCH ₂	-CH=CH C ₆ H ₅	Ph	-
m ^c	-	PhCH ₂	p-tolyl	Ph	83
n ^c	-	PhCH ₂	Ph	Ph	72
o	pyridine	PhCH ₂	p-tolyl	Ph	87
p ^c	diphos	PhCH ₂	p-tolyl	Ph	-

^a0.57 mmol imine, 0.57 mmol acid chloride, 1 atm CO with 5 mol % Pd₂(dba)₃·CHCl₃ and 10 mol% ligand for 4 days at 55 °C. ^bIsolated yield. ^c 24 h. ^d 48 h.

The efficiency of this coupling does show some dependence upon the electronic nature of the imine substrate employed. While good to excellent yields are obtained with the relatively electron rich p-CH₃C₆H₄, and p-CH₃SC₆H₄ aldimines, limitations

arise from imines that incorporate electron withdrawing groups. For example, the less electron rich $p\text{-ClC}_6\text{H}_4(\text{H})\text{C}=\text{NBn}$ gives slightly lower yields than its corresponding $p\text{-tolyl}$ derivative, while the nitro substituted $p\text{-NO}_2\text{C}_6\text{H}_4(\text{H})\text{C}=\text{NBn}$ (entry g) does not react to form imidazoline products. Similarly, $N\text{-aryl}$ substituted imines fail to yield any imidazoline-carboxylate product (entry h). This electronic effect may be attributed to the lower nucleophilicity of these imines, which could inhibit their interaction with acid chloride (*vide infra*). In addition, neither alkyl (entry k) nor alkenyl (entry l) substituents at the R_2 position are tolerated under these reaction conditions. The former may be related to the lower stability of alkyl-imines in the presence of acid chlorides.⁹ In spite of these limitations, this four component coupling strategy provides easy access to a range of diversely substituted imidazoline derivatives from inexpensive, flexible and readily available starting materials.

3.1.3 Mechanistic Studies: Palladium Catalysis

This imidazoline-carboxylate synthesis involves the coupling of four separate components (two imines, an acid chloride and carbon monoxide), and the generation of at least five separate bonds, all via a one-pot, palladium catalyzed process. From an analysis of the structure of the imidazoline carboxylate, the individual constituents can be seen (Figure 3.3). This structure might be considered to arise from the dipolar cycloaddition of an imine with a mesoionic 1,3-oxazolium-5-oxide (**3.5**) intermediate, which itself could be generated from imine, acid chloride and carbon monoxide. Consistent with this potential formulation, performing the catalytic reaction with

^{13}C O leads to the incorporation of the carbon-13 label into the carboxylate position of 3.4.

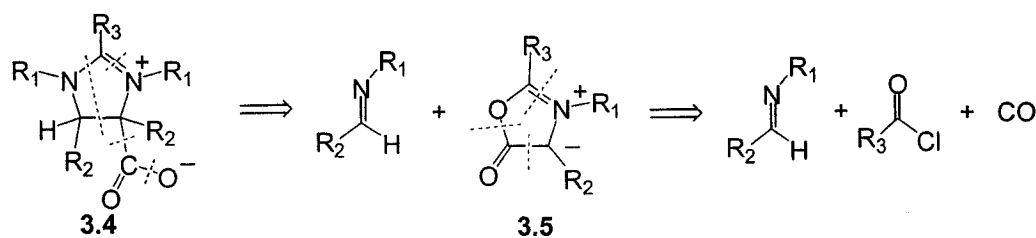
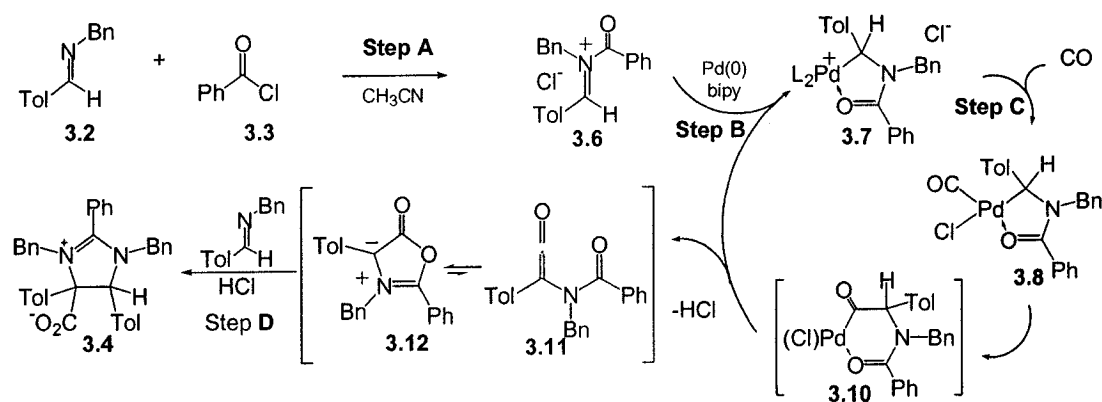


Figure 3.3 4-Component Coupling Approach to Imidazoline-Carboxylates

In order to further understand how this overall transformation proceeds, a series of mechanistic experiments have been performed, in which the catalytic cycle has been broken down into individual steps (Scheme 3.1). Firstly, monitoring the reaction *in situ* by ^1H and ^{13}C NMR clearly reveals that imine **3.2** with acid chloride **3.3** react immediately upon mixing, prior to the addition of $\text{Pd}_2(\text{dba})_3\text{CHCl}_3$, bipyridine, or carbon monoxide, to form the N-acyliminium salt **3.6** (Step **A**, Scheme 3.1).¹⁰ The structure of **3.6** can be confirmed by its independent synthesis from imine and acid chloride. The conversion of **3.2** and **3.3** to this iminium salt is essentially quantitative by ^1H NMR.

We have previously reported that N-acyliminium salts can undergo rapid oxidative addition to low valent metals to generate metal-chelated amides.¹¹ Similarly, the addition of the catalyst (5 mol% $\text{Pd}_2(\text{dba})_3\text{CHCl}_3$ and 10% bipyridine) to this solution of **3.6** (Step **B**, Scheme 3.1) results in the rapid conversion of the palladium source into a new complex (**3.7**). This same complex **3.7** can be prepared and isolated upon the stoichiometric reaction of **3.6**, 0.5 equiv. $\text{Pd}_2(\text{dba})_3\text{CHCl}_3$ and 0.5 equiv.

bipyridine in CH₃CN, and has been characterized to be the amide-chelated palladium complex (bipy)Pd[η²-CH(Tol)NBn(CO)Ph]⁺Cl⁻ (**3.7**). Of note, the ¹H NMR of **3.7** shows the presence of the methine iminium salt hydrogen singlet shifted upfield to 5.11 ppm, consistent with the reduction of the C=N upon addition to palladium, and the presence of diastereotopic benzylic hydrogens (δ 4.32, dd). In addition, the amide carbonyl resonance is shifted downfield of a free amide to 180.5 ppm in the ¹³C NMR, consistent with its chelation to the palladium center. All other spectroscopic and mass spectrometry data are consistent with this structure, and directly analogous to the previously reported (bipy)Pd[η²-C(H)TolNBnCOCH₃]⁺OTf.¹²



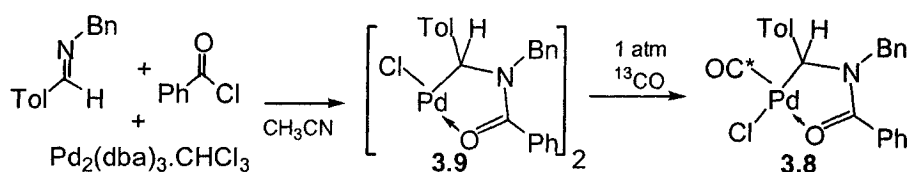
Scheme 3.1 Mechanism of Imidazoline-Carboxylate Formation

The addition of 1 atm ¹³CO to the CD₃CN solution of **3.6** and **3.7** generates the final catalysis mixture, and also allows the observation of a third potential intermediate in the catalytic cycle (Step C, Scheme 3.1). Examination of this solution by ¹H and ¹³C NMR reveals the presence of a stoichiometric amount of **3.6**, palladium catalyst **3.7**, and the partial conversion (ca. 10%) of complex **3.7** into a new structure. This

compound, **3.8** has ^1H and ^{13}C NMR resonances for an amide ligand analogous to that in complex **3.7** (δ 6.13 (s, 1H, C(H)Tol), 4.58 (dd, 2H, CH_2Ph), though shifted downfield from the original complex. In addition, the ^{13}C NMR of the catalytic mixture reveals the presence of a labeled carbonyl resonance at 174.9 ppm, suggesting the coordination of a CO ligand in **3.8**. Our original postulate for the structure of **3.8** was that CO coordination to Pd occurred via dechelation of the amide oxygen, in analogy to the reactivity observed in palladium catalyzed sequential olefin/CO insertion.¹³ Once again, the identity of this reaction intermediate has been determined by its independent synthesis.

The reaction of equimolar amounts of imine **3.2** and acid chloride **3.3** with 0.5 equivalents of $\text{Pd}_2(\text{dba})_3\cdot\text{CHCl}_3$ in CH_3CN leads to the generation of $\{\text{Pd}(\text{Cl})[\eta^2\text{-CH}(\text{Tol})\text{NBnCOPh}]\}_2$ (**3.9**), which can be isolated as a yellow powder (Eq. 3.1). The addition of ^{13}CO to a CD_3CN solution of this complex results in its rapid reaction, and generation of the same complex observed in the catalytic reaction mixture. The formation of **3.8** in the absence of bipyridine demonstrates that this ligand has dissociated from the metal center in the catalytic reaction. IR ($\nu_{\text{CO}} = 2114 \text{ cm}^{-1}$ in CH_3CN) and ^{13}C NMR (174.9 ppm) confirms the presence of a single coordinated CO ligand in **3.8**, as well as the chelated amide ligand (179.1 ppm). In addition, no IR stretch was observed between 1650 and 1800 cm^{-1} , suggesting that CO has not undergone insertion into the palladium-carbon bond. The structure of **3.8** has been tentatively assigned as the CO coordinated amide-chelated complex shown. Thus, it appears that during catalysis the chloride and carbon monoxide together act to create

an empty coordination site on the palladium center for CO via the displacement of the bipyridine ligand, rather than dechelation of the amide oxygen. Consistent with this hypothesis, imidazoline formation is inhibited by the use of a strongly coordinating diphos ligand (Table 3.1, entry p), while the absence of any ligand (which should facilitate the generation of **3.8**) results in a significantly increased rate of catalysis (24h vs. 4 days, entry m).

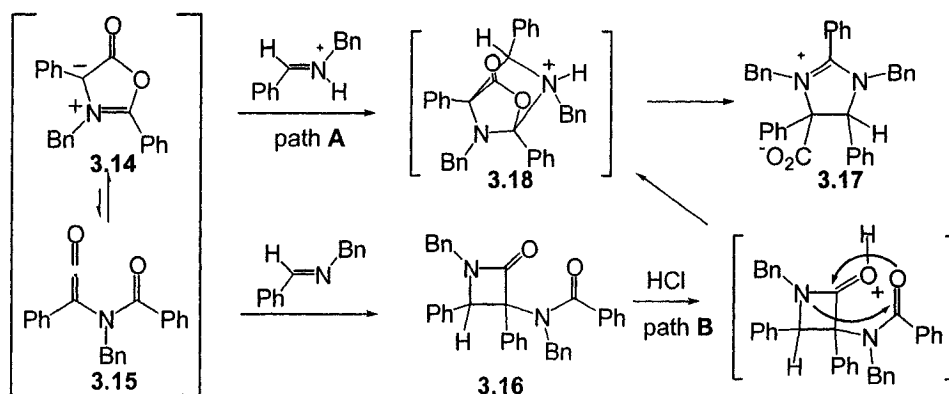


Equation 3.1 Carbonylation of Complex **3.9** to generate **3.8**

While warming the catalysis mixture to 55°C (Step **D**, Scheme 3.1) leads to no other observable reaction intermediates, the generation of intermediate **3.8** would allow the series of steps shown in Scheme 3.1. Insertion of the coordinated CO into the palladium-carbon bond would lead to the overall coupling of acid chloride, imine and carbon monoxide in complex **3.10**. The subsequent loss of HCl from **3.10**, either via direct deprotonation or β -H elimination, would form the α -amide substituted ketene **3.11**. The latter is known to be in rapid equilibrium with its cyclic mesoionic 1,3-oxazolium-5-oxide tautomeric **3.12**.¹⁴ These steps would lead to the liberation of the Pd(0) catalyst, which can return to the catalytic cycle.

3.1.4 Mechanistic Studies: Münchnone Reactivity

1,3-oxazolium-5-oxides, commonly referred to as Münchnones, are well-known substrates in 1,3-dipolar addition reactions.^{14, 15} This reactivity has been extensively exploited in the cyclization of alkynes and alkenes to access pyrrole and pyrroline derivatives, respectively.¹⁵ However, to our knowledge, N-alkyl substituted imines have not been previously reported to undergo dipolar cyclization with **3.14**, and instead typically react the ketene valence tautomer **3.15** in a formal [2+2] cycloaddition to generate β -lactams, **3.16**. In order to explore the potential intermediacy of Münchnones in this catalytic imidazoline synthesis, **3.14** has been generated independently upon the dehydration of PhCON(Bn)CH(Tol)CO₂H (**3.13**) with dicyclohexyl carbodiimide (Scheme 3.2).^{14, 15} Consistent with previously reports, the addition of imine to this Münchnone and heating to 55 °C for 24 hours leads to the formation of the amide-substituted β -lactam **3.16**.^{14, 15} However, the presence of acid, which is generated in the palladium catalyzed synthesis of imidazolines, has been found to have a dramatic affect upon the cyclization chemistry of imines with **3.14**. Thus, the reaction of the independently formed **3.14** with imine in the presence of 1 equiv. HCl results in the extremely rapid (< 5 min) formation of imidazoline-carboxylate **3.17** in high yield (81%). To our knowledge, the ability of HCl to divert the reaction of imines with Münchnones from β -lactam to imidazoline formation has not been previously reported.



Scheme 3.2 Reactivity of Münchnone **3.14** with Ph(H)C=NBn

The role of acid in influencing the cyclization of **3.14** with imines towards imidazolines products is at present unclear. One possibility is suggested by the work of Ferraccioli and Croce¹⁶, who have shown that the electronic nature of the imine can have a significant influence upon its reactivity with Münchnone. In particular, while N-alkyl substituted imines react with Münchnones to form β-lactams, more electron poor imines, such as the N-tosyl substituted substrates, have been found to undergo a 1,3-dipolar cyclization with **3.14** to form imidazoles.¹⁶ In our case, the role of acid may be in protonation of the imine substrate, thereby creating a more electrophilic C=N which can undergo a dipolar cycloaddition with **3.14** (path A, Scheme 3.2). Subsequent heterolysis of the C-O bond in **3.18**, would yield the observed imidazoline-carboxylate **3.17**.

Alternatively, control experiments show that the addition of HCl to the β-lactam product formed from reaction of imines with **3.14** leads to its quantitative rearrangement into the imidazoline-carboxylate product **3.17** (path B, Scheme 3.2). This acid induced reaction likely proceeds in a similar fashion to previously reported

amide-substituted β -lactam rearrangements¹⁷, whereby lactam protonation induces C-N bond-cleavage to reduce ring-strain, in this case leading to the generation of intermediate **3.18**. While at present we cannot rule out either of these mechanistic possibilities, it is notable that imine cyclization with **3.14** to generate β -lactams is a slow transformation (>24h at 55°C), relative to the almost instantaneous addition of imine to **3.14** in the presence of HCl to form imidazolines, arguing against the intermediacy of β -lactams in this transformation. Regardless of the precise role of HCl, these experiments confirm the plausible intermediacy of Münchnones in this palladium catalyzed imidazoline-carboxylate synthesis.

3.3 Conclusions

These studies have shown that the palladium catalyzed coupling imines, CO and acid chlorides is a viable and general route for the synthesis of a new class of peptide-based imidazolines. Mechanistic studies suggest this four-component coupling reaction proceeds via the *in situ* formation of Münchnone intermediates, which undergo cyclization with imines in the presence of acid to yield the observed product. The use of this chemistry to access other amino acid and/or heterocyclic target molecules is currently the subject of research in our laboratories.

3.4 Experimental Section

Unless otherwise noted, all manipulations were performed under an inert atmosphere in a Vacuum Atmospheres 553-2 dry box or by using standard Schlenk or vacuum line techniques. Tris(dibenzylideneacetone)dipalladium chloroform adduct was obtained from Strem Chemical Co. (Catalog No.46-3010) and was used without further purification. Carbon monoxide (99.99%) was purchased from Matheson and used as received. Carbon-13 labeled carbon monoxide was obtained from Cambridge Isotope Laboratories. Imines were all prepared using literature procedures.²⁰ All other reagents were purchased from Aldrich[®] and used as received.

Tetrahydrofuran (THF) was distilled from sodium/benzophenone ketyl under nitrogen. Acetonitrile and methylene chloride were distilled from CaH₂ under nitrogen. Deuterated solvents were dried as their protonated analogues, but were transferred under vacuum from the drying agent, and stored over 3Å molecular sieves. ¹H, and ¹³C were recorded on JEOL-270, Varian 400, and Unity 500 spectrometers. Infrared spectra were recorded on a Bruker IFS-48 spectrometer and on a Nicolet Avatar Spectrometer.

General Procedure for Catalytic Formation of Imidazolines Imine (0.57 mmol) and acid chloride (0.57 mmol) were dissolved in 5 mL of dry acetonitrile and stirred for 15 min. The previous solution was then added to a solution of Pd₂(dba)₃·CHCl₃ (dba = *trans, trans*-dibenzylideneacetone) (5 mol%) in 10 mL of dry acetonitrile. The reaction

mixture was transferred to a 100 mL reaction bomb and left to stir at room temperature for 1/2 hour resulting in a clear yellow solution. CO (760 torr) was added and the reaction mixture was left to stir at 55°C overnight. The resulting solution was cooled, filtered through celite, and washed with dilute HCl, saturated NaHCO₃ solution, water, saturated solution of NaCl, and dried over Na₂SO₄. Filtration, followed by evaporation of solvent, addition of anhydrous diethyl ether, and cooling at -40°C afforded the imidazoline product as a white solid.

1,3-dibenzyl-4-carboxylate-2-phenyl-4,5-(p-tolyl)-2-imidazoline (3.4a). Yield: 82%. ¹H NMR (500 MHz, CD₃CN): δ 7.58 (t, 2H), 7.45 (m, 5H), 7.33 (m, 10H), 7.20 (d, 2H), 7.08 (t, 1H), 7.00 (t, 2H), 6.95 (d, 2H), 6.68 (d, 2H), 5.68 (s, 1H, NCH), 4.57 (dd, 2H, NCH₂Ph), 4.20 (dd, 2H, NCH₂Ph), 2.38 (s, 3H, C₆H₅CH₃), 2.34 (s, 3H, C₆H₅CH₃). ¹³C NMR (125 MHz, CD₃CN): δ 166.4, 165.2, 140.8, 140.4, 134.1, 132.6, 131.2, 130.0, 129.5, 129.4, 129.3, 128.2, 127.9, 127.7, 127.6, 127.5, 127.4, 126.9, 122.3, 81.4, 72.2, 53.3, 49.6, 21.0, 20.6. IR (KBr): ν_{CO} = 1645.2, 1564.1 cm⁻¹ HRMS. Calculated for C₃₈H₃₄N₂O₂ + H⁺: 551.269854; found: 551.269830.

1,3-dimethyl-4-carboxylate-2-phenyl-4,5-(p-tolyl)-2-imidazoline (3.4b). Yield: 92%. ¹H NMR (500 MHz, CD₃CN): δ 7.77 (t, 1H), 7.71 (d, 2H), 7.69 (d, 2H), 7.64 (d, 2H), 7.36 (t, 2H), 7.28 (m, 4H), 5.74 (s, 1H, NCH), 2.83 (s, 3H, NCH₃), 2.80 (s, 3H, NCH₃), 2.40 (s, 3H, C₆H₅CH₃), 2.36 (s, 3H, C₆H₅CH₃). ¹³C NMR (125 MHz, CD₃CN): δ 167.5, 167.4, 140.3, 140.0, 133.4, 130.1, 129.8, 129.7, 128.8,

128.3, 128.0, 80.8, 76.1, 33.4, 32.9, 20.2, 19.9. IR (KBr): $\nu_{\text{CO}} = 1649.3, 1595.3$ cm^{-1} HRMS. Calculated for $\text{C}_{26}\text{H}_{27}\text{N}_2\text{O}_2 + \text{H}^+$: 399.207253; found: 399.207390.

1,3-dimethoxyethyl-4-carboxylate-2-phenyl-4,5-(p-tolyl)-2-imidazoline (3.4c).

Yield: 78%. ^1H NMR (270 MHz, CD_2Cl_2): δ 7.83 (d, 2H), 7.63 (m, 5H), 7.16 (m, 6H), 5.57 (s, 1H, NCH), 3.39 (s, 3H, OCH_3), 3.36 (m, 6H), 2.79 (s, 3H, OCH_3), 2.73 (m, 2H), 2.34 (s, 3H, $\text{C}_6\text{H}_5\text{CH}_3$), 2.32 (s, 3H, $\text{C}_6\text{H}_5\text{CH}_3$). ^{13}C NMR (67.5 MHz, CD_2Cl_2): δ 166.4, 165.2, 139.0, 138.6, 138.4, 132.1, 132.0, 129.9, 129.4, 129.1, 128.3, 123.9, 82.7, 74.6, 69.3, 67.3, 58.8, 57.7, 46.6, 45.0, 21.0, 20.8. IR (KBr): $\nu_{\text{CO}} = 1643.6, 1566.6$ cm^{-1} HRMS. Calculated for $\text{C}_{30}\text{H}_{34}\text{N}_2\text{O}_4 + \text{H}^+$: 487.2596638; found: 487.259660.

1,3-dibenzyl-4-carboxylate-2-phenyl-4,5-(4-methylthiophenyl)-2-imidazoline

(3.4d). Yield: 73%. ^1H NMR (270 MHz, CD_2Cl_2): δ 7.46 (d, 2H), 7.39 (m, 10H), 7.29 (t, 1H), 7.12 (d, 2H), 7.04 (t, 2H), 6.95 (d, 2H), 6.92 (t, 2H), 6.66 (d, 2H), 5.36 (s, 1H, NCH), 4.68 (dd, 2H, $J=15$ Hz, NCH_2Ph), 4.10 (dd, 2H, $J=14$ Hz, NCH_2Ph), 2.54 (s, 3H, $\text{C}_6\text{H}_5\text{SCH}_3$), 2.45 (s, 3H, $\text{C}_6\text{H}_5\text{SCH}_3$). ^{13}C NMR (67.5 MHz, CD_2Cl_2): δ 165.4, 165.0, 140.3, 139.7, 136.5, 135.7, 132.3, 132.2, 130.5, 130.0, 129.4, 129.3, 129.2, 128.7, 128.4, 128.1, 127.9, 127.2, 127.1, 126.1, 125.8, 123.6, 83.7, 72.6, 51.0, 49.1. IR (KBr): $\nu_{\text{CO}} = 1639.1, 1552.7$ cm^{-1} HRMS. Calculated for $\text{C}_{38}\text{H}_{34}\text{N}_2\text{O}_2\text{S}_2 + \text{H}^+$: 615.213997; found: 615.214040.

1,3-dibenzyl-4-carboxylate-2-phenyl-4,5-(4-chlorophenyl)-2-imidazoline. (3.4e).

Yield: 62%. ^1H NMR (270 MHz, CD_2Cl_2): δ 7.51(t, 2H), 7.42 (m, 5H), 7.23 (m, 10H), 7.20 (d, 2H), 7.00 (t, 1H), 6.97 (t, 2H), 6.90 (d, 2H), 6.64 (d, 2H), 5.40 (s, 1H, NCH), 4.70 (dd, 2H, NCH_2Ph), 4.13 (dd, 2H, NCH_2Ph). ^{13}C NMR 67.5 MHz, CD_2Cl_2): δ 166.1, 164.3, 138.2, 135.4, 135.3, 134.6, 132.5, 132.4, 132.0, 130.5, 130.2, 129.5, 129.4, 128.8, 128.6, 128.5, 128.2, 128.0, 127.4, 127.2, 122.4, 83.6, 72.6, 51.3, 49.3. IR (KBr): $\nu_{\text{CO}} = 1646.0, 1559.8 \text{ cm}^{-1}$ HRMS. Calculated for $\text{C}_{36}\text{H}_{28}\text{Cl}_2\text{N}_2\text{O}_2 + \text{H}^+$: 591.16061; found: 591.16084.

1,3-dibenzyl-4-carboxylate-2-methyl-4,5-(p-tolyl)-2-imidazoline (3.4f).. Yield:

70%. ^1H NMR (400 MHz, CDCl_3): δ 7.42 (s, 1H), 7.40 (s, 1H), 7.38 (t, 3H), 7.15 (t, 4H), 7.11 (m, 3H), 7.00 (m, 4H), 6.81 (m, 2H), 5.38 (s, 1H, NCH), 4.80 (dd, 2H, NCH_2Ph), 4.40 (dd, 2H, NCH_2Ph), 2.20 (s, 3H, $\text{C}_6\text{H}_5\text{CH}_3$), 2.26 (s, 3H, $\text{C}_6\text{H}_5\text{CH}_3$), 2.21(s, 3H, $\text{C}_6\text{H}_5\text{CH}_3$), 2.20 (s, 3H, COCH_3). ^{13}C NMR (100 MHz, CDCl_3): δ 166.3, 165.0, 139.5, 138.7, 135.8, 135.7, 133.0, 130.4, 129.8, 129.7, 129.5, 129.4, 129.3, 129.1, 128.1, 128.0, 127.4, 84.1, 74.0, 51.1, 48.9, 21.6, 20.2, 13.7. IR (KBr): $\nu_{\text{CO}} = 1643.6, 1593.2 \text{ cm}^{-1}$ HRMS Calculated for $\text{C}_{33}\text{H}_{32}\text{N}_2\text{O}_2 + \text{H}^+$: 489.254004; found: 489.25408.

1,3-difurfuryl-4-carboxylate-2-phenyl-4,5-(phenyl)-2-imidazoline (3.4i).. Yield:

67%. ^1H NMR (400 MHz, CDCl_3): δ 7.90-7.80 (d, 1H), 7.75-7.50 (m, 5H), 7.55 (m, 1H), 7.40-7.25 (d, 5H), 7.23-7.15 (t, 4H), 7.00 (s, 2H), 6.32 (s, 1H), 5.96 (s, 1H),

5.85 (s, 1H), 5.26 (s, 1H), 5.22 (s, 1H), 4.90 (d, 1H), 4.69 (d, 1H), 4.35 (d, 1H), 3.96 (d, 1H). ^{13}C NMR (100 MHz, CDCl_3) δ 166.1, 165.1, 147.9, 145.9, 144.0, 141.9, 139.5, 133.6, 132.7, 131.7, 131.7, 130.2, 130.2, 130.0, 129.7, 129.6, 129.4, 129.0, 128.8, 128.7, 128.5, 128.4, 128.1, 123.3, 111.6, 111.1, 110.8, 109.7, 83.9, 75.8, 44.4, 42.5. IR (CH_2Cl_2): $\nu_{\text{CO}} = 1655.9, 1563.0 \text{ cm}^{-1}$

1,3-dibenzyl-4-carboxylate-2-phenyl-4,5-(2-piperonyl)-2-imidazoline (3j) Yield: 51%. ^1H NMR (400 MHz, CDCl_3): δ 7.70-7.50 (m, 3H), 7.40-7.30 (m, 4H), 7.20-6.70 (m, 12H), 6.68 (d, 1H), 6.47 (d, 2H), 5.96 (s, 2H), 5.90 (s, 2H), 5.39 (s, 1H), 4.90 (d, 1H), 4.51 (d, 1H), 4.34 (d, 1H), 4.04 (d, 1H). ^{13}C NMR (100MHz, CDCl_3). δ 165.8, 165.2, 148.8, 148.2, 148.0, 148.0, 135.7, 132.4, 130.2, 129.5, 129.5, 129.4, 128.6, 128.3, 128.3, 128.3, 128.2, 127.5, 123.8, 123.0, 110.5, 108.7, 108.4, 101.6, 101.5, 84.3, 73.6, 51.7, 49.5. IR(CH_2Cl_2): $\nu_{\text{CO}} = 1654.2, 1563.4 \text{ cm}^{-1}$.

1,3-dibenzyl-4-carboxylate-2-phenyl-4,5-(phenyl)-2-imidazoline (3.17) Yield: 72%. ^1H NMR (400 MHz, CDCl_3): δ 7.65-7.50 (m, 5H), δ 7.50-7.25 (m, 12H), 7.05-6.85 (m, 6H), 6.31 (d, 2H), δ 5.54 (t, 1H), 4.97 (d, 1H), 4.54 (d, 1H), 4.34 (d, 1H), 3.96 (s, 1H). ^{13}C NMR (100MHz, CDCl_3): δ 165.7, 165.2, 139.7, 135.7, 133.6, 132.3, 132.3, 131.6, 130.1, 129.7, 129.6, 129.4, 129.3, 129.0, 128.9, 128.7, 128.6, 128.4, 128.2, 128.1, 127.5, 127.4, 127.2, 123.9, 84.8, 73.6, 51.8, 49.5. IR (CH_2Cl_2): $\nu_{\text{CO}} = 1654.0, 1562.9 \text{ cm}^{-1}$

Crystallographic details for N,N-dimethyl-2-phenyl-4,5-(p-tolyl)-imidazole-4-carboxylate.¹⁹⁻²² Crystals of the imidazole for diffraction analysis were grown by cooling in a chloroform solution and mounted on a capillary. X-ray data was collected at 293 K on an Enraf-Nonius CAD4 diffractometer with Cu K α radiation. The space groups were confirmed by the PLATON program. Data reduction was performed using a locally modified version of the NRC-2 program. The structure was solved by direct method using SHELXS97 and difmap synthesis using SHELXTL and SHELXL96. All non-hydrogen atoms were refined anisotropically, and the hydrogen atoms were refined isotropically. Hydrogen atoms were constrained to the parent site using a riding model; SHELXL96 defaults, C-H 0.93 to 0.98 Å. The isotropic factors, U_{iso} were adjusted to a 50% higher value of the parent site (methyl) and 20% higher (others). Two models were used to describe part of the molecule (two different unit cells). Occupancy factor of model A was refined to 0.58 (1) and was fixed to 0.60 in the last cycles. The occupancy factor of model B was fixed to 0.40. Some restraints (SADI), EADP constraints, and ideal phenyl rings description (AFIX 66) were applied to help convergence. A final verification of possible voids was performed using the VOID routine of the PLATON program.

Empirical formula for N,N-dimethyl-2-phenyl-4,5-(p-tolyl)-imidazole-4-carboxylate, $\text{C}_{26}\text{H}_{26}\text{N}_2\text{O}_2$; Fw, 398.488; temp K_m , 293 (2); wavelength (Å), 1.54056; cryst syst, Orthorhombic; space group, Pca2₁; a (Å), 16.788 (5); b (Å), 10.594 (8); c (Å), 12.525 (4); V (Å³), 2227.6 (19); Z (mm⁻¹), 4; d (calcd) (Mg m⁻³), 1.1882; μ , 0.594; reflections with $>2\sigma(I)$, 1837; no. of rflns collected, 28074; no. of indep. rflns, 4228;

θ_{\max} (deg), 69.96°; R [$F^2 > 2\sigma(F^2)$] = 0.0385 R₁; wR (F^2) = 0.0654, S = 0.874; Min, max A_p (e/Å³), -0.124, 0.113

Tol(H)C=N(CH₂Ph)COPh⁺ Cl⁻ (3.6)¹¹ Using a modified literature procedure, an equimolar mixture of (PhCH₂)N=C(H)Tol (100 mg, 0.48 mmol) and PhCOCl (67 mg, 0.48 mmol) were combined in CH₃CN (3 mL) and stirred for 10 minutes. The solvent is subsequently removed *in vacuo* to provide a **3.6** as a white solid, which was washed with ether prior to use (80% yield). ¹H NMR (400 MHz, CD₃CN): δ 7.64 (d, 2H), 7.71-7.45 (m, 3H), 7.44 (d, 2H), 7.35 (s, 1H), 7.23- 7.12 (m, 5H), 7.09 (d, 2H), 4.59 (s, 1H), 2.33 (s, 3H), ¹³C NMR (100 MHz, CD₃CN): δ 172.3, 139.4, 137.8, 135.5, 133.9, 130.7, 129.3, 129.1, 128.2, 127.7, δ 127.4, 126.9, 78.5, 46.8, 20.8.

[(bipy)Pd[η²-C(Tol)HN(CH₂Ph)COPh]]⁺Cl⁻ (3.7) Pd₂(dba)₃·CHCl₃ (424.2 mg, 0.41 mmol) was added to an acetonitrile (15 mL) solution of **3.6** (286.2 mg, 0.82 mmol), followed by 2,2'-bipyridine (255.8 mg, 1.6 mmol). The mixture was left to stir overnight at room temperature, resulting in a clear yellow solution. The solution was concentrated to 5 mL, diethyl ether (10 mL) added, and cooled to -40°C overnight. Complex **3.7** was isolated as a pale yellow solid (92 % yield). ¹H NMR (CD₂Cl₂, 270MHz): δ 9.15 (d, 2H), 8.58 (s, 1H), 8.21 (s, 2H), 7.86 (s, 1H), 7.55 (m, 6H), 7.38 (m, 6H), 7.14 (d, 2H), 7.02 (d, 2H), 5.11 (s, 1H, CH-N), 4.32 (dd, 2H, CH₂Ph), 2.27 (s, 3H, C₆H₄CH₃). ¹³C NMR (CD₂Cl₂, 67.5 MHz): δ 180.5 (COPh), 150.0, 148.0, 141.5, 138.2, 138.0, 133.9, 132.3, 131.5, 130.4, 129.5, 128.8, 128.3, 127.7, 127.6,

65.2 (C-N), 52.7 (CH₂Ph), 21.1 (C₆H₄CH₃) IR (KBr): $\nu_{\text{CO}} = 1552.2 \text{ cm}^{-1}$ HRMS
Calculated for C₃₂H₂₈N₃O¹⁰⁶Pd⁺: 576.126713; found: 576.126790.

Cl(CO)Pd[η^2 -C(Tol)HN(CH₂Ph)COPh] (3.8) An equimolar mixture of (PhCH₂)N=C(H)Tol and PhCOCl were combined in CH₃CN and stirred for 10 minutes. To this solution is added 0.50 equiv. of Pd₂(dba)₃·CHCl₃. The solvent was removed *in vacuo* to provide a yellow solid, which was washed with diethyl ether prior to use to give complex **3.9**. Complex **3.9** (20mg, 0.03 mmol) was dissolved in acetonitrile-d₃ (0.5 mL) and transferred to a J-Young capped NMR tube. CO (g) (760 torr) was then added resulting in the formation of **3.8**. Complex **3.8** is too unstable to isolate, and was characterized by *in situ* NMR techniques. ¹H NMR (CD₃CN, 400MHz): δ 7.68 (m, 2H), 7.56 (m, 2H), 7.46 (m, 4H), 7.37 (m, 4H), 7.20 (m, 2H), 6.13 (s, 1H, CH-N), 4.52 (dd, 2H, CH₂Ph), 2.45 (s, 3H, C₆H₄CH₃). ¹³C NMR (CD₃CN, 101 MHz): δ 179.1 (COPh), 174.9 (PdCO), 138.2, 134.7, 133.0, 131.4, 130.1, 130.0, 129.9, 129.3, 128.7, 126.6, 66.2 (C-N), 54.0 (CH₂Ph), 21.3 (C₆H₄CH₃). IR (CH₃CN): $\nu_{\text{CO}} = 2114 \text{ cm}^{-1}, 1553 \text{ cm}^{-1}$.

Reaction of 3.14 with Ph(H)C=N(CH₂Ph). This reaction was performed using modified literature procedures.^{15, 17} To a solution of HO₂CCH(Tol)N(CH₂Ph)COPh (**13**) (75 mg, 0.22 mmol) in CH₃CN (3 mL) was added dicyclohexyl carbodiimide (47 mg, 0.24 mmol). The reaction mixture was stirred for 5 minutes to allow the formation of **3.14**. To this solution was added (Bn)NCH(Ph) (43 mg, 0.22 mmol) and the solution was allowed to stir at 55°C for 24 hours. β -lactam product **3.16** was

isolated by column chromatography (62% yield). $^1\text{H-NMR}$ (400 MHz, CD_3CN): δ 7.42 (d, 2H, 8Hz), 7.35-7.09 (15H, m), 6.94 (d, 2H, 8Hz), 6.62 (d, 2H, 8Hz), 6.56 (d, 2H, 8Hz), 5.48(s, 1H), 4.80 (d, 1H, 15Hz), 4.76 (d, 1H, 17 Hz), 4.66 (d, 1H, 17Hz), 3.91(d, 1H, 15Hz), 3.81(s, 3H), 3.70 (s, 3H). $^{13}\text{C NMR}$ (100 MHz, CD_3CN): δ 174.0, 165.6, 138.3, 137.0, 135.6, 135.1, 134.3, 134.3, 130.0, 129.9, 129.6, 129.2, 128.1, 128.4, 128.3, 128.2, 128.1, 126.8, 126.8, 126.7, 81.2, 66.3, 52.3, 44.4. IR (KBr): ν_{CO} : 1753 cm^{-1} , 1639 cm^{-1} .

Reaction of 3.14 with $\text{Ph(H)C=N(CH}_2\text{Ph)H}^+ \text{Cl}^-$. To a solution of $\text{HO}_2\text{CCH(Tol)N(CH}_2\text{Ph)COPh}$ (75 mg, 0.22 mmol) in CH_3CN (3 mL) was added dicyclohexyl carbodiimide (47 mg, 0.24 mmol). The reaction mixture was stirred for 5 minutes to allow the formation of **3.14**. To this solution was added $(\text{Bn})\text{NCH(Ph)HCl}$ (60 mg, 0.26 mmol), and the mixture was allowed to stir at 55°C for 12 hours. ^1H and $^{13}\text{C-NMR}$ (CD_3CN) of the reaction mixture show the formation of 1,3-dibenzyl-4-carboxylate-2-phenyl-4,5-(phenyl)-2-imidazoline (**3.17**) in ca. 72% NMR yield.

Reaction of 16 with HCl to yield 3.17. β -lactam **3.16** (75 mg, 0.14 mmol) was dissolved in CH_3CN (3mL). To this solution was added HCl in dioxanes (4.0 M, 36 μL , 0.14 mmol). The solution was heated to 50°C for 10 minutes. The solvent was subsequently removed *in vacuo* to provide an oil, which was dissolved in CHCl_3 and washed with aqueous NaHCO_3 . Removal of the solvent *in vacuo* provided imidazoline **3.17** (87% yield).

3.5 References:

1. a) Olson, G.L.; Bolin, D.R.; Bonner, M.P.; Bos, M.; Cook, C.M.; Fry, D.C.; Graves, B.J.; Hatada, M.; Hill, D.E.; Kahn, M.; Madison, V.S.; Rusiecki, V.K.; Sarabu, R.; Sepinwall, J.; Vincent, G.P.; Voss, M.E. *J. Med. Chem.* **1993**, *36*, 3039. b) Goodman, M.; Zhang, J. *Chemtracts-Org. Chem.* **1997**, *10*, 629.
2. a) Jones, R.C.F.; Ward, G.J. *Tetrahedron Lett.* **1988**, *29*, 3853. b) Gilbert, I.H.; Rees, D.C.; Richardson, R.S. *Tetrahedron Lett.* **1991**, *32*, 2277. c) Gilbert, I.H.; Rees, D.C. *Tetrahedron* **1995**, *51*, 6315.
3. Zhou, X.T.; Lin, Y.R.; Dai, L.X.; Sun, J.; Xia, L.J.; Tang, M.H. *J. Org. Chem.* **1999**, *64*, 1331.
4. Hayashi, T.; Kishi, E.; Soloshonok, V.A.; Uozumi, Y. *Tetrahedron Lett.* **1996**, *37*, 4969.
5. Lin, Y.R.; Zhou, X.T.; Dai, L.X.; Sun, J. *J. Org. Chem.* **1997**, *62*, 1799.
6. Dghaym, R.D.; Dhawan, R.; Arndtsen, B.A. *Angew. Chem. Int. Ed.* **2001** *40*, 3228.
7. Some of the data in this manuscript has been communicated previously (see reference 6).
8. 0.50 equiv. of the acid chloride starting material is regenerated at the completion of the reaction.
9. a) Hiemstra, H.; Speckamp, N. In: B.M. Trost, I. Fleming, ed. *Comprehensive Organic Synthesis*. New York: Pergamon Press, pg. 1047-1081, **1991**. b) B.R.

Brown. *Chemistry of Aliphatic Carbon-Nitrogen Compounds*. New York: Oxford Science Publications, 1994.

10. Ratts, K.; Chupp, J. *J. Org. Chem.* **1974**, *39*, 3300.
11. Lafrance, D.; Davis, J.L.; Dhawan, R.; Arndtsen, B.A. *Organometallics* **2001**, *20*, 1128.
12. Dghaym, R.D.; Yaccato, K.J.; Arndtsen, B.A. *Organometallics* **1998**, *17*, 4.
13. Drent, E.; Budzelaar, P.H.M. *Chem. Rev.* **1996**, *96*, 663.
14. a) Huisgen, R.; Gotthardt, H.; Bayer, H.O.; Schaefer, F.C. *Angew. Chem.* **1964**, *76*, 185. b) Huisgen, R.; Gotthardt, H.; Bayer, H.O.; Schaefer, F.C. *Chem. Ber.* **1970**, *103*, 2611.
15. Gingrich, H.L.; Baum, J.S. In: I.J. Turchi. ed. *The Chemistry of Heterocyclic Compounds: Oxazoles*. New York: Wiley, **1986**, pg. 731-961.
16. Consonni, R.; Croce, P.D.; Ferraccioli, R.; La Rosa, C. *J. Chem. Res.* **1991**, *7*, 188.
17. Croce, P.D.; Ferraccioli, R.; La Rosa, C. *Tetrahedron* **1995**, *51*, 9385.
18. For spectral data, see reference 6.
19. Spek, A.L. PLATON Molecular Geometry Program. July **1995** version; University of Utrecht, Utrecht, Holland.
20. Ahmed, F.R.; Hall, S.R.; Pippy, M.E.; Huber, C.P. (1973) NRC Crystallographic Computer Programs for the IBM/360. Accession Nos. 133-147 in *J. Appl. Cryst.* **6**, 309-346.
21. Sheldrick, G.M. (1997) SHELXS97. Program for the Solution of Crystal Structures. University of Gottingen, Germany.

22. Sheldrick, G.M. (1996) SHELXL96. Program for the Refinement of Crystal Structures. University of Gottingen, Germany. SHELXTL (1997) Release 5.10; The Complete Software Package for Single Crystal Structure Determination, Bruker AXS Inc., Madison, WI 53719-1173.

CHAPTER FOUR

The Development of the First Catalytic Synthesis to Münchnones: A Simple Four Component Coupling Approach to α -Amino Acid Derivatives*

Preface

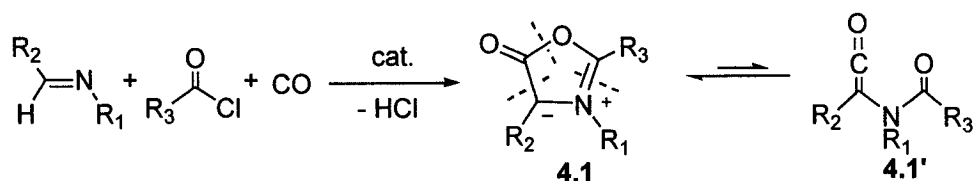
In Chapter 3 the mechanism of imidazoline-carboxylate and β -lactam formation was discussed. This mechanistic analysis identified the key reaction intermediate as being a 1,3-oxazolium-5-oxide or Münchnone. Chapter 4 of this thesis describes a palladium catalyzed route to prepare Münchnones directly from imine, acid chloride and carbon monoxide building blocks. This methodology has been utilized to design a new catalytic synthesis of α -amino acid derivatives via a one-pot coupling process.

4.0 Introduction

Mesoionic 1,3-oxazolium-5-oxides (e.g. Münchnones, **4.1**), and their α -amide substituted ketene tautomer (**4.1'**), are an important family of substrates for the synthesis of biologically relevant molecules.¹ Münchnones are versatile 1,3-dipolar addition substrates, and have proven key in the construction of a range of natural

* Previously Published: Dhawan, R.; Dghaym, R.D.; Arndtsen, B.A. *J. Am. Chem. Soc.* **2003**, *125*, 1474.

products and pharmacologically relevant heterocycles, including pyrroles,^{1,2a,b} imidazoles,^{2c,d} pyrrolines,^{2e} and indole derivatives.^{2f} Alternatively, the less stable ketene **4.1'** can serve as a precursor to α -amino acid and peptide derivatives, via reaction with alcohols or N-terminated peptides,^{3a} and their cycloaddition with imines provides access to peptide-based β -lactams.^{3b} While the diversity of products accessible from **4.1** makes them attractive synthetic targets, their preparation to date has typically involved multistep processes. For example, the most common approach involves the dehydration of the appropriately substituted N-acyl amino acid derivative.¹ This route limits the utility of these compounds in the actual synthesis of amino acids, and also imposes a necessary initial preparation of the amino acid precursor. As such, alternative transition metal-based syntheses of these compounds have become of growing relevance.⁴ Perhaps the most well-established of these is the carbonylation of pre-synthesized chromium-carbenes,^{4a,5,6} which has been employed to develop stoichiometric syntheses of a variety of α -amino acid derivatives, peptides, β -lactams and pyrroles.



Equation 4.1. Generation of 1,3-Oxazolium-5-oxides (Münchnones)

Despite the obvious potential advantages of a metal catalyzed method to form Münchnones directly from readily available materials, to date this has not been reported. We⁷ and others⁸ have recently suggested the possibility of preparing

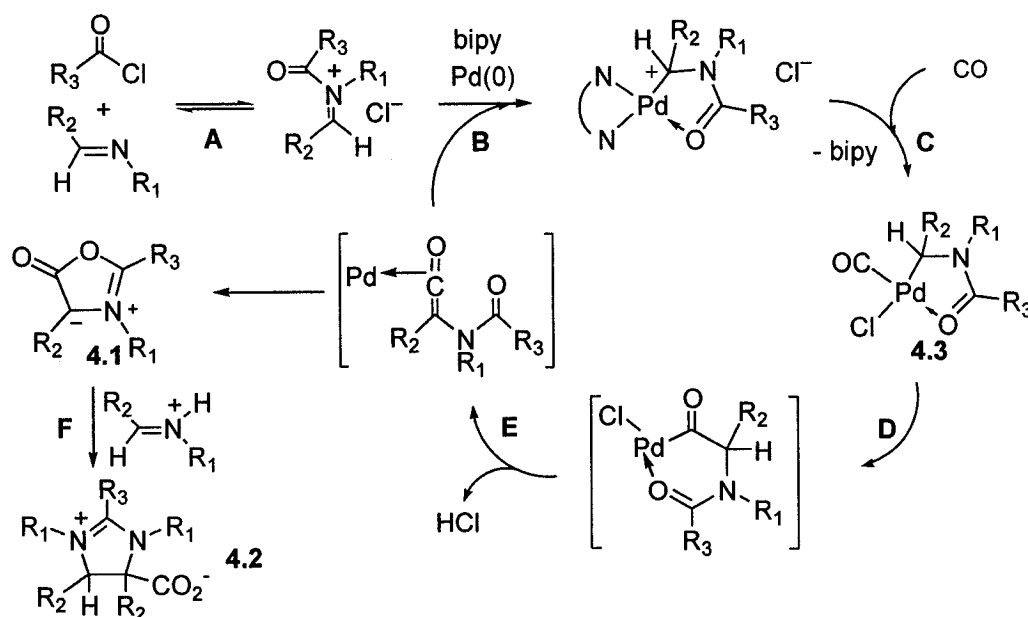
peptide-based products from simple imine and carbon monoxide units, rather than the traditional routes employing α -amino acids. As described below, these investigations have led to the discovery of a metal catalyzed method to prepare stable Münchnones, via a catalytic coupling of imines, carbon monoxide and acid chlorides. The utility of this transformation is demonstrated in the design of a new one-pot catalytic synthesis of diprotected α -amino acid derivatives.

4.1 Results and Discussion

4.1.1 Palladium Catalyzed Synthesis of Münchnones: Mechanistic Considerations

Our approach to the catalytic synthesis of Münchnones is shown in Eq. 4.1, and based upon our recently observed palladium catalyzed synthesis of imidazolines, the postulated mechanism for which is in Scheme 4.1.^{7a,9} In particular, we surmised that oxidative addition of imine and acid chloride to Pd(0) (steps A, B), CO coordination (C), insertion (D), and β -hydride elimination (E) might provide a pathway to construct **4.1**, provided subsequent cycloaddition (F) to form **4.2** could be inhibited. During the course of these studies, it was observed that the HCl generated during catalysis is critical for the Münchnone cycloaddition step (F), implying that its removal might allow the build-up of **4.1**. Indeed, the reaction of (p-tolyl)HC=NBn, PhCOCl and 1 atm CO with 5 mol% Pd₂(dba)₃·CHCl₃, bipyridine and NEt(ⁱPr)₂ base leads to the disappearance of starting materials over 4 days, and generation of **4.1a** as

a minor product (5% yield, Table 4.1, entry 1). The formation of **4.1a**, albeit in very low yield, suggested this approach might indeed allow the development of a one-pot synthesis catalytic of Münchnones from three basic building blocks (Eq. 1), which could be employed in a range of further transformations. With a working hypothesis for the mechanism of this transformation, we set out to improve the efficiency of this process.



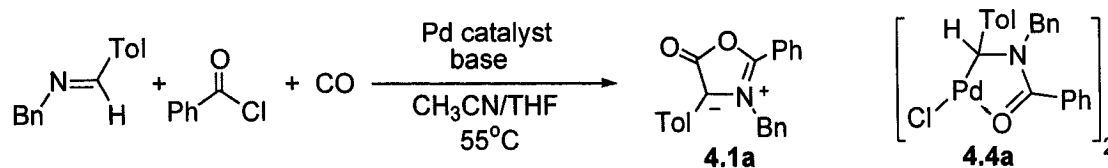
Scheme 4.1. Mechanistic rationale for Münchnone formation

4.1.2 Palladium Catalyzed Synthesis of Münchnones: Method Development

Firstly, it was noted that the imine and acid chloride are consumed during the catalysis, implying that the low yields of **4.1a** may result from the decomposition of the reactive Münchnone product,^{1, 10} rather than incomplete reaction. Our attention therefore turned towards tuning the palladium catalyst to allow for a more selective

and mild reaction. In principle, this might be accomplished by allowing more facile access to CO-coordinated intermediate **4.3** (C), since steps A and B are known to be rapid.^{7a} Consistent with this, the removal of bipy from the catalytic reaction increased the rate of Münchnone formation (from 4 days to 24 h), and led to a doubling of the yield (ca. 10%, entry 3).¹¹ Increasing the pressure of CO further facilitates the generation of **4.3**, and increases the yield of **4.1a** to 13% (entry 4). However, this also led to the incomplete conversion of imine and acid chloride, due to the precipitation of palladium from the reaction.

The formation of palladium sediments can be inhibited by the addition of Cl⁻ and Br⁻ sources, as previously noted in “ligandless” catalysis,¹² and leads to a dramatic increase the yield of **4.1a** (entries 5-7). In the case of Bu₄N⁺ Br⁻, this allows the formation of **4.1a** in a synthetically useful 69% yield.¹¹ The efficiency of the catalysis can be further improved by removal of the potentially coordinating dba ligand from the Pd(0) source via the use of [Pd(Cl)[η²-CH(p-tolyl)NBn(COPh)] (**4.4a**), generated by pre-treating Pd₂(dba)₃·CHCl₃ with imine and acid chloride.¹³ The use of catalyst **4.4a** leads to the formation of **4.1a** as essentially the only significant reaction product (83% yield, entry 8). Overall, this optimized protocol (Table 1) provides a straightforward and high yield catalytic route to prepare stable Münchnones.

Table 4.1 Catalytic Synthesis of **4.1a**^a

#	[CO]	Pd catalyst	Base	Additive	% 4.1a , (% 4.2) ^b
1	1 atm	Pd ₂ (dba) ₃ ·CHCl ₃	NEt(ⁱ Pr) ₂	bipy, 5%	5 % (-) ^c
2	1 atm	Pd ₂ (dba) ₃ ·CHCl ₃	-	bipy, 5%	- (82%) ^c
3	1 atm	Pd ₂ (dba) ₃ ·CHCl ₃	NEt(ⁱ Pr) ₂	-	10 %
4	4 atm	Pd ₂ (dba) ₃ ·CHCl ₃	NEt(ⁱ Pr) ₂	-	13 %
5	4 atm	Pd ₂ (dba) ₃ ·CHCl ₃	NEt(ⁱ Pr) ₂	LiCl	30 %
6	4 atm	Pd ₂ (dba) ₃ ·CHCl ₃	NEt(ⁱ Pr) ₂	LiBr	50 %
7	4 atm	Pd ₂ (dba) ₃ ·CHCl ₃	NEt(ⁱ Pr) ₂	Bu ₄ NBr	69 %
8	4 atm	4.4a	NEt(ⁱ Pr) ₂	Bu ₄ NBr	83 %

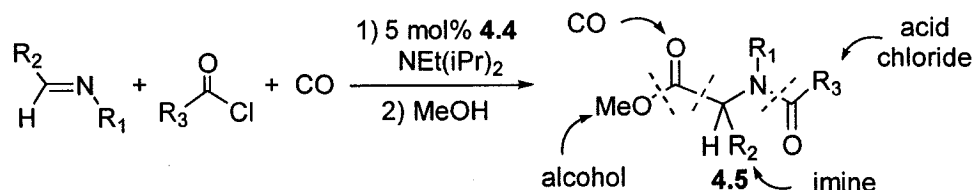
^a 0.48 mmol imine and additive, 0.67 mmol acid chloride, 0.74 mmol base and 5 mol% catalyst for 24-30 h at 55°C. ^b NMR Yield. ^c 4 days.

A useful feature of this catalytic reaction is the simplicity of the three separate building blocks, which are either commercially available (CO) or easily prepared (imines and acid chlorides). As such, this chemistry can be generalized to prepare a range of Münchnones, many of which have not been previously reported. Notably, functionalities such as aryl-halides, esters, ethers and thioethers are tolerant to the catalysis conditions (Table 4.2), and both alkyl and aryl acid chloride and N-substituted imines can be employed. However, C-alkyl substituted imines do not yield Münchnones under these conditions. This is likely related to the established

lower stability of these products,^{1,14} and may be addressable in the future with the use of *in situ* traps.

4.1.3 Palladium Catalyzed Synthesis of Diprotected α -Amino Acids

Considering the wide scope of products available from 4.1 and 4.1', this procedure should prove useful in the design of new catalytic syntheses for a range of Münchnone-based targets. As a preliminary illustration of this feature, we have used this catalytic Münchnone synthesis, followed by the addition of methanol, to design a new one-pot, four-component coupling route to diprotected α -amino acid derivatives (Eq. 4.2).



Equation 4.2. Generation of Diprotected α -Amino Acids

α -Aryl amino acids have been demonstrated to be of utility in antimicrobial agents and enzyme inhibitors.¹⁵ As shown in Table 4.2, diversely substituted amino acid derivatives can be prepared by modification of the starting imine and acid chloride. In addition to its simplicity, this transformation also provides what is to our knowledge the first example of the catalytic construction of α -amino acids from imines and carbon monoxide.

Table 4.2 Scope of Palladium Catalyzed Munchnone Synthesis^a

Cpd	Imine	Acid Chloride	Munchnone 4.1 (% yield) ^b	Amido Ester 4.5 (% yield)
a,b		PhCOCl		
c		PhCOCl		
d		PhCOCl		
e		PhCOCl		
f				
g		PhCOCl	R = OCO(p-C ₆ H ₄ CH ₃)"/>	
h		PhCOCl		
i		PhCOCl	R=p-CH ₃ OC ₆ H ₄ "/>	

^aAnalogous to Table 4.1, # 8. ^b¹³C NMR. ^c Pd₂(dba)₃ CHCl₃ cat. ^d96 h.

4.2 Conclusions

In summary, this report has described the development of the first catalytic synthesis of Münchnones, providing direct access to this general class of compounds from basic building blocks. Experiments directed towards the development of multi-component catalytic syntheses of other peptidic and/or heterocyclic products based on 4.1 are currently underway.

4.3 Experimental

General Procedures

Unless otherwise noted, all manipulations were performed under an inert atmosphere in a Vacuum Atmospheres 553-2 dry box or by using standard Schlenk or vacuum line techniques. Tris(dibenzylideneacetone) dipalladium chloroform adduct was synthesized according to a modified literature procedure starting from Na_2PdCl_4 .¹⁶ Carbon monoxide (99.99%) was purchased from Matheson and used as received. Imines were prepared using literature procedures.¹⁷ All other reagents were purchased from Aldrich® and used as received. Tetrahydrofuran (THF) was distilled from sodium/benzophenone ketyl under nitrogen. Acetonitrile was distilled from CaH_2 under nitrogen. Deuterated solvents were dried as their protonated analogues, but were transferred under vacuum from the drying agent, and stored over 3 Å molecular sieves.

^1H , and ^{13}C were recorded on JEOL 270, Varian Mercury 300 MHz, Mercury 400 MHz, and Unity 500 MHz spectrometers. Infrared spectra were recorded on a Nicolet Avatar Infrared Spectrometer. Mass spectra were obtained from the Université de Sherbrooke and McGill University mass spectral facilities. Elemental analyses were obtained from QTI, Whitehouse N.J.

Typical Procedure for Synthesis of $[\text{Pd}(\text{Cl})\{\eta^2\text{-CH}(\text{R}^1)\text{NR}^2(\text{COR}^3)\}]$ (4.4)

(4- $\text{CH}_3\text{C}_6\text{H}_4$) $\text{HC}=\text{N}(\text{CH}_2\text{Ph})$ (62.5 mg, 0.298 mmol) and benzoyl chloride (42.0 mg, 0.298 mmol) were dissolved in 10 mL of CH_3CN and stirred for 15 minutes. $\text{Pd}_2(\text{dba})_3\cdot\text{CHCl}_3$ (150.1 mg, 0.145 mmol) was added to this solution, and the mixture stirred overnight at ambient temperature. The solvent volume was reduced to 2 mL and diethyl ether (10 mL) was added and cooled to -40°C , resulting in the precipitation of the product $[\text{PdCl}(\eta^2\text{-CH}(4\text{-C}_6\text{H}_4\text{CH}_3)\text{N}(\text{CH}_2\text{C}_6\text{H}_5)(\text{COC}_6\text{H}_5))]_2$ **4.4a** as a yellow solid (92% yield). ^1H NMR (CD_2Cl_2 , 270 MHz): δ 7.70-7.42 (m, 5H), 7.40-7.26 (m, 3H), 7.20-7.05 (m, 4H), 7.04-6.94 (m, 2H), 5.06 (s, 1H), 4.28 (dd, 2H), 2.29 (s, 3H). ^{13}C NMR (CD_2Cl_2 , 270 MHz): δ 182.3, 138.2, 136.6, 133.9, 132.3, 131.0, 130.3, 129.1, 128.7, 128.3, 128.1, 127.7, 127.5, 65.7, 52.3, 21.6. IR (KBr): 1547 cm^{-1} . Analysis: Calculated for $\text{C}_{22}\text{H}_{20}\text{NOCIPd}$: C, 57.91; H, 4.42; N, 3.07; found: C, 58.24; H, 4.56; N, 3.01.

Typical Procedure for Catalytic Formation of Münchnone Formation

(4-CH₃C₆H₄)HC=N(CH₂Ph) (100.0 mg, 0.48 mmol) and benzoyl chloride (94.0 mg, 0.68 mmol) were dissolved in 5 mL of acetonitrile and stirred for 15 min. The previous solution was then added to a solution of [Pd(Cl)[η²-CH(4-CH₃C₆H₄)NCH₂Ph(COPh)]₂ (21.8 mg, 0.024 mmol) in 5 mL of dry acetonitrile. The reaction mixture was transferred to a 50 mL reaction bomb and Bu₄N⁺Br⁻ (154 mg, 0.48 mmol) and EtNⁱPr₂ (96.0 mg, 0.74 mmol) were added in 10 mL of tetrahydrofuran. The solution was degassed and carbon monoxide (60 psi) was added to the reaction mixture, which was left to stir at 55°C for 30 hours. ¹H NMR yields were obtained using 1,3-dimethoxybenzene as an internal standard.

Typical Procedure for Catalytic Formation of Münchnone formation (for isolation)

(4-CH₃C₆H₄)HC=N(CH₂Ph) (100.0 mg, 0.48 mmol) and benzoyl chloride (94.0 mg, 0.68 mmol) were dissolved in 5 mL of acetonitrile and stirred for 15 min. The previous solution was then added to a solution of [Pd(Cl)[η²-CH(4-CH₃C₆H₄)NCH₂Ph(COPh)]₂ (21.8 mg, 0.024 mmol) in 5 mL of dry acetonitrile. The reaction mixture was transferred to a 50 mL reaction bomb and LiBr (42 mg, 0.48 mmol) and EtNⁱPr₂ (96.0 mg, 0.74 mmol) were added in 10 mL of tetrahydrofuran. The solution was degassed and carbon monoxide (60 psi) was added to the reaction

mixture, which was left to stir at 55°C for 30 hours. After removal of the solvent, the oil is dissolved in THF (10 mL) and dried K₃PO₄ (2.5 g) is added in order to remove the EtN⁺Pr₂H⁺Cl⁻ from the reaction mixture. The solution is allowed to stir for 7 hours and subsequently filtered. Removal of the solvent in vacuo, followed by dissolution in acetonitrile or acetonitrile/diethyl ether and cooling to -40°C led to the precipitation of the Münchnone **4.1a** (29.5 mg, 18%) as a yellow solid. A significant amount product was typically sacrificed in order to crystallize the Münchnone in high purity.

3-benzyl-2-phenyl-4-p-tolyl-1,3-oxazolium 5-oxide (4.1a)

NMR Yield: 83%. Isolated Yield: 18%. ¹H NMR (400 MHz, CD₃CN): δ 7.65 (d, 2H), 7.54-7.46 (m, 3H), 7.38-7.26 (m, 5H), 7.16 (d, 2H), 7.12 (d, 2H), 5.48 (s, 2H), 2.29 (s, 3H), ¹³C NMR (100 MHz, CD₃CN): δ 160.9, 143.1, 136.1, 134.9, 131.2, 129.5, 129.3, 129.3, 128.3, 128.0, 127.8, 126.5, 126.2, 123.5, 95.0, 50.7, 20.6. IR (NaCl): ν_{CO} = 1709.8 cm⁻¹. HRMS calculated for C₂₃H₁₉NO₂: 341.1416; found: 341.1420.

3-ethyl-2-phenyl-4-p-tolyl-1,3-oxazolium 5-oxide (4.1b)

NMR Yield: 85%. Isolated Yield: 32%. ¹H NMR (300 MHz, CD₃CN): δ 7.77 (m, 2H), 7.60 (m, 3H), 7.40 (d, 2H), 7.25 (d, 2H), 4.32 (q, 2H), 2.40 (s, 3H), 1.20 (t, 3H).

^{13}C NMR (75 MHz, CD_3CN): δ 161.1; 142.3; 136.2; 131.0; 129.5; 129.4; 128.4; 128.3; 127.0; 123.8; 93.8; 42.6; 20.6; 14.1. IR (NaCl): $\nu_{\text{CO}} = 1712.7$ (s) cm^{-1} . HRMS calculated for $\text{C}_{18}\text{H}_{17}\text{NO}_2$: 279.1259; found: 279.1256.

3-ethyl-2-phenyl-4-naphthyl-1,3-oxazolium 5-oxide (4.1c):

NMR Yield: 93%. Isolated Yield: 48%. ^1H NMR (300 MHz, CD_2Cl_2): δ 8.00-7.82 (m, 6H), 7.80 (m, 2H), 7.60 (m, 2H), 7.60-7.43 (m, 2H), 4.43 (m, 2H), 1.20 (t, 3H). ^{13}C NMR (75 MHz, CD_2Cl_2): δ 161.2; 142.9; 133.9; 132.0; 131.2; 129.6; 128.5; 128.2; 127.9; 127.7; 127.2; 126.5; 126.3; 125.9; 125.8; 123.3; 94.7; 43.0; 14.9. IR (NaCl): $\nu_{\text{CO}} = 1712.6$ cm^{-1} (s). HRMS calculated for $\text{C}_{21}\text{H}_{17}\text{NO}_2$: 315.1259; found: 315.1262.

3-ethyl-2-phenyl-4-(benzo[1,3]-dioxol-yl)-1,3-oxazolium 5-oxide (4.1d):

NMR Yield: 63%. Isolated Yield: 17%. ^1H NMR (300 MHz, CD_3CN): δ 7.73-7.70 (m, 2H), 7.60-7.56 (m, 3H), 7.01-6.92 (m, 3H); 6.02 (s, 2H), 4.27 (q, 2H), 1.20 (t, 3H). ^{13}C NMR (75 MHz, CD_3CN): δ 161.0; 148.1; 146.5; 142.0; 131.0; 129.4; 128.3; 123.8; 123.5; 122.8; 109.4; 108.7; 101.7; 93.7; 42.5; 14.1. IR (NaCl): $\nu_{\text{CO}} = 1709.0$ cm^{-1} (s). HRMS calculated for $\text{C}_{18}\text{H}_{15}\text{NO}_4$: 309.1001; found: 309.0991.

3-ethyl-2-phenyl-4-(4-bromophenyl)-1,3-oxazolium 5-oxide (4.1e):

NMR Yield: 88%. Isolated Yield: 31%. ¹H NMR (300 MHz, CD₃CN): δ 7.75 (m, 2H), 7.45-7.70 (m, 7H), 4.37 (q, 2H), 1.20 (t, 3H). ¹³C NMR (75 MHz, CD₃CN): δ 160.8; 143.7; 131.8; 131.4; 129.7; 129.5; 128.7; 128.6; 123.5; 118.4; 92.8; 43.1; 14.1. IR (NaCl): ν_{CO} = 1712.9 cm⁻¹ (s). HRMS calculated for C₁₇H₁₄BrNO₂: 343.0208; found: 343.0215.

3-ethyl-2-isopropyl-4-p-tolyl-1,3-oxazolium 5-oxide (4.1f):

NMR Yield: 59%. Isolated Yield: 8%. ¹H NMR (300 MHz, CD₃CN): δ 7.33 (d, 2H), 7.21 (d, 2H), 4.05 (q, 2H), 3.30 (m, 1H), 2.35 (s, 3H), 1.40 (d, 6H), 1.20 (t, 3H). ¹³C NMR (75 MHz, CD₃CN): δ 161.3; 150.7; 135.2; 129.4; 127.6; 127.5; 89.7; 40.7; 26.2; 20.5; 19.5; 14.7. IR (NaCl): ν_{CO} = 1738.4 cm⁻¹ (s). HRMS calculated for C₁₅H₁₉NO₂: 245.1416; found: 245.1411.

3-benzyl-2-phenyl-4-(4-methyl-benzoic acid-4-phenyl ester)-1,3-oxazolium 5-oxide (4.1g):

NMR Yield: 32%. Isolated Yield: 21%. ¹H NMR (300 MHz, CD₂Cl₂): δ 8.05 (d, 2H), 7.60-7.15 (m, 16H), 5.53 (s, 2H), 2.45 (s, 3H). ¹³C NMR (75 MHz, CD₂Cl₂): δ 165.2; 160.7; 149.2; 148.1; 144.8; 143.2; 134.5; 131.2; 130.2; 129.7; 129.5; 129.5;

128.7; 128.3; 127.6; 126.9; 126.8; 125.9; 123.0; 122.2; 95.4; 51.2; 21.9. IR (NaCl): $\nu_{\text{CO}} = 1735.0 \text{ cm}^{-1}$ (s), 1714.5 cm^{-1} (s). HRMS calculated for $\text{C}_{30}\text{H}_{23}\text{NO}_4$: 461.1627; found: 461.1637.

3-ethyl-2-phenyl-4-(4-methylsulfanyl-phenyl)-1,3-oxazolium 5-oxide (4.1h):

NMR Yield: 85%. Isolated Yield: 24%. ^1H NMR (300 MHz, CD_2Cl_2): δ 7.65 (m, 2H), 7.58 (m, 3H), 7.50 (d, 2H), 7.35 (d, 2H), 4.36 (q, 2H), 2.53 (s, 3H), 1.21 (t, 3H). ^{13}C NMR (75 MHz, CD_2Cl_2): δ 161.0; 142.8; 136.0; 131.2; 129.4; 128.4; 128.2; 126.9; 126.7; 123.7; 93.4; 42.8; 15.2; 14.1. IR (NaCl): $\nu_{\text{CO}} = 1709.7 \text{ cm}^{-1}$ (s). HRMS calculated for $\text{C}_{18}\text{H}_{17}\text{NO}_2\text{S}$: 311.0980; found: 311.0977.

3-(4-methoxyphenyl)-2-phenyl-4-p-tolyl-1,3-oxazolium 5-oxide (4.1i):

NMR Yield: 55%. Isolated Yield: 36%. ^1H NMR (300 MHz, CD_2Cl_2): δ 7.35-7.20 (m, 8H), 7.10-6.90 (m, 5H), 3.78 (s, 3H), 2.25 (s, 3H). ^{13}C NMR (75 MHz, CD_2Cl_2): δ 161.3; 160.1; 141.0; 134.8; 130.3; 129.0; 128.9; 128.5; 127.3; 126.2; 126.2; 123.2; 115.8; 97.6; 56.0; 21.1. IR (NaCl): $\nu_{\text{CO}} = 1715.8 \text{ cm}^{-1}$. HRMS calculated for $\text{C}_{23}\text{H}_{19}\text{NO}_3$: 357.1365; found: 357.1374.

General Procedure for Formation of Amido Esters

~20 eq. of methanol was added to the solution of Münchnone, and the solution was allowed to stir for 2 hours. The solvent was subsequently removed *in vacuo*, and the resulting oil was chromatographed on Silica Gel 60 using hexanes/ethyl acetate as eluent.

Benzeneacetic acid, α -(benzoylbenzylamino)-4-methyl-, methyl ester (4.5a).

Yield: 75%. ^1H NMR (500 MHz, CDCl_3): δ 7.48 (d, 2H, 7.8 Hz), 7.40-7.28 (m, 3H), 7.22-7.15 (m, 5H), 7.07 (d, 2H, 7.8 Hz), 6.97 (m, 2H), 5.59 (s, 1H), 4.73 (d, 1H), 4.40 (m, 1H), 3.73 (s, 3H), 2.34 (s, 3H). ^{13}C NMR (100 MHz, CDCl_3): δ 173.1, 170.6, 138.6, 137.6, 136.3, 131.1, 129.9, 129.7, 129.3, 128.6, 128.3, 127.2, 127.0, 127.0, 63.6, 52.6, 51.6, 21.4. IR (NaCl): $\nu_{\text{CO}} = 1746.7, 1644.0 \text{ cm}^{-1}$ HRMS calculated for $\text{C}_{24}\text{H}_{23}\text{NO}_3$: 373.1678; found: 373.1678.

Benzeneacetic acid, α -(benzoylethylamino)-4-methyl-, methyl ester (4.5b).

Yield: 83%. ^1H NMR (400 MHz, CDCl_3 , 50°C): δ 7.46-7.40 (m, 2H), 7.40-7.35 (m, 3H), 7.28-7.32 (m, 4H), 5.88 (s, br, 1H), 3.78 (s, 3H), 3.32 (q, br., 2H), 2.36 (s, 3H), 0.78 (t, br, 3H). ^{13}C NMR (100 MHz, CDCl_3): δ 172.4, 171.0, 138.6, 136.9, 131.7, 129.6, 129.6, 129.3, 128.6, 126.6, 62.6, 52.5, 41.9, 21.4, 21.4, 14.9. IR (NaCl): $\nu_{\text{CO}} = 1747.5, 1637.6 \text{ cm}^{-1}$ HRMS calculated for $\text{C}_{19}\text{H}_{21}\text{NO}_3$: 311.1521; found: 311.1516.

2-naphthaleneacetic acid, α -(benzoylethylamino)-, methyl ester (4.5c).

Yield: 91%. ^1H NMR (400 MHz, CDCl_3): δ 7.88-7.76 (m, 4H), 7.55-7.45 (m, 5H), 7.44-7.38 (m, 3H), 6.08 (s, br, 1H), 3.84 (s, 3H), 3.49 (q, br, 2H), 0.81 (t, br, 3H). ^{13}C NMR (100 MHz, CDCl_3): δ 172.6, 170.9, 136.8, 133.3, 133.3, 132.3, 129.7, 128.8, 128.7, 128.3, 127.8, 126.9, 63.3, 52.7, 42.2, 15.0. IR (NaCl): ν_{CO} = 1746.7, 1636.3 cm^{-1} . HRMS calculated for $\text{C}_{22}\text{H}_{21}\text{NO}_3$: 347.1521; found: 347.1530.

Benzo[1,3]dioxol-5-yl-(benzoyl-ethyl-amino)-acetic acid methyl ester (4.5d).

Yield: 57%. ^1H NMR (400 MHz, CDCl_3): δ 7.45-7.35 (m, 5H), 6.90-6.75 (m, 3H), 5.97 (s, 2H), 5.81 (s, br, 1H), 3.79 (s, 3H), 3.32 (q, br., 2H), 0.75 (m, 3H). ^{13}C NMR (100 MHz, CDCl_3): δ 172.4, 170.8, 148.2, 148.0, 136.8, 129.6, 128.6, 128.4, 126.6, 123.2, 109.8, 108.6, 101.5, 62.8, 52.6, 42.5, 15.0. IR (NaCl): ν_{CO} = 1746.9, 1635.8 cm^{-1} . HRMS calculated for $\text{C}_{19}\text{H}_{19}\text{NO}_5$: 341.1263; found: 341.1254.

Benzeneacetic acid, α -(benzoylethylamino)-4-bromo-, methyl ester (4.5e).

Yield: 85%. ^1H NMR (400 MHz, CDCl_3): δ 7.51 (d, 2H), 7.46-7.35 (m, 5H), 7.30-7.18 (m, 2H), 5.74 (s, br, 1H), 3.79 (s, 3H), 3.33 (q, br, 2H), 0.84 (m, 3H). ^{13}C NMR (100 MHz, CDCl_3): δ 172.4, 170.2, 136.5, 134.1, 132.0, 131.0, 129.8, 128.7, 126.6,

122.9, 62.6, 52.7, 42.6, 14.9. IR (NaCl): $\nu_{\text{CO}} = 1747.1, 1637.2 \text{ cm}^{-1}$ HRMS calculated for $\text{C}_{18}\text{H}_{18}\text{BrNO}_3$: 375.0470; found: 375.0476.

Benzeneacetic acid, α -(ethylisobutyrylamino)-4-methyl-, methyl ester (4.5f).

Yield: 49%. ^1H NMR (400 MHz, CDCl_3 , 50°C): δ 7.15 (m, 4H), 6.04 (s, br, 1H), 3.72 (s, 3H), 3.40–3.20 (m, 2H), 2.81 (m, 1H), 2.35 (s, 3H), 1.18 (d, 6H), 0.82 (m, 3H). ^{13}C NMR (100 MHz, CDCl_3): δ 178.1, 171.4, 138.4, 132.1, 129.6, 129.5, 61.4, 52.3, 40.4, 31.2, 21.4, 20.1, 20.0, 16.1. IR (NaCl): $\nu_{\text{CO}} = 1748.6, 1652.5 \text{ cm}^{-1}$. HRMS calculated for $\text{C}_{16}\text{H}_{23}\text{NO}_3$: 277.1678; found: 277.1686.

4-Methyl-benzoic acid 4-[(benzoyl-benzyl-amino)-methoxycarbonyl-methyl]-phenyl ester (4.5g):

Yield: 31%. ^1H NMR (400 MHz, CD_3CN): δ 8.07 (d, 2H), 7.40-7.51 (m, 9H), 7.12-7.36 (m, 7H), 5.53 (s, 1H), 4.76 (d, 1H), 4.47 (d, 1H), 3.76 (s, 3H), 2.49 (s, 3H). ^{13}C NMR (100 MHz, CDCl_3): δ 172.6, 170.2, 165.1, 151.3, 145.1, 137.3, 136.3, 132.4, 131.1, 130.2, 130.1, 130.0, 129.7, 128.8, 128.5, 127.2, 126.9, 126.7, 122.1, 62.8, 52.4, 51.6, 21.2. IR (NaCl): $\nu_{\text{CO}} = 1737.4, 1642.6 \text{ cm}^{-1}$. HRMS calculated for $\text{C}_{31}\text{H}_{27}\text{NO}_5$: 493.1889; found: 493.1895.

Benzeneacetic acid, α -(benzoylethylamino)-4-methylsulfanyl-, methyl ester (4.5h).

Yield: 75%. ^1H NMR (400 MHz, CDCl_3): δ 7.46-7.34 (m, 5H), 7.30-7.18 (m, 4H), 5.82 (s, br, 1H), 3.78 (s, 3H), 3.32 (q, br., 2H), 2.48 (s, 3H), 0.81 (m, 3H). ^{13}C NMR (100 MHz, CDCl_3): δ 172.4, 170.7, 139.6, 136.7, 131.4, 129.8, 129.7, 128.6, 126.8, 126.6, 62.7, 52.6, 42.0, 16.0, 14.9. IR (NaCl): $\nu_{\text{CO}} = 1746.7, 1636.0 \text{ cm}^{-1}$. HRMS calculated for $\text{C}_{19}\text{H}_{21}\text{NO}_3\text{S}$: 343.1242; found: 343.1237.

Benzeneacetic acid, α -(benzoyl(4-methoxyphenyl)amino)-4-methyl-, methyl ester (4.5i).

Yield: 53%. ^1H NMR (400 MHz, CDCl_3 , 50°C): δ 7.26 (m, 2H), 7.20-7.08 (m, 3H), 7.04 (m, 4H), 6.84-6.74 (m, 2H), 6.49 (d, 2H), 6.27 (s, 1H), 3.80 (s, 3H), 3.65 (s, 3H), 2.29 (s, 3H). ^{13}C NMR (100 MHz, CDCl_3): δ 171.5, 171.3, 158.6, 138.4, 136.4, 133.5, 132.0, 131.4, 130.4, 129.5, 129.2, 128.7, 127.7, 113.6, 64.7, 55.4, 52.4, 21.3. IR (NaCl): $\nu_{\text{CO}} = 1746.8, 1644.8 \text{ cm}^{-1}$. HRMS calculated for $\text{C}_{24}\text{H}_{23}\text{NO}_4$: 389.1627; found: 389.1621.

4.4 References

1. a) Gingrich, H.L.; Baum, J.S. In *Oxazoles*; Turchi, I.J., Ed.; Wiley; New York, 45, 1986, p. 731. b) Potts, K.T. In *1,3-Dipolar Cycloaddition Chemistry* Padwa A. Ed, Wiley, New York; vol. 2, 1984, p. 1.
2. a) Keating, R. A.; Armstrong, R. W. *J. Am. Chem. Soc.* **1996**, *118*, 2574.; b) Santiago, B.; Dalton, C. R.; Huber, E. W.; Kane, J. M. *J. Org. Chem.* **1995**, *60*, 4947.; c) Bilodeau, M. T.; Cunningham, A. M. *J. Org. Chem.* **1998**, *63*, 2800.; d) Consonni, R.; Dalla Croce, P.; Ferraccioli, R.; La Rosa, C. *J. Chem. Res. Synop.* **1991**, *7*, 188. e) Huisgen, R.; Gotthardt, H.; Bayer, H.O. *Chem. Ber.* **1970**, *103*, 2368. f) Nayyar, N. K.; Hutchison, D. R.; Martinelli, M. J. *J. Org. Chem.* **1997**, *62*, 982.
3. a) Bayer, H.O.; Huisgen, R.; Knorr, R.; Schaefer, F. C. *Chem. Ber.* **1970**, *103*, 2581. b) Funke, E.; Huisgen, R.; *Chem. Ber.* **1971**, *104*, 3222
4. a) Merlic, C. A.; Baur, A.; Aldrich, C. C. *J. Am. Chem. Soc.* **2000**, *122*, 7398; b) Alper, H.; Tanaka, M. *J. Am. Chem. Soc.* **1979**, *101*, 4345.
5. For chromium-ketene complexes: a) Hegedus, L. S. *Acc. Chem. Res.* **1995**, *28*, 299. b) Hegedus, L. S. *Tetrahedron.* **1997**, *53*, 4105.
6. For examples of related carbonylative cyclizations: a) Colquhoun, H.; Thompson, D.J.; Twigg, M. V. *Carbonylation*, Plenum Press: New York 1991. b) Khumtaveeporn, K.; Alper, H. *Acc. Chem. Res.* **1995**, *28*, 414. c) Tanaka, H.; Abdul Hai, A.K.M.; Sadakane, M.; Okumoto, H.; Torii, S. *J. Org. Chem.* **1994**, *59*, 3040. d) Cho, C.S.; Jiang, L.H.; Shim, S.C. *Synth. Comm.* **1999**, *29*, 2695. e) Van den Hoven, B.G.; Alper, H. *J. Am. Chem. Soc.*, **2001**, *123*, 10214. f)

- Mahadevan, V.; Getzler, Y.; Coates, G.W. *Angew. Chem. Int. Ed.* **2002**, *41*, 2781.
- g) Chatani, N.; Morimoto, T.; Fukumoto, Y.; Murai, S. *J. Am. Chem. Soc.* **1998**, *120*, 5335. h) Chatani, N.; Kamitani, A.; Murai, S. *J. Org. Chem.* **2002**, *67*, 7014.
7. a) Dghaym, R. D.; Dhawan, R.; Arndtsen, B. A. *Angew. Chem. Int. Ed.* **2001**, *40*, 3228. b) Dghaym, R. D.; Yaccato, K. J.; Arndtsen, B. A. *Organometallics* **1998**, *17*, 4. c) Lafrance, D.; Davis, J. L.; Dhawan, R.; Arndtsen, B. A. *Organometallics* **2001**, *20*, 1128.
8. Kacker, S.; Kim, J. S.; Sen, A. *Angew. Chem. Int. Ed.* **1998**, *37*, 1251.
9. This mechanism is similar to those postulated for amidocarbonylation: a) Beller, M.; Eckert, M.; Vollmuller, F.; Bogdanovic, S.; Geissler, H. *Angew. Chem., Int. Ed.* **1997**, *36*, 1494. b) Beller, M.; Eckert, M. *Angew. Chem. Int. Ed.* **2000**, *39*, 1010.
10. Control reactions show **4.1a** decomposes in the presence of Pd₂(dba)₃·CHCl₃
11. Compound **4.2** is not observed in these reactions, nor are there any major (i.e. >5% yield) identifiable products other than **4.1**.
12. a) Beletskaya, I. P.; Cheprakov, A. V. *Chem. Rev.* **2000**, *100*, 3009. b) Jeffrey, T. *Tetrahedron* **1996**, *52*, 10113.
13. See experimental section for the synthesis of **4.1**, **4.4**, and **4.5**.
14. Side reactions of these N-acyl iminium salts may also inhibit **4.1** formation: enamides are observed in these reactions in ca. 30% yield.
15. Williams, R. M. and Hendrix, J. A. *Chem. Rev.* **1992**, *92*, 889.
16. Ukai, R.; Kawazura, H.; Ishii, Y. *J. Organomet. Chem.* **1974**, *65*, 253.
17. Layer, R. W. *Chem. Ber.* **1963**, *63*, 489.

CHAPTER FIVE

Palladium Catalyzed Multicomponent Coupling of Imines, Alkynes and Acid Chlorides: A Direct and Modular Approach to Pyrrole Synthesis*

Preface

In Chapter 4, we described the palladium catalyzed multicomponent coupling of imines, acid chlorides and CO to generate Münchnones. In Chapter 5 we describe a highly modular, one step, three component coupling of imine, acid chloride and alkynes to generate multisubstituted pyrroles. In addition, we discuss further improvements for catalytic Münchnone generation by employing sterically bulky ligands in the coupling process. These improvements have lead to increased rates of Münchnone formation and an expanded reaction scope to include non-enolizable alkyl-imines.

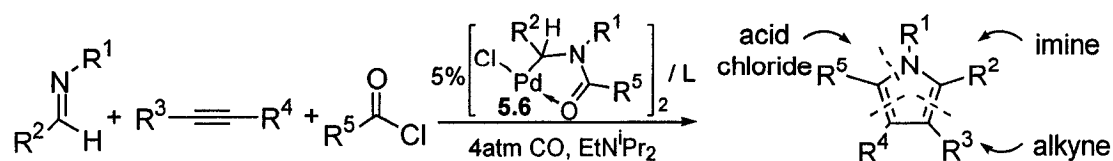
5.0 Introduction

Of the various synthetic and naturally occurring heterocyclic structures, the pyrrole nucleus is among the most prevalent. Pyrroles are found in a tremendous range of natural products¹ and bioactive molecules,² including the blockbuster drug

* Previously Published: Dhawan, R.; Arndtsen, B.A. *J. Am. Chem. Soc.* **2004**, *126*, 468

Atorvastatin Calcium,^{2a} as well as important anti-inflammatories,^{2b} antitumor agents,^{2c} and immunosuppressants.^{2d} Similarly, polypyrroles are of growing relevance in material science as conjugated polymers.³ While this broad utility has made pyrroles important synthetic targets, traditional routes to their preparation are multistep reactions, as illustrated by the Paal-Knorr cyclization of amines with pre-formed 1,4-diketones.⁴ This has stimulated interest in the design of alternative metal-based routes to pyrroles.⁵ Examples include the isomerization of unsaturated imines,^{5a} isonitrile/ketone couplings,^{5c} and imine additions to chromium-carbenes,^{5d} many of which provide structures not easily generated by classical routes.

Despite these advances, a common feature of most pyrrole syntheses is their requisite use of pre-assembled precursor(s) for cyclization.^{1,4,5} This not only imposes further steps on the overall synthesis, but can also complicate structural diversification. In principle, a more ideal way to construct complex molecules would involve their preparation in one step, directly from simple, readily available and easily varied substrates, in a fashion similar to the Pauson-Khand reaction for carbocycle synthesis⁶ and other multicomponent reactions.⁷ We report below our design of such a direct synthesis of pyrroles. This has been done by assembling the pyrrole core via metal catalysis, from the basic building blocks shown in Eq. 5.1.



Equation 5.1 Four Component Coupling in the Generation of Pyrroles

5.1 Results and Discussion

Our approach to this synthesis is based upon the ability of alkynes to undergo 1,3-dipolar addition to 1,3-oxazolium-5-oxides (Münchnones, **5.1**) to form pyrroles.⁸ While Münchnones are typically prepared *in situ* from amino acid derivatives, we have recently reported their generation by the palladium catalyzed coupling of imines, acid chlorides and carbon monoxide.⁹ This suggested a potential pathway to construct pyrroles, outlined in Scheme 5.1. By performing these steps simultaneously, this would provide overall a method to convert imines, alkynes and acid chlorides directly into a pyrrole. However, examination of this reaction under the conditions reported to generate **5.1**⁹ formed only a trace of pyrrole **5.2a** (5%, Eq. 5.2). Indeed, while mechanistically plausible, this process involves four separate reagents, base and a catalyst all proceeding selectively through over eight separate steps. Considering the reactivity of the intermediates formed in this cycle (**5.1**, **5.7-5.11**), this suggests the potential for numerous other reactions. Thus, we have undertaken a series of mechanistic studies on this process, with the goal of designing a metal catalyst that could mediate this synthesis in a selective fashion.

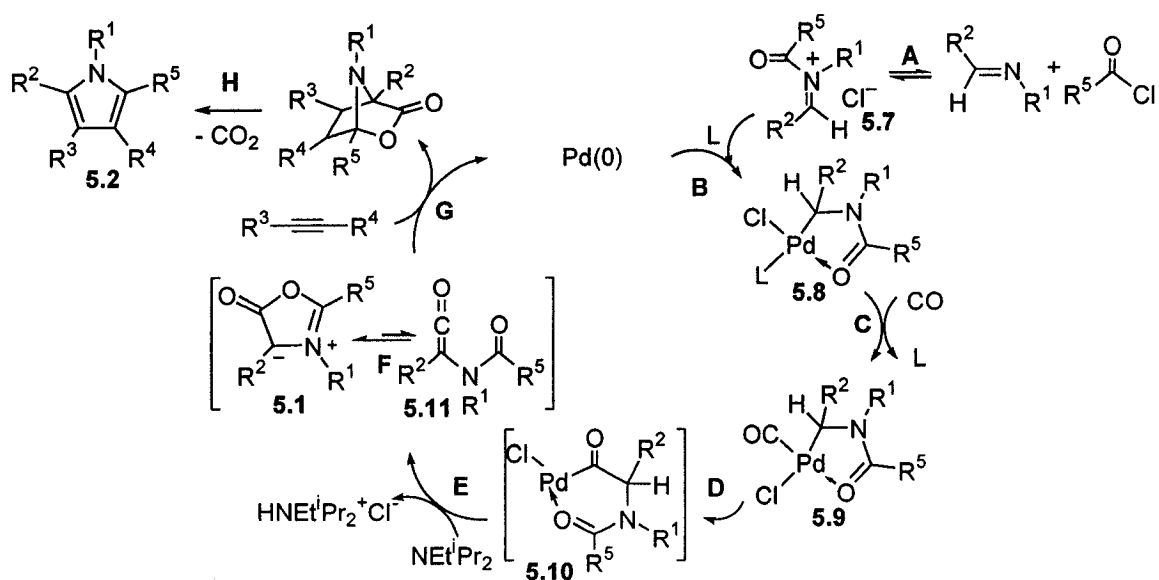
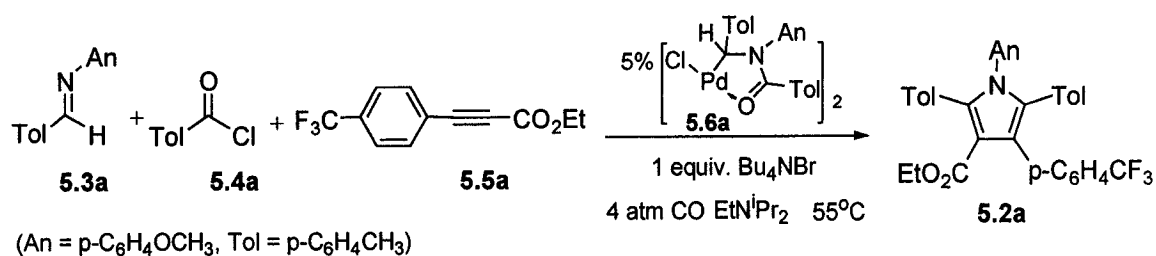


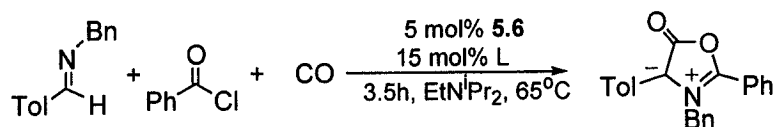
Figure 5.1. Catalytic Cycle For Pyrrole Formation

While there are several stages in this cycle wherein the reaction might be inhibited, a useful observation came from mechanistic studies on the Münchnone synthesis itself, which show that the oxidative addition of iminium salt **5.7** to Pd(0) (step B) is rate determining. This is evidenced by kinetic studies (the formation of **5.1** is first order in **5.7**), and consistent with *in situ* NMR data (the catalyst resting state is not **5.8-5.10**).¹⁰ Considering that catalyst **5.6**¹¹ forms an unligated 14 e⁻ intermediate **5.8** (- L) for carbonylation (steps C-E), a slow oxidative addition is not surprising, and suggests that the inhibition of pyrrole formation may potentially arise from the alkyne further slowing this step in the catalytic cycle. Consistent with this postulate, examination of the products of Eq. 5.2 reveals significant quantities of **5.7** after catalysis.



Equation 5.2 Pyrrole Formation in the Presence Weakly Coordinating Halide Salts

A method to accelerate iminium salt oxidative addition (step B) would be to add donor ligands (L) to stabilize **5.8**. However, simple phosphines were found to completely inhibit Münchnone formation even without alkynes (Table 5.1, entry 2-4), presumably due to tight coordination to **5.8** blocking subsequent CO binding (step C).⁹ A more favorable scenario would be a ligand that could both stabilize **5.8**, as well as be sufficiently labile to allow the subsequent catalysis steps. As has been noted in other systems,¹² these features can be obtained by the use of sterically encumbered phosphines. In the case of P(o-tolyl)₃, this generates a catalyst that is several times more reactive for Münchnone formation (entry 8). More importantly, this catalyst is also capable of mediating these steps in the presence of alkyne (Scheme 4.1). Thus, the addition of 15 mol% P(o-tolyl)₃ to the **5.6a** catalyzed reaction of imine, acid chloride, alkyne (**5.3a-5.5a**), 4 atm CO and NEtⁱPr₂ results in disappearance of these reagents over 16 h, and the formation of pyrrole **5.2a** as essentially the only significant reaction product (81% yield, Table 5.2).¹³ Overall, this optimized protocol provides a straightforward catalytic method to construct a pyrrole in one step from three separate and readily available building blocks.

Table 5.1. Ligand Influence on Münchnone Formation^a

entry	Ligand	Yield ^b	entry	Ligand	Yield ^b
1	- ^c	33%	5	P ^t Bu ₃	29%
2	PCy ₃	-	6	P ^t Bu ₂ (2-biphenyl)	31%
3	PPh ₃	-	7	P(1-naphthyl) ₃	51%
4	dppe	-	8	P(o-tolyl) ₃	78%

^aSee Experimental Section for details. ^bNMR yield. ^c1 equiv. Bu₄NBr

In addition to its simplicity, a useful feature of this synthesis is the nature of the substrates employed, each of which can be easily varied. As shown in Table 5.2, catalysis is tolerant to a range of functionalities (*e.g.* esters, indoles, halides, thioethers). Aryl, heteroaryl and alkyl substituents can be incorporated into the pyrrole from the acid chloride or imine-nitrogen, as can a variety of bis-, mono-, and unsubstituted alkynes. While unsymmetrical alkynes can lead to mixtures, steric and electronic effects provide a reasonable degree of selectivity (5:1 ratio in **5.2c**).^{8b} Even electron rich alkynes, typically less potent Münchnone trapping reagents,^{8a} form pyrroles in reasonable yield (**5.2f**, **5.2g**). Considering the nature of the substrates and number of bonds generated in one-pot, these all represent effective syntheses of **5.2a-5.2n**.

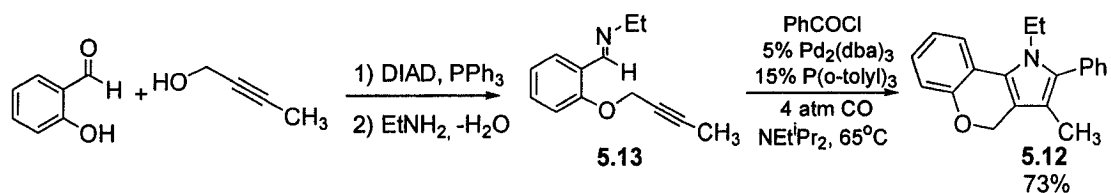
Table 5.2. Palladium Catalyzed Pyrrole Synthesis (Eq. 5.1).^{a,b}

cpd	imine	acid chloride	alkyne	5.2 (% yield)
a		TolCOCl		
b ^c		PhCOCl		
c ^d		PhCOCl		
d				
e				
f ^c		PhCOCl		
g		TolCOCl		
h		TolCOCl		
i ^d		PhCOCl		
j		TolCOCl		
k		TolCOCl		
l		PhCOCl		
m ^c		PhCOCl		
n ^c		PhCOCl		

^aImine (0.7 equiv), acid chloride, alkyne (1.4 equiv.), NEt^iPr_2 , CO (4 atm), 5% **5.6** and 15% $\text{P}(\text{o-tolyl})_3$ in $\text{CH}_3\text{CN}/\text{THF}$, 16h, 65°C. ^b Pd_2dba_3 or $[\text{Pd}(\text{allyl})\text{Cl}]_2$ are viable catalysts at ca. 10% lower yield. ^cAlkyne added to preformed **5.1**. ^d75°C, 1 equiv. LiOTf , **5.6f** cat. ^eMajor isomer (5:1 ratio).

Interestingly, the phosphine-based catalyst system can also form pyrroles of Münchnones not previously accessible by catalysis, as shown by the synthesis of pyrroles of both C-aromatic and C-alkyl imines (**5.2c**). The latter represents a significant expansion in scope of the Münchnone synthesis, which without P(o-tolyl)₃ is inert towards these imines.⁹ In general, while there are some limitations brought on by the complex series of reactions occurring during catalysis,¹⁴ this process provides a method to construct pyrroles wherein each of the five substituents (R¹-R⁵) can be independently controlled and varied by modulation of the three substrates. A method to accomplish the latter in a single step reaction is, to our knowledge, previously unknown.

As illustrated in Eq. 5.3, this process can also be useful in the incorporation of further levels of product complexity (**5.12**) into the pyrrole product with minimal steps. This class of multicyclic pyrroles are of utility as potential therapeutics and retinoic acid regulators,¹⁵ in this case generated in three steps from an aldehyde, alkyne, amine and acid chloride.



Equation 5.3 Generation of Multicyclic Pyrroles

5.3 Conclusions

In conclusion, these studies have shown that pyrroles can be considered as the product of three basic building blocks coupled via palladium catalysis, providing a modular method to construct these heterocycles with facile diversity and high atom economy. Experiments directed towards understanding of the role of P(o-tolyl)₃ in this catalysis, as well as the application of this approach to other heterocyclic targets, are underway.

5.4 Experimental

I. General Procedures

Unless otherwise noted, all manipulations were performed under an inert atmosphere in a Vacuum Atmospheres 553-2 dry box or by using standard Schlenk or vacuum line techniques. The catalysts, [Pd(Cl)[η^2 -CH(R¹)NR²(COR⁵)]₂, were prepared according to previous literature procedures.¹⁶ Carbon monoxide (99.99%) was purchased from Matheson and used as received. Imines were prepared using standard literature procedures.¹⁷ **5.5a**¹⁸ and dibenzoylacetylene¹⁹ were prepared using literature procedures. All other reagents were purchased from Aldrich® and used as received. Tetrahydrofuran (THF) was distilled from sodium/benzophenone ketyl under nitrogen. Acetonitrile was distilled from CaH₂ under nitrogen. Deuterated

solvents were dried as their protonated analogues, but were transferred under vacuum from the drying agent, and stored over 3Å molecular sieves.

^1H and ^{13}C were recorded on JEOL 270, Varian Mercury 300 MHz, Mercury 400 MHz, and Unity 500 MHz spectrometers. Mass spectra were obtained from the McGill University Mass Spectral Facility.

II. General Procedure for Pyrrole formation²⁰

Imine (0.272 mmol) and acid chloride (0.381 mmol) were dissolved in 4.5 mL of acetonitrile. This solution was added to $[\text{Pd}(\text{Cl})[\eta^2\text{-CH}(\text{R}^1)\text{NR}^2(\text{COR}^5)]_2$ (5 mol%) and $\text{P}(\text{o-tolyl})_3$ (15 mol%) in 4.5 mL of acetonitrile. The reaction mixture was transferred to a 50 mL reaction bomb, and alkyne (0.54 mmol) (in 4.5 mL of THF) and EtN^iPr_2 (0.44 mmol) (in 4.5 mL of THF) were added. The solution was evacuated, carbon monoxide (60 psi) added, and the solution stirred at 65°C for 18 hours. In the case of dimethoxyacetylenedicarboxylate (DMAD) and acetylene, the alkyne was added to the pre-formed Münchnone solution after catalysis. Products were purified by silica gel chromatography using hexanes/ethyl acetate as eluent.

1-(4-Methoxy-phenyl)-2,5-di-p-tolyl-4-(4-trifluoromethyl-phenyl)-1H-pyrrole-3-carboxylic acid ethyl ester (5.2a)

Yield: 81% ¹H NMR (300 MHz, CDCl₃): δ 7.46 (d, 2H, 8.80 Hz), 7.35 (d, 2H, 8.80 Hz), 7.12-7.00 (m, 4H), 6.88-6.74 (m, 6H), 6.66-6.59 (m, 2H), 4.00 (q, 2H), 3.70 (s, 3H), 2.31 (s, 3H); 2.22 (s, 3H); 0.89 (t, 3H). ¹³C NMR (75 MHz, CD₃CN): δ 165.4, 158.6, 139.8, 138.9, 137.5, 137.0, 133.4, 131.3, 131.1, 131.0, 130.8, 130.2, 129.0, 128.7, 128.4, 128.2, 127.9, 127.4 (q), 124.5 (q), 122.5, 113.8, 113.7, 60.0, 55.5, 21.7, 21.5, 14.0 HRMS. Calculated for C₃₅H₃₀F₃NO₃: 569.21778; found: 569.21829.

1-Ethyl-2-phenyl-5-[1-(toluene-4-sulfonyl)-1H-indol-3-yl]-1H-pyrrole-3,4-dicarboxylic acid dimethyl ester (5.2b)

Yield: 71%. ¹H NMR (400 MHz, CDCl₃): δ 8.02 (d, 1H), 7.84-7.74 (m, 3H), 7.50-7.40 (m, 5H), 7.40-7.30 (m, 2H), 7.28-7.20 (m, 3H), 3.80-3.60 (2H, m), 3.66 (s, 3H), 3.47 (s, 3H), 2.34 (s, 3H), 0.78 (t, 3H). ¹³C NMR (100 MHz, CDCl₃): δ 165.4, 165.0, 145.4, 137.6, 135.2, 134.8, 130.9, 130.7, 130.5, 130.1, 129.1, 128.6, 127.7, 127.1, 126.9, 125.4, 124.1, 120.5, 116.7, 115.3, 114.0, 112.9, 52.0, 51.8, 40.5, 22.0, 16.8. HRMS. Calculated for C₃₁H₂₈N₂O₆S: 556.16681; found: 556.16671 .

1-Benzyl-5-tert-butyl-2,4-diphenyl-1H-pyrrole-3-carboxylic acid methyl ester

(5.2c):

(major isomer: 67%) ^1H NMR (400 MHz, CDCl_3): δ 7.60-7.10 (m, 13H), 6.72 (d, 2H, 8.22 Hz), 5.36 (s, 2H), 3.27 (s, 3H), 1.26 (s, 9H). ^{13}C NMR (100 MHz, CDCl_3): δ 165.7, 139.6, 139.6, 139.5, 137.5, 133.0, 131.5, 130.8, 128.5, 128.1, 127.8, 127.2, 127.1, 126.5, 125.7, 123.8, 115.3, 50.7, 50.7, 34.7, 33.2. HRMS. Calculated for $\text{C}_{29}\text{H}_{29}\text{NO}_2$: 423.21983; found: 423.21868. 1-Benzyl-2-tert-butyl-4,5-diphenyl-1H-pyrrole-3-carboxylic acid methyl ester) (minor isomer: 13%) ^1H NMR (400 MHz, CDCl_3): δ 7.19-7.03 (m, 11H), 6.96 (d, 2H, 8.22 Hz), 6.65 (d, 2H, 6.45 Hz), 5.30 (s, 2H), 3.64 (s, 3H), 1.44 (s, 9H). ^{13}C NMR (100 MHz, CDCl_3): δ 170.8, 139.4, 138.3, 135.0, 132.9, 132.2, 131.7, 129.4, 128.4, 128.2, 127.9, 127.6, 126.9, 125.8, 125.7, 122.0, 115.3, 77.5, 52.3, 50.2, 34.2, 31.6. HRMS. Calculated for $\text{C}_{29}\text{H}_{29}\text{NO}_2$: 423.21983; found: 423.21944.

[4-Benzoyl-5-(4-bromo-phenyl)-2-cyclohexyl-1-ethyl-1H-pyrrol-3-yl]-phenyl-methanone (5.2d):

Yield: 63%. ^1H NMR (400 MHz, CDCl_3): δ 7.42-7.39 (m, 4H), 7.33-7.10 (m, 8H), 7.04 (m, 2H), 3.93 (q, 2H), 2.83 (m, 1H), 2.00-1.60 (m, 7H), 1.40-1.24 (m, 3H), 1.24 (t, 3H). ^{13}C NMR (100 MHz, CDCl_3): δ 194.9, 192.0, 141.2, 140.5, 139.7, 134.7, 132.8, 132.1, 131.7, 131.5, 130.4, 129.0, 128.9, 128.1, 127.8, 124.3, 123.1, 122.0,

39.9, 37.8, 32.6, 27.6, 26.0, 17.4. HRMS. Calculated for $C_{32}H_{30}NO_2Br$: 539.14559; found: 539.14541.

[4-Benzoyl-1-ethyl-2-furan-2-yl-5-(4-methylsulfanyl-phenyl)-1H-pyrrol-3-yl]-phenyl-methanone (5.2e):

Yield: 73%. 1H NMR (400 MHz, $CDCl_3$): δ 7.52-7.38 (m, 5H), 7.34-7.23 (m, 4H), 7.21-7.06 (m, 6H); 6.66 (m, 1H), 6.35 (m, 1H), 4.04 (q, 2H, 7.04 Hz), 2.45 (s, 3H), 1.12 (t, 3H). ^{13}C NMR (75 MHz, $CDCl_3$): δ 192.0, 191.8, 143.6, 143.4, 139.9, 139.5, 139.3, 137.8, 132.1, 132.0, 131.3, 129.1, 129.1, 128.0, 128.0, 126.8, 126.0, 125.8, 125.3, 124.0, 113.8, 111.5, 41.4, 16.6, 15.8. HRMS. Calculated for $C_{31}H_{25}NO_3S$: 491.15551; found: 491.15630.

1-Ethyl-2-phenyl-5-p-tolyl-1H-pyrrole (5.2f):²¹

Yield: 77%. 1H NMR (400 MHz, $CDCl_3$): δ 7.56-7.26 (m, 9H), 6.33 (d, 1H), 6.31 (d, 1H), 4.17 (q, 1H), 2.47 (s, 3H), 0.93 (t, 3H). ^{13}C NMR (100 MHz, $CDCl_3$): δ 137.0, 136.2, 135.8, 134.4, 131.4, 129.4, 129.3, 128.7, 127.2, 109.7, 109.5, 40.4, 21.8, 16.7. HRMS. Calculated for $C_{19}H_{19}N$: 261.15175; found: 261.15123.

1-Benzyl-3-phenyl-2,5-di-p-tolyl-1H-pyrrole (5.2g).

Yield: 56%. ^1H NMR (500 MHz, CDCl_3): δ 7.36 (d, 2H), 7.31 (d, 2H), 7.26-7.08 (m, 12H), 6.76 (d, 2H), 6.62 (s, 1H), 5.15 (s, 2H), 2.40 (s, 3H), 2.38 (s, 3H). ^{13}C NMR (75.5 MHz, CDCl_3): δ 139.6, 137.5, 137.1, 136.6, 135.6, 132.3, 131.4, 130.8, 130.4, 129.4, 129.4, 129.2, 128.4, 128.3, 127.8, 126.9, 126.2, 125.3, 123.2, 109.4, 48.7, 21.8, 21.7. Calculated for $\text{C}_{31}\text{H}_{27}\text{N}$: 413.21435; found: 413.21484.

1-Methoxycarbonylmethyl-2-methyl-5-p-tolyl-4-(4-trifluoromethyl-phenyl)-1H-pyrrole-3-carboxylic acid ethyl ester (5.2h).

Yield: 65%. ^1H NMR (300 MHz, CDCl_3): δ 7.43 (d, 2H), 7.38-7.30 (m, 4H), 7.24 (d, 2H), 7.12-7.04 (m, 4H), 4.34 (s, 2H), 3.93 (q, 2H), 3.61 (s, 3H), 2.42 (3H, s), 2.34 (s, 3H), 0.83 (t, 3H). ^{13}C NMR (75.5 MHz, CDCl_3): δ 169.2, 164.9, 139.5, 139.5, 138.8, 138.5, 133.2, 131.2, 131.1, 130.7, 129.5, 129.1, 128.9, 127.9, 127.4 (q), 126.5, 124.3 (q), 123.0, 113.3, 59.7, 52.6, 47.1, 21.8, 21.6, 13.9. HRMS. Calculated for $\text{C}_{31}\text{H}_{28}\text{F}_3\text{NO}_4$: 535.19704; found: 535.19775.

Acetic acid 1-(3,4-dibenzoyl-1-benzyl-5-phenyl-1H-pyrrol-2-yl)-1-methyl-ethyl ester (5.2i):

Yield: 56%. ¹H NMR (400 MHz, CDCl₃): δ 7.90 (d, 2H), 7.41 (t, 1H), 7.38-7.24 (m, 3H), 7.22-7.08 (m, 4H), 7.00-6.90 (m, 7H), 6.65 (d, 2H), 5.43 (s, 2H), 4.21 (s, 2H), 1.86 (s, 3H). ¹³C NMR (100 MHz, CDCl₃): δ 196.1, 192.1, 170.8, 140.4, 139.6, 138.8, 138.1, 135.9, 132.7, 131.3, 131.2, 130.7, 129.4, 129.3, 128.7, 128.4, 128.3, 127.9, 127.4, 127.4, 125.5, 125.4, 124.3, 71.6, 50.7, 38.4, 24.5, 21.1. HRMS. Calculated for C₃₇H₃₃NO₄: 555.24096; found: 555.24053.

1-Benzyl-4-phenyl-2,5-di-p-tolyl-1H-pyrrole-3-carboxylic acid methyl ester (5.2j):

Yield: 95%. ¹H NMR (400 MHz, CDCl₃): δ 7.40-7.05 (m, 9H), 7.05-6.95 (m, 7H), 6.70 (m, 2H), 5.03 (s, 2H), 3.51 (s, 3H), 2.42 (s, 3H), 2.31 (s, 3H). ¹³C NMR (100 MHz, CDCl₃): δ 166.1, 139.1, 138.5, 138.2, 137.6, 135.7, 133.0, 131.5, 130.9, 130.9, 129.4, 129.1, 128.9, 128.9, 128.5, 127.5, 127.2, 126.3, 126.1, 124.5, 113.3, 51.1, 48.8, 21.9, 21.7. HRMS. Calculated for C₃₃H₂₉NO₂: 471.21983; found: 471.22052.

1-Benzyl-3-phenyl-4-(toluene-4-sulfonyl)-2,5-di-p-tolyl-1H-pyrrole (5.2k):

NMR Yield: 74%. ¹H NMR (300 MHz, CDCl₃): δ 7.22 (d, 2H), 7.20-7.08 (d, 12H), 6.98 (d, 2H), 6.91 (m, 5H), 6.58-6.52 (m, 2H), 4.88 (s, 2H), 2.40 (s, 3H), 2.32 (s, 3H),

2.22(s, 3H). ^{13}C NMR (75 MHz, CD_3CN): δ 142.4, 141.0, 138.9, 137.7, 137.7, 137.6, 133.7, 132.1, 131.5, 131.1, 129.0, 128.9, 128.7, 128.4, 128.0, 127.9, 127.9, 127.4, 127.3, 127.3, 126.8, 126.3, 123.5, 121.4, 49.0, 22.0, 21.9, 21.7. HRMS. Calculated for $\text{C}_{38}\text{H}_{33}\text{NO}_2\text{S}$: 567.22320; found: 567.22409 .

{4-Benzoyl-1-ethyl-5-phenyl-2-[1-(toluene-4-sulfonyl)-1H-indol-3-yl]-1H-pyrrol-3-yl}-phenyl-methanone (5.2l)

Yield: 66%. ^1H NMR (300 MHz, CDCl_3): δ 7.95 (m, 2H); 7.75 (d, 2H), 7.50-7.38 (m, 7H), 7.38-7.24 (m, 5H), 7.24-7.06 (m, 6H), 7.04-6.96 (m, 2H), 3.95 (t, 2H), 2.22 (s, 3H), 0.85 (t, 3H). ^{13}C NMR (75.5 MHz, CDCl_3): δ 192.2, 191.8, 145.3, 136.9, 139.4, 138.2, 135.0, 134.7, 132.0, 131.9, 130.9, 130.8, 130.6, 130.1, 130.1, 129.1, 128.9, 128.8, 128.6, 128.0, 127.8, 127.5, 127.1, 125.8, 125.3, 124.4, 124.1, 120.3, 114.0, 112.2, 41.1, 22.0, 16.7. Calculated for $\text{C}_{41}\text{H}_{32}\text{N}_2\text{O}_4\text{S}$: 648.20828; found: 648.20933

2-Benzo[1,3]dioxol-5-yl-1-ethyl-5-phenyl-1H-pyrrole-3,4-dicarboxylic acid dimethyl ester (5.2m)

Yield: 81%. ^1H NMR (400 MHz, CDCl_3): δ 7.43-7.35 (m, 5H), 6.87 (m, 3H), 6.01 (s, 2H), 3.69 (s, 3H), 3.32 (q, 2H), 3.68 (s, 3H), 3.63 (s, 3H), 0.84 (t, 3H). ^{13}C NMR (100 MHz, CDCl_3): δ 165.6, 165.5, 148.2, 147.6, 136.3, 135.9, 131.1, 130.6, 128.9,

128.5, 124.7, 124.4, 114.6, 114.5, 111.0, 108.5, 101.6, 52.0, 51.9, 40.2, 16.6. HRMS. Calculated for $C_{23}H_{21}NO_6$: 407.13689; found: 407.13644.

1-Ethyl-2-naphthalen-2-yl-5-phenyl-1H-pyrrole-3,4-dicarboxylic acid dimethyl ester (5.2n)

Yield: 88%. 1H NMR (400 MHz, $CDCl_3$): δ 7.97-7.86 (m, 4H), 7.58-7.42 (m, 8H), 3.81 (q, 2H), 3.69 (s, 3H), 3.64 (s, 3H), 0.84 (t, 3H). ^{13}C NMR (100 MHz, $CDCl_3$): δ 165.6, 165.6, 136.7, 136.4, 133.4, 133.1, 131.2, 130.7, 130.2, 129.0, 128.6, 128.6, 128.5, 128.2, 128.0, 128.0, 127.0, 126.7, 115.0, 114.9, 52.0, 51.9, 40.4, 16.6. HRMS. Calculated for $C_{26}H_{23}NO_4$: 413.16271; found: 413.16317.

1-Ethyl-3-methyl-2-phenyl-1,4-dihydro-5-oxa-1-aza-cyclopenta[a]naphthalene (5.12)

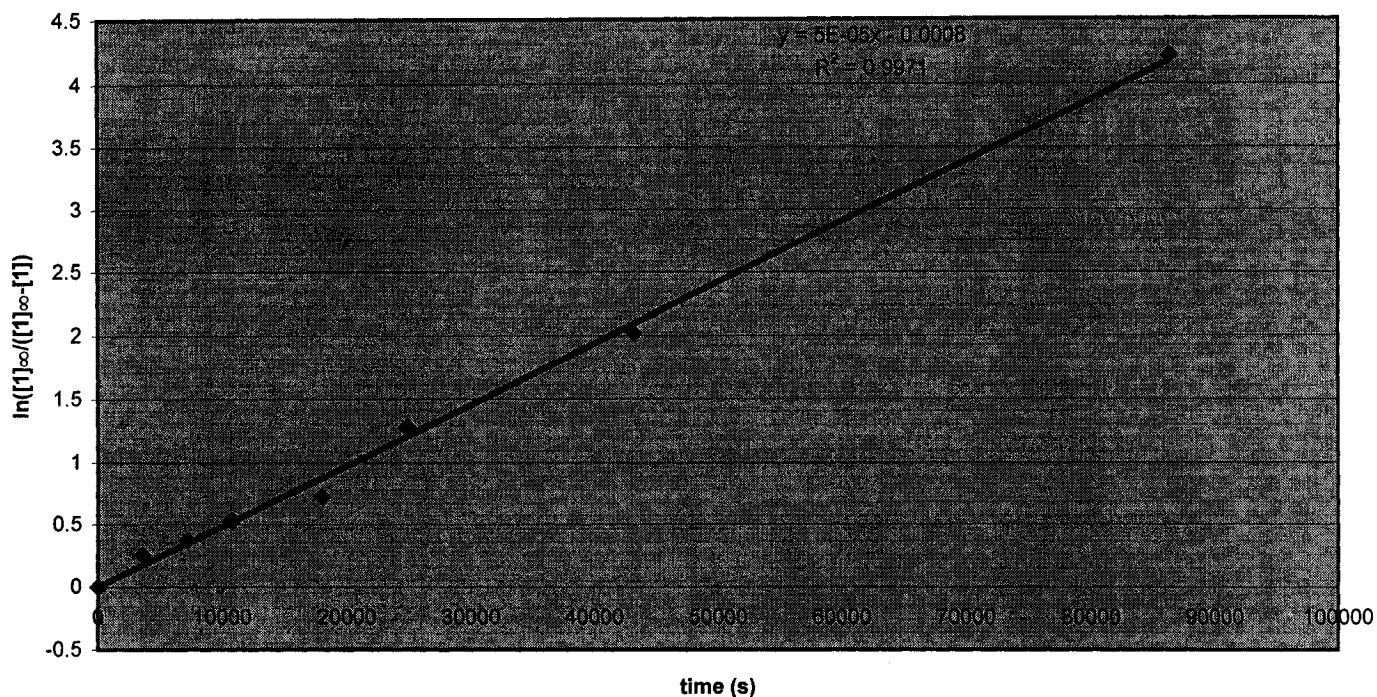
Imine **5.13**²² (188 mg, 0.93 mmol) and benzoyl chloride (184 mg, 1.30 mmol) were dissolved in 6 mL of acetonitrile. This solution was added to $Pd_2(dba)_3 \cdot CHCl_3$ (2.5 mol%) and $P(o\text{-tolyl})_3$ (10 mol%) in 6 mL of acetonitrile. The reaction mixture was transferred to a 100 mL reaction bomb and EtN^iPr_2 (184 mg, 1.43 mmol) (in 12 mL of THF) was added. The solution was evacuated, carbon monoxide (60 psi) added, and stirred at 55°C for 18 hours. The product was purified by silica gel chromatography using hexanes/ethyl acetate as eluent.

Yield: 73%. ^1H NMR (400 MHz, CDCl_3): δ 7.60-7.40 (m, 6H), 7.15-7.00 (m, 3H), 5.29 (s, 2H), 4.16 (q, 2H), 2.01 (s, 3H), 1.30 (t, 3H). ^{13}C NMR (100 MHz, CDCl_3): δ 153.4, 134.2, 132.6, 131.1, 128.7, 127.8, 126.5, 122.6, 121.9, 120.6, 120.2, 117.6, 116.6, 112.6, 65.3, 40.8, 17.2, 10.0. HRMS. Calculated for $\text{C}_{20}\text{H}_{19}\text{NO}_3$: 289.14666; found: 289.14589.

III. Kinetic Studies on Münchnone Formation

p-tolyl(H)C=Nbn (114 mg, 0.54 mmol) was combined with benzoyl chloride (107 mg, 0.76 mmol) in 8 mL of acetonitrile. To this solution was added $[\text{Pd}(\text{Cl})[\eta^2\text{-CH}(\text{p-tolyl})\text{NBn}(\text{COPh})]_2$ (5 mol%, 24.6 mg) in 8 mL of acetonitrile, Bu_4NBr (176 mg, 0.54 mmol) in 8 mL of THF and EtN^iPr_2 (0.86 mmol, 111 mg) in 8 mL of THF. The solution was divided into 8 portions and added to 50 mL reaction bombs, followed by the addition of carbon monoxide (60 psi). The solutions were warmed to 55°C , and the reactions were stopped at intervals of 0, 1, 2, 3, 5, 7, 12, and 24 hours. The yield of Münchnone generated was determined by ^1H NMR (utilizing benzyl benzoate as an internal standard). See plot below.

Plot of $\ln([\text{Munchnone}]_{\infty}/([\text{Munchnone}]_{\infty}-[\text{Munchnone}]))$ vs time



IV. Conditions for Ligand Scanning (Table 5.1)

p-tolyl(H)C=NBn (156 mg, 0.75 mmol) was combined with benzoyl chloride (147 mg, 1.04 mmol) in 16 mL of acetonitrile. To 1/8 of this solution was added $[\text{Pd}(\text{Cl})[\eta^2\text{-CH}(\text{p-tolyl})\text{NBn}(\text{COPh})]_2$ (4.3 mg, 0.0047 mmol) and the ligand (0.012 mmol, 15 mol%) in 3 mL of acetonitrile, followed by EtN^iPr_2 (19 mg, 0.11 mmol) in 4.5 mL of THF. The solution was evacuated, carbon monoxide (60 psi) added, and stirred at 65°C for 3.5 hours. The yields of Münchnone were determined by ^1H NMR (utilizing benzyl benzoate as an internal standard)

5.5 References

1. *Pyrroles, Part II* Jones, R. A. Ed., Wiley: New York, **1992**.
2. a) Thompson, R. B. *FASEB J.* **2001**, *15*, 1671. b) Muchowski, J.M. *Adv. Med. Chem.* **1992**, *1*, 109. c) Cozzi, P.; Mongelli, N. *Curr. Pharm. Des.* **1998**, *4*, 181. d) Fürstner, A.; Szillat, H.; Gabor, B.; Mynott, R. *J. Am. Chem. Soc.* **1998**, *120*, 8305.
3. Skotheim, T. A.; Elsenbaumer, R. L.; Reynolds, J. R. Eds. *Handbook of Conducting Polymers 2nd Ed.*; Marcel Dekker: New York, **1998**.
4. Knorr, L. *Ber.* **1884** *17*, 1635. b) Paal, C. *Ber.* **1885**, *18*, 367.
5. Representative examples: a) Kel'in, A.V.; Sromek, A.W.; Gevorgyan, V. *J. Am. Chem. Soc.* **2001**, *123*, 2074. b) Gabriele, B.; Salerno, G.; Fazio, A. *J. Org. Chem.* **2003**, *68*, 7853. c) Takaya, H.; Kojima, S.; Murahashi, S.-I. *Org. Lett.* **2001**, *3*, 421. d) Lee, C.-F.; Yang, L.-M.; Hwu, T.-Y.; Feng, A.S.; Tseng, J.-C.; Luh, T.-Y. *J. Am. Chem. Soc.* **2000**, *122*, 4992 e) Merlic, C.A.; Baur, A.; Aldrich, C.C. *J. Am. Chem. Soc.* **2000**, *122*, 7398 f) Braun, R.U.; Zeitler, K.; Müller, T.J. *Org. Lett.* **2001**, *3*, 3297. g) Nishibayashi, Y.; Yoshikawa, M.; Inada, Y.; Milton, M.D.; Hidai, M.; Uemura, S. *Angew. Chem., Int. Ed.* **2003**, *42*, 2681. h) Deng, G.S.; Jiang, N.; Ma, Z.H.; Wang, J.B. *Synlett*, **2002**, 1913. i) Wang, Y; Zhu, S. *Org. Lett.* **2003**, *5*, 745. j) Dieter, R.K.; Yu, H. *Org. Lett.* **2001**, *3*, 3855.
6. Gibson, S. E.; Stevenazzi, A. *Angew. Chem. Int. Ed.* **2003**, *42*, 1800.

7. Representative examples: a) Beller, M.; Eckert, M. *Angew. Chem. Int. Ed.* **2000**, *39*, 1010. b) Montgomery, J. *Acc. Chem. Res.* **2000**, *33*, 467. c) Dghaym, R. D.; Dhawan, R.; Arndtsen, B. A. *Angew. Chem. Int. Ed.* **2001**, *40*, 3228. d) Kamijo, S.; Jin, T.; Huo, Z.; Yamamoto, Y. *J. Am. Chem. Soc.* **2003**, *125*, 7786. e) Trost, B. M.; Pinkerton, A. B. *J. Am. Chem. Soc.* **2000**, *122*, 8081. f) Cao, C.; Shi, Y.; Odom, A. L. *J. Am. Chem. Soc.* **2003**, *125*, 2880.
8. a) Gribble, G. W. In *The Chemistry of Heterocyclic Compounds*, Padwa, A. Ed. Wiley: New York. **2002**, *59*, p. 681. b) Coppola, B.P.; Noe, M. C.; Schwartz, D.J.; Abdon, R.L.; Trost, B.M. *Tetrahedron* **1994**, *50*, 93.
9. Dhawan, R.; Dghaym, R.D.; Arndtsen, B.A. *J. Am. Chem. Soc.* **2003**, *125*, 1474.
10. See Supporting Information for full details.
11. **5.6** is formed by pre-treating Pd₂dba₃ with imine and acid chloride (ref. 8).
12. For example: Stambuli, J. P.; Bühl, M; Hartwig, J. F. *J. Am. Chem. Soc.* **2002**, *124*, 9346, and references therein.
13. Pd₂dba₃ or [Pd(allyl)Cl]₂ are also viable catalysts at ca. 10% lower yield.
14. Enolizable R² are not stable, though these units can be incorporated into the 2-pyrrole position via the acid chloride (**5.2d**). Strong dipolarophiles react with **5.7**, and must be added to a preformed **5.1** (**5.2b,m,n**).
15. Yoshimura, H.; Nagai, M.; Hibi, S.; Kikuchi, K.; Abe, S.; Hida, T.; Higashi, S.; Hishinuma, I.; Yamanaka, T. *J. Med. Chem.* **1995**, *38*, 3163.

16. Dhawan, R.; Dghaym, R.D.; Arndtsen, B.A. *J. Am Chem. Soc.* **2003**, *125*, 1474.
17. Layer, R. W. *Chem. Ber.* **1963**, *63*, 489.
18. Eckert, T.; Ipaktschi, J. *Syn. Comm.* **1998**, *28*, 327.
19. Zhang, J.-J.; Schuster, G. B. *J. Am. Chem. Soc.* **1989**, *111*, 7149.
20. Reactions of C-alkyl substituted imines (**5.2c**, **5.2i**) were performed at 75°C with 1 eq. of LiOTf, and $[\text{Pd}(\text{Cl})[\eta^2\text{-CH}(\text{Tol})\text{NEt}(\text{COPh})]_2$ catalyst, in CH_3CN .
21. 60 psi of acetylene is added to the solution of Münchnone and stirred at 50°C for 8 hours.
22. Perez-Serrano, L.; Blanco-Urgoiti, J.; Casarrubios, L.; Dominguez, G.; Perez-Castells, J. *J. Org. Chem.* **2000**, *65*, 3513.

CHAPTER SIX

Palladium Catalyzed Synthesis of Münchnones: Characterization of Intermediates and Mechanistic Analysis of the Reaction

Preface

In Chapter 2-5, we described the development of palladium catalyzed synthetic routes to prepare α -amino acid derivatives, β -lactams, and pyrroles, all via the initial formation of Münchnones. In Chapter 6, we will discuss characterization of several suspected catalytic intermediates in Münchnone generation. This, coupled with other mechanistic studies, will provide additional insight into the mechanism by which this mesoionic heterocycle is formed.

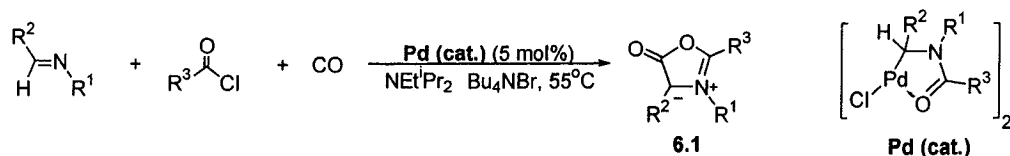
6.0 Introduction

Multicomponent coupling methodologies can greatly facilitate synthetic efforts in comparison to linear synthetic strategies.^{1,2} This approach to synthesis can aid in the generation of complex products from three or more precursors by conducting multiple bond forming processes in a single synthetic step. In addition, the reaction constituents can be varied independently of each other, which is ideal for generating compound libraries.² However, a significant limitation to the development of new multicomponent coupling reactions that generate more complex products is that the

requisite reaction substrates are also generally complex. In principle, the use of metal catalysis can significantly facilitate the design of new multicomponent coupling reactions, by employing the diverse reactivity of metal complexes to mediate the coupling of traditionally unreactive precursors into more complex products.³ When designed well, this can provide a method to directly couple basic building blocks into useful products, as demonstrated by reactions such as the cyclotrimerization of alkynes,⁴ amidocarbonylation,⁵ and the Pauson Khand reaction.⁶ A challenge in developing new classes of these reactions remains how to control the manner in which the multiple building blocks, along with the reactive catalyst, come together to selectively generate a single reaction product. In particular, these reactions can be very mechanistically complex, involving numerous sequential steps on the metal center. Developing a precise knowledge of these steps can be critical for designing efficient catalysts, selectively forming specific products, controlling the numerous potential side reactions, and extrapolating these reactions to the design of new syntheses.

We have recently developed a number of palladium catalyzed multicomponent coupling routes to construct imidazoline carboxylates,⁷ α -amino acid derivatives,⁸ β -lactams⁹ and pyrroles,¹⁰ all in one step from basic building blocks. Each of these processes is believed to be proceeding through the same catalytic formation of 1,3-oxazolium-5-oxides (Münchnones) **6.1**, formed via the coupling of imines, acid chlorides and carbon monoxide (Equation 6.1).¹¹ We describe herein the results of our mechanistic studies on this reaction, which include examination of catalyst resting

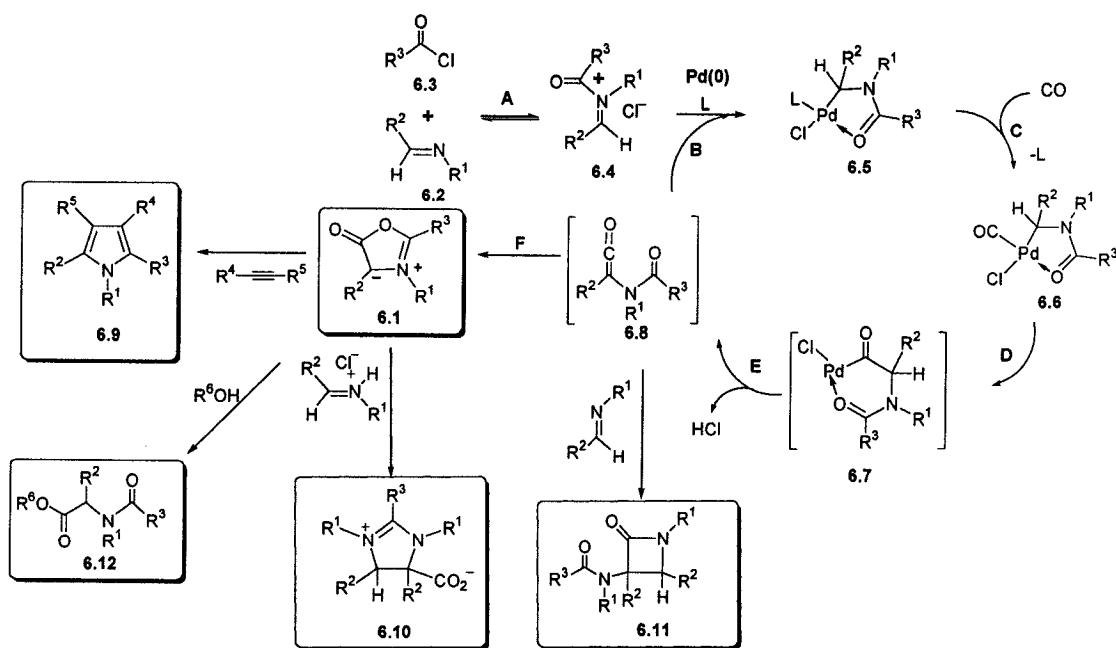
states, reaction kinetics, and studies on the various reaction steps. These suggest not only the route by which Münchnones are formed, but also the importance of balancing the factors that favour oxidative addition, carbonylation, and palladium (0) stabilization in facilitating efficient catalysis.



Equation 6.1 Münchnone Generation

6.1 Results and Discussion

Our working hypothesis for the palladium catalyzed synthesis of Münchnones from imines, acid chlorides, and carbon monoxide is shown in Scheme 6.1.^{7, 8} This involves the initial nucleophilic attack of imine on the acid chloride to form *N*-acyliminium salt **6.4** (Step A) which is followed by oxidative addition of **6.4** to Pd(0) to form palladacycle **6.5** (Step B). Subsequent CO coordination to the metal center (Step C), CO insertion (Step D), β -hydride elimination, reductive elimination (Step E) and finally cyclization (Step F) forms the Münchnone product and regenerates Pd(0) for further catalysis. Depending upon the specific reaction conditions utilized, a range of different products can be formed in this catalytic process (Scheme 6.1).



Scheme 6.1 Mechanistic Rationale for Münchnone Formation

Evidence for the mechanism comes from monitoring the reaction by $^1\text{H-NMR}$ spectroscopy, which shows the immediate formation of *N*-acyliminium salt **6.4** upon mixing of the reagents.¹² We have previously shown that *N*-acyliminium salts react at ambient temperature with Pd(0) sources to generate palladacycles of the form **6.5**,⁸ which has been completely characterized in the case of a similar compound: $\{[\text{bipy}]\text{Pd}[\eta^2\text{-CH}(\text{Tol})\text{N}(\text{Bn})\text{COCH}_3]^+\text{OTf}^-$ (Tol = $p\text{-C}_6\text{H}_4\text{CH}_3$, Bn = CH_2Ph).¹³ Similarly, control experiments show that the independently generated dimeric **6.5a** ($\text{Cl-Pd}[\eta^2\text{-CH}(\text{Tol})\text{NBn}(\text{COPh})]_2$) can react with CO to form $[\text{Pd}(\text{CO})(\text{Cl})[\eta^2\text{-CH}(\text{Tol})\text{NBn}(\text{COPh})]]_2$ **6.6a**, and that the latter complex can eventually yield Münchnone derived imidazoline-carboxylate products.⁷

Considering that our early experiments showed the palladacycle **6.5** could be formed rapidly upon addition of *N*-acyliminium salt **6.4** to Pd(0), our preliminary postulate for Münchnone formation was that the oxidative addition step (Step B) was rapid. As such, our catalyst development focused on facilitating carbonylation (CO coordination (Step C) & insertion (Step D)),⁷ by favouring the formation of CO coordinated intermediate **6.6** (Scheme 6.1).⁸ The latter was approached by attempting to form **6.5**, in the absence of any coordinating ligands. This was done by pre-treating Pd₂(dba)₃·CHCl₃ with acid chloride and imine to form palladacycle intermediate (Cl-Pd[η²-CH(R²)NR¹(COR³)]₂) **6.5** and employing the latter as the reaction catalyst. While the use of this catalyst by itself leads to the formation of palladium sediments, the addition of halide salts (ie. Bu₄NBr) can stabilize Pd(0) through weak halide coordination, and allow for efficient catalytic Münchnone generation.⁸

6.1.1 Catalyst Resting State

In principle, a rapid oxidative addition, followed by a rate determining carbonylation, should leave the palladacycle **6.5** as the catalyst resting state. This was probed by monitoring the catalytic coupling of Tol(H)C=NBn **6.2a**, PhCOCl **6.3a**, and CO (4 atm) with [Pd(Cl)[η²-CH(Tol)NBn(COPh)]₂ **6.5a** (12.5 mol%), Bu₄NBr (1 eq.), and NEtⁱPr₂ (1.6 eq.) by ¹H-NMR spectroscopy (Figure 6.2).

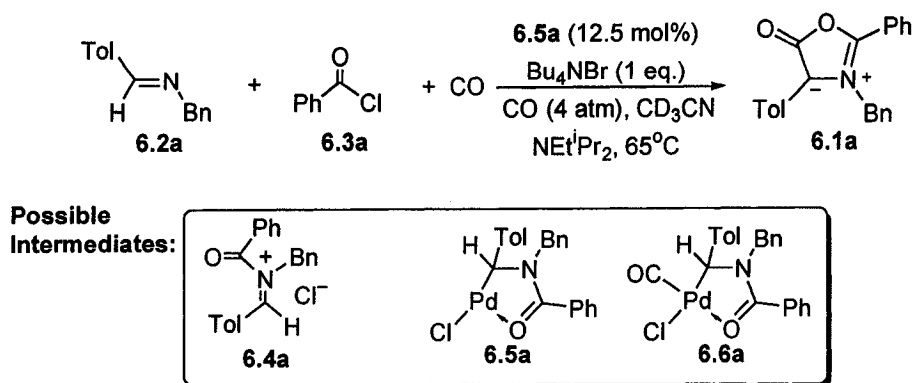


Figure 6.2 Determination of the Catalyst Resting State

The initial reaction spectrum shows the immediate and essentially quantitative formation of *N*-acyliminium salt **6.4a**. In addition, it shows the presence of palladacycle **6.5a** and the carbonylated intermediate **6.6a** in an approximate 1:3 ratio. Monitoring the reaction at 65°C in the NMR spectrometer shows the slow disappearance of *N*-acyliminium salt **6.4a** and the concomitant formation of Münchnone **6.1a** over the course of 22 hours. However, after ca. 3 hours of reaction time, there is no evidence for any organometallic species (i.e. **6.5a** and **6.6a**) by ^1H -NMR spectroscopy. Bearing in mind that a fast equilibrium could exist between *N*-acyliminium salt **6.4a** and palladium complexes **6.5a** or **6.6a**, the reaction solution was cooled down to -20°C . However, ^1H -NMR analysis once again revealed only the presence of *N*-acyliminium salt and Münchnone and no observable palladium-containing complex. Considering the mechanism of this reaction, the lack of any observable organopalladium intermediates during catalysis suggests that the majority of palladium exists as $\text{Pd}(0)$.

6.1.2 Preliminary Kinetic Analysis of Münchnone Formation

The role of oxidative addition in the rate of Münchnone formation was further probed by examining the kinetics of this reaction. Münchnone formation was monitored in the palladium catalyzed coupling of Tol(H)C=NBn **6.2a** (1 eq.), benzoyl chloride **6.3a** (1.4 eq.), and CO (4 atm) at 55°C by stopping the reaction at various times, and obtaining ¹H-NMR spectra of the reaction products.^{10, 14}

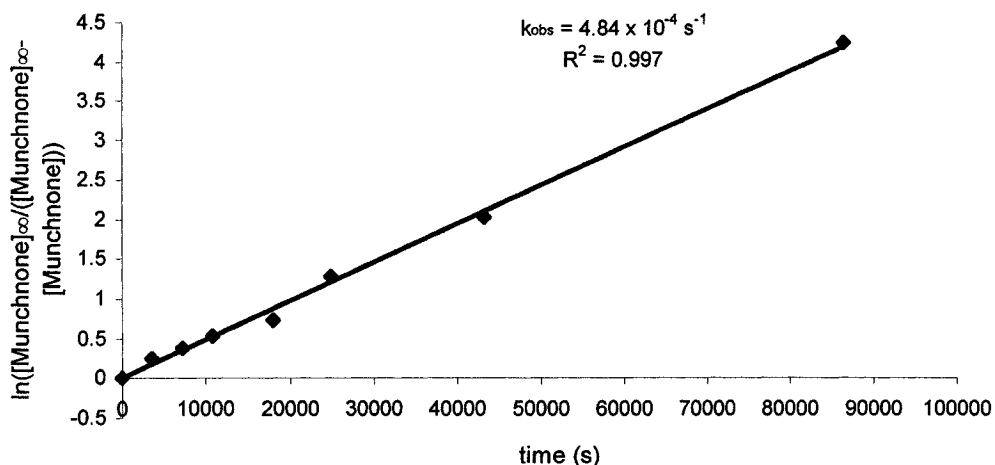


Figure 6.3 Plot of $\ln([\text{Münchnone}]_{\infty}/([\text{Münchnone}]_{\infty} - [\text{Münchnone}])$ vs time. (Reaction of Tol(H)C=NBn (114 mg, 0.54 mmol), PhCOCl (107 mg, 0.76 mmol), Bu₄NBr (176 mg, 0.54 mmol) and NEtⁱPr₂ (640 mg, 4.94 mmol) with [Pd(Cl)[η²-CH(Tol)NBn(COPh)]₂ (24.6 mg, 5 mol%) in a THF/CH₃CN mixture ([N-Acyliiminium salt]₀ = 0.0169 M). The reaction is divided into 8 portions and pressurized with carbon monoxide (4 atm). Reactions heated at 65°C and stopped at intervals of 0, 1, 2, 3, 5, 7, 12, and 24 hours. Yields are determined by ¹H-NMR).

As shown in Figure 6.3, the plot of $\ln[\text{Münchnone}]$ as a function of time provides a linear fit, consistent with a first order rate of Münchnone formation.¹⁰ Considering that the base (NEt^iPr_2) and carbon monoxide were used under pseudo-zero order conditions, the presence of this linear correlation suggests that the reaction is first order with respect to *N*-acyliminium salt concentration. Since, a rapid oxidative addition of *N*-acyliminium salt **6.4** to Pd(0) during catalysis should result in a rate of Münchnone formation that is iminium salt concentration independent, this data further supports the resting state studies: that oxidative addition is a rate-determining step.

6.1.3 Probing the Oxidative Addition of *N*-Acyliminium Salts to Pd(0)

Considering that the preliminary analysis of the mechanistic data suggests that the oxidative addition of *N*-acyliminium salt **6.4** to Pd(0) is a rate limiting step in Münchnone formation, a more thorough study of this reaction step was undertaken. This was done by reacting $\text{Pd}_2(\text{dba})_3\cdot\text{CHCl}_3$ (0.5 eq.) with equimolar amounts of $\text{Tol}(\text{H})\text{C}=\text{NBn}$ (**6.2a**) (1 eq.) and PhCOCl (**6.3a**) (1 eq.). In contrast to the results obtained under catalytic conditions, this stoichiometric reaction leads to the rapid formation of $\{\text{Pd}(\text{Cl})[\eta^2\text{-CH}(\text{Tol})\text{NBnCOPh}]\}_2$ **6.5a** in ~45 minutes at ambient temperature.¹⁵

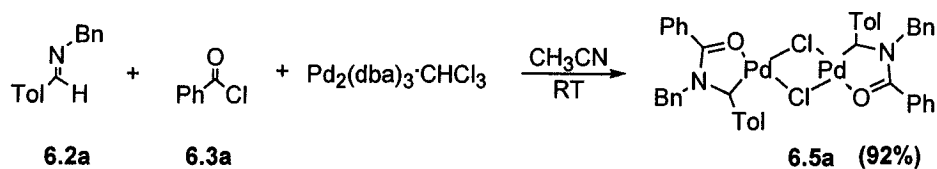


Figure 6.4 Formation of $\{\text{Pd}(\text{Cl})[\eta^2\text{-CH}(\text{Tol})\text{N}(\text{Bn})\text{COPh}]\}_2$ **6.5a**

As previously reported, the $^{13}\text{C}\{^1\text{H}\}$ NMR spectrum of complex **6.5a** displays an amide carbonyl resonance at δ 180.1 ppm, while the former imine carbon signal is shifted from δ 172.0 to δ 59.4, indicating the reduction of this center.⁸ The ^1H -NMR spectrum of this same complex shows an upfield shift of the former imine proton from δ 8.10 to δ 5.28. All other spectroscopic data is consistent with the formation palladium chelated amide complex **6.5a**.⁸ Electrospray mass spectroscopy of complex **6.5a** shows a major mass peak at 948.37, which is consistent with the dimeric structure assigned.¹⁶

Unequivocal structural determination of **6.5a** could not be obtained by X-ray crystallography due to the difficulty in obtaining crystalline material. As such, an analogue of this complex was generated by the reaction of equimolar amounts of Tol(H)C=N(PMB) **6.2b** (PMB = $-(\text{CH}_2)(p\text{-C}_6\text{H}_4\text{OCH}_3)$) and PhCOCl **6.3a** with 0.5 equivalents of $\text{Pd}_2(\text{dba})_3\cdot\text{CHCl}_3$ in CH_3CN . This similarly lead to the generation of $\{\text{Pd}(\text{Cl})[\eta^2\text{-CH}(\text{Tol})\text{N}(\text{PMB})\text{COPh}]\}_2$ (**6.5b**), which was isolated as a yellow powder in a 74% yield (Figure 6.5).¹⁷ Recrystallization from toluene at -40°C provided complex **6.5b** as orange crystals. Complex **6.5b** was characterized by X-ray diffraction, which shows it to indeed have a dimeric structure (Figure 6.6).

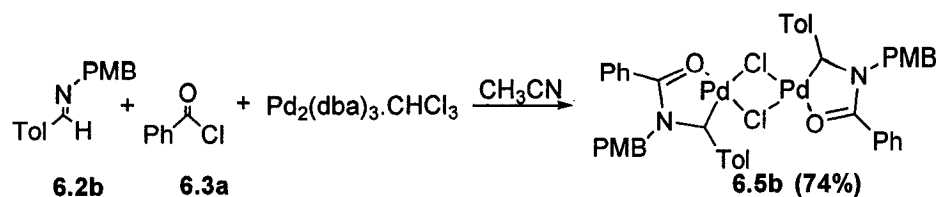


Figure 6.5 Formation of $\{\text{Pd}(\text{Cl})[\eta^2\text{-CH}(\text{Tol})\text{N}(\text{PMB})\text{COPh}]\}_2$ **6.5b**

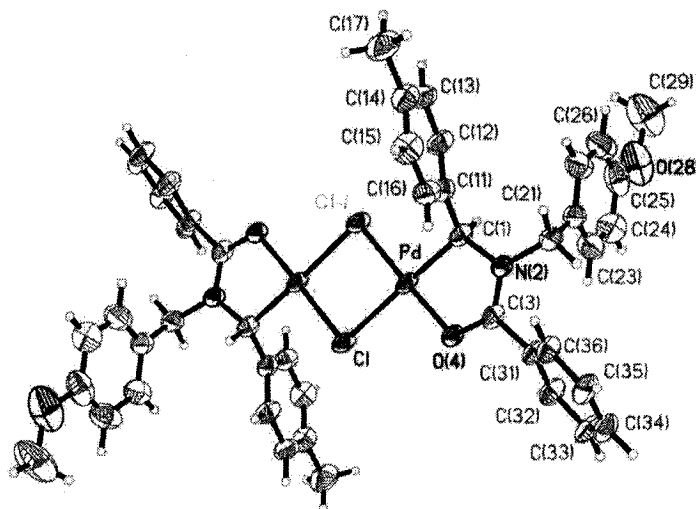


Figure 6.6 Crystal Structure of $\{\text{Pd}(\text{Cl})[\eta^2\text{-CH}(\text{Tol})\text{N}(\text{PMB})\text{COPh}]\}_2$ (PMB= $p\text{-C}_6\text{H}_4\text{OCH}_3$) (**6.5b**). Selected bond lengths (Å) and angles (deg.): Pd-O(4), 2.2028 (4); O(4)-C(3), 1.264 (7); C(3)-N(2), 1.312 (8); N(2)-C(1), 1.519 (7); C(1)-Pd, 1.976 (6); Pd-Clⁱ, 2.3198(16); Pd-Cl, 2.4655 (18); Cl-Pdⁱ, 2.3198 (16); C(3)-C(31), 1.498 (8); N(2)-C(21), 1.479 (8); C(1)-C(11), 1.490 (8). Pdⁱ-Cl-Pd, 93.08 (6); Pd-O(4)-C(3), 111.8 (4); O(4)-C(3)-N(2), 121.6 (5); C(3)-N(2)-C(1), 166.6 (5); N(2)-C(1)-Pd, 106.4 (4); C(1)-Pd-O(4), 83.6 (4); C(1)-Pd-Clⁱ, 94.29 (17); O(4)-C(3)-C(31), 117.7 (6); C(31)-C(3)-N(2), 120.7 (6); C(21)-N(2)-C(1), 116.3 (5). The disordered solvate species (toluene) in the lattice has been excluded for clarity.

Complex **6.5b** has a pseudo-square planar geometry about the metal center, with a sum of the four angles about the palladium center of 360.0°. As expected, the Pd-Cl

bond length (*cis* to the amide oxygen O(4)) is longer than the Pd-Clⁱ bond. This is in part attributable to C(1) having a greater *trans* influence than the amide oxygen O(4). The C-O bond length is 1.264Å is slightly longer than that observed in simple amides (*N,N*-dimethylbenzamide: C=O = 1.231 Å).¹⁸ In addition, the amide C-N bond length (1.312Å) in **6.5b** is contracted compared to non-chelated amides (*N,N*-dimethylbenzamide: C-N = 1.368Å). This bond in dimeric complex **6.5b** is similar in length to that observed in {[bipy]Pd[η²-CH(Tol)N(Bn)COCH₃]OTf} (C-N = 1.328 Å), and is consistent with a significant contribution of resonance form **6.5b'** to the structure of **6.5b** (Figure 6.7).¹⁹

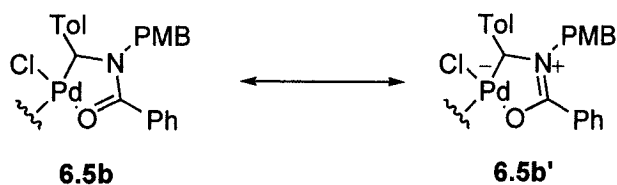


Figure 6.7 Bond Lengths in Palladium Chelated Amides

6.1.4 Probe for a Heterogeneous Palladium Catalyst

The rapid room temperature oxidative addition of *N*-acyliminium salt to Pd₂(dba)₃·CHCl₃ in stoichiometric experiments contrasts with our observations on catalysis, which suggests that the iminium salt oxidative addition is a rate determining step for catalysis at 55°C. In considering this apparent discrepancy, one difference in these two systems that may play a role is the sources of palladium. While the dba (*trans*-,*trans*-dibenzylideneacetone) ligated palladium complex ([Pd₂(dba)₃·CHCl₃]) was employed in the stoichiometric experiment, the mechanism of catalysis suggests

that the formation of Münchnone would liberate an unligated Pd(0). One might anticipate this Pd(0) fragment would also undergo rapid oxidative addition of *N*-acyliminium salt **6.4**, however, in the absence of strongly coordinating ligands, palladium (0) catalysts are known to deactivate through the initial formation of clusters and subsequently with the formation of sediments.²⁰ In addition, according to a recent mechanistic study, Pd(II) sources (i.e. [Pd(OAc)₂]) can be activated towards the generation of catalytically active colloidal Pd(0) in the presence of Bu₄NBr.²¹ Considering that this system is similar to our “ligand free” Münchnone forming conditions, we considered the possibility that colloidal palladium might be formed during catalysis.

A useful test for the presence of heterogeneous species in a reaction involves the use of catalyst poisons such as mercury.²² In these studies, it is generally found that heterogeneous reactions are more readily poisoned than their homogeneous variants. In order to probe for the presence of heterogeneous palladium catalysts in the Münchnone synthesis, the catalytic coupling of Tol(H)C=NBn **6.2a** (1 eq), PhCOCl **6.3a** (1.4 eq.) and CO (4 atm.) was allowed to proceed to partial completion (2 hours, 24 % Münchnone yield) (Figure 6.8). Mercury (320 eq.) was then added to the degassed solution and stirred vigorously for 2 hours. After celite filtration, the solution was added to a reaction vessel and again heated at 65°C with CO (4 atm) for another 2 hours. Examination of the reaction mixture showed no further catalysis after the mercury addition and filtration.²³

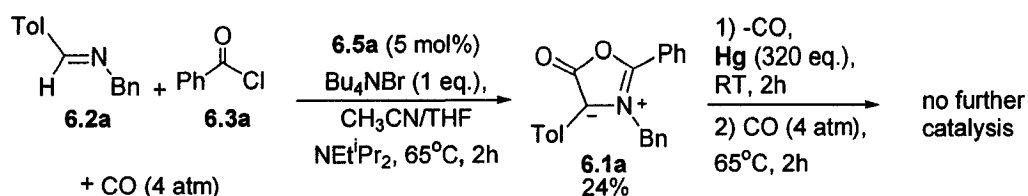


Figure 6.8 Probe for Heterogeneous Processes with Halide Salts

Although the poisoning of catalytic Münchnone formation by mercury is indicative of the presence of colloidal or heterogeneous palladium, multiple tests are required for definitive proof.^{22a} However, if colloidal palladium is indeed present, it could either play the role of the actual active palladium catalyst, or act as a deactivated form of $\text{Pd}(0)$. Both of these possibilities could lead to the observed slow iminium salt oxidative addition relative to the stoichiometric studies.

6.1.5 Triphenylphosphine in Münchnone Formation

Colloidal palladium formation can be inhibited through the utilization of strongly coordinating phosphine ligands, such as PPh_3 .²⁰ These ligands are also known to increase rates of oxidative addition, are therefore potentially useful for the generation of Münchnones.²⁰ In order to probe the ability of phosphine ligands to facilitate Münchnone generation, the catalytic coupling of $\text{TolHC}=\text{NBn}$ **6.2a**, PhCOCl **6.3a** and CO was examined with $[\text{Pd}(\text{Cl})[\eta^2\text{-CH}(\text{Tol})\text{NBn}(\text{COPh})]_2$ **6.5a** (5 mol%) and PPh_3 (15 mol%). However, the presence of PPh_3 during the catalytic reaction was found to completely inhibit Münchnone formation.²⁴

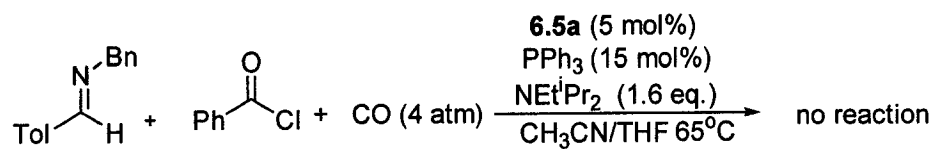


Figure 6.9 Utilization of PPh₃ in Münchnone Generation

In order to better understand this result, reactions stoichiometric in palladium were studied. The phosphine bound palladacycle complex **6.5d** can be readily generated by the addition of PPh₃ (2 eq.) to **6.5c** in CH₂Cl₂ (Figure 6.10). This leads to the formation of triphenylphosphine complex [PPh₃]Pd(Cl)[η²-CH(Tol)N(Et)COPh] **6.5d** as a yellow solid in 90% yield.

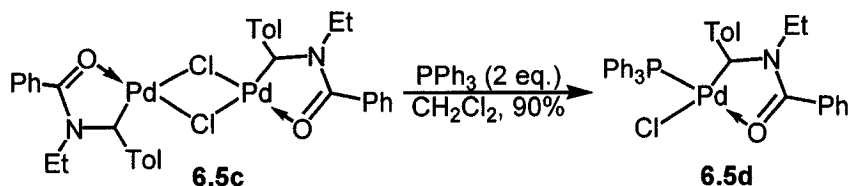


Figure 6.10 Synthesis of [PPh₃]Pd(Cl)[η²-CH(Tol)N(Et)COPh]

Examination of the ¹H-NMR spectrum of **6.5d** at 22°C showed a new methine resonance at 4.42 ppm (d, ³J_{P-H} = 4.10Hz), consistent with the formation of the *cis*-isomer of the palladium bound phosphine complex.²⁵ Furthermore, the ³¹P-NMR spectra also shows the presence of a single phosphorus resonance at 28.7 ppm, which is consistent with the formation of a palladium complex with one coordinated phosphine.

Considering that complex **6.5d** is readily formed and is stable, it is unlikely that the formation of this intermediate (Step B in Scheme 6.1) is a problem step in

Münchnone generation with PPh_3 . As such, the ability of **6.5d** to act as a carbonylation precursor (Steps C and D) was examined by $^1\text{H-NMR}$ spectroscopy (Figure 6.11). On monitoring the reaction of $[\text{PPh}_3]\text{Pd}(\text{Cl})[\eta^2\text{-CH}(\text{Tol})\text{N}(\text{Et})\text{COPh}]$ **6.5d** with CO (4 atm) in CD_3CN , no change was apparent, even upon prolonged heating at 65°C . Instead, **6.5d** slowly decomposed with the formation of palladium sediments.

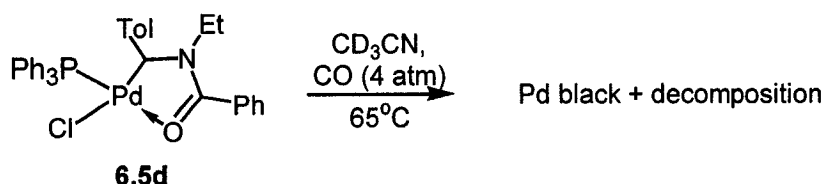


Figure 6.11 Reaction of $\{[\text{PPh}_3]\text{Pd}(\text{Cl})[\eta^2\text{-CH}(\text{Tol})\text{N}(\text{Et})\text{COPh}]\}$ **6.5d** with CO

In comparison to phosphine complex **6.5d**, the non-phosphine bound dimeric palladium complex $[\text{Pd}(\text{Cl})[\eta^2\text{-CH}(\text{Tol})\text{NBn}(\text{COPh})]_2$ **6.5a** is found to readily react with CO (1 atm) to form the carbonylated complex **6.6a** within 5 minutes (Figure 6.12). This complex shows a shift of the methine proton to δ 6.13 ppm and a concomitant downfield shift of the diastereotopic benzylic group to δ 4.58 ppm. The presence of a palladium bound carbonyl is also confirmed through utilizing infrared spectroscopy ($\nu_{\text{CO}} = 2114 \text{ cm}^{-1}$ in CH_3CN).²⁶ However, no IR stretch is observable between 1650 and 1800 cm^{-1} , indicating that CO insertion into the palladium-carbon bond has not occurred. The *N*-ethyl substituted complex $[\text{Pd}(\text{Cl})[\eta^2\text{-CH}(\text{Tol})\text{NEt}(\text{COPh})]_2$ **6.5c** shows analogous behaviour, forming **6.6c** rapidly upon exposure to CO (1 atm). Complex **6.6c** is not stable in the absence of a CO environment, and rapidly reverts to **6.5c**. In addition, **6.5c** partially decomposes to

palladium sediments on standing for extended periods of time (>8 hours) in the presence of CO, with complete decomposition occurring at elevated temperatures (demonstrated by **6.6c**).

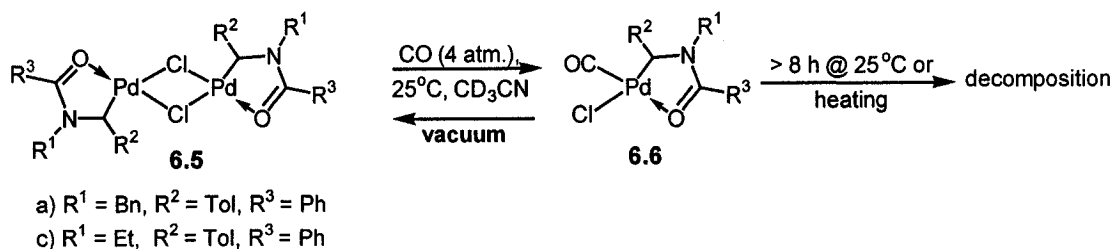


Figure 6.12 Addition of CO to **6.5** $[\text{Pd}(\text{Cl})[\eta^2\text{-CH}(\text{Tol})\text{NR}(\text{COPh})]_2$

The inability to generate Münchnone in the presence of PPh_3 is possibly a direct consequence of this ligand remaining tightly bound to the palladium center and thereby not enabling the carbonylation steps to occur (Step C and D, Scheme 6.1). As such, ligands that can more readily dissociate from the metal center could serve as better candidates for stabilizing the palladium center without binding so strongly as to prevent formation of the carbonylated intermediate **6.6** (Scheme 6.1). For this reason, sterically bulky ligands were examined for their competency in generating Münchnones.²⁷

6.1.6 Second Generation Münchnone Catalyst: Utilization of Sterically Hindered Phosphines

As previously described (Chapter 5),¹⁰ while smaller phosphines such as a PCy_3 and PPh_3 completely inhibit Münchnone formation, sterically bulky phosphines including

P^tBu_3 , $P^tBu_2(2\text{-biphenyl})$, $P(1\text{-naphthyl})_3$ and $P(o\text{-Tol})_3$ were found to promote product formation. Of these, the bulky $P(o\text{-Tol})_3$ not only facilitated catalysis, but also allowed it to proceed 2-3 times faster than with added Bu_4NBr (Figure 6.13).¹⁰

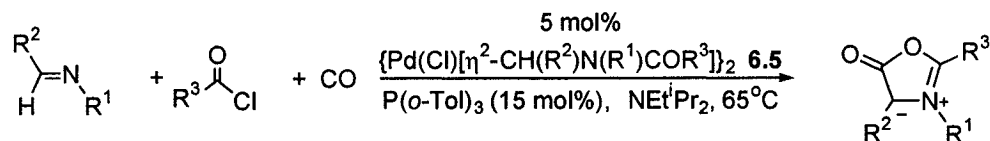


Figure 6.13 Generation of Münchnones Utilizing $P(o\text{-Tol})_3$

In order to better understand the increased catalytic activity obtained with sterically bulky phosphine ligands, the reaction of $P(o\text{-Tol})_3$ with $\{Pd(Cl)[\eta^2\text{-CH}(Tol)N(PMB)COPh]\}_2$ was examined. As shown in Figure 6.14, this results in the formation of $\{[P(o\text{-Tol})_3]Pd(Cl)[\eta^2\text{-CH}(Tol)N(PMB)COPh]\}$ **6.5e** in 84% yield. Crystals of complex **6.5e** suitable for X-ray diffraction were grown from CH_2Cl_2 and toluene at -40°C , and the formulation of this complex was confirmed by X-ray crystallography (Figure 6.15).²⁸

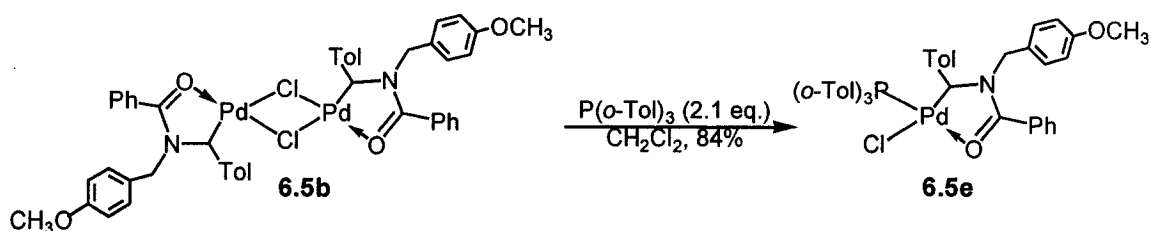


Figure 6.14 Formation of $\{[P(o\text{-Tol})_3]Pd(Cl)[\eta^2\text{-CH}(Tol)N(PMB)COPh]\}$ **6.5e**

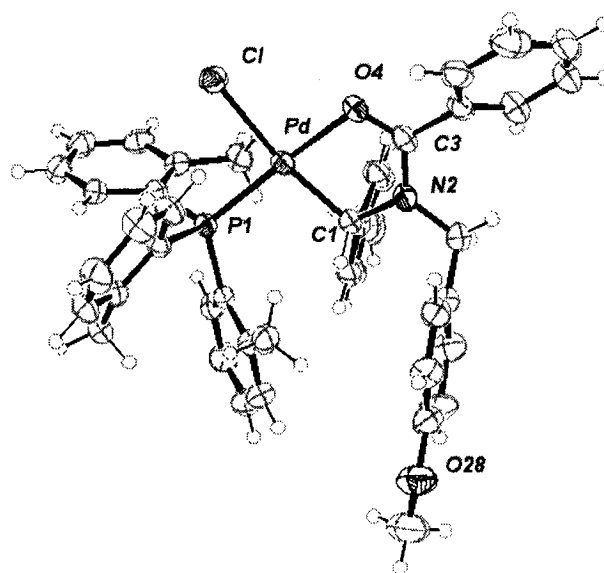


Figure 6.15 X-ray of $\{[P(o\text{-Tol})_3]Pd(Cl)[\eta^2\text{-CH(Tol)N(PMB)COPh}]\}$ **6.5e**. Selected bond lengths (Å) and angles (deg.): Pd-C(1), 2.050(3); Pd-O(4), 2.078(2); Pd-P(1), 2.2563(7); Pd-Cl, 2.4030(8); C(1)-N(2), 1.495(4); C(1)-C(11), 1.506(4); N(2)-C(3), 1.324(4); N(2)-C(21), 1.476(4); C(3)-O(4), 1.262(4); C(3)-C(31), 1.498(4); C(1)-Pd-O(4), 81.01(10); C(1)-Pd-P(1), 98.50(8); O(4)-Pd-P(1), 173.29(6); C(1)-Pd-Cl, 170.36(8); O(4)-Pd-Cl, 91.37(6); P(1)-Pd-Cl, 89.76(3); N(2)-C(1)-C(11), 109.9(2); N(2)-C(1)-Pd, 105.17(19); C(11)-C(1)-Pd, 112.5(2); C(3)-N(2)-C(21), 125.7(3); C(3)-N(2)-C(1), 118.2(3); C(21)-N(2)-C(1), 115.7(2); O(4)-C(3)-N(2), 120.3(3); O(4)-C(3)-C(31), 117.4(3); N(2)-C(3)-C(31), 122.3(3); C(3)-O(4)-Pd, 112.45(18). The disordered solvate species (CH_2Cl_2) in the lattice has been excluded for clarity.

Examination of the structure reveals that Pd, Cl, P(1), C(1), and O(4) atoms are slightly out of square-planar geometry, with the sum of bond angles at the palladium center of 360.64° . The carbonyl bond length in **6.5e** (1.262 Å) is similar to that previously found in $\{[bipy]Pd[\eta^2\text{-CH(Tol)N(Bn)COCH}_3]\}OTf$ (1.265 Å) and

$\{\text{Pd}(\text{Cl})[\eta^2\text{-CH}(\text{Tol})\text{N}(\text{PMB})\text{COPh}]\}_2$ (**6.5b**) (1.264 Å). In addition, the amide C-N bond is slightly longer at 1.324 Å than that seen in complex **6.5b** (1.312 Å), but still smaller than those found in simple amides like *N,N*-dimethylbenzamide (1.368 Å).¹⁸ This again suggests a significant contribution of resonance form **6.5e'** to the structure of **6.5e** (Figure 6.16). In addition, the $\angle\text{C-Pd-O}$ bond angle is slightly compressed in **6.5e** (81.01°), in comparison to **6.5b** (83.6°), presumably due to the steric bulk of the phosphine ligand forcing the carbon bound to the palladium closer to the amide oxygen.

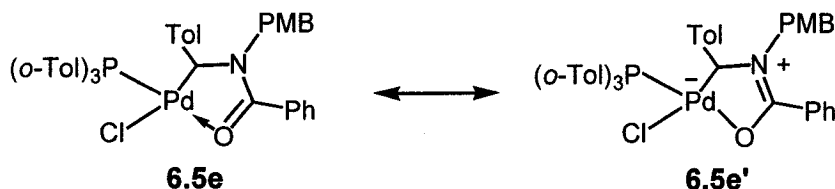


Figure 6.16 Bond Lengths in Palladium Chelated Amides

While both PPh_3 and $\text{P}(o\text{-Tol})_3$ appear to form similar mono-ligated palladium complexes, their behaviour in solution is distinct. In contrast to the PPh_3 complex **6.5d**, the $^1\text{H-NMR}$ spectrum of **6.5e** in CD_2Cl_2 at 22°C shows two broad methoxy resonances at δ 3.82 (s) and δ 3.72 (s) in a 4:1 ratio, as well as a broad methine δ 5.34 (s, 1H) and benzylic peaks δ 4.20 (d, 2H). The $^{31}\text{P}\{^1\text{H}\}$ -NMR spectrum of **6.5e**, also shows two peaks at δ 29.5 and δ 22.9 in a 4:1 ratio. These are presumably cis and trans isomers shown in Figure 6.17. In addition, three different *o*-tolyl methyl resonances for the phosphine ligand are seen, indicating that steric interaction between the bulky phosphine ligand and the substituents on the chelated amide results

in restricted rotation about the Pd-P bond. Heating this complex to 45°C results in the coalescence of the two methoxy peaks into one at δ 3.85 in the $^1\text{H-NMR}$ spectrum, as well as the broadening of the phosphine *o*-tolyl-methyl signals. Examination of the $^{31}\text{P}\{^1\text{H}\}$ NMR spectrum of this compound at 45°C also shows a single phosphine resonance, with no free $\text{P}(o\text{-Tol})_3$. As $16e^-$ square planar complexes are known to be structurally rigid, it is likely that this isomerization is taking place through some unseen intermediate, possibly through a phosphine ligation-deligation equilibrium process shown below (Figure 6.17).²⁹ Steric interactions of the bulky phosphine may help to labilize this ligand, thereby facilitating the low barrier isomerization.

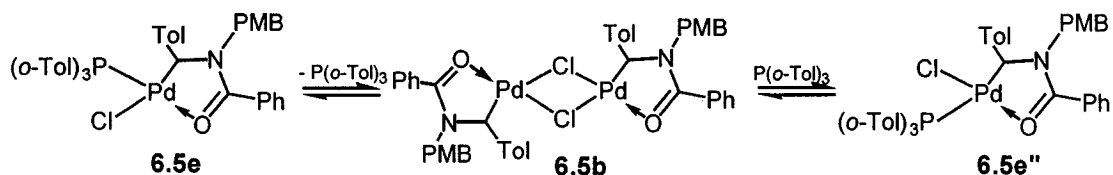


Figure 6.17 Cis-trans Isomerization of $[\text{P}(o\text{-Tol})_3]\text{Pd}(\text{Cl})[\eta^2\text{CH}(\text{Tol})\text{N}(\text{PMB})\text{COPh}]$
6.5b

6.1.7 Catalyst Resting State with $\text{P}(o\text{-Tol})_3$

The facile formation of $\text{P}(o\text{-Tol})_3$ coordinated complex **6.5e** suggests the role of this ligand in accelerated Münchnone formation might be in favouring *N*-acyliminium salt oxidative addition to $\text{Pd}(0)$. This was once again probed by examining the catalyst resting state for Münchnone formation. Monitoring the catalytic coupling of $\text{Tol}(\text{H})\text{C}=\text{NBn}$ **6.2a**, PhCOCl **6.3a**, and CO (4 atm) with $[\text{Pd}(\text{Cl})[\eta^2\text{-CH}(\text{Tol})\text{NBn}(\text{COPh})_2]$ **6.5a** (12.5 mol%), $\text{P}(o\text{-Tol})_3$ (30 mol%), NEt^iPr_2 (1.6 eq.) by

^1H - and ^{31}P -NMR spectroscopy showed the rapid formation of *N*-acyliminium salt **6.4a** and its slow conversion to Münchnone (Figure 6.18). However, once catalysis had begun, no organometallic species were visible in the ^1H -NMR spectrum, even at temperatures down to -20°C . Similarly, ^{31}P -NMR spectrum showed no signal assignable to **6.5e**. Instead, resonances were observed for free $\text{P}(o\text{-Tol})_3$ (~75%), as well as several other non-identifiable phosphine complexes (~25%). These signals were not consistent with $\text{Pd}[\text{P}(o\text{-Tol})_3]_2$.³⁰ While preliminary, this lack of any observable **6.5e** or **6.6a** is once again consistent with a $\text{Pd}(0)$ catalyst resting state for catalysis, perhaps in the form of an as of yet undetermined complex ($[\text{P}(o\text{-Tol})_3\text{PdL}]$ ($\text{L} = \text{NEt}^i\text{Pr}_2, \text{Cl}^-, \text{etc.}$)).

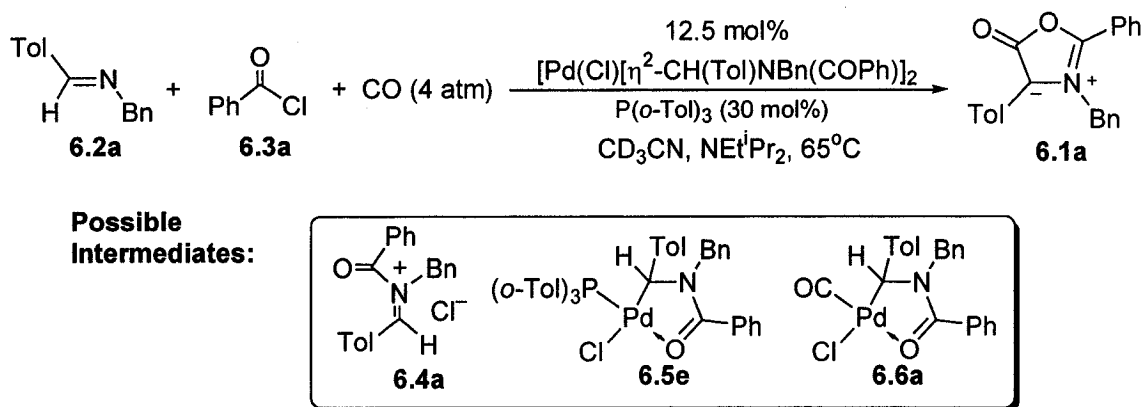


Figure 6.18 Catalyst Resting State Determination

6.1.8 Kinetic Analysis of Münchnone Formation

Preliminary kinetic experiments on Münchnone formation in the presence of $\text{P}(o\text{-Tol})_3$ are also consistent with a $\text{Pd}(0)$ resting state for catalysis. This was

determined in the reaction of Tol(H)C=NBn **6.2a** (1 eq.), PhCOCl **6.3a** (1.4 eq.), and CO (4 atm) with [Pd(Cl)[η^2 -CH(Tol)NBn(COPh)]₂ **6.5a** (5 mol%), P(*o*-Tol)₃ (15 mol%) and NEtⁱPr₂ (1.6 eq.) by stopping the catalytic reaction at various times and obtaining ¹H-NMR spectra. Plotting the $\ln([\text{Münchnone}]_{\infty}/([\text{Münchnone}]_{\infty} - [\text{Münchnone}]))$ as a function of time, once again appears to show a linear correlation (Figure 6.19).³¹ Thus, even in the presence of electron rich P(*o*-Tol)₃, the oxidative addition of *N*-acyliminium salt to Pd(0) appears to be at least partially rate determining for Münchnone formation.

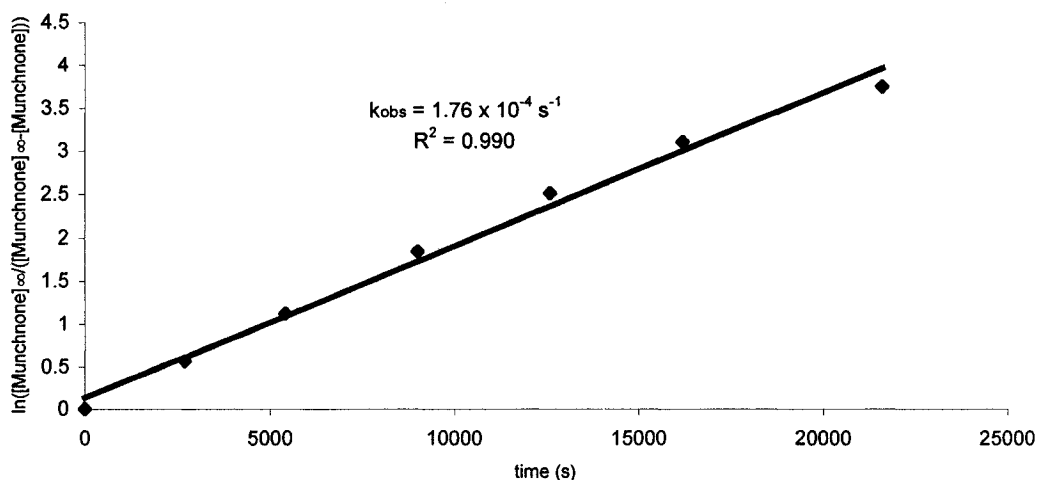


Figure 6.19 Plot of $\ln([\text{Münchnone}]_{\infty}/([\text{Münchnone}]_{\infty} - [\text{Münchnone}]))$ vs time. (Reaction of Tol(H)C=NBn (114 mg, 0.54 mmol), PhCOCl (107 mg, 0.76 mmol), NEtⁱPr₂ (640 mg, 4.94 mmol) with [Pd(Cl)[η^2 -CH(Tol)NBn(COPh)]₂ (24.6 mg, 5 mol%) and P(*o*-Tol)₃ (15 mol%) in a THF/CH₃CN mixture ([N-Acyliiminium Salt]₀ = 0.0169 M). The reaction mixture is divided into 8 portions and pressurized with carbon monoxide (4 atm). Reactions heated at 65°C and stopped at intervals of 0, 3/4, 1.5, 2.5, 3.5, 4.5, 6 and 18 hours. Yields determined by ¹H NMR.)

6.1.9 Probe for a Heterogeneous Palladium Catalyst with P(*o*-Tol)₃

In order to probe for the presence of a heterogeneous palladium species in the Münchnone synthesis with P(*o*-Tol)₃, the catalytic coupling of Tol(H)C=NBn (1 eq), PhCOCl (1.4 eq.) and CO (4 atm) (Figure 6.20) was allowed to proceed to partial completion (1.5 hours, 21 % Münchnone yield). Mercury (320 eq.) was then added to the degassed solution and stirred vigorously for 2 hours. After celite filtration, the catalysis mixture was added to a reaction vessel and again heated for 2 hours at 65°C in the presence of CO (4 atm) (Figure 6.20). In contrast to the results obtained with Bu₄NBr, this reaction mixture showed that further catalysis had indeed occurred following mercury addition, and at a rate similar to that before mercury addition.

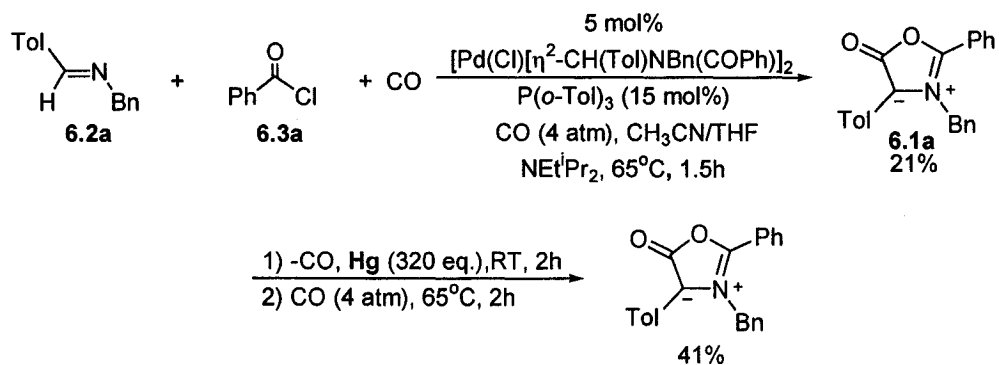


Figure 6.20 Probe for Heterogeneous Processes with Phosphine Ligands

6.1.10 Mechanistic Considerations: Probe for Radical-Based Processes

Reactions that proceed through an apparent oxidative addition step can in fact be radical based processes.³² Therefore eliminating this possibility is required to guide further improvements to the reaction being examined. In order to probe for radical intermediates during Münchnone formation, 9,10-dihydroanthracene (7.3 eq.) was added to the catalytic coupling mixture of Tol(H)C=NEt (1 eq.), PhCOCl (1.4 eq.) and CO (4 atm) (Figure 6.21). The same reaction was conducted in the absence of the radical trap. After 2 hours of reaction time the yields of the Münchnone were identical in both the presence and absence of the radical trap, within experimental error.³³ In addition, anthracene was not formed when the reaction was carried out in the presence of 9,10-dihydroanthracene. This is suggestive of the Münchnone formation proceeding through standard oxidative addition/reductive elimination steps, and not through radical processes.

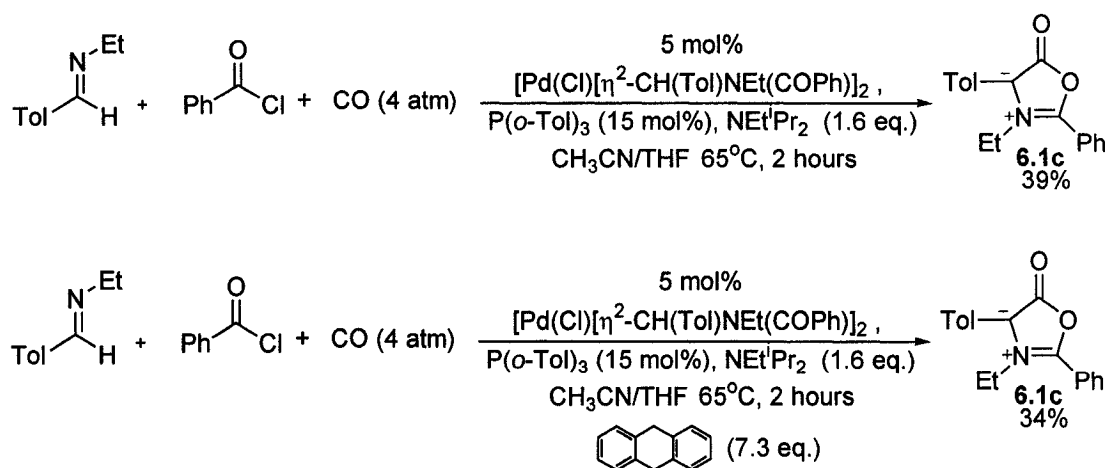


Figure 6.21 Test for Radical Pathways Utilizing 9,10-Dihydroanthracene

6.1.10 Carbonylation Studies with $\{[P(o\text{-Tol})_3]Pd(Cl)[\eta^2\text{-CH(Tol)N(Et)COPh}]\}$

As shown in Scheme 6.1, the formation of Münchnones requires initial displacement of a coordinating ligand by carbon monoxide to generate the carbonylated intermediate **6.6** (Scheme 6.1). This is subsequently followed by the insertion of CO into the palladium-carbon bond to generate **6.7**. However, without initial ligand displacement, the carbonylation step does not occur, as seen when PPh_3 is employed as a reaction constituent. In contrast to PPh_3 , $P(o\text{-Tol})_3$ allows for Münchnone generation. In order to compare these two phosphine ligands, $\{[P(o\text{-Tol})_3]Pd(Cl)[\eta^2\text{-CH(Tol)N(Et)COPh}]\}$ **6.5f** was dissolved in CD_3CN and the NMR tube pressurized with CO (1 atm). As shown in Figure 6.22, this results in the partial conversion of **6.5f** to the CO coordinated complex **6.6c** in approximately a 5:1 ratio (Figure 6.22). While this ratio remains intact for several hours, the reaction mixture slowly decomposes over several days to yield palladium black, trace amounts of Münchnone **6.1c** (2%) and protonated imine **6.13c** (10%).

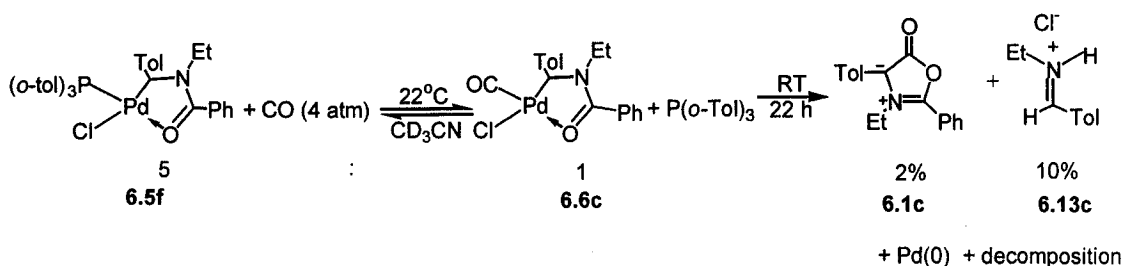


Figure 6.22 Reaction of $\{[P(o\text{-Tol})_3]Pd(Cl)[\eta^2\text{-CH(Tol)N(Et)COPh}]\}$ **6.6f** with CO

As anticipated, the addition of excess $P(o\text{-Tol})_3$ (2 eq.) to the reaction of **6.5f** with carbon monoxide (4 atm) suppresses the formation of **6.6c** (Table 6.1), consistent with the equilibrium between $P(o\text{-Tol})_3$ and CO coordinated to the palladium. Surprisingly, however, $^1\text{H-NMR}$ analysis reveals the immediate formation of Münchnone in approximately 10% yield. Monitoring the reaction further reveals only small amounts of Münchnone derived products forming along with protonated imine **6.13c**.

Table 6.1 Reaction of $\{[P(o\text{-Tol})_3]_2\text{Pd}(\text{Cl})[\eta^2\text{-CH}(\text{Tol})\text{N}(\text{Et})\text{COPh}]\}$ with CO and $P(o\text{-Tol})_3$ (2 eq.)

Conditions	6.5f	6.6c	6.1c	6.13c	6.14c
5 minutes	90%	<1%	~10%	0	0
2 hours	60%	< 2%	15%	10%	0
22 hours	~40%	0	~10%	~10%	~10%

The rapid, room temperature formation of Münchnone in the presence of excess $P(o\text{-Tol})_3$, is intriguing, especially since this ligand inhibits the generation of **6.6c**. Considering the mechanism of Münchnone formation, one possible rationale is that the $P(o\text{-Tol})_3$ serves as a base to quench the HCl generated during the formation of Münchnone. However, its effect as a ligand could also account for the reactivity seen. It has been noted previously that sterically bulky bidentate ligands can

dramatically increase rates of CO migratory insertion.³⁴ Although, phosphine assisted CO insertion is not normally seen or utilized to increase rates of carbonyl insertion, the presence of this ligand could account for the increased level of Münchnone formation. This could possibly arise through the binding of the bulky phosphine ligand to the fifth coordination site of the carbonylated intermediate $[\text{Pd}(\text{Cl})(\text{CO})[\eta^2\text{-CH}(\text{R}^2)\text{NR}^1(\text{COR}^3)]$ **6.6**. The formation of this intermediate would presumably create unfavourable steric interactions, which could be relieved by carbonyl insertion.

6.2 Mechanistic Conclusions

Our initial postulate for the palladium catalyzed synthesis of Münchnones from imines, acid chlorides, and carbon monoxide was that the oxidative addition of the *N*-acyliminium salt to Pd(0) (Step B, Scheme 6.1) was rapid and the carbonylation step was rate controlling. With this in mind, our initially developed catalyst, $[\text{Pd}(\text{Cl})[\eta^2\text{-CH}(\text{R}^2)\text{NR}^1(\text{COR}^3)]_2$ **6.5**, was designed to allow for the facile formation of an empty coordination site for CO binding. However, under these conditions, the liberation of Pd(0) during catalysis led to the generation of palladium sediments. This was attributable to colloidal palladium forming at even a faster rate than what was thought to be a rapid *N*-acyliminium salt oxidative addition. While palladium black formation can be inhibited in the presence of bromide anions, as shown by kinetics experiments and the analysis of the palladium resting state in the catalytic reaction, this still does not lead to rapid *N*-acyliminium salt oxidative addition. Instead, and despite control

experiments that show that stoichiometric palladacycle generation is rapid with $\text{Pd}_2(\text{dba})_3\text{CHCl}_3$, *N*-acyliminium salt oxidative addition to Pd(0) appears to be a rate determining step in catalysis. While conclusive statements as to why oxidative addition remains slow under the catalytic conditions cannot be made at this stage, preliminary experiments suggest that this could be due to palladium colloids being generated during the reaction. The presence of these heterogeneous palladium species might adversely affect the rates of oxidative addition by decreasing the effective catalyst concentration due to the sequestration of active Pd(0), and thereby lead to a decreased rate of Münchnone formation.

Based upon these results, the accelerating influence of $\text{P}(o\text{-Tol})_3$ on Münchnone generation takes on a different light. In particular, while our initial postulate was that $\text{P}(o\text{-Tol})_3$ favours Münchnone formation by aiding mono-metallic Pd(0) in undergoing oxidative addition, a more reasonable scenario may be that this ligand also acts to inhibit colloidal palladium generation, while retaining its lability for subsequent CO binding. Indeed, the accelerating effect of this ligand might be solely based upon blocking colloid formation, and $\text{P}(o\text{-Tol})_3$ coordination may actually slow down *N*-acyliminium salt oxidative addition. This was suggested from kinetic studies, which showed that Münchnone formation with $\text{P}(o\text{-Tol})_3$ still shows a first order dependence on the *N*-acyliminium salt concentration, despite the fact that palladium colloids were not present in this reaction. Considering that ^{31}P -NMR data suggests the existence of several unidentifiable palladium-phosphine complexes, the palladium catalyst could be in a form that requires ligand labilization (e.g.

[P(*o*-Tol)₃], NEt^tPr₂, solvent, etc.) prior to oxidative addition of the *N*-acyliminium salt.

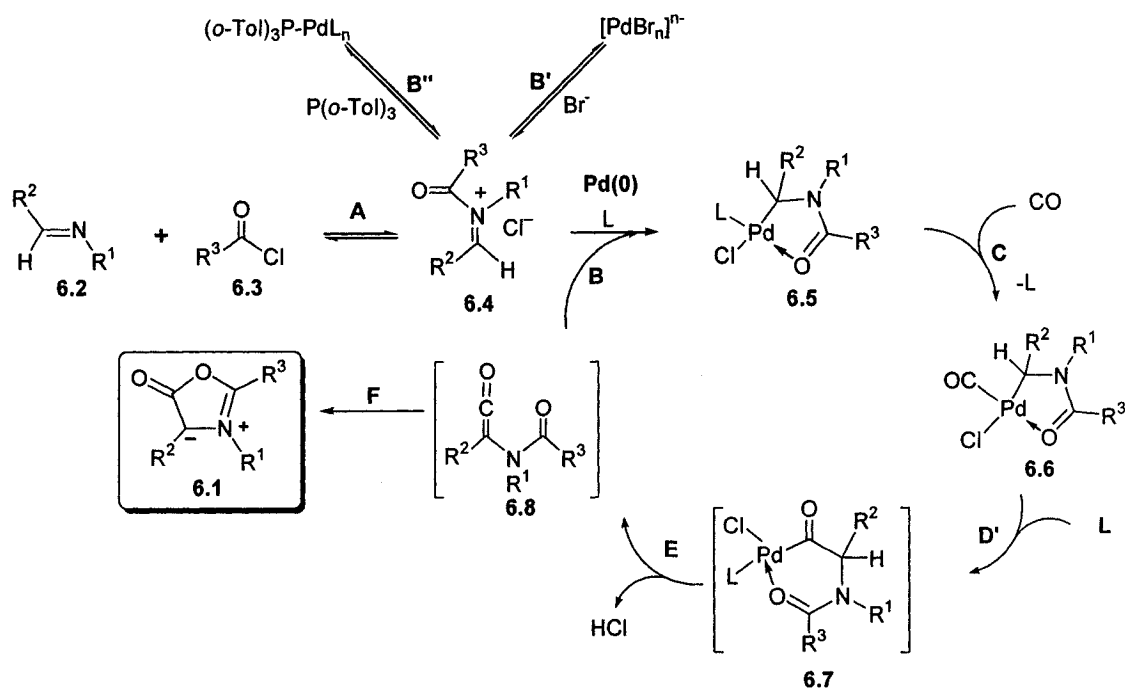
The lability of the bulky P(*o*-Tol)₃ ligand is also certainly critical for Münchnone formation. While the catalytic generation of Münchnone did not proceed in the presence of PPh₃, it progressed efficiently in the presence of a sterically bulky P(*o*-Tol)₃ ligand. This was rationalized based upon the steric bulk of P(*o*-Tol)₃ (cone angle: 195°), which promotes its labilization from the palladium center, and hence subsequent CO binding.³⁵ This is supported by the examination of ¹H-NMR data of {[P(*o*-Tol)₃]Pd(Cl)[η²-CH(Tol)N(PMB)COPh]}, which suggests that rotation about the palladium-phosphine bond is restricted. This is in sharp contrast to PPh₃ (cone angle: 145°), which remains tightly bound to the palladium center, even at high temperatures. While access to the CO coordinated adduct is less facile than without phosphines, this inhibition appears to be more than offset by the ability of this ligand to facilitate other steps in the catalysis (e.g. prevent palladium colloid formation or accelerate oxidative addition). In addition, as shown in stoichiometric experiments that utilize excess P(*o*-Tol)₃ during catalysis, this ligand may actually aid in the conversion of the carbonylated intermediate [Pd(Cl)(CO)[η²-CH(R²)NR¹(COR³)] **6.6** to Münchnone. At the present time, however, this is still speculative.

Overall, this data suggests a more complex mechanism for Münchnone formation, as shown in Scheme 6.2. First, the form in which Pd(0) is present during the catalysis is found to vary depending upon the additives utilized and this in turn is found to be

critical in efficiently generating Münchnone. When weakly coordinating halide salts are employed in the catalysis, this data suggests the rapid formation of colloidal palladium. Alternatively, if the catalysis proceeds on monometallic Pd(0), the deactivated colloidal palladium must undergo an equilibration to generate an active Pd(0) species (Step B', Scheme 6.2). Alternatively, the colloidal Pd(0) may in fact, be the active catalyst for Münchnone formation in the presence of halide salts. In this case, it can presumably enter the catalytic cycle immediately. The catalytic Münchnone synthesis in the presence of P(*o*-Tol)₃ engenders a homogeneous catalytic system, in which ligand labilization from the catalyst resting state is likely required prior to oxidative addition of the *N*-acyliminium salt (Step B''). The presence of this electron rich phosphine ligand could also perhaps increase the rates of oxidative addition, as well as possibly increasing the rates of carbonylation.

In summary, these studies have demonstrated the importance of finely balancing all steps in a multi-step metal catalyzed multicomponent coupling reaction, such as the synthesis of Münchnones from imines, acid chloride and carbon monoxide. In particular, this palladium catalyzed synthesis of Münchnones shows the requirement for careful control of several catalytic features, including Pd(0) stabilization, oxidative addition, ligand labilization and carbonylation in achieving efficient catalysis. These studies suggest that ligands should be designed to not only stabilize the metal center from colloid formation, but also undergo ready labilization for carbon monoxide coordination. Further studies aimed at developing these concepts

and confirming the mechanistic postulates developed in this work, will be the subject of future reports.



Scheme 6.2 Mechanistic Rationale for Münchnone Formation

6.3 Experimental

Unless otherwise noted, all manipulations were performed under an inert atmosphere in a Vacuum Atmospheres 553-2 dry box or by using standard Schlenk or vacuum line techniques. The catalysts, $[\text{Pd}(\text{Cl})[\eta^2\text{-CH}(\text{R}^1)\text{NR}^2(\text{COR}^5)]_2$, were prepared according to previous literature procedures.⁸ Carbon monoxide (99.99%) was purchased from Matheson and used as received. Imines were prepared using standard literature procedures.³⁶ All other reagents were purchased from Aldrich[®] and used as received. Tetrahydrofuran (THF) was distilled from sodium/benzophenone ketyl

under nitrogen. Acetonitrile was distilled from CaH_2 under nitrogen. Deuterated solvents were dried as their protonated analogues, but were transferred under vacuum from the drying agent, and stored over 3\AA molecular sieves.

^1H and ^{13}C were recorded on JEOL 270, Varian Mercury 300 MHz, Mercury 400 MHz, and Unity 500 MHz spectrometers. Mass spectra were obtained from the McGill University Mass Spectral Facility.

Test for Heterogeneity of the Reactions

Reactions were set up as described previously.^{8, 10} Tol(H)C=NBn (28.0 mg, 0.133 mmol) and benzoyl chloride (22 μL , 0.188 mmol) were dissolved in 2.5 mL of CH_3CN and stirred for 15 min. The previous solution was then added to a solution of $\{\text{Pd}(\text{Cl})[\eta^2\text{-CH}(\text{Tol})\text{NBnCOPh}]\}_2$ **6.5a** (6.2 mg, 0.0068 mmol), and $\text{P}(o\text{-Tol})_3$ (6.2 mg, 0.0205 mmol) in 2.5 mL of dry CH_3CN . The reaction mixture was transferred to a 50 mL reaction bomb and NEt^iPr_2 (36 μL , 0.21 mmol) were added in 5 mL of tetrahydrofuran. The solution was degassed and carbon monoxide (60 psi) was added to the reaction mixture, which was left to stir at 65°C for 2 hours. In the case of Bu_4NBr , (43 mg, 0.133 mmol), was added instead of the $\text{P}(o\text{-Tol})_3$. The reactions were stopped after 2 hours and showed 24% formation of Münchnone with the utilization of Bu_4NBr and 21% with $\text{P}(o\text{-Tol})_3$. After degassing, the solutions were each stirred vigorously in the presence of mercury (8.7 g, 42.6 mmol) over a 2 hour period. After celite filtration, the solutions were added to their respective reaction vessels, pressurized with CO (4 atm), heated to 65°C and allowed to react for another

2 hours. The respective yields of Münchnone were 24% in the case of Bu₄NBr and 41% with P(*o*-Tol)₃.

Test for Radical-Based Products

Tol(H)C=NBn (57.0 mg, 0.27 mmol) and benzoyl chloride (44 μ L, 0.38 mmol) were dissolved in 5 mL of CH₃CN and stirred for 15 min. The previous solution was then added to a solution of {Pd(Cl)[η^2 -CH(Tol)NBnCOPh]}₂ **6.5a** (12.4 mg, 0.013 mmol), and P(*o*-Tol)₃ (12.4 mg, 0.041 mmol) in 5 mL of dry CH₃CN. The reaction mixture was transferred to a 50 mL reaction bomb and NEtⁱPr₂ (71 μ L, 0.42 mmol) and 9,10-dihydroanthracene (180 mg, 1.03 mmol) were added in 10 mL of THF. The solution was degassed and carbon monoxide (4 atm) was added to the reaction mixture, which was left to stir at 65°C for 2 hours. The same reaction was conducted in the absence of the radical trap. After 2 hours of reaction time the yields of the Münchnone were 34% and 39% presence and absence of the radical trap, respectively.¹⁰ No anthracene was formed in the reaction as well. ¹H-NMR yields were obtained using 1,3-dimethoxybenzene as an internal standard.

Table 6.1 Crystallographic Details for Complexes 6.5b and 6.5e.³⁷⁻⁴⁰

	6.5b	6.5e
empirical formula	C ₄₆ H ₄₄ Cl ₂ N ₂ O ₄ Pd ₂ · 4(C ₇ H ₈)	C ₄₄ H ₄₃ Cl NO ₂ P Pd ₂ · 2(CH ₂ Cl ₂)
Fw	1341.07	960.47
temp (K)	220 (2)	220 (2)
wavelength, Å	1.54178	1.54178
cryst. syst.	monoclinic	Monoclinic
space group	P2 ₁ /c	P2 ₁ /c
a (Å)	17.5028 (11)	16.833 (3)
b (Å)	9.7001 (5)	16.4443 (4)
c (Å)	20.2231 (13)	16.6678 (4)
α (deg)		
β (deg)	103.052 (3)	96.4340 (10)
γ (deg)		
V (Å ³)	3344.8 (4)	4396.85 (17)
Z	2	4
d(calcd) (Mg m ⁻³)	1.332	1.451
μ (mm ⁻¹)	5.450	6.844
F(000)		
no. of reflns collected	42029	35168
no. of indep. Reflns	4165	8663
θ _{min} , θ _{max} (deg)	3.02-54.49	3.61-72.72
goodness of fit on F ²	1.031	1.041
R [F ² > 2σ (F ²)]	0.0689	0.0448
wR(F ²)	0.1882	0.1184
min, max, Δρ(e/ Å ³)	-1.216, 2.063	-0.580, 1.268

Kinetic Studies on Münchnone Formation: Bu₄NBr

Tol(H)C=NBn (114 mg, 0.54 mmol) was combined with PhCOCl (107 mg, 0.76 mmol) in 8 mL of CH₃CN. To this solution was added [Pd(Cl)[η²-CH(Tol)NBn(COPh)]₂ (5 mol%, 24.6 mg) in 8 mL of CH₃CN, Bu₄NBr (176 mg, 0.54 mmol) in 8 mL of THF and NEt^tPr₂ (4.94 mmol, 640 mg) in 8 mL of THF. The solution was divided into 8 portions and added to 50 mL reaction bombs, followed by the addition of carbon monoxide (60 psi). The reactions were heated at 65°C and stopped at intervals of 0, 1, 2, 3, 5, 7, 12, and 24 hours. The yield of Münchnone generated was determined by ¹H NMR (utilizing benzyl benzoate as an internal standard).

Kinetic Studies on Münchnone Formation: P(*o*-Tol)₃

Tol(H)C=NBn (114 mg, 0.54 mmol) was combined with PhCOCl (107 mg, 0.76 mmol) in 8 mL of CH₃CN. To this solution was added [Pd(Cl)[η²-CH(Tol)NBn(COPh)]₂ (5 mol%, 24.6 mg) in 8 mL of CH₃CN, P(*o*-Tol)₃ (24.8 mg, 0.082 mmol) in 8 mL of THF and EtNⁱPr₂ (0.86 mmol, 111 mg) in 8 mL of THF. The solution was divided into 8 portions and added to 50 mL reaction bombs, followed by the addition of carbon monoxide (60 psi). The solutions were heated at 65°C and stopped at intervals of 0, ¼, 1.5, 2.5, 3.5, 4.5, 6 and 18 hours. The yield of Münchnone was determined by ¹H-NMR (utilizing benzyl benzoate as an internal standard).

Münchnone Generation Utilizing PPh₃

Tol(H)C=NBn (114 mg, 0.54 mmol) was combined with PhCOCl (107 mg, 0.76 mmol) in 8 mL of CH₃CN. To this solution was added [Pd(Cl)[η²-CH(Tol)NBn(COPh)]₂ (5 mol%, 24.6 mg) in 8 mL of CH₃CN, PPh₃ (21.5 mg, 0.082 mmol) in 8 mL of THF and EtNⁱPr₂ (0.86 mmol, 111 mg) in 8 mL of THF. The solution was evacuated, carbon monoxide (60 psi) added, and the solution stirred at 65°C for 18 hours. Analysis of the reaction mixture did not show the presence of Münchnone.

{Pd[η^2 -C(Tol)HN(PMB)COPh]}₂ (6.5b)

Tol(H)C=N(PMB) (231 mg, 0.966 mmol) was reacted with PhCOCl (136 mg, 0.966 mmol) and added to Pd₂(dba)₃·CHCl₃ (500 mg, 0.242 mmol) in CH₃CN (10 mL) and stirred for 2 hours at room temperature. The solution is subsequently filtered through celite and the solvent is removed *in vacuo* to provide a yellow residue. This residue is washed with diethyl ether (3 x 10 mL) to yield {Pd(Cl)[η^2 -CH(Tol)N(PMB)COPh]}₂ (**6.5b**), which was isolated as a yellow powder in a 74% yield. Recrystallization from toluene at -40°C provided complex **6.5b** as orange crystals.

Yield: 74%. ¹H NMR (CD₃CN, 400 MHz, 60°C): δ 7.64-7.57 (m, 7H), 7.23 (d, 2H, 7.43 Hz), 7.18 (d, 2H, 7.43 Hz), 6.138 (d, 2H, 7.43 Hz), 6.132 (d, 2H, 7.43 Hz), 5.28 (s, 1H), 4.48 (d, 1H, 15.26 Hz), 3.88 (d, 1H, 15.26 Hz), 3.83 (s, 3H); 2.29 (s, 3H). ¹³C NMR (CD₃CN, 75.5 MHz, 60°C): δ 180.1, 159.7, 139.5, 136.0, 132.3, 131.6, 130.0, 129.6, 129.4, 127.8, 126.3, 126.18, 114.4, 59.4, 55.2, 52.0, 20.8. IR (KBr): 1550 cm⁻¹
ESI MS: 970.07- [Cl]

Crystal Structure of {Pd(Cl)[η^2 -CH(Tol)N(PMB)COPh]}₂ (PMB = p-C₆H₄OCH₃) **6.5b**

Crystals of this dimeric palladium complex for diffraction analysis were grown by cooling in a toluene solution and mounted on a capillary after being removed from

toluene. X-ray data was collected at 293 K on an Enraf-Nonius CAD4 diffractometer with Cu K α radiation. The space groups were confirmed by the PLATON program. Data reduction was performed using a locally modified version of the NRC-2 program. The structure was solved by direct method using SHELXS97 and difmap synthesis using SHELXTL and SHELXL96. All non-hydrogen atoms were refined anisotropically, and the hydrogen atoms were refined isotropically. Hydrogen atoms were constrained to the parent site using a riding model; SHELXL96 defaults, C-H 0.93 to 0.98 Å. The isotropic factors, U_{iso} were adjusted to a 50% higher value of the parent site (methyl) and 20% higher (others). Two models were used to describe part of the molecule (two different unit cells). Occupancy factor of model A was refined to 0.58 (1) and was fixed to 0.60 in the last cycles. The occupancy factor of model B was fixed to 0.40. Some restraints (SADI), EADP constraints, and ideal phenyl rings description (AFIX 66) were applied to help convergence. A final verification of possible voids was performed using the VOID routine of the PLATON program.

{[P(*o*-Tol)₃]Pd(Cl)[η^2 -CH(Tol)N(PMB)COPh]} (6.5e)

P(*o*-Tol)₃ (32 mg, 0.105 mmol) was added to {Pd(Cl)[η^2 -CH(Tol)N(PMB)COPh]}₂ (**6.5b**) (50 mg, 0.051 mmol) in CH₂Cl₂ (5 mL) and stirred at room temperature for 30 minutes to form {[P(*o*-Tol)₃]Pd(Cl)[η^2 -CH(Tol)N(PMB)COPh]} **6.5e**. The solvent was removed *in vacuo* and the impure solid was washed with ether (3 x 5 mL), which resulted in the formation of **6.5e** in 84% yield as a yellow solid. This yellow solid

was recrystallized from toluene at -40°C to yield crystals of complex **6.5e** suitable for X-ray diffraction.

Yield: 84% ^1H NMR (CD_2Cl_2 , 400 MHz, 45°C): δ 9.64-9.30 (m (br.), 1H), 7.77-7.62 (m, 2H), 7.62-7.49 (m, 2H), 7.49-6.50 (m, 20H), 5.34 (s, 1H), 4.46 (d, 1H, 14.6 Hz), 3.84 (s, 3H), 3.65 (d, 1H, 14.6 Hz); 2.28 (s, 3H); 2.28 (m, 9H). ^{13}C NMR (CD_2Cl_2 , 75.5 MHz, 45°C): δ 179.0, 159.9, Aromatic Peaks, 114.5, 69.2, 55.7, 52.6, tolyl peak \sim 22, 21.1. ^{31}P NMR (200 MHz): δ 29.5; 22.9 (4:1). IR (KBr): 1551 cm^{-1} ESI MS: 789.18 – $[\text{P}(o\text{-Tol})_3] + [\text{H}^+]$

Crystal Structure of $\{\text{P}(o\text{-Tol})_3\}\text{Pd}(\text{Cl})[\eta^2\text{-CH}(\text{Tol})\text{N}(\text{PMB})\text{COPh}\}$ **6.5e.**

Crystals of this monophosphine palladium complex for diffraction analysis were grown by cooling in a dichloromethane solution and mounted on a capillary. X-ray data was collected at 293 K on an Enraf-Nonius CAD4 diffractometer with Cu $K\alpha$ radiation. The space groups were confirmed by the PLATON program. Data reduction was performed using a locally modified version of the NRC-2 program. The structure was solved by direct method using SHELXS97 and difmap synthesis using SHELXTL and SHELXL96. All non-hydrogen atoms were refined anisotropically, and the hydrogen atoms were refined isotropically. Hydrogen atoms were constrained to the parent site using a riding model; SHELXL96 defaults, C-H 0.93 to 0.98 Å. The isotropic factors, U_{iso} were adjusted to a 50% higher value of the parent site (methyl) and 20% higher (others). Two models were used to describe part

of the molecule (two different unit cells). Occupancy factor of model A was refined to 0.58 (1) and was fixed to 0.60 in the last cycles. The occupancy factor of model B was fixed to 0.40. Some restraints (SADI), EADP constraints, and ideal phenyl rings description (AFIX 66) were applied to help convergence. A final verification of possible voids was performed using the VOID routine of the PLATON program.

{Pd[η^2 -C(Tol)HN(Et)COPh] }₂ (6.5c)

Tol(H)C=NEt (73 mg, 0.495 mmol) was reacted with PhCOCl (69 mg, 0.495 mmol) and added to Pd₂(dba)₃·CHCl₃ (250 mg, 0.242 mmol) in CH₃CN (10 mL) and stirred for 2 hours at room temperature. The solution is subsequently filtered through celite and the solvent is removed *in vacuo* to provide a yellow residue. This residue is washed with diethyl ether (3 x 10 mL) to yield {Pd(Cl)[η^2 -CH(Tol)N(Et)COPh]}₂ (6.5c), which was isolated as a yellow powder in a 78% yield.

Yield: 78%. ¹H NMR (CD₂Cl₂, 400MHz, 40°C): δ 7.60-7.49 (m, 5H), 7.28-7.20 (m, 2H), 7.18-7.08 (m, 2H), 5.65 (s, 1H), 3.31-3.22(m, 1H), 3.02-2.93 (m, 1H), 2.25 (s, 3H); 1.02 (t, 3H). ¹³C NMR (CD₂Cl₂, 101 MHz, 40°C): δ 179.8 , 139.1, 136.4, 132.3, 131.4, 130.0, 129.0, 127.4, 125.8, 60.4, 44.1, 21.6, 13.3. IR (KBr): 1558 cm⁻¹ ESI MS: 786.02 + [Cl⁻]

3-benzyl-2-phenyl-4-p-tolyl-1,3-oxazolium 5-oxide (6.1)

NMR Yield: 83%. Isolated Yield: 18%. ^1H NMR (400 MHz, CD_3CN): δ 7.65 (d, 2H), 7.54-7.46 (m, 3H), 7.38-7.26 (m, 5H), 7.16 (d, 2H), 7.12 (d, 2H), 5.48 (s, 2H), 2.29 (s, 3H), ^{13}C NMR (100 MHz, CD_3CN): δ 160.9, 143.1, 136.1, 134.9, 131.2, 129.5, 129.3, 129.3, 128.3, 128.0, 127.8, 126.5, 126.18, 123.5, 95.0, 50.7, 20.6. IR (NaCl): $\nu_{\text{CO}} = 1709.8 \text{ cm}^{-1}$. HRMS calculated for $\text{C}_{23}\text{H}_{19}\text{NO}_2$: 341.1416; found: 341.1420.

{[PPh₃]Pd(Cl)[η^2 -CH(Tol)N(Et)COPh]} (6.5d)

PPh_3 (100 mg, 0.127 mmol) was added to $\{\text{Pd}(\text{Cl})[\eta^2\text{-CH}(\text{Tol})\text{N}(\text{Et})\text{COPh}]\}_2$ (**6.5c**) (68 mg, 0.26 mmol) in CH_2Cl_2 (5 mL) and stirred at room temperature for 30 minutes to form $\{[\text{PPh}_3]\text{Pd}(\text{Cl})[\eta^2\text{-CH}(\text{Tol})\text{N}(\text{Et})\text{COPh}]\}$ **6.5d**. The solvent was removed *in vacuo* and the impure solid was washed with ether (3 x 5 mL), which resulted in the formation of **6.5d** in 90% yield as a yellow solid.

Yield: 90% ^1H NMR (CD_2Cl_2 , 400MHz, 25°C): δ 7.64-7.48 (m, 8H), 7.46-7.34 (m, 12H), 6.134 (d, 2H, 7.43 Hz), 6.32 (d, 2H, 7.43 Hz), 4.54 (d, 1H, 4.10 Hz), 3.19 (m, 1H), 2.73 (m, 1H), 2.30 (s, 3H), 0.95 (t, 3H) ^{13}C NMR (CD_3CN , 75.5 MHz, 25°C): δ 179.0, 139.4, 139.3, 136.5, 136.4, 135.0, 134.9, 133.3, 133.3, 130.9, 130.9, 130.7, 130.7, 130.2, 129.2, 128.9, 128.3, 128.2, 127.3, 126.6, 12.6, 69.1 (d, 3.18 Hz), 44.3,

21.2, 13.4. ^{31}P NMR (CD_2Cl_2 , 200MHz, 25°C): δ 28.7. IR (KBr): 1549 cm^{-1} . ESI MS: 655.10 = (429.8 + PPh_3 + $[\text{Cl}^-]$)

6.4 References

- 1 a) Capdevilla, E.; Rayó, J.; Carrión, F.; Jové, I.; Borrel, J.I.; Teixidó, J. *Afinidad*, **60**, 317. b) Bienaymé, H.; Hulme, C.; Odon, G.; Schmitt, P. *Chem. Eur. J.* **2000**, *6*, 3321. c) Tietze, L.F.; Modi, A. *Med. Res. Rev.* **2000**, *20*, 304. d) Posner, G.H. *Chem. Rev.* **1986**, *86*, 831.
- 2) Armstrong, R.W.; Combs, A.P.; Tempest, P.A.; Brown, S.D.; Keating, T.A. *Acc. Chem. Res.* **1996**, *29*, 123.
- 3) Hegedus, L.S. *Transition Metals in the Synthesis of Complex Organic Molecules*, 2nd Edition. University Science Books, **1999**.
- 4 a) Saito, S.; Yamamoto, Y.; *Chem. Rev.* **2000**, *100*, 2901. b) Frühauf, H.-W.; *Chem. Rev.* **1997**, *97*, 523. c) Ojima, I.; Tzamarioudaki, M.; Zhaoyang, L.; Donovan, R.J.; *Chem. Rev.* **1996**, *96*, 635. d) Lautens, M.L.; Klute, W.; Tam, W. *Chem. Rev.* **1996**, *96*, 46. e) Schore, N.E. *Chem. Rev.* **1988**, *88*, 1081. f) Vollhardt, K.P.C. *Angew. Chem. Int. Ed.* **1984**, *23*, 536. g) Grotjahn, D.B. In *Comprehensive Organometallic Chemistry II*; Ed. Abel, Stone, Wilkinson, Hegedus. Pergammon Press: Oxford, **1995**; vol. 12, pp 741-770.
- 5) For Reviews on Amidocarbonylation, see: a) Beller, M. and Eckert, M. *Angew. Chem. Int. Ed.* **2000**, *39*, 1010. b) Knifton, J.F. Amidocarbonylation. In *Applied Homogeneous Catalysis with Organometallic Compounds*. 2nd Ed. **2002**, 156-164.

- 6) For Reviews on the Pauson Khand Reaction, see: a) Gibson, S.E.; Stevenazzi, A. *Angew. Chem. Int. Ed.* **2003**, *42*, 1800. b) Chung, Y.K. *Coord. Chem. Rev.* **1999**, *188*, 297. c) Frühauf, H.-W. *Chem. Rev.* **1997**, *97*, 523. d) Geis, O.; Schmalz, H.-G. *Angew. Chem. Int. Ed.* **1998**, *37*, 911. e) Brummond, K.M.; Kent, J.L. *Tetrahedron*, **2000**, *56*, 3263. f) Schore, N.E. *Organic Reactions* vol. 40. **1991**, Wiley. New York.
- 7 a) Dghaym, R. D.; Dhawan, R.; Arndtsen, B. A. *Angew. Chem. Int. Ed.* **2001**, *40*, 3228 b) Dhawan, R.; Dghaym, R.D.; Arndtsen, B.A. *Catalysis of Organic Reactions.* **2003**, *89*, 499.
- 8) Dhawan, R.; Dghaym, R.D.; Arndtsen, B.A. *J. Am. Chem. Soc.* **2003**, *125*, 1474.
- 9) Dhawan, R.; St. Cyr, D.; Dghaym, R.D.; Arndtsen, B.A. *Org. Letters*, to be submitted. (Chapter 2)
- 10) Dhawan, R.; Arndtsen, B. A. *J. Am. Chem. Soc.* **2004**, *126*, 468.
- 11) For Reviews on Münchnone chemistry, see: a) Mesoionic Ring Systems by K.T. Potts in *1,3 Dipolarcycloaddition Chemistry* A. Padwa ed. pg. 1-81. **1983** John Wiley & Sons Inc. New York b) Mesoionic Oxazoles by H.L. Gingrich and J.S. Baum in *Oxazoles*. I.J. Turchi Ed. 731-958. **1984** John Wiley & Sons Inc. New York c) Mesoionic Ring Systems by G.W. Gribble in *Synthetic Applications of 1,3-Dipolar Cycloaddition Chemistry Toward Heterocycles and Natural Products.* **2002** John Wiley & Sons Inc. New York . A. Padwa Ed. pg. 681-753. d) Mesoionic Oxazoles by G.W. Gribble in *Oxazoles: Synthesis, Reactions, and Spectroscopy Part. A.* Ed. D.C. Palmer **2003**, John Wiley & Sons. New York.

- 12) Determined by $^1\text{H-NMR}$ spectroscopy. See Ref. 7. Also see: Ratts, K.; Chupp, J. *J. Org. Chem.* **1974**, *39*, 3300.
- 13) Dghaym, R.D.; Yaccatto, K.J.; Arndtsen, B.A. *Organometallics* **1998**, *17*, 4.
- 14) See Experimental Section for Details.
- 15) Reaction of Tol(H)C=NBn (1 eq.), PhCOCl (1 eq.), and $\text{Pd}_2(\text{dba})_3\cdot\text{CHCl}_3$ (0.5 eq.) is seen to occur within 15 minutes at room temperature in CH_2Cl_2 ($[\text{Pd}_2(\text{dba})_3\cdot\text{CHCl}_3]$ is sparingly soluble in $\text{CH}_3\text{CN}/\text{THF}$ and therefore requires longer reaction times).
- 16) Davis, J.L.; Dhawan, R.; Arndtsen, B. A. *Angew. Chem. Int. Ed.* **2004**, *43*, 590.
- 17) See Experimental Section for complete experimental details and the X-ray structure.
- 18) Adler, M.; Marsch, M.; Nudelman, N.S.; Boche, G. *Angew. Chem. Int. Ed.* **1999**, *38*, 1261.
- 19) Also seen with similar compounds: See Ref. 13.
- 20) Beletskaya, I. P.; Cheprakov, A. V. *Chem. Rev.* **2000**, *100*, 3009.
- 21) Reetz, M.; Westermann, E. *Angew. Chem. Int. Ed.* **2000**, *39*, 165.
- 22 a) Widegren, J.A.; Finke, R.G. *J. Mol. Cat. A.* **2003**, *198*, 317. b) Davies, I.W.; Matty, L.; Hughes, D.L.; Reider, P.J. *J. Am. Chem. Soc.* **2001**, *123*, 10139
- 23) Performing the same sequence of steps, without the addition of mercury results in further catalysis.
- 24) See Experimental Section for further details.
- 25) An analogous compound $\{(\text{L}_2\text{Pd}[\eta^2\text{-CH}(\text{Ph})\text{N}(\text{Ph})\text{COCH}_3])^+\text{BF}_4^-\}$, $\text{L}_2 = \text{Ph}_2\text{P}(\text{CH}_2)_3\text{PPh}_2$ previously reported, shows the methine proton as a doublet of

doublets at $\delta = 4.27$ ($^3J_{P-H} = 4.8, 8.0$ Hz). Kacker, S.; Kim, J.S.; Sen, A. *Angew. Chem. Int. Ed. Engl.* **1998**, *37*, 1251. Coupling constants for cis coupling are generally smaller than those for trans coupling (Crabtree, R.H. *The Organometallic Chemistry of the Transition Metals* 2nd Ed. Wiley Interscience, **1994**, New York. pg. 236-266) As such, the assignment is suggested.

- 26) Data also reported in Chapter 4 of this thesis. See Ref. 7b
- 27) For example: Stambuli, J. P.; Bühl, M.; Hartwig, J. F. *J. Am. Chem. Soc.* **2002**, *124*, 9346, and references therein.
- 28) See Experimental Section for full details.
- 29) For examples of cis-trans isomerization with palladium complexes, see: a) Casado, A.L.; Espinet, P. *Organometallics* **1998**, *17*, 954. b) Amatore, C.; Jutand, A. *J. Organomet. Chem.* **1999**, *576*, 254. c) Amatore, C.; Jutand, A. *Acc. Chem. Res.* **2000**, *33*, 314.
- 30 a) Paul, F.; Patt, J.; Hartwig, J.F.; *J. Am. Chem. Soc.* **1994**, *116*, 5969. b) Paul, F.; Patt, J.; Hartwig, J.F.; *Organometallics* **1995**, *14*, 3030.
- 31) Data reported is preliminary.
- 32) For examples of this type of processes, see: a) Kramer, A.V.; Labinger, J.A.; Bradley, J.S.; Osborn, J.A. *J. Am. Chem. Soc.* **1974**, *96*, 7145. b) Kochi, J.K. *Pure Appl. Chem.* **1980**, *52*, 571. c) Paonessa, R.S.; Thomas, N.C.; Halpern, J. *J. Am. Chem. Soc.* **1985**, *107*, 4333. d) Ishiiyama, T.; Murata, M.; Suzuki, A. *Chem. Commun.* **1995**, 295.
- 33) See Experimental Section for Details.

- 34) Gonsalvi, L.; Adams, H.; Sunley, G.J.; Ditzel, E.; Haynes, A. *J. Am. Chem. Soc.* **1999**, *121*, 11233.
- 35) Tolman, C.A. *Chem. Rev.* **1977**, *77*, 313.
- 36) Layer, R. W. *Chem. Ber.* **1963**, *63*, 489.
- 37) Spek, A.L. PLATON Molecular Geometry Program. July **1995** version; University of Utrecht, Utrecht, Holland.
- 38) Ahmed, F.R.; Hall, S.R.; Pippy, M.E.; Huber, C.P. (**1973**) NRC Crystallographic Computer Programs for the IBM/360. Accession Nos. 133-147 in *J. Appl. Cryst.* *6*, 309-346.
- 39) Sheldrick, G.M. (**1997**) SHELXS97. Program for the Solution of Crystal Structures. University of Gottingen, Germany.
- 40) Sheldrick, G.M. (**1996**) SHELXL96. Program for the Refinement of Crystal Structures. University of Gottingen, Germany. SHELXTL (**1997**) Release 5.10; The Complete Software Package for Single Crystal Structure Determination, Bruker AXS Inc., Madison, WI 53719-1173.

CHAPTER SEVEN

Conclusions, Contributions to Original Knowledge, and Suggestions for Future Work

This chapter gives a brief synopsis of the results and conclusions that were presented in this thesis, as well as providing the contributions to original knowledge. In addition, based upon the results obtained in this thesis, suggestions for future work are also presented herein.

7.0 Conclusions and Contributions to Original Knowledge

This thesis has shown how a range of complex molecules can be thought of as arising through the coupling of simpler precursors that are assembled via a single step transition metal catalyzed process. More specifically, these studies focused on developing a palladium catalyzed methodology to construct Münchnones. By carefully controlling the sequence of reactions that happen at the palladium center, as well as manipulating the structure of the catalyst, a method was developed to convert three basic building blocks (i.e. imines, acid chlorides and carbon monoxide) directly into Münchnones. This methodology was then utilized to generate a range of heterocycles and peptide-based molecules, where essentially every position of the respective molecule can be varied independently.

In addition to reactions that happen on the metal catalyst itself, the constituents of the catalytic mixture are also critical in influencing the products obtained. This was clearly demonstrated in our design of a catalytic β -lactam synthesis. Previous work had shown that imidazoline-carboxylates could be generated from coupling two imines, an acid chloride and carbon monoxide. Mechanistic studies on this reaction suggested that the HCl generated during catalysis could mediate the 1,3-dipolar cycloaddition of an imine to the Münchnone to form imidazoline-carboxylates. The addition of base to this reaction mixture sequestered the *in situ* generated acid, and allowed the imine to undergo a [2+2] cycloaddition with the ketene tautomer of the Münchnone, yielding small amounts of 3-amido substituted β -lactams. The utilization of ligands, addition of base, and fine-tuning reactant ratios enabled β -lactam generation to proceed in moderate to good yields. Subsequent studies suggested that imidazoline-carboxylate formation could also occur through an acid catalyzed rearrangement of β -lactams.

Perhaps the work of greatest impact presented in this thesis involves the catalytic coupling of imine, acid chloride and carbon monoxide to construct Münchnones. This reaction, which represents the first metal catalyzed synthesis of these mesoionic heterocycles, was developed based upon a thorough mechanistic understanding of β -lactam and imidazoline-carboxylate formation. In order to favour Münchnone generation, reaction development focused on specifically designing the catalyst, controlling the reactant ratios, and removing the *in situ* generated acid from the reaction mixture. The catalyst was initially designed to readily undergo carbonylation

through the exclusion of ligands in the reaction. However, the absence of these stabilizing additives was seen to result in the formation of palladium sediments. In order to facilitate carbonylation while preventing catalyst deactivation, weakly coordinating halides (i.e. Bu₄NBr) were employed, and allowed for the generation of Münchnones in good yields. The utility of this process was demonstrated through the addition of alcohol to this intermediate to form diprotected α -amino acids.

Considering the importance of the pyrrole nucleus as a pharmaceutically relevant core, new routes for its preparation are of significant interest. Following considerable catalyst development, sterically bulky phosphine ligands such as P(*o*-Tol)₃ were found to effectively stabilize the catalytic intermediates in Münchnone generation and allowed for the development of a one-step three-component coupling methodology to construct multisubstituted pyrroles. This methodology is potentially of significant utility in the preparation of tetra- and pentasubstituted pyrroles. Not only are these heterocycles constructed in a single step from readily available precursors, the modular nature of their formation potentially enables a large assortment of products to be generated in a facile manner. Moreover, the newly developed catalytic system also enables non-enolizable alkyl imines to be employed for Münchnone formation.

In order to gain insight into the mechanism of Münchnone formation, several of the catalytic intermediates were identified through isolation, or if unstable, characterized *in situ*. X-ray diffraction data was obtained on the dimeric palladium complex, {Pd(Cl)[η^2 -CH(Tol)N(PMB)COPh]}₂, which is employed in the generation of

Münchnones. In addition, a crystal structure for the possible catalytic intermediate, $\{[P(o\text{-Tol})_3]Pd(Cl)[\eta^2\text{-CH(Tol)N(PMB)COPh}]\}$ was also obtained. This structural data was useful in understanding some of the reactivity patterns of the catalytic intermediates. Preliminary evidence also suggested that the utilization of Bu_4NBr in the reaction results in a palladium catalyst that is heterogeneous, while with phosphine ligands it is likely that a monomeric Pd(0) catalyst exists during catalysis. This understanding should be of significant utility in further improving the methodology to prepare Münchnones.

7.1 Suggestions for Future Work

These studies have demonstrated that the palladium catalyzed multicomponent coupling of imine, acid chloride and carbon monoxide is a viable approach to construct Münchnones. Future work should focus on further improving the catalytic reaction by decreasing the catalyst loadings, while lowering pressures of carbon monoxide. Obtaining these improvements could perhaps involve more extensively surveying sterically bulky phosphine ligands, such as those that have been utilized in palladium catalyzed cross-coupling reactions (Figure 7.1). In addition, mechanistic studies have suggested that reactions involving the utilization of Bu_4NBr , are proceeding through the generation of colloidal palladium. Considering that the activity of colloids is dependent upon a multiple factors, including their composition and method of preparation, examination of a range of colloidal palladium sources could perhaps allow for increased catalytic activities. Furthermore, other metal

catalysts including rhodium and nickel complexes could be significantly more active in Münchnone generation.

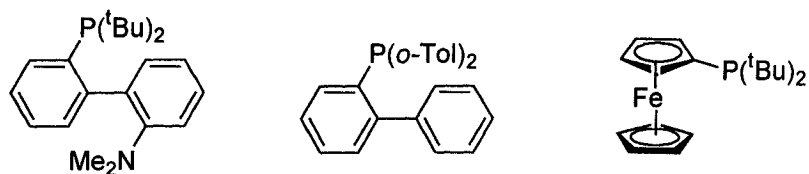


Figure 7.1 Potential Ligands for Improving the Catalytic Reaction

Considering that the pyrrole nucleus is ubiquitous in a range of different biologically active compounds, this methodology could be utilized to generate specific target molecules. For instance, reacting imine **7.1**, isobutyryl chloride **7.2**, alkyne **7.3** and carbon monoxide could generate a direct precursor to Atorvastatin Calcium (Lipitor®) **7.5** (Figure 7.2).¹

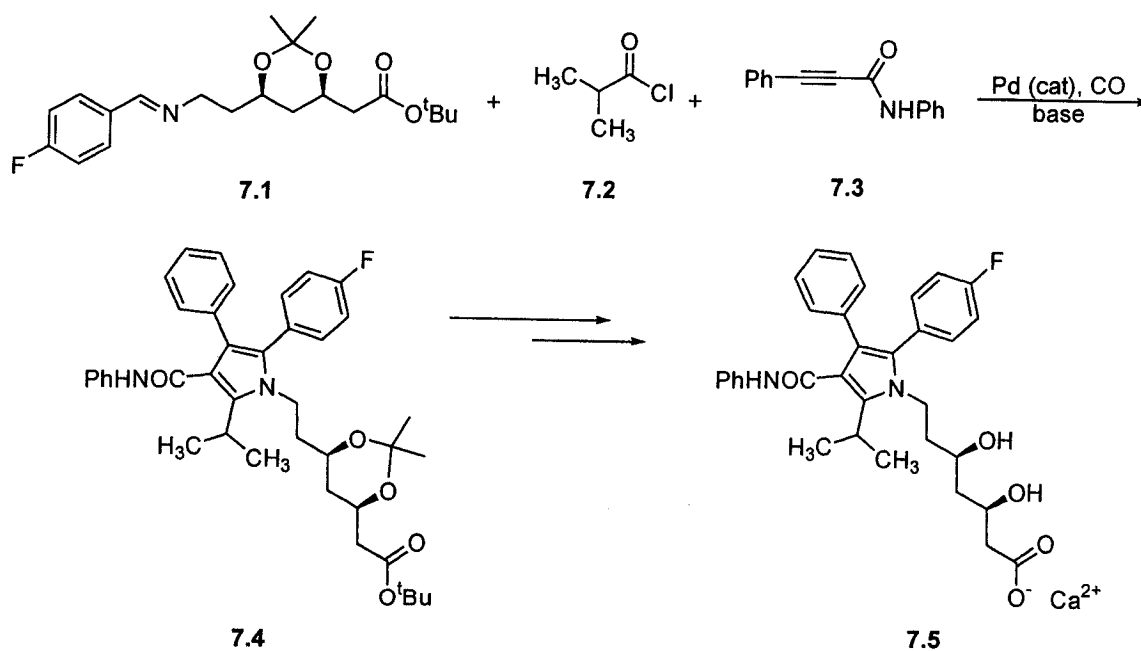


Figure 7.2 Potential Route to Lipitor

We have also demonstrated the potential that intramolecular processes have in generating significant levels of molecular complexity in a single step. Incorporating an alkyne dipolarophile on the imine or acid chloride precursors and subsequently subjecting the reaction mixture to the catalytic conditions, could potentially construct a diverse array of multicyclic products from simple precursors (Figure 7.3). In addition to alkynyl dipolarophiles, olefin-tethered precursors could readily enable the generation of a large number of new heterocyclic molecules. Considering the vast amount of literature available that utilizes Münchnone intermediates, this protocol could also be useful in developing more facile routes to a range of different compounds.

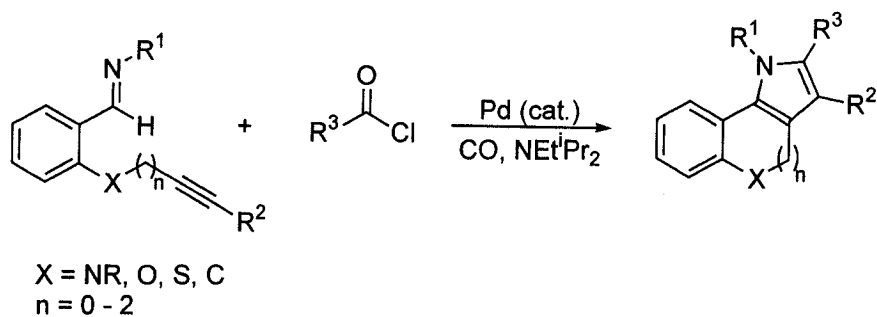


Figure 7.3 Products Potentially Available from Intramolecular Processes

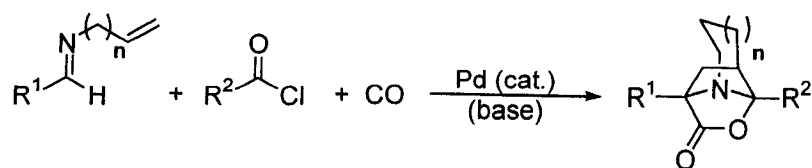


Figure 7.4 Products Potentially Available from Intramolecular Processes

7.2 References

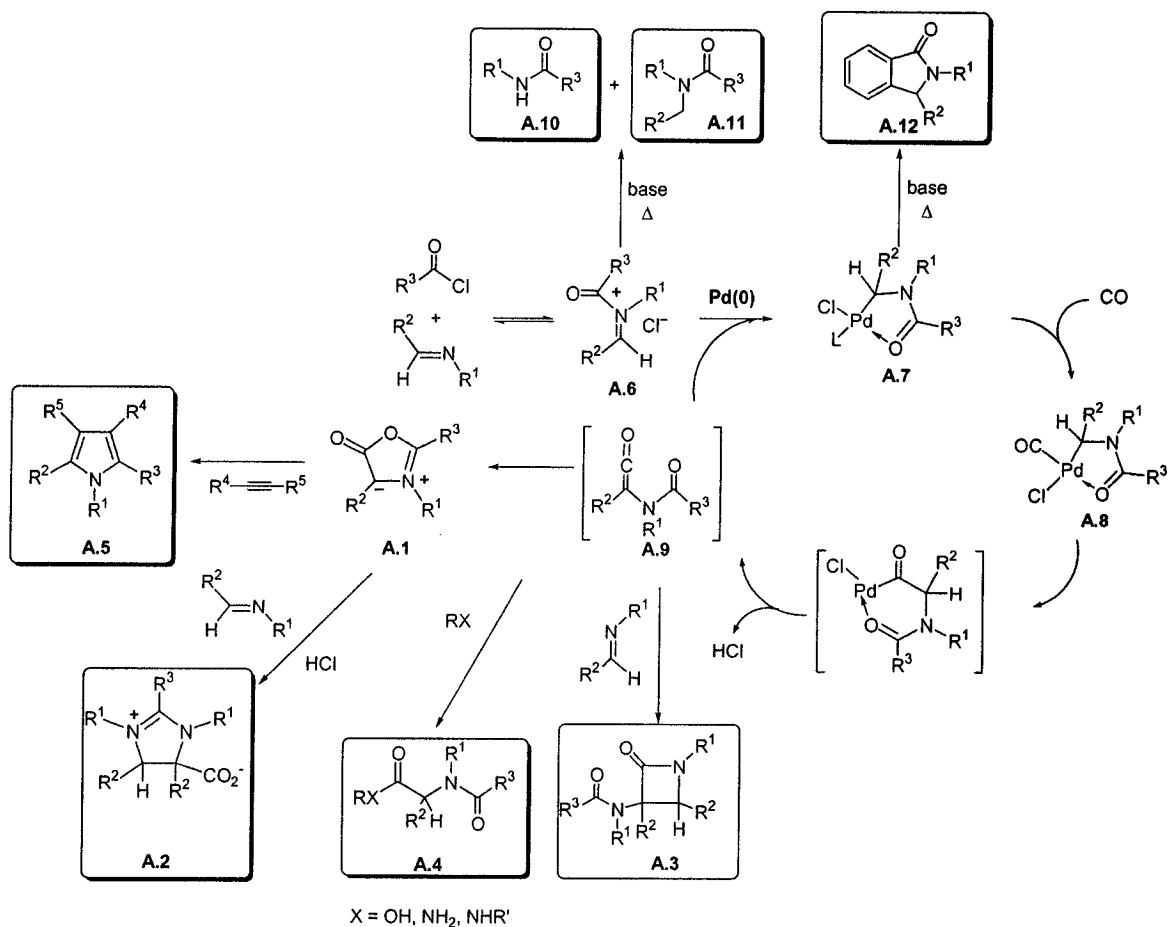
- 1 a) Roth, B.D. U.S. Patent 4,681,893 **1987** b) Graul, A.; Castaner, J. *Drugs of the Future* **1997**, 22, 956.

APPENDIX A

Further Studies on the Scope and Limitations on the Palladium Catalyzed Synthesis of Münchnones, Peptides, Pyrroles and Multicyclic Products

A.0 Introduction

We have shown throughout this thesis, that the palladium catalyzed coupling of imines, acid chlorides and carbon monoxide can generate Münchnones **A.1** (Scheme A.1).¹ By employing the diverse reactivity of these mesoionic heterocycles, this methodology can be used to catalytically form imidazoline-carboxylates **A.2**,² 3-amido substituted β -lactams **A.3**,³ diprotected α -amino acids **A.4**,¹ and pyrroles **A.5**⁴ in a highly modular manner from readily available building blocks (Scheme A.1). This account more completely discusses the scope and limitations of the catalytic Münchnone synthesis. In addition, competent imine and acid chloride precursors employable in pyrrole synthesis, and applications of this reaction for the generation of peptide derivatives and multicyclic products, is also presented herein.



Scheme A.1 Catalytic Generation of Münchnone Derived Products

A.1 Results and Discussion

In catalytic processes, both desired and undesired products can be generated, depending upon the reaction conditions employed. As such, careful control of factors including the solvent polarity, temperature, and substrate ratios is often necessary to favour pathways that yield desired compounds. This can be illustrated by examining the products that can be constructed in the palladium catalyzed coupling of imines, acid chlorides and carbon monoxide (Scheme A.1). We have observed that the

absence of base, palladium catalysis can couple two imines, acid chloride and carbon monoxide to generate imidazoline-carboxylates **A.2**.² The addition of base to this reaction mixture inhibits the formation of this product and instead forms Münchnones **A.1** or β -lactams **A.3**, depending upon the presence of free imine in the reaction mixture. However, these proton scavengers can also slowly convert *N*-acyliminium salt **A.6** to *N*-alkylamide **A.10**⁵ or *N,N*-dialkylamide **A.11**.⁶ In addition, the palladacycle intermediate **A.7** can form isoindolones **A.12**, through a C-H activation process.⁷ Any and all of these compounds can potentially be formed in the same reaction vessel depending upon the conditions employed. Hence, careful control of the reaction conditions, which favour the generation of desired products, while minimizing formation of unwanted side products, is of utmost importance.

A.2.1 *N*-Acyliminium Ions

The palladium catalyzed reactions that generate Münchnones, imidazoline-carboxylates, β -lactams, α -amino acid derivatives, and pyrroles involve the intermediate formation of *N*-acyliminium ions.¹⁻⁴ As such, a discussion concerning their utility and stability will be presented. *N*-acyliminium ions **A.6**, which are in equilibrium with a covalent form **A.6'**, are typically prepared and trapped *in situ* to generate cyclic and acyclic amine derivatives (Figure A.1).⁸ A variety of counteranions, X are also found in these molecules, including alkoxides, thiolates, triflates, halides, sulfonates, azides and acetates. Of these, the alkoxyiminium ions⁸

(X = OR) have garnered the most attention, while their chloro analogues,⁹ utilized in this thesis, have received significantly less.

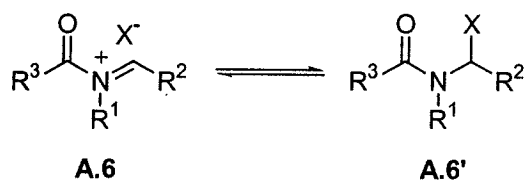


Figure A.1 Equilibrium in *N*-Acyliminium Salts

Considering the importance of these intermediates, a brief discussion concerning their reactivity under the conditions utilized for Münchnone generation will be presented. This analysis includes their stability on heating, heating in the presence of metallacycle, [Pd(Cl)[η²-CH(R²)NR¹(COR³)]₂ **A.7**, and heating in the presence of NEt^tPr₂. The *N*-acyliminium salt **A.6a** is stable when heated to 65°C for 24 hours in CD₃CN and while in the presence of metallacycle **A.7** (Scheme A.1).¹⁰ However, when exposed to NEt^tPr₂, the *N*-acyliminium salt completely decomposes at 65°C over 3 days to a range of identifiable and non-identifiable products.¹¹ This decomposition is faster at elevated temperatures (Figure A.2).

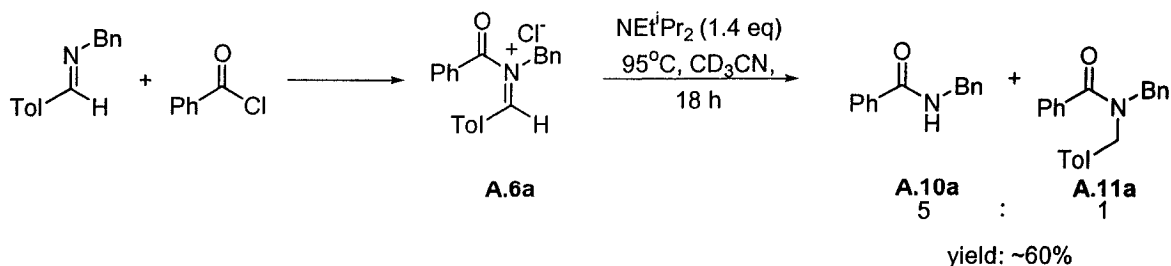


Figure A.2 Stability of *N*-Acyliminium Salts

The base can presumably serve as a hydride source that can react with the *N*-acyliminium salt **A.6a** to yield *N,N*-dialkylamide **A.11a**.⁶ The mechanism of *N*-benzylbenzamide **A.10a** formation is as of yet unknown, but could be consistent with the deprotonation of the *N*-acyliminium salt.⁵ Considering that the decomposition of *N*-acyliminium salt **A.6** occurs at temperatures and times similar to that of Münchnone formation (65°C, ~18 hours), careful control of reaction temperature and duration are necessary for optimal conversion of this intermediate to Münchnone.

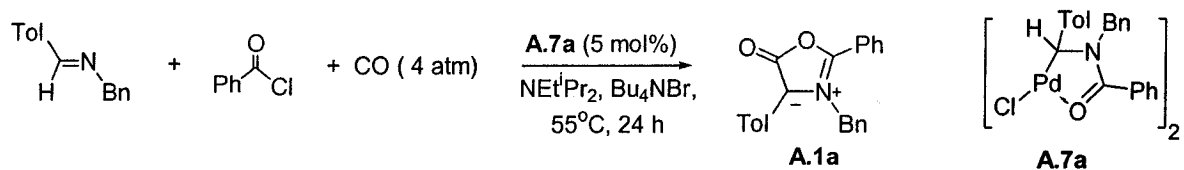


Figure A.3 Generation of Münchnones

A.2.2 Generation of Peptide Derivatives

We have previously shown that the addition of alcohols to catalytically generated Münchnone generates α -amino acid derivatives.¹ This trapping of Münchnones presumably occurs via the nucleophilic attack of the alcohol on the ketene tautomer of the Münchnone **A.9** (Scheme A.1). Considering that primary amines are also potent nucleophiles, we considered the possibility that they could react with Münchnones to provide a direct synthesis of peptides.¹² In principle, this can be done by employing an *N*-terminated amino acid residue as a trap for the catalytically formed Münchnone. The ability of Münchnones to generate dipeptides was probed by the addition of glycine methyl ester to Münchnone **A.1b**, which resulted in the

formation of dipeptide **A.13** in 70% yield (Figure A.4).^{12b} This preliminary result suggests a potentially useful palladium catalyzed four-component coupling route to construct peptides, in which one peptide residue is constructed directly from CO and imine building blocks.

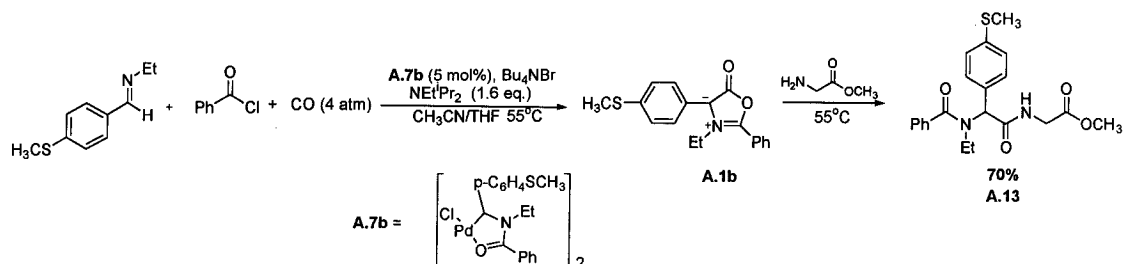
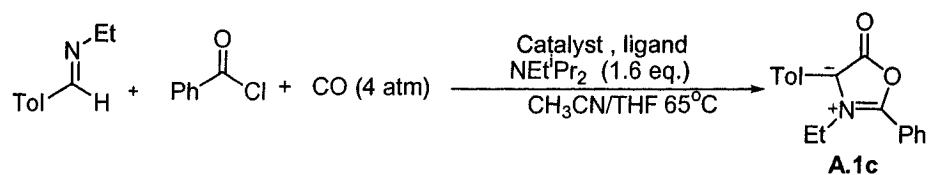


Figure A.4 Generation of Dipeptides from Münchnones

A.2.3 Catalytic Münchnone Synthesis: Catalyst Optimization

In general, the source of palladium catalyst utilized in a reaction can dramatically effect product yields.¹³ Palladium (0) sources, such as $\text{Pd}_2(\text{dba})_3 \cdot \text{CHCl}_3$, $\text{Pd}(\text{PPh}_3)_4$, Pd/C and Pd/Al are directly able to participate in oxidative addition reactions without a pre-activation step.¹⁴ However, not all $\text{Pd}(0)$ sources are equally amenable to efficiently facilitating a catalytic reaction. For instance, a palladium (0) source such as $\text{Pd}(\text{PPh}_3)_4$ would inevitably inhibit Münchnone formation, as PPh_3 strongly binds to the Pd center, thereby preventing carbonylation (Chapter 6).⁴ Alternatively, palladium (II) precursors such as $\text{Pd}(\text{OAc})_2$, Na_2PdCl_4 , and $[(\pi\text{-C}_3\text{H}_5)\text{PdCl}]_2$ require pre-activation; that is, they must be reduced *in situ* to $\text{Pd}(0)$ by an external source (e.g. phosphine, CO or an amine base) prior to undergoing oxidative addition.¹² This

activation step can pose problems as the oxidized reaction constituent could interfere with the catalytic reaction. On examining a range of palladium sources as catalysts for Münchnone formation, it was found that palladium precursors that require pre-activation, such as Na_2PdCl_4 (entry 3, Table A.1), gave lower Münchnone yields (32%). An exception to this was $[(\pi\text{-C}_3\text{H}_5)\text{PdCl}]_2$, which showed almost as high activity as the dimeric complex, $[\text{Pd}(\text{Cl})[\eta^2\text{-CH}(\text{R}^2)\text{NR}^1(\text{COR}^3)]_2$, at 81% yield (entry 8). Considering that the Pd(II) phosphine palladacycle precursor *trans*-di(μ -acetato) bis[*o*-tolyl-phosphino]benzyl]dipalladium (II), (Herrmann's catalyst) exhibits turnover numbers that approach 1,000,000 in the Heck reaction, it was also examined as a catalyst (entry 2).¹⁶ However, this complex was found to not catalyze Münchnone formation, even at temperatures above 85°C (entry 2). In attempts to simplify Münchnone generation, heterogeneous air stable palladium (0) sources such as Pd/C and Pd/Al were also examined. These palladium sources were found to be viable catalysts, though not as efficient as $\text{Pd}_2(\text{dba})_3\text{CHCl}_3$ and $[\text{Pd}(\text{Cl})[\eta^2\text{-CH}(\text{R}^2)\text{NR}^1(\text{COR}^3)]_2$. Control reactions suggest that Münchnone adsorption onto the charcoal surface could account for the lower yields seen on utilizing Pd/C as a catalyst.¹⁵

Table A.1. Palladium Catalyst Optimization

Entry	Catalyst	% Yield of A.1c ^a
1 ^d	$\text{Pd}_2(\text{dba})_3 \cdot \text{CHCl}_3$	59
2 ^{b,d}		0 ^c
3 ^d	Na_2PdCl_4	32
4 ^d	$\{\text{Pd}(\text{Cl})[\eta^2\text{-CH}(\text{Tol})\text{NEtCOPh}]\}_2$	>90
5	Pd/C	53
6 ^e	Pd/Al	44
7 ^f	Pd/Al	65
8 ^d	$[(\pi\text{-C}_3\text{H}_5)\text{PdCl}]_2$	81

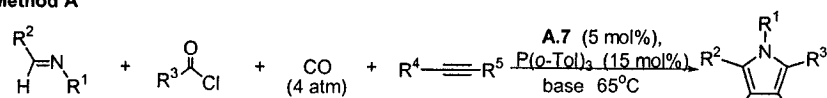
Catalyst: 5 mol% unless otherwise state ^aNMR Yield. ^b See Ref. 16 for preparation. ^c Reaction temperatures of up to 85°C. ^d Ligand: 15 mol% P(o-tol)₃, ^e Ligand: 0 mol% Bu₄NBr. ^f Ligand: 100 mol% Bu₄NBr, 5% Pd/Al.

A.3 Generation of Pyrroles

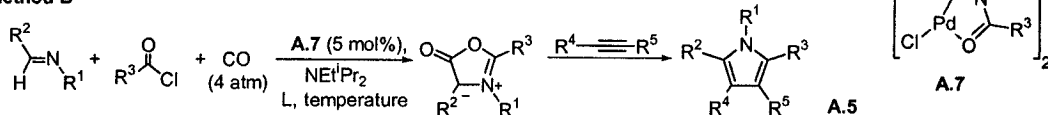
In Chapter 5 we described that the palladium catalyzed coupling of imines, acid chlorides and alkynes can be employed to construct pyrroles.⁴ In addition to those products described previously, this approach can also generate a range of other tetra- and penta substituted pyrroles (Table A.2). These products can be prepared either via the simultaneous reaction of imine, acid chloride, carbon monoxide and alkyne (Method A) or, in the case of reactive alkynes, via the initial formation of Münchnone, followed by addition of alkyne to the reaction mixture (Method B). A summary of the various pyrroles generated, and not described in Chapter 5, is shown in Table A.2.

Table A.2 Palladium Catalyzed Generation of Pyrroles

Method A



Method B



cpd	Method	Imine	acid chloride	Alkyne	A.5 (% yield)
a ^a	B		PhCOCl		 A.5a, 53%
b ^b	B		PhCOCl		 A.5b, 63%
c ^b	B		PhCOCl		 A.5c, 80%
d ^a	B		TolCOCl		 A.5d, 77%
e ^c	B		TolCOCl		 A.5e, 74%
f ^c	B		TolCOCl		 A.5f, 65%
g ^{e,g}	A		PhCOCl		 A.5g, 66% ^o
h ^f	A				 A.5h, 53%
i ^{e,g}	A		PhCOCl		 A.5i, 50%
j ^d	A		TolCOCl		 A.5j, 92%
k ^d	A		TolCOCl		 A.5k, 67%

Experimental Details: In all reactions, imine (0.272 mmol) and acid chloride (0.381 mmol) were dissolved in 4.5 mL of acetonitrile. This solution was added to Pd(Cl)[η^2 -CH(R¹)NR²(COR⁵)]₂ (5 mol%) and ligand in 4.5 mL of acetonitrile. The reaction mixture was transferred to a 50 mL reaction bomb and EtNⁱPr₂ (0.44 mmol) (n 4.5 mL of THF) were added. The solution was evacuated, carbon monoxide (4 atm) added, and the solution stirred at 55°C (for Bu₄NBr) or 65°C (P(*o*-Tol)₃) for 18 hours. a) (Method B) L = Bu₄NBr (1 eq.); alkyne (1.3 eq.) added and solution heated at 55°C for 18 h. b) (Method B) L = Bu₄NBr (1 eq.); alkyne (1.1 eq.) added and reaction stirred at RT for 15 minutes. c) (Method B) L = P(*o*-Tol)₃ (15 mol%); alkyne (1.1 eq.) added and reaction stirred at RT for 15 minutes. d) (Method A) base = NEtⁱPr. e) (Method A) base = NEtⁱPr₂; LiOTf (1 eq.) also added and reaction heated at 75°C. f) (Method A) base = collidine. g) A.7 = Pd(Cl)[η^2 -CH(Tol)NEt(COPh)]₂

A.3.1 Alkyne Reaction Scope in Pyrrole Synthesis

A range of substituted alkynes can be employed in pyrrole syntheses. As shown in entries b,c and e-j (Table A.1), pyrrole formation proceeds in highest yields with electron poor substituents on the alkyne (i.e. DMAD and methylpropiolate).¹⁷ However, these alkynes also react with *N*-acyliminium salts to generate a range of different products, and therefore can only be employed in Method B (addition to a preformed Münchnone).¹⁸ Alternatively, moderately electron poor alkynes, such as ethynyl pyridine (entry d), 3-phenylpropynoic acid, methyl-phenyl-amide (entry a), methyl phenylpropiolate (entry j) and 2-methyl-5-phenyl-3-propanone (entry k) react slowly with *N*-acyliminium salts, and can be utilized in pyrrole synthesis via either method. Electron rich alkynes, including 1-hexyne and 3-hexyne require forcing conditions and generate pyrroles in low yields (by NMR < 20%).¹⁹

A.3.2 Imine Reaction Scope in Pyrrole Synthesis

As shown in entry i (Table A.2), in addition to the previously reported use of aromatic and *tert*-butyl alkyl imines, functionalized, non-enolizable substrates such as (AcOCH₂C(CH₃)₂C(H)=NBn) **A.14** are also found to be competent reaction precursors. Although more functionality is incorporated in the case of imine (AcOCH₂C(CH₃)₂C(H)=NBn) **A.14**, there are no heteroatoms directly attached to the imine α -carbon. To address this issue, **A.15**²⁰ was reacted with acid chloride under the catalytic conditions; however, this did not result in Münchnone formation.

Instead, the reaction was arrested at the iminium salt stage (confirmed through the addition of water to the reaction mixture after catalysis, which yields the parent aldehyde) (Figure A.5). Examination of different additives including LiOTf, LiCl, and LiI, also did not result in Münchnone formation. Furthermore, the utilization of less coordinating counteranions, including OTf⁻ and I⁻, also failed to generate the desired product. This lack of reactivity could be ascribed to the steric bulk of this *N*-acyliminium salt **A.6d**, which possibly prevents its oxidative addition to Pd(0). In addition, the electron poor nature of the α -imine carbon could also decrease the stability of the CO insertion product (**A.8** \rightarrow **A.9**), and thereby inhibit Münchnone formation.²¹

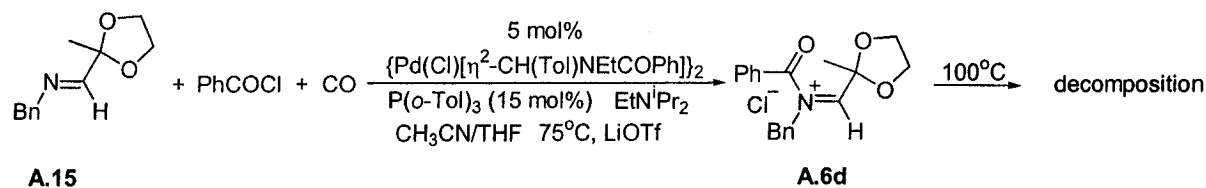


Figure A.5 Increasing Alkyl Imine Diversity

Enolizable alkyl imines were also examined as potential reagents. However, subjecting benzyl-isobutyridene-amine **A.16** to the standard Münchnone reaction conditions did not result in product formation (Figure A.6). Instead, enamide **A.17** (characterized by ¹H-NMR and ¹³C-NMR spectroscopy) was formed immediately on addition of the acid chloride to the imine. Control experiments demonstrate that this *N*-acyliminium salt intermediate is stable only at temperatures below -45°C, well below that required for Münchnone formation.²²

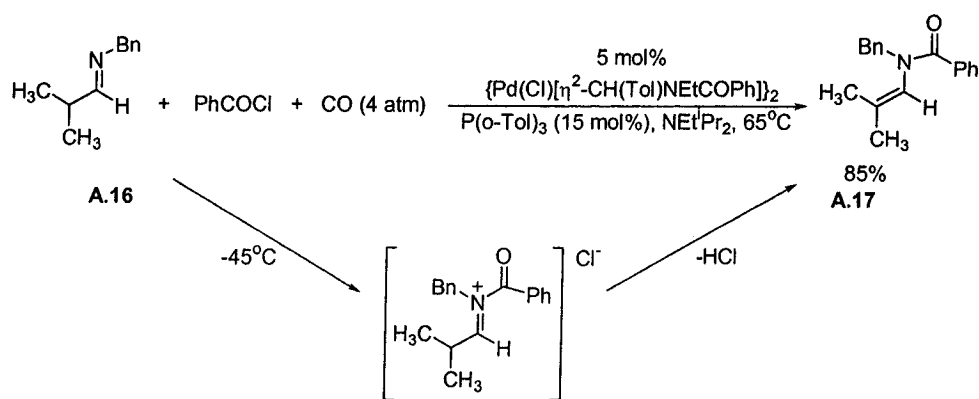


Figure A.6 Utilization of Enolizable Alkyl Imines

Considering that the ring strain in cyclopropane carboxaldehyde imine **A.18** could potentially deter enolization and subsequent enamide formation, this substrate was also reacted with PhCOCl (1.4 eq.), CO (4 atm.), NEtⁱPr₂ (1.6 eq.), {Pd(Cl)[η²-CH(Tol)NEtCOPh]}₂ (5 mol%), and P(*o*-Tol)₃ (15 mol%) at 65°C (Figure A.7). However, once again the 1,3-oxazolium-5-oxide did not form. Instead, these conditions, as well as lower reaction temperatures, resulted in the generation of a ring-opened cyclopropyl ring product **A.19** in 88% yield. This product was characterized by ¹H and ¹³C-NMR spectroscopy, and the bond connectivity was determined by COSY; however, no attempts were made to determine the stereochemistry about the olefin.

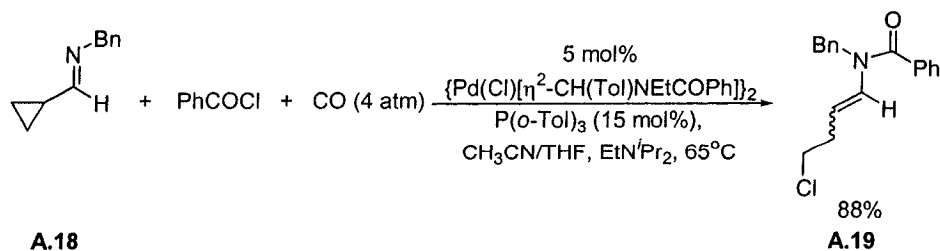


Figure A.7 Utilization of a Cyclopropyl Imine

A.3.3 Acid Chloride Scope in Pyrrole Synthesis

As shown in Table A.1, both aryl and bulky alkyl substituted acid chlorides can be used in pyrrole synthesis. However, when the steric bulk of acid chlorides with α -protons is reduced (e.g. acetyl chloride), no pyrrole or even Münchnone formation is seen. Instead, control experiments show that the *N*-acyliminium salt formed with acetyl chloride undergoes immediate dehydrohalogenation in the presence of NEt^iPr_2 base.²³ This illustrates yet another factor important to Münchnone formation, which is the nature of the base employed to sequester the HCl formed during Münchnone synthesis. Without sequestration, this acid converts the *N*-acyliminium salt to imine and free acid chloride. Subsequently, this imine-HCl complex can undergo 1,3-dipolar cycloaddition with Münchnone to form imidazoline-carboxylate (Scheme A.1).²⁴

Considering the sensitivity of this reaction, the number of bases employable in the Münchnone synthesis is limited. First, the reaction requires completely dry bases, as adventitious moisture can dramatically decrease product yield and even completely arrest the reaction progress. In addition, the bases cannot be strongly nucleophilic, as they can add to the *N*-acyliminium ion. Finally, as mentioned previously, alkyl acid chlorides with acidic α -hydrogens undergo direct deprotonation of the acid chloride with amine bases.²⁵

Acetyl chloride has previously been utilized to generate imidazoline-carboxylates,² suggesting that Münchnones can be prepared with this acid halide, provided that a sufficiently unreactive base is employed (in this case, the imine itself). As such, an examination of potential bases that can be used in Münchnone synthesis was undertaken. This was first probed with the established reaction of TolC(H)=NBn (1 eq.), PhCOCl (1.4 eq.), and CO (4 atm) in the presence of {Pd(Cl)[η^2 -CH(Tol)NBnCOPh]}₂ **A.7b** (5 mol%), Bu₄NBr (1 eq.) and base. As shown in Table A.3, the use of K₃PO₄ forms small amounts of Münchnone (<5%) and instead generates palladium sediments. However, when this same reaction is conducted without halide sources and in the presence of P(*o*-Tol)₃ (15 mol %), Münchnone **A.1b** was generated in 45% yield (entry 2, Table A.3). Considering these findings, acetyl chloride was assessed to determine its propensity for Münchnone formation in the presence of K₃PO₄ (Figure A.8).²⁶ However, this only generated decomposition products: benzyl acetamide²⁷ (26% yield) and free imine (20% yield).²⁸ The presence of free imine signified consumption of acetyl chloride from the reaction mixture. However, even with 5 equivalents of acetyl chloride, benzyl acetamide and free imine products were still observed (Figure A.8). Cs₂CO₃ was also examined in both DMF and dioxanes; however, Münchnone formation was not obtained.

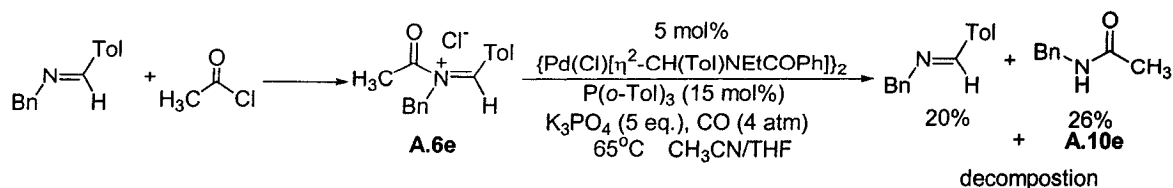
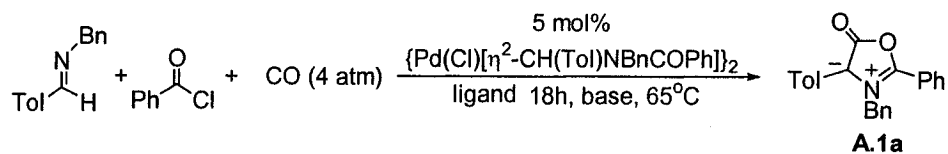
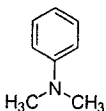
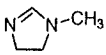
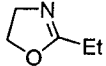
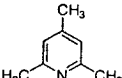


Figure A.8 Utilization of Acetyl Chloride

Table A.3 Base Influence on Münchnone Formation^a

entry	Base	Yield ^b
1	K ₃ PO ₄	<5% ^c
2	K ₃ PO ₄	45% ^d
3	Cs ₂ CO ₃	20% ^{d, e}
4		0% ^d
5		18% ^d
6		18% ^d
7		78% ^d

^aCO (4 atm.); ^bNMR yield; ^cligand: 1 equiv., Bu₄NBr; ^dligand: 15 mol% P(*o*-Tol); ^edioxanes

In the case of soluble organic bases, weak amine bases including *N,N*-dimethylaniline (entry 4), *N*-methylimidazole (entry 5) and 2-ethylisoxazole (entry 6) were studied, but provided low Münchnone yields (Table A.3). However, on changing the base to 2,4,6-trimethylpyridine (collidine), the desired product was obtained in 78% yield (entry 7). Considering the lower basicity of collidine, as well as its efficiency in Münchnone formation, this base was also examined with acetyl chloride under various conditions. Heating **A.6e** at 65°C for 2 hours in the presence of collidine resulted in its decomposition by 33%; however, it was stable at 45°C over this same period of time (Figure A.9). However, as shown in Table A.4, none of the conditions examined resulted in Münchnone formation exceeding 5%.

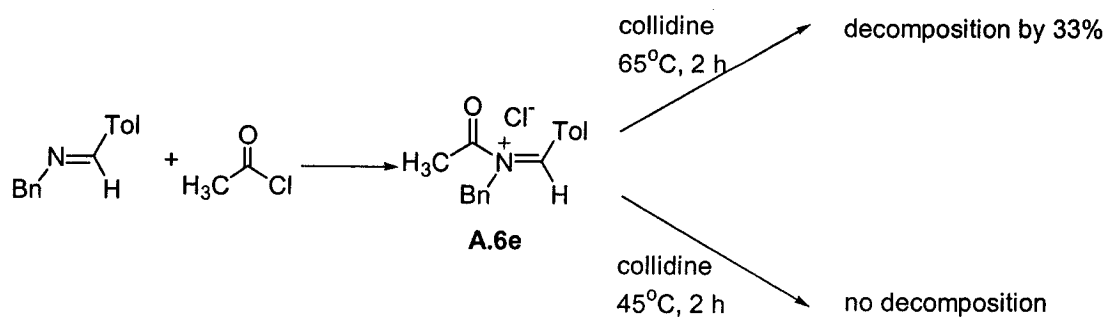
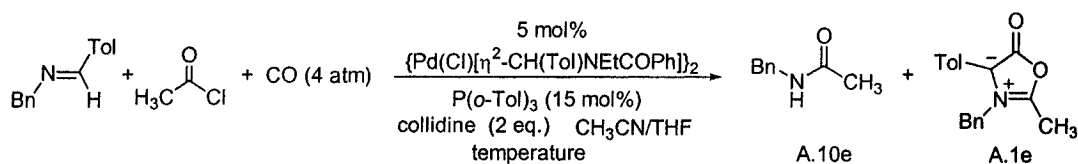


Figure A.9 Stability of *N*-Acyliminium Salt **A.6e**

Table A.4 Synthesis of Münchnones Utilizing Acetyl Chloride



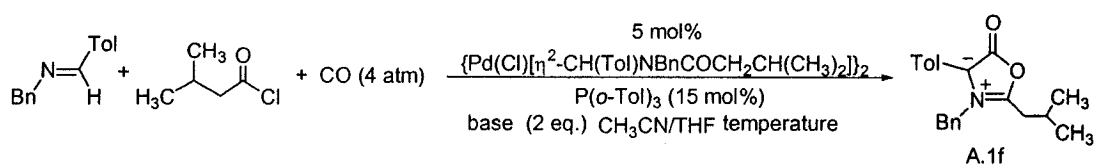
entry	temp. (°C)	CH ₃ COCl (eq.)	Yield ^a	
			A.10e	A.1e
1	45	1	50%	<5% ^b
2	45	5	8%	-
3	55	2	-	-
4	55	1	-	<5%
5	55	5	-	<5%

^aNMR yield (The Münchnone was characterized *in situ* both chemically and spectroscopically from an analogous species). ^bPalladium sediments formed. The balance consists of unidentifiable baseline products.

Isovaleryl chloride ($[(\text{CH}_3)_2\text{CHCH}_2\text{COCl}]$), which is more bulky at the α -carbon than acetyl chloride, was also studied as a potential reagent for Münchnone formation. On reacting ToIc(H)=NBn , $(\text{CH}_3)_2\text{CHCH}_2\text{COCl}$ (1.4 eq.), $\{\text{Pd(Cl)}[\eta^2\text{-CH(Tol)NBnCO}(\text{CH}_2\text{CH}(\text{CH}_3)_2)]_2$ (5 mol%), $\text{P}(o\text{-Tol})_3$ (15 mol%) and NEt^iPr_2 (1.6 eq.) at 65°C, Münchnone was formed in 14% yield (entry 1, Table A.5).

Changing the base from NEt^iPr_2 to collidine (2 eq.) and conducting the reaction at 65°C generated **A.1f** in a slightly higher yield of 22% (entry 2, Table A.5). However, decreasing the temperature to 45°C , while utilizing collidine, generated the Münchnone **A.1f** in 70% yield (entry 5, Table A.5). Subsequent addition of DMAD to this solution produced pyrrole in a 53% yield (isolated) (entry h, Table A.2).

Table A.5 Synthesis of Münchnones Utilizing Isovaleryl Chloride



Entry	Temp. ($^\circ\text{C}$)	Base	Acid Chloride (eq.)	Yield ^{a,b} A.1f
1	65	NEt^iPr_2	1.4	14%
2	65		1.4	22%
3	65		3	20%
4	45	NEt^iPr_2	1.4	~10%
5	45		1.4	70%

^a NMR Yield (The Münchnone was characterized *in situ* both chemically and spectroscopically from an analogous species). ^b Palladium sediments formed.

A.4 The Synthesis of Multicyclic Products via Münchnone Chemistry

Multicomponent coupling reactions are frequently utilized to assemble complex products from simple precursors. When these processes are conducted intramolecularly, they can generate multicyclic products.²⁹ We have described one such reaction in Chapter 5 and as shown below, this intramolecular cyclization appears to be somewhat general. For example, the reaction of the alkene tethered imine **A.20** with PhCOCl (1.4 eq.), in the presence of NEtⁱPr₂ (1.6 eq.) and Pd₂(dba)₃·CHCl₃ (5 mol%), and CO (1 atm) at 55°C for 18 hours leads to the formation of the tricyclic amino acid derivative **A.21** in 70% yield (Figure A.9). The structure was determined utilizing HMQC, HMBC, and COSY; however, unequivocal determination was obtained by X-ray crystallography.³⁰ This compound arises from an intramolecular 1,3-dipolar cycloaddition of the alkene on the intermediate Münchnone **A.22**. Although unactivated olefins are typically not potent 1,3-dipolar cycloaddition substrates, the intramolecular nature of this process presumably makes this an entropically favourable process.³³

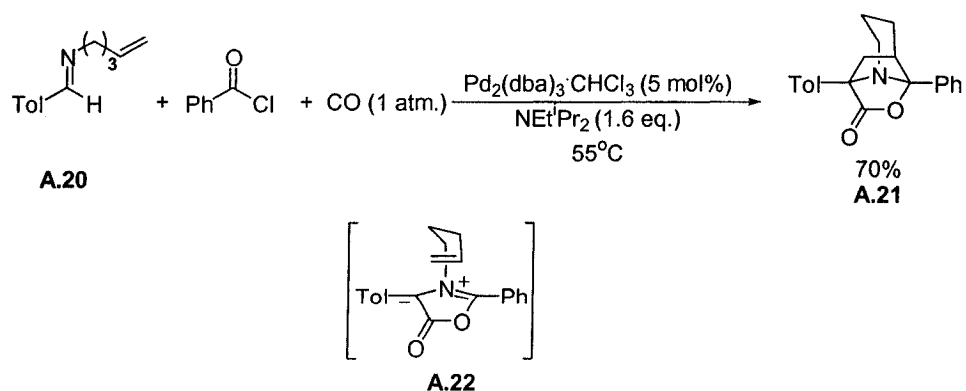


Figure A.10 Intramolecular Cyclization in the Generation of Multicyclic Products

We have previously shown that alkynyl functionality on the imine allows for the generation of multicyclic pyrroles.⁴ Depending upon the length of the methylene linker in the imine, different types of pyrroles can be generated. In order to construct other classes of products, aldehyde **A.23** was prepared by initial Mitsunobu coupling between salicylaldehyde and 3-pentyn-1-ol.³² Subsequent addition of ethylamine generated imine **A.24**.

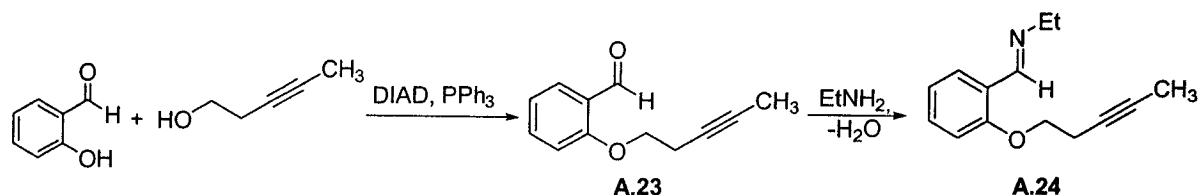


Figure A.11 Synthesis of the Alkyne Tethered Imine

The reaction of this imine with benzoyl chloride and CO, in the presence of $\text{Pd}_2(\text{dba})_3\cdot\text{CHCl}_3$ (2.5 mol%) and $\text{P}(o\text{-Tol})_3$ (10 mol%) generated the multicyclic pyrrole **A.25** in 50% yield (Figure A.12). This 7-membered ring-containing product is generated in a lower yield than the analogous 6-membered ring system.

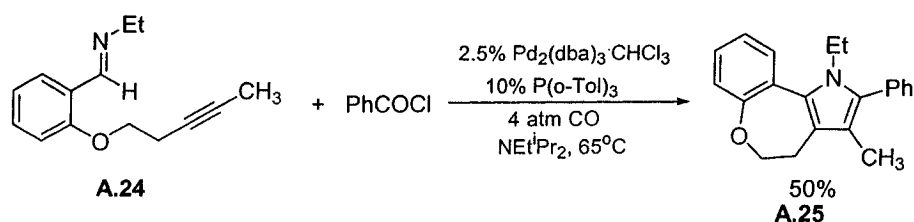


Figure A.12 Generation of Multicyclic Pyrroles

A.5 Experimental

Unless otherwise noted, all manipulations were performed under an inert atmosphere in a Vacuum Atmospheres 553-2 dry box or by using standard Schlenk or vacuum line techniques. The catalysts, $[\text{Pd}(\text{Cl})[\eta^2\text{-CH}(\text{R}^1)\text{NR}^2(\text{COR}^5)]_2$, were prepared according to previous literature procedures.^{1, 2} Carbon monoxide (99.99%) was purchased from Matheson and used as received. All other reagents were purchased from Aldrich[®] and used as received. Tetrahydrofuran (THF) was distilled from sodium/benzophenone ketyl under nitrogen. Acetonitrile was distilled from CaH_2 under nitrogen. Deuterated solvents were dried as their protonated analogues, but were transferred under vacuum from the drying agent, and stored over 3Å molecular sieves.

^1H and ^{13}C were recorded on JEOL 270, Varian Mercury 300 MHz, Mercury 400 MHz, and Unity 500 MHz spectrometers. Mass spectra were obtained from the McGill University Mass Spectral Facility.

Stability of N- α -chloro-alkylamides

In order to determine the stability of the N- α -chloro-alkylamides, $(\text{ToI})\text{HC}=\text{N}(\text{CH}_2\text{Ph})$ (50 mg, 0.24 mmol) and benzoyl chloride (33 mg, 0.24 mmol) were dissolved in 5 mL of CH_3CN and heated at 95°C in the presence of NEt^iPr_2 (48 mg, 0.37 mmol). Following solvent removal *in vacuo*, the products were purified using column chromatography, utilizing hexanes/ethyl acetate as eluent

N-benzyl-benzamide (A.10a)

Yield: 77%. ¹H-NMR (400 MHz, CDCl₃): δ 7.87-7.85(m, 2H); 7.80-7.78 (s (br.), 1H); 7.60-7.44 (m, 3H); 7.41-7.24 (m, 5H); 4.57 (d, 2H, 6.26 Hz). ¹³C-NMR (101 MHz, CDCl₃): δ 174.2, 142.6, 137.7, 134.0, 129.3, 129.2, 129.1, 129.0, 128.9, 128.8, 128.7, 127.7, 50.8, 21.8.

N-Benzyl-N-(4-methyl-benzyl)-benzamide (A.11a)

Yield: 15%. ¹H-NMR (400 MHz, CDCl₃): δ 7.49-7.00 (m, 14H); 4.67 (d, 2H, 12.45 Hz); 4.37 (d, 2H, 10.62Hz); 2.36 (s, 3H). ¹³C-NMR (101 MHz, CDCl₃): δ 172.5, 136.5, 129.8, 129.8, 129.6, 129.1, 128.9, 128.8, 127.9, 127.7, 127.3, 127.0, 51.5, 46.8, 21.4.

[2-(Benzoyl-ethyl-amino)-2-(4-methylsulfonyl-phenyl)-acetylamino]-acetic acid methyl ester (A.13).

(p-SCH₃C₆H₄)HC=N(Et) (100.0 mg, 0.48 mmol) and benzoyl chloride (94.0 mg, 0.68 mmol) were dissolved in 5 mL of acetonitrile and stirred for 15 min. The previous solution was then added to a solution of [Pd(Cl)[η²-CH(p-SCH₃C₆H₄)NEt(COPh)]₂ (21.8 mg, 0.024 mmol) in 5 mL of dry acetonitrile. The reaction mixture was transferred to a 50 mL reaction bomb and Bu₄N⁺Br⁻ (154 mg, 0.48mmol) and EtNⁱPr₂ (96.0mg, 0.74mmol) were added in 10 mL

tetrahydrofuran. The solution was degassed and carbon monoxide (60 psi) was added to the reaction mixture, which was left to stir at 55°C for 18 hours. After heating, this solution was again degassed, and brought into a glovebox, where glycine methyl ester (21.8 mg, 0.024 mmol) was added. This solution was allowed to stir for a further 18 hours at 55°C. Following removal of solvent *in vacuo*, the residue was purified on silica gel chromatography, utilizing hexanes/ethyl acetate as eluent.

Yield: 66%. ¹H NMR (400 MHz, CDCl₃, 50°C): δ 7.56-7.30 (m, 7H), 7.27-7.21 (m, 2H), 6.86-6.66 (s (br.), 1H), 5.86-5.70 (s (br.), 1H), 4.02 (d, 2H, 5.50 Hz), 3.72 (3H, s), 3.50-3.25 (q. (br.), 2H), 2.46 (s, 3H); 0.83 (t, 3H, 6.88 Hz), ¹³C NMR (100 MHz, CDCl₃, 50 °C): δ 172.6, 170.0, 166.7, 139.5, 136.7, 131.8, 129.9, 129.7, 128.6, 126.8, 126.6, 63.7 (br.), 52.4, 43.0 (br.), 41.7, 16.0, 14.9. HRMS. Calculated for C₂₁H₂₄N₂O₄S: 400.14633; found: 400.14682.

Procedure for Pyrrole Generation: Bu₄NBr

(p-CH₃C₆H₄)HC=N(CH₂Ph) (100.0 mg, 0.48 mmol) and benzoyl chloride (94.0 mg, 0.68 mmol) were dissolved in 5 mL of acetonitrile and stirred for 15 min. The previous solution was then added to a solution of [Pd(Cl)[η²-CH(4-CH₃C₆H₄)NCH₂Ph(COPh)]₂ (21.8 mg, 0.024 mmol) in 5 mL of dry acetonitrile. The reaction mixture was transferred to a 50 mL reaction bomb and Bu₄N⁺Br⁻ (154 mg, 0.48 mmol) and EtN⁺iPr₂ (96.0 mg, 0.74 mmol) were added in 10 mL of tetrahydrofuran. The solution was degassed and carbon monoxide (60 psi) was added

to the reaction mixture, which was left to stir at 55°C for 30 hours. To this solution was added the alkyne (2 eq.) and the solution stirred. Electron poor alkynes, such as DMAD and ethyl propiolate reacted within 10 minutes at room temperature. Electron rich alkynes, such as Ph-C≡C-C(O)NHPH, required heating at 55°C for 18 hours.

II. General Procedure for Pyrrole formation³

Imine (0.272 mmol) and acid chloride (0.381 mmol) were dissolved in 4.5 mL of acetonitrile. This solution was added to [Pd(Cl)[η²-CH(R¹)NR²(COR⁵)]₂ (5 mol%) and P(o-tolyl)₃ (15 mol%) in 4.5 mL of acetonitrile. The reaction mixture was transferred to a 50 mL reaction bomb, and alkyne (0.54 mmol) (in 4.5 mL of THF) and EtNⁱPr₂ (0.44 mmol) (in 4.5 mL of THF) were added. The solution was evacuated, carbon monoxide (60 psi) added, and the solution stirred at 65°C for 18 hours. In the case of dimethoxyacetylenedicarboxylate (DMAD) and acetylene, the alkyne was added to the pre-formed Münchnone solution after catalysis. Products were purified by silica gel chromatography using hexanes/ethyl acetate as eluent.

1-Ethyl-4-phenyl-2,5-di-p-tolyl-1H-pyrrole-3-carboxylic acid methyl-phenylamide (A.5a)

Yield: 63%. ¹H NMR (400 MHz, CDCl₃): δ 7.32 (d, 2H, 7.92 Hz), 7.24 (d, 2H, 7.92 Hz) 7.18-7.02 (m, 9H), 7.00-6.92 (m, 3H), 6.42-6.24 (m, 2H), 3.90-3.65 (q. (br.) 2H), 3.10 (s, 3H), 2.43 (s, 3H), 2.33 (s, 3H), 0.74 (t, 3H, 6.89 Hz). ¹³C NMR (100 MHz,

CDCl₃): δ 168.6, 144.2, 137.4, 137.3, 135.7, 132.5, 131.6, 131.3, 130.3, 130.0, 129.9, 129.5, 129.2, 129.1, 128.0, 127.7, 126.0, 125.5, 122.2, 119.7, 40.1, 37.4, 21.6, 21.5, 16.3. HRMS. Calculated for C₃₄H₃₂N₂O: 484.25146; found: 484.25092

2-(4-Bromo-phenyl)-1-ethyl-5-phenyl-1H-pyrrole-3,4-dicarboxylic acid dimethyl ester (A.5b)

Yield: 80%. ¹H NMR (400 MHz, CDCl₃): δ 7.56 (d, 2H, 8.21 Hz), 7.45-7.38 (m, 5H), 7.29 (2H, d, 8.21 Hz), 3.71 (q, 2H, 7.04 Hz), 3.65 (s, 3H), 3.63 (s, 3H), 0.82 (t, 3H, 7.04 Hz). ¹³C NMR (100 MHz, CDCl₃): δ 165.5, 165.2, 136.6, 135.2, 132.4, 131.8, 130.9, 130.6, 130.1, 129.1, 128.9, 128.6, 123.5, 115.0, 114.7, 52.0, 52.0, 40.3, 16.5. HRMS. Calculated for C₂₂H₂₀⁷⁹BrNO₄: 441.05757; found: 441.05714

1-Ethyl-2-(4-methylsulfonyl-phenyl)-5-phenyl-1H-pyrrole-3,4-dicarboxylic acid dimethyl ester (A.5c)

Yield: 63%. ¹H NMR (400 MHz, CDCl₃): δ 7.45-7.37 (m, 5H), 7.33 (d, 2H, 8.44 Hz), 7.29 (d, 2H, 8.44 Hz), 3.72 (q, 2H, 7.10 Hz), 3.67 (s, 3H), 3.64 (s, 3H), 2.52 (s, 3H), 0.83 (t, 3H, 7.10 Hz). ¹³C NMR (100 MHz, CDCl₃): δ 165.5; 165.5; 139.9; 136.5; 136.0; 131.0; 131.0; 130.6; 129.0; 128.5; 127.3; 125.8; 125.8; 114.7; 114.6; 52.0; 52.0; 40.3; 16.5; 15.6. HRMS. Calculated for C₂₃H₂₃NO₄S: Exact Mass: 409.13478; found: 409.13560

2-(1-Benzyl-2,5-di-p-tolyl-1H-pyrrol-3-yl)-pyridine (A.5d)

Yield: 63%. ¹H NMR (400 MHz, CDCl₃): δ 8.57-8.54 (m, 1H), 7.47-7.23 (m, 11H), 6.93-6.88 (m, 1H), 6.82-6.79 (m, 1H), 3.94 (q, 2H, 7.33 Hz), 2.43 (s, 3H), 2.41 (s, 3H), 0.86 (t, 3H, 7.33 Hz). ¹³C NMR (100 MHz, CDCl₃): δ 155.3, 149.4, 138.0, 137.1, 135.6, 135.1, 133.4, 131.2, 131.1, 130.6, 129.8, 129.4, 129.3, 123.2, 121.9, 120.0, 109.7, 40.1, 21.8, 21.7, 16.7. HRMS. Calculated for C₂₅H₂₄N₂: 352.19395; found: 352.19300

1-Ethyl-2,5-di-p-tolyl-1H-pyrrole-3-carboxylic acid methyl ester (A.5e)

Yield: 63%. ¹H NMR (400 MHz, CDCl₃): δ 7.42-7.20 (m, 8H), 6.66 (s, 1H), 3.89 (q, 2H, 7.04 Hz), 3.69 (s, 3H), 2.45 (s, 3H), 2.43 (s, 3H), 0.91 (t, 3H, 7.04 Hz). ¹³C NMR (100 MHz, CDCl₃): δ 165.3, 139.6, 138.3, 137.7, 134.3, 130.7, 130.3, 129.8, 129.5, 129.5, 129.1, 113.2, 110.5, 51.2, 40.1, 21.9, 21.7, 16.7. HRMS. Calculated for C₂₂H₂₃NO₂: 333.17288; found: 333.17364

1-(4-Methoxy-phenyl)-2,5-di-p-tolyl-1H-pyrrole-3,4-dicarboxylic acid dimethyl ester (A.5f)

Yield: 63%. ¹H NMR (300 MHz, CDCl₃): δ 7.24-7.14 (m, 5H), 7.07 (d, 2H, 7.62 Hz), 7.01 (d, 2H, 7.92 Hz), 6.76 (d, 2H, 8.50 Hz), 6.58 (d, 2H, 8.50 Hz), 3.74 (s, 3H), 3.72 (s, 3H), 3.67 (s, 3H), 2.29 (s, 3H). ¹³C NMR (75.5 MHz, CDCl₃): δ 165.9, 165.8,

158.8, 138.0, 137.2, 131.0, 130.8, 130.7, 130.0, 128.6, 128.2, 127.8, 127.6, 114.8, 114.7, 113.9, 55.6, 52.2, 52.1, 21.7. HRMS. Calculated for $C_{26}H_{23}N_4O_4$: 455.17193; found: 455.17242.

1-Benzyl-2-tert-butyl-5-phenyl-1H-pyrrole-3,4-dicarboxylic acid dimethyl ester

(A.5g)

Yield: 63%. 1H NMR (400 MHz, $CDCl_3$): δ 7.26-7.12 (m, 6H), 7.00 (d, 2H, 7.92 Hz), 6.61 (d, 2H, 7.92 Hz), 5.19 (s, 2H), 3.91 (s, 3H), 3.51 (s, 3H), 1.39 (s, 9H). ^{13}C NMR (100 MHz, $CDCl_3$): δ 170.1, 164.1, 140.3, 138.4, 137.9, 131.7, 130.6, 128.5, 128.5, 127.8, 127.2, 125.7, 115.8, 112.0, 52.8, 51.4, 50.3, 34.2, 31.2. HRMS. Calculated for $C_{25}H_{27}NO_4$: 405.19535; found: 405.19521.

1-Benzyl-2-isobutyl-5-p-tolyl-1H-pyrrole-3,4-dicarboxylic acid dimethyl ester

(A.5h)

Yield: 63%. 1H NMR (400 MHz, $CDCl_3$): δ 7.27-7.20 (m, 3H), 7.08-7.04 (m, 4H), 6.80-6.77 (m, 2H), 5.01 (s, 2H); 3.82 (s, 3H) 3.66 (s, 3H); 2.66 (d, 2H, 7.33 Hz), 2.33 (s, 3H), 1.90 (m, 1H), 0.93 (d, 6H, 6.45 Hz). ^{13}C NMR (100 MHz, $CDCl_3$): δ 166.4, 165.7, 138.7, 138.7, 137.4, 136.1, 130.5, 129.1, 129.0, 128.7, 127.6, 125.7, 115.4, 113.0, 52.0, 51.7, 48.1, 34.3, 29.9, 22.8, 21.7. HRMS. Calculated for $C_{26}H_{29}NO_4$: 419.20966; found: 409.20878

2-(2-Acetoxy-1,1-dimethyl-ethyl)-1-benzyl-5-phenyl-1H-pyrrole-3,4-dicarboxylic acid dimethyl ester (A.5i)

Yield: 50%. ¹H NMR (400 MHz, CDCl₃): δ 7.16-7.10 (m, 6H), 7.08-7.00 (m, 2H), 6.65-6.60 (m, 2H), 5.20 (s, 2H), 4.15 (s, 2H); 3.91 (s, 3H), 3.52 (s, 3H), 2.02 (m, 3H), 1.39 (s, 3H). ¹³C NMR (100 MHz, CDCl₃): δ 170.9, 169.7, 164.0, 140.8, 138.0, 133.1, 131.5, 130.5, 128.7, 128.6, 127.9, 127.4, 125.5, 118.4, 112.4, 77.6, 70.9, 52.9, 51.4, 50.4, 38.2, 26.4, 21.2. HRMS. Calculated for C₂₇H₂₉NO₆: 463.19949; found:

1-Ethyl-4-phenyl-2,5-di-p-tolyl-1H-pyrrole-3-carboxylic acid methyl ester (A.5j)

Yield: 63%. ¹H NMR (400 MHz, CDCl₃): δ 7.45 (d, 2H, 7.92 Hz), 7.34 (d, 2H, 7.92 Hz), 7.29-7.10 (m, 9H), 3.86 (q, 2H, 7.33 Hz), 3.50 (s, 3H), 2.50 (s, 3H), 2.39 (s, 3H), 0.95 (t, 3H, 7.33 Hz). ¹³C NMR (100 MHz, CDCl₃): δ 166.1, 138.3, 138.2, 137.7, 135.8, 132.1, 131.4, 130.9, 130.8, 129.9, 129.4, 129.3, 129.1, 127.4, 126.0, 124.3, 112.8, 50.9, 40.2, 21.9, 21.8, 16.8. HRMS. Calculated for C₂₈H₂₇NO₂: 409.20418; found: 409.20502.

1-(1-Benzyl-4-phenyl-2,5-di-p-tolyl-1H-pyrrol-3-yl)-2-methyl-propan-1-one (A.5k)

Yield: 63%. ¹H NMR (400 MHz, CDCl₃): δ 7.28-7.10 (m, 12H), 7.04 (d, 2H, 8.21 Hz); 6.99 (d, 2H, 8.21 Hz), 6.72-6.64 (m, 2H), 5.00 (s, 2H), 2.51 (m, 1H), 2.38 (s,

1H), 2.29 (s, 1H), 0.94 (s, 3H); 0.93 (s, 3H). ¹³C NMR (100 MHz, CDCl₃): δ 205.3, 138.6, 138.4, 137.6, 136.5, 135.8, 132.7, 131.4, 130.9, 130.5, 129.3, 129.1, 129.0, 129.0, 128.4, 127.9, 127.1, 126.2, 126.2, 123.8, 123.8, 48.6, 39.7, 21.8, 21.7, 19.3. HRMS. Calculated for C₃₅H₃₃NO: 483.25621; found: 483.25692.

N-Benzyl-N-(2-methyl-propenyl)-benzamide (A.17)

Yield: 85%. ¹H NMR (400 MHz, CDCl₃): δ 7.62-7.22 (m, 10H), 5.79 (s, 1H), 4.77 (s, 2H), 1.43 (s, 3H); 1.12 (s, 3H), ¹³C NMR (100 MHz, CDCl₃): δ 170.7, 137.3, 136.8, 134.4, 129.9, 129.0, 128.6, 128.3, 127.7, 127.5, 124.5, 51.7, 22.1, 18.1.

N-Benzyl-N-(5-chloro-pent-2-enyl)-benzamide (A.19)

Yield: 88%. ¹H NMR (400 MHz, CDCl₃, 60°C): δ 7.53-7.22 (m, 10H), 6.80 (m, 1H), 5.04-4.95 (m, 3H), 3.37 (t, 2H, 7.04 Hz); 2.38-2.31 (m, 2H), ¹³C NMR (100 MHz, CDCl₃): δ 170.5, 137.1, 135.6, 131.5, 130.5, 128.8, 128.6, 128.0, 127.3, 126.9, 108.6, 48.5, 44.7, 33.9..

1-Phenyl-8-p-tolyl-10-oxa-2-aza-tricyclo[4.4.0.0^{2,8}]decan-9-one (A.21)

Imine **A.20** (100.0 mg, 0.48 mmol) and benzoyl chloride (94.0 mg, 0.68 mmol) were dissolved in 5 mL of acetonitrile and stirred for 15 min. The previous solution was then added to a solution of Pd₂(dba)₃·CHCl₃ (21.8 mg, 0.024 mmol) in 5 mL of

acetonitrile. The reaction mixture was transferred to a 50 mL reaction bomb and EtNⁱPr₂ (96.0 mg, 0.74 mmol) was added. The solution was degassed and carbon monoxide (60 psi) was added to the reaction mixture, which was left to stir at 55°C for 30 hours. Following removal of solvent *in vacuo*, the residue was purified on silica gel chromatography utilizing hexanes/ethyl acetate as eluent.

Yield: 70% ¹H NMR (400 MHz, CDCl₃): δ 7.78-7.76 (d, 2H, 7.71 Hz), 7.50-7.47 (m, 4H), 7.31-7.29 (m, 2H, 7.71 Hz), 3.43-3.40 (m, 1H), 3.13-3.05 (m, 1H), 2.87-2.81 (m, 1H), 2.08-1.93 (m, 1H), 1.81-1.73 (m, 1H); 1.45-1.31 (m, 1H); 1.07-0.98 (m, 1H). ¹³C NMR (101 MHz, CDCl₃): δ 174.4, 138.8, 131.8, 130.0, 129.7, 129.6, 129.5, 129.1, 128.8, 102.4, 74.1, 43.5, 39.2, 33.0, 26.9, 21.8, 16.9 HRMS. Calculated for C₂₁H₂₁NO₂: 319.15723; found: 319.15680. IR: 1790.0 cm⁻¹

1-Ethyl-3-methyl-2-phenyl-4,5-dihydro-1H-6-oxa-1-aza-benzo[e]azulene (A.25)

Imine A.24 (188 mg, 0.93 mmol) and benzoyl chloride (184 mg, 1.30 mmol) were dissolved in 6 mL of acetonitrile. This solution was added to Pd₂(dba)₃·CHCl₃ (2.5 mol%) and P(*o*-tolyl)₃ (10 mol%) in 6 mL of acetonitrile. The reaction mixture was transferred to a 100 mL reaction bomb and EtNⁱPr₂ (184 mg, 1.43 mmol) (in 12 mL of THF) was added. The solution was evacuated, carbon monoxide (60 psi) added, and stirred at 55°C for 18 hours. The product was purified by silica gel chromatography using hexanes/ethyl acetate as eluent.

Yield: 50%. ¹H NMR (400 MHz, CDCl₃): δ 7.48-7.30 (m, 6H), 7.22-7.17 (m, 3H), 4.54 (t, 2H, 6.55 Hz), 4.09 (q, 4H, 6.88 Hz), 2.82 (t, 2H, 6.55 Hz), 2.06 (3H, s), 0.89 (t, 3H, 6.88 Hz), ¹³C NMR (100 MHz, CDCl₃): δ 156.8, 133.8, 133.5, 130.7, 128.5, 127.8, 127.8, 127.7, 127.2, 126.9, 123.8, 122.9, 121.4, 116.5, 76.9, 41.1, 26.0, 16.4, 10.2. HRMS. Calculated for C₂₁H₂₁NO: 303.16231; found: 303.16206.

A.3 References

- 1) Dhawan, R.; Dghaym, R.D.; Arndtsen, B.A. *J. Am. Chem. Soc.* **2003**, *125*, 1474.
- 2 a) Dghaym, R. D.; Dhawan, R.; Arndtsen, B. A. *Angew. Chem. Int. Ed.* **2001**, *40*, 3228. b) Dhawan, R.; Dghaym, R.D.; Arndtsen, B.A. *Catalysis of Organic Reactions.* **2003**, *89*, 499-508.
- 3) Dhawan, R.; St. Cyr, D.; Dghaym, R.D.; Arndtsen, B.A. *Org. Lett.* (Chapter 2) (manuscript in preparation)
- 4) Dhawan, R.; Arndtsen, B.A. *J. Am. Chem. Soc.* **2004**, *126*, 468.
- 5) Authentic sample obtained from reaction of equimolar amounts of benzylamine and benzoyl chloride in the presence of Et₃N.
- 6) See Experimental Section for details.
- 7) Ph.D. Dissertation: Rania D. Dghaym. pp. 181.
- 8 a) Hiemstra, H.; Speckamp, N. In: B.M. Trost, I. Fleming, ed. *Comprehensive Organic Synthesis*. New York: Pergamon Press, pg. 1047-1081, **1991**. b) Speckamp, W.N.; Moolenaar, M.J. *Tetrahedron* **2000**, *56*, 3817.
- 9) Ratts, K.; Chupp, J. *J. Org. Chem.* **1974**, *39*, 3300.

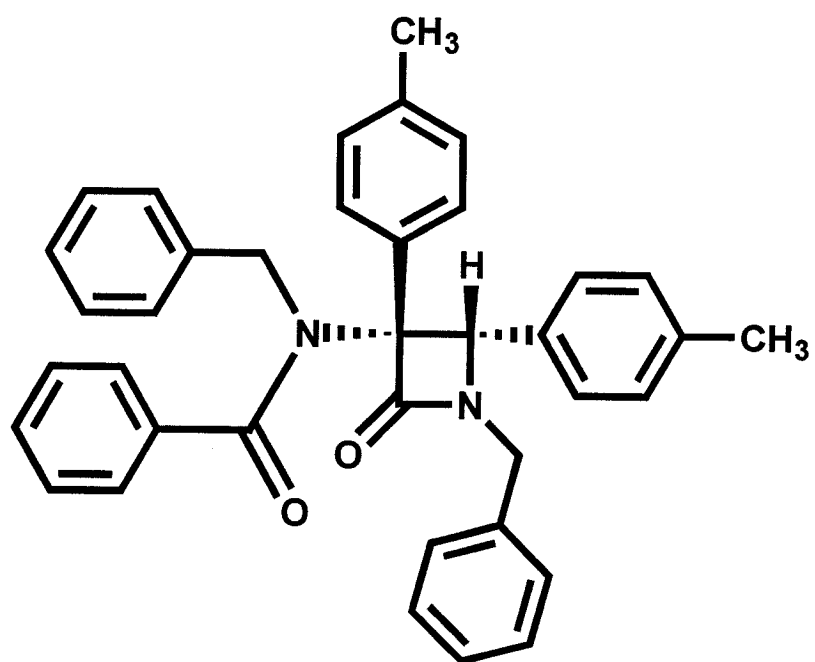
- 10) Suggested by control reactions in CD₃CN and determined by ¹H-NMR spectroscopy
- 11) Determined by ¹H-NMR spectroscopy in CD₃CN
- 12a) Mesoionic Ring Systems by K.T. Potts in *1,3 Dipolarcycloaddition Chemistry* A. Padwa Ed. pg. 1-81. 1983 John Wiley & Sons Inc. New York b) Mesoionic Oxazoles by H.L. Gingrich and J.S. Baum in *Oxazoles*. I.J. Turchi Ed. 731-958. 1984 John Wiley & Sons Inc. New York c) Mesoionic Ring Systems by G.W. Gribble in *Synthetic Applications of 1,3-Dipolar Cycloaddition Chemistry Toward Heterocycles and Natural Products*. 2002 John Wiley & Sons Inc. New York . A. Padwa Ed. pg. 681-753. d) Mesoionic Oxazoles by G.W. Gribble in *Oxazoles: Synthesis, Reactions, and Spectroscopy Part. A*. Ed. D.C. Palmer 2003, John Wiley & Sons. New York.
- 13) Hegedus, L.S. Organopalladium Chemistry. In *Organometallics in Synthesis*; Schlosser, M., Ed.; Wiley: New York, 2002; p. 1193.
- 14) Beletskaya, I. P.; Cheprakov, A. V. *Chem. Rev.* **2000**, *100*, 3009.
- 15) (Benzoyl-benzyl-amino)-phenylacetic acid (12.5 mg, 0.036 mmol) was added to a CD₃CN (1 mL) solution of *N,N*-dicyclohexylcarbodiimide (8.9 mg, 0.043 mmol). To this, now intense yellow solution of Münchnone (3-benzyl-2,4-diphenyl-oxazolium-5-oxide) was added Pd/C (2 mg) and heated at 60°C for 24 hours. This showed a diminution of Münchnone concentration by 50%.
- 16) Herrmann, W.A.; Brossmer, C.; Öfele, K.; Reisinger, C.P.; Priermeier, J.; Beller, M.; Fischer, H. *Angew. Chem. Int. Ed.* **1995**, *34*, 1844
- 17) See Chapter 1., Part II of this thesis and Ref. 17.

- 18) Control reactions suggest that on addition of DMAD to *N*-acyliminium salt **A.6** ($R^1 = \text{Bn}$, $R^2 = \text{Tol}$, $R^3 = \text{Ph}$), in CD_3CN , a large range of unidentifiable products are formed.
- 19) Use of Method A and Method B (Table A.1)
- 20) Johnson, P.R.; White, J.D. *J. Org. Chem.* **1984**, *49*, 4424.
- 21) Collman, J.P.; Hegedus, L.S.; Norton, J.R.; Finke, R.G. *Principles and Applications of Organotransition Metal Chemistry*, 2nd Edition. University Science Books, **1987**, 235-458.
- 22) Stability of the to *N*-acyliminium salt was probed through the addition of imine **A.16** to PhCOCl at -45°C in CD_2Cl_2 . A $^1\text{H-NMR}$ of this reaction was obtained at -20°C , which showed that this *N*-acyliminium salt was stable at this temperature for at least 20 minutes (monitoring time). Formation of enamide **A.17** ensued on warming the reaction mixture up to room temperature. Conversion to enamide is significantly faster in CD_3CN .
- 23) Tidwell, T. *Ketenes* pp. 57-65. J.W. Wiley & Sons, **1995**. New York.
- 24) Bernard, D.; Poutheau, A.; Gore, J. *Tetrahedron* **1987**, *43*, 2721.
- 25) Determined from *in situ* examination of the reaction. Also see Ref. 7.
- 26) Control reactions also suggested that *N*-acyliminium salt **A.6e** was not stable in the presence of K_3PO_4 as it leads to formation of unidentifiable products.
- 27) Compared to an authentic sample prepared from acetyl chloride and benzylamine.
- 28) Determined from $^1\text{H-NMR}$ using phenyl trimethylsilane as internal standard.
- 29) Poli, G.; Giambastiani, G.; Heumann, A. *Tetrahedron*, **2000**, *56*, 5959.
- 30) See Appendix C for X-ray data.

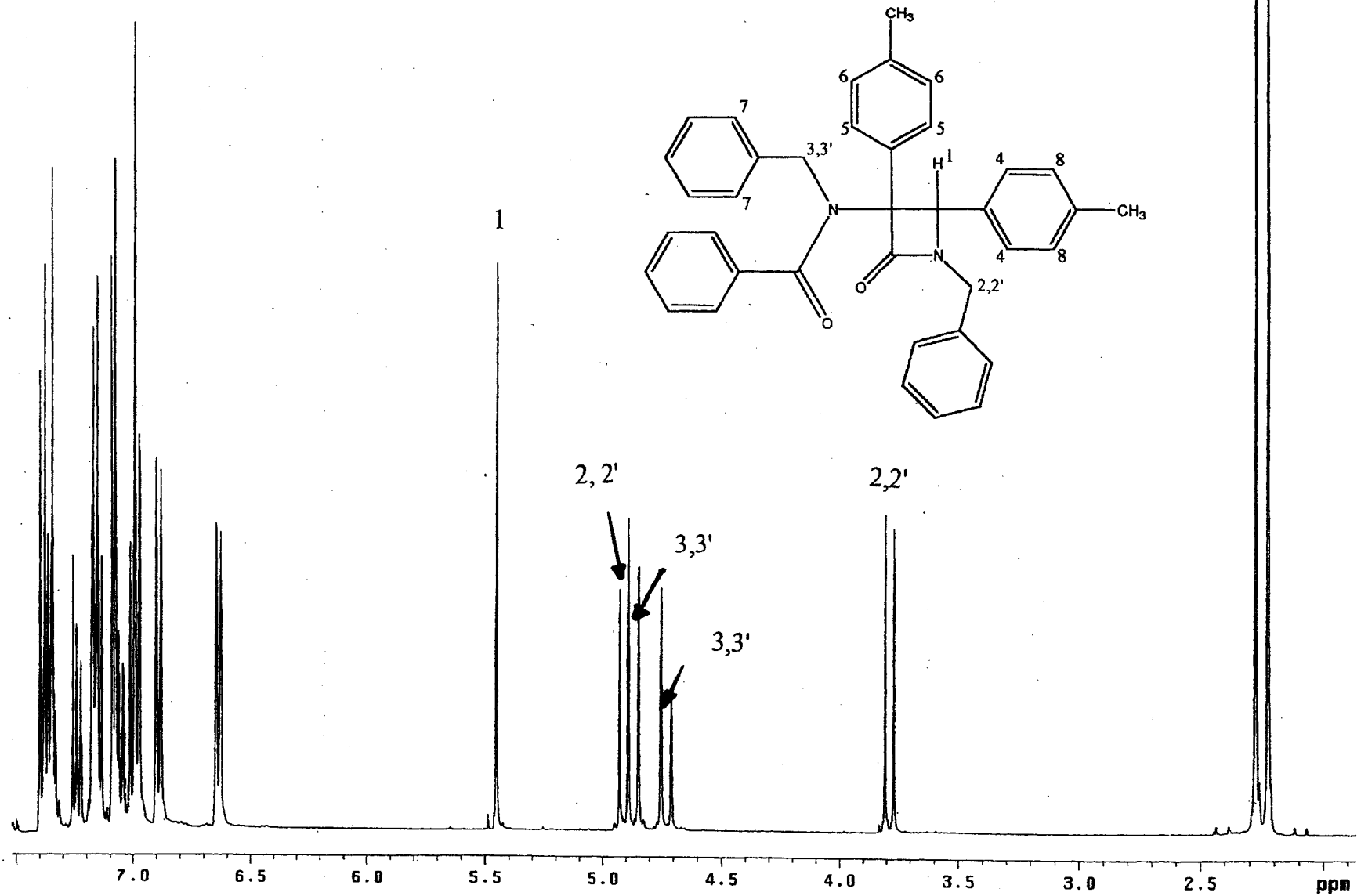
- 31 a) Padwa, A.; Lim, R.; MacDonald, J. G.; Gingrich, H.L.; Kellar, S.M. *J. Org. Chem.* **1985**, *50*, 3816. b) Padwa, A.; Gingrich, H.L.; Lim, R. *J. Org. Chem.* **1982**, *47*, 2447 c) Padwa, A.; Gingrich, H.L.; Lim, R. *Tetrahedron Lett.* **1980**, *21*, 3419.
- 32) Pérez-Serrano, L.; Blanco-Urgoiti, J.; Casarrubios, L.; Domínguez, G.; Pérez-Castells, J. *J. Org. Chem.* **2000**, *65*, 3513.
- 33) March, J.M *Advanced Organic Chemistry: Reactions, Mechanism & Structure*. Pg. 212, 4th ed., J.Wiley & Sons, **1992**, New York

Appendix B

2D-NMR and X-ray Structural Data for Complex 2.1b



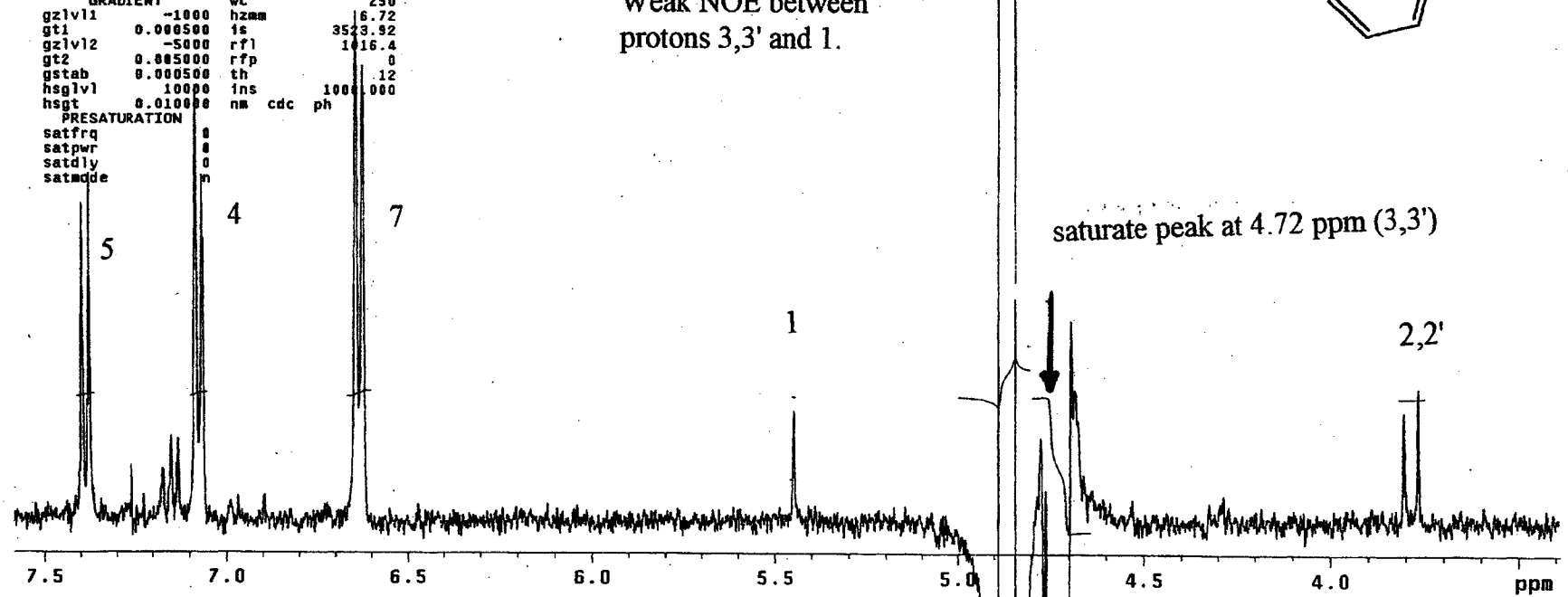
^1H for 1-Benzyl-3-(1-benzyl-2-oxo-2-phenylethyl)-3,4-di-*p*-tolyl-azetidin-2-one



NOESY1D for 1-Benzyl-3-(1-benzyl-2-oxo-2-phenyl-ethyl)-3,4-di-*p*-tolyl-azetidin-2-one

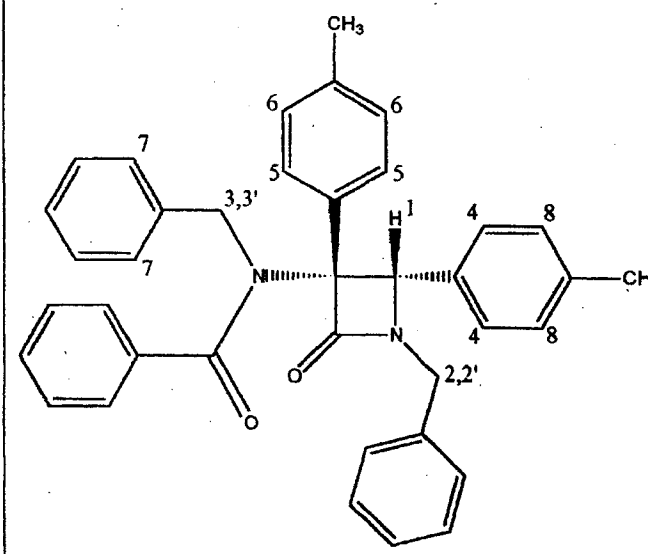
```

exp2 NOESY1D
ACQUISITION          DECOUPLER
sw 5998.8 dn H1
at 1.995 dm nnn
np 23936 SAMPLE
fb 3480 date Oct 9 2000
bs 16 solvent CDC13
ss -2 file /export/home/~
d1 1.000 rdh/mix_7.fid
nt 2048 SPECIAL
ct 2048 temp not used
TRANSMITTER          gain 28
tn H1 spin 0
sfrq 400.133 pw90 14.200
tof 0
tpwr 57 sspul y
pw 14.200 il n
NOESY in n
mix 0.700 dp y
sweep1 57 hs nn
sweep2 14.000
sweep3p hard lb 0.50
SEL PULSE fn not used
sel1 91.7
selshape NOESY1D_4~ sp 1356.3
sel2 73p wp 1678.8
sel3 0 ve 2355
sel4 20129.4 sc 0
GRADIENT wc 250
gzlv1 -1000 hzmm 16.72
gt1 0.000500 is 3523.92
gzlv2 -5000 rfl 1416.4
gt2 0.005000 rfp 0
gstab 0.000500 th 12
hsglv1 10000 ins 1000.000
hsgt 0.010000 nm cdc ph
PRESATURATION
sat1 0
sat2 0
sat3 0
sat4 0
satmode n
  
```



Strong NOE between protons 3,3' and 4.

Weak NOE between protons 3,3' and 1.

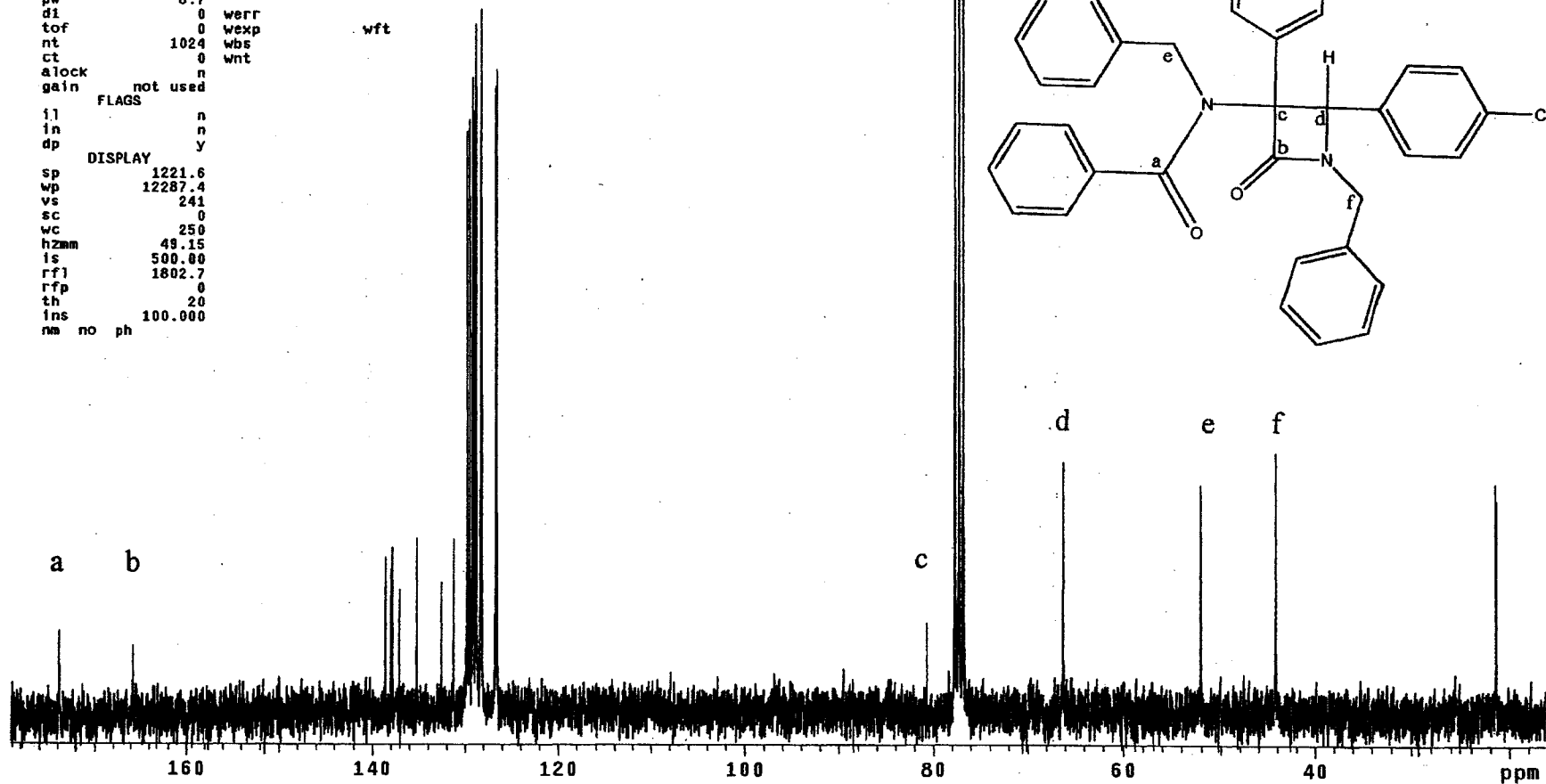


saturate peak at 4.72 ppm (3,3')

¹³C-NMR for 1-Benzyl-3-(1-benzyl-2-oxo-2-phenyl-ethyl)-3,4-di-p-tolyl-azetidin-2-one

```

exp2 std13c
SAMPLE          DEC. & VT
date Sep 26 2000 dfrq 300.075
solvent CDC13   dn H1
file exp dpwr 35
ACQUISITION    dof 0
sfrq 75.461   dm  yyy
tn C13        dm  w
at 1.815     dmf 7400
np 68106     PROCESSING
sw 18761.7   lb 1.00
fb 10400     wf file
bs 16        proc ft
tpwr 57      fn not used
pw 8.7
di 0         werr
tof 0        wexp wft
nt 1024     wbs
ct 0         wnt
alock n
gain not used
FLAGS
il n
in n
dp y
DISPLAY
sp 1221.6
wp 12287.4
vs 241
sc 0
wc 250
hzmm 49.15
is 500.00
rf1 1802.7
rfp 0
th 20
ins 100.000
na no ph
    
```



STANDARD 1H OBSERVE

Pulse Sequence: gCOSY

Solvent: CDCl3
Ambient temperature
File: rdh347cosy
Mercury-300 "m300"

PULSE SEQUENCE: gCOSY
Relax. delay 0.800 sec
Acq. time 0.220 sec
Width 2331.0 Hz
2D Width 2331.0 Hz
4 repetitions
128 increments

OBSERVE H1, 300.0738816 MHz

DATA PROCESSING

Sine bell 0.110 sec

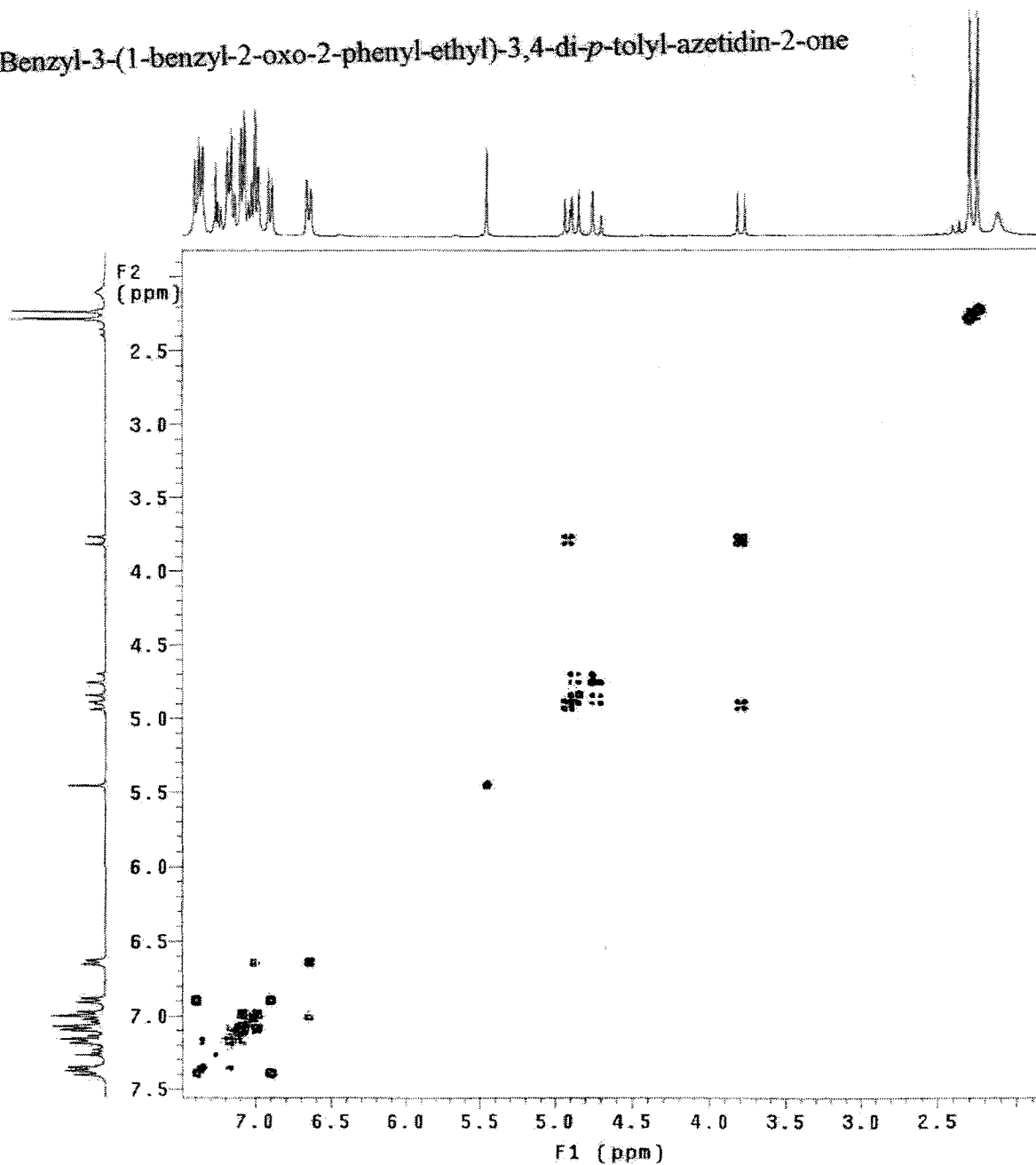
F1 DATA PROCESSING

Sine bell 0.055 sec

FT size 2048 x 2048

Total time 10 min, 19 sec

COSY for 1-Benzyl-3-(1-benzyl-2-oxo-2-phenyl-ethyl)-3,4-di-*p*-tolyl-azetidin-2-one



STANDARD 1H OBSERVE

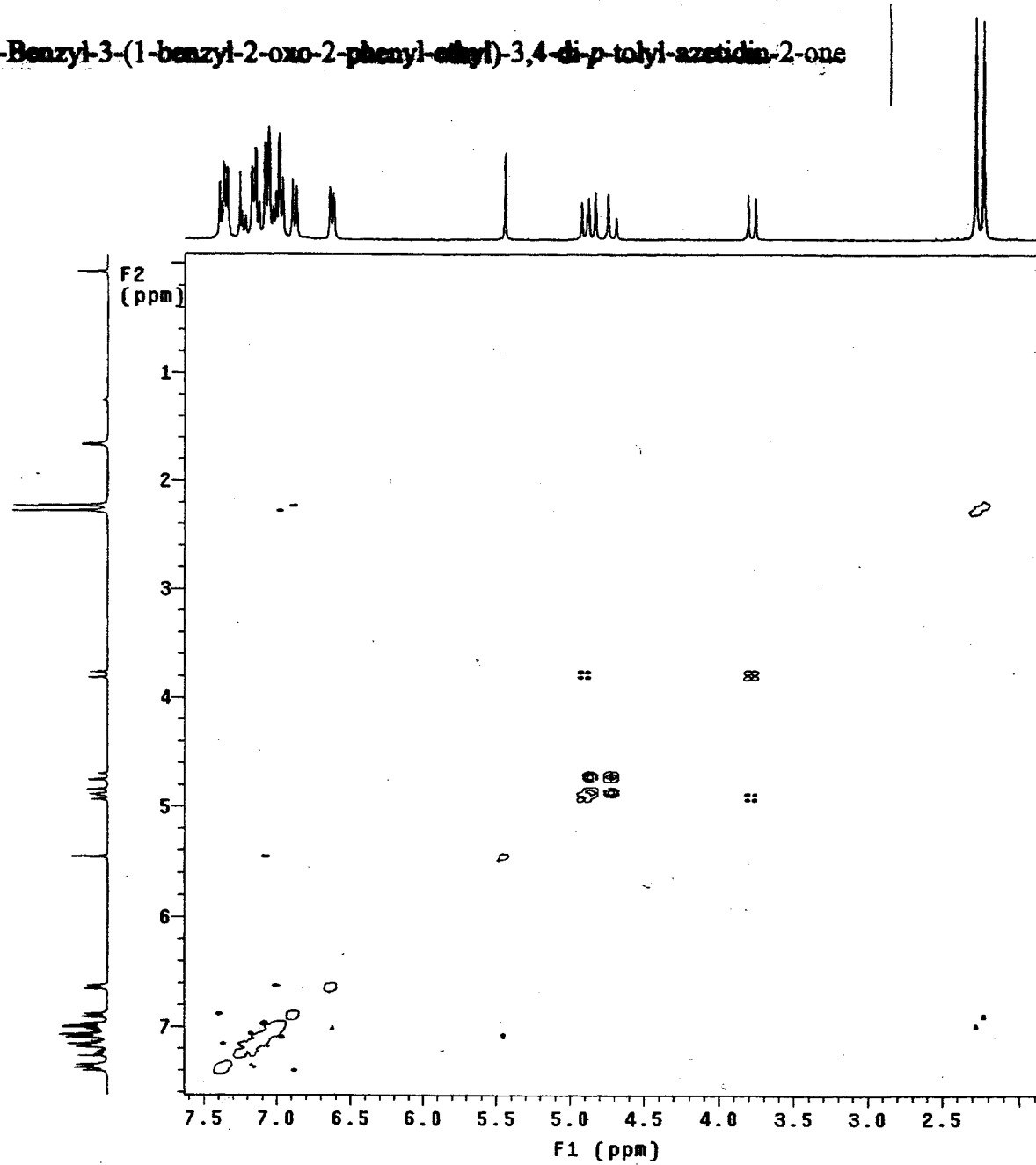
Pulse Sequence: NOESY

Solvent: CDCl3
Ambient temperature
Mercury-300 "m300"

PULSE SEQUENCE: NOESY
Relax. delay 1.500 sec
Mixing 0.700 sec
Acq. time 0.220 sec
Width 2531.0 Hz
2D Width 2531.0 Hz
8 repetitions
2 x 256 increments

OBSERVE F1, 300.0738816 MHz
DATA PROCESSING
Gauss apodization 0.101 sec
F1 DATA PROCESSING
Gauss apodization 0.079 sec
FT size 4096 x 4096
Total time 2 hr, 55 min, 5 sec

NOESY for 1-Benzyl-3-(1-benzyl-2-oxo-2-phenylethyl)-3,4-dip-tolyl-azetidin-2-one



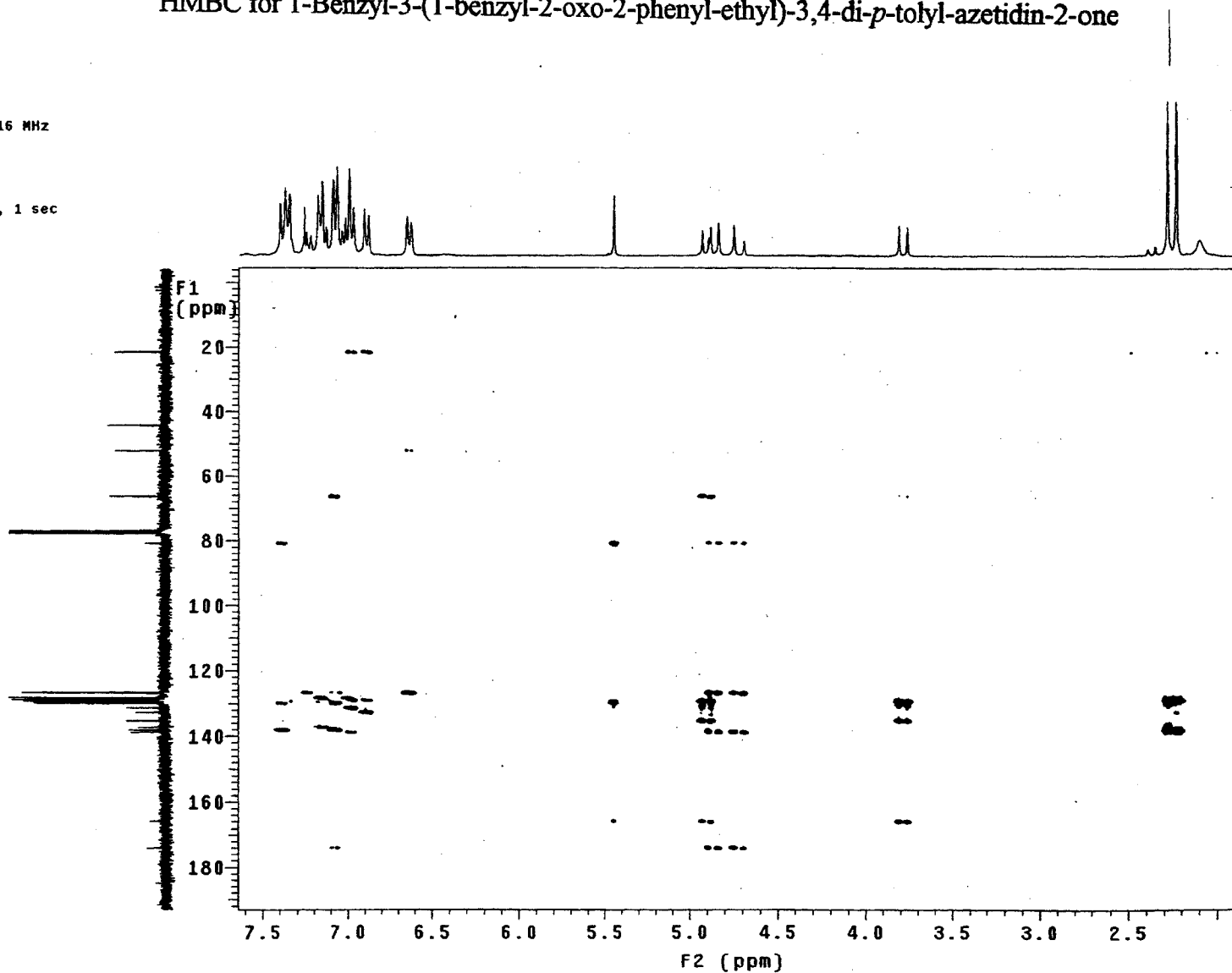
STANDARD 1H OBSERVE

Pulse Sequence: gHMBC

Solvent: CDC13
Ambient temperature
File: rdhmbc
Mercury-300 "m300"

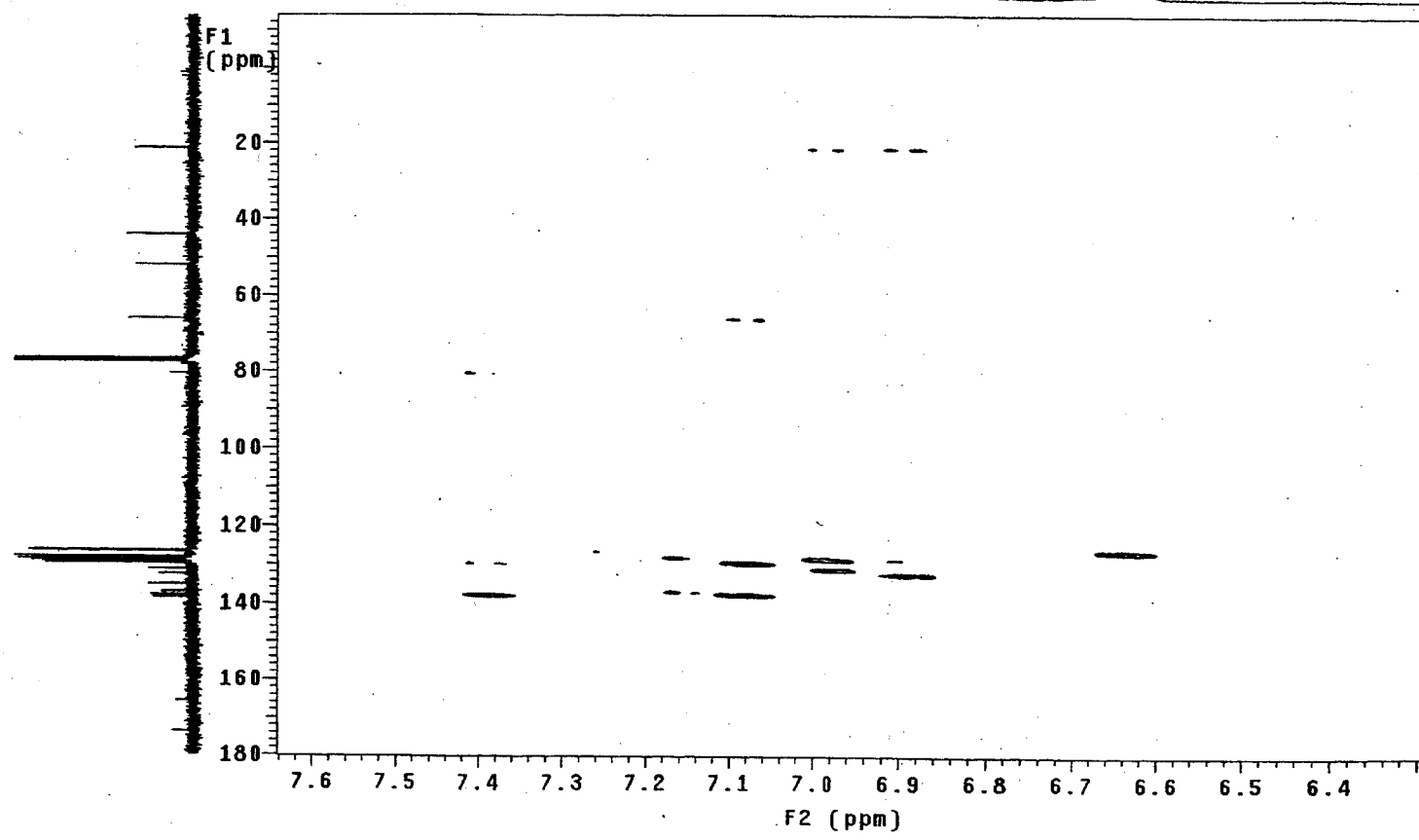
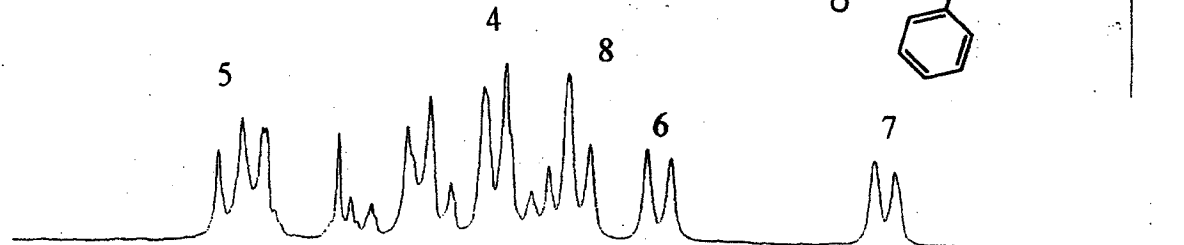
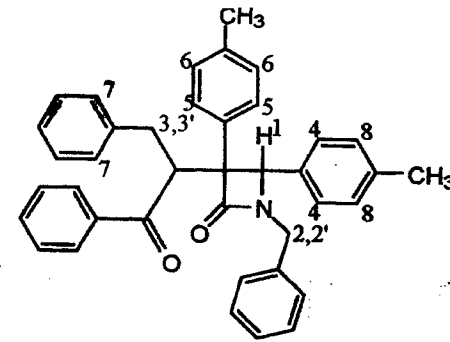
PULSE SEQUENCE: gHMBC
Relax. delay 1.000 sec
Mixing 0.700 sec
Acq. time 0.220 sec
Width 2331.0 Hz
2D Width 18107.7 Hz
8 repetitions
400 increments
OBSERVE H1, 300.0738816 MHz
DATA PROCESSING
Sine bell 0.110 sec
F1 DATA PROCESSING
Sine bell 0.044 sec
FT size 1024 x 8192
Total time 1 hr, 14 min, 1 sec

HMBC for 1-Benzyl-3-(1-benzyl-2-oxo-2-phenyl-ethyl)-3,4-di-*p*-tolyl-azetid-2-one



STANDARD 1H OBSERVE

Pulse Sequence: gHMBC
Solvent: CDCl3
Ambient temperature
Mercury-300 "m300"
PULSE SEQUENCE: gHMBC
Relax. delay 1.000 sec
Acq. time 0.220 sec
Width 2331.0 Hz
2D Width 18107.7 Hz
8 repetitions
400 increments
OBSERVE H1, 300.0738816 MHz
DATA PROCESSING
Sine bell 0.110 sec
F1 DATA PROCESSING
Sine bell 0.011 sec
FT size 1024 x 8192
Total time 1 hr, 14 min, 1 sec



STANDARD 1H OBSERVE

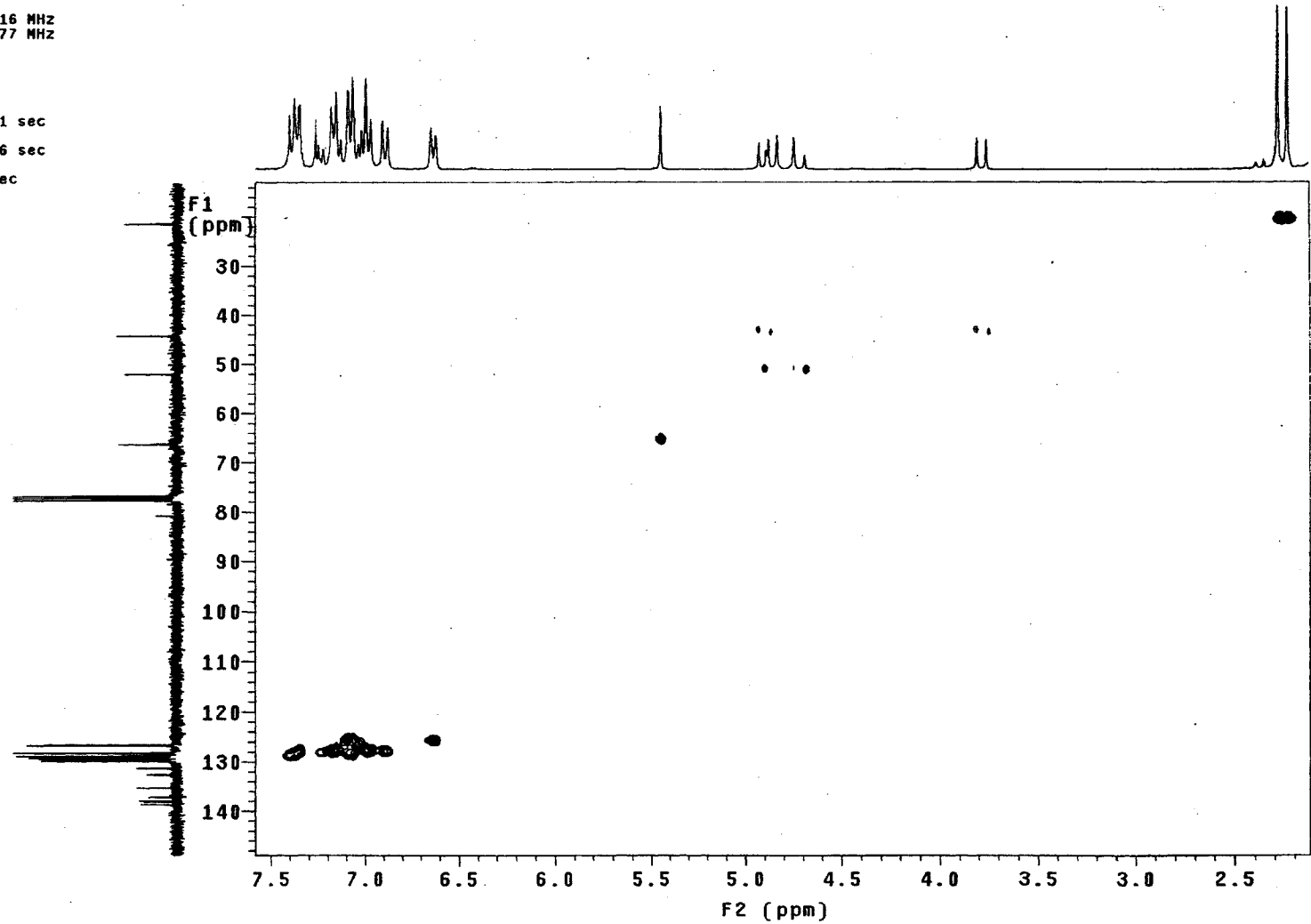
Pulse Sequence: gHMOC

Solvent: CDCl3
Ambient temperature
File: rdhmqc
Mercury-300 "m300"

PULSE SEQUENCE: gHMOC
Relax. delay 1.000 sec
Acq. time 0.220 sec
Width 2331.0 Hz
2D Width 18761.7 Hz
8 repetitions
2 x 64 increments

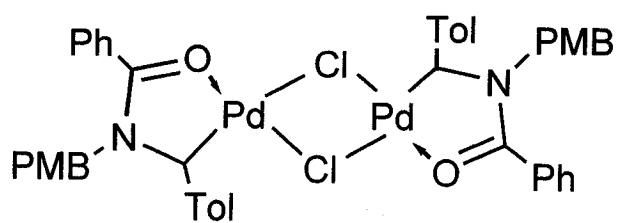
OBSERVE H1, 300.0738816 MHz
DECOUPLE C13, 75.4611977 MHz
Power 42 dB
on during acquisition
off during delay
GARP-1 modulated
DATA PROCESSING
Gauss apodization 0.101 sec
F1 DATA PROCESSING
Gauss apodization 0.006 sec
FT size 1024 x 2048
Total time 23 min, 34 sec

HMOC for 1-Benzyl-3-(1-benzyl-2-oxo-2-phenyl-ethyl)-3,4-di-*p*-tolyl-azetidin-2-one

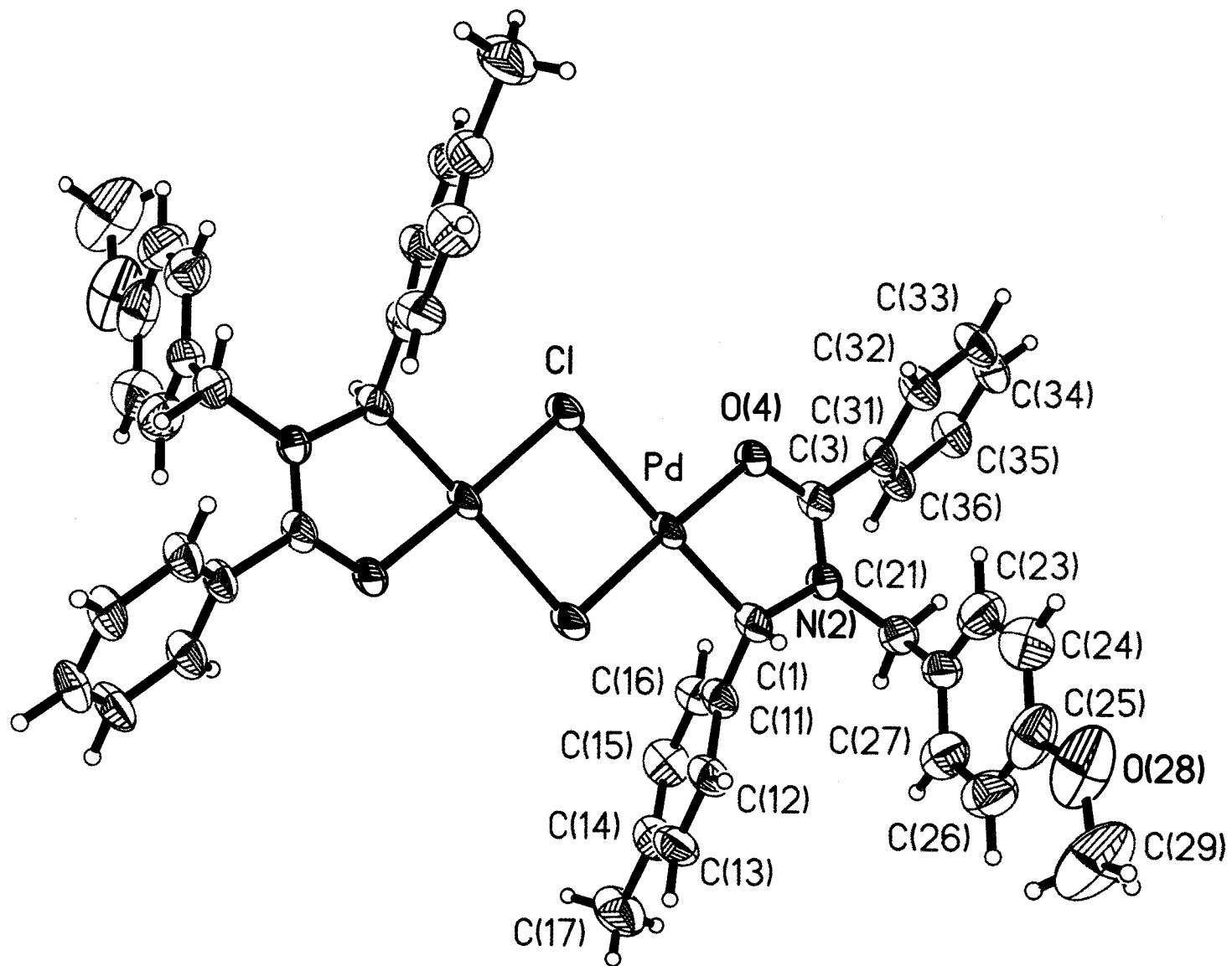


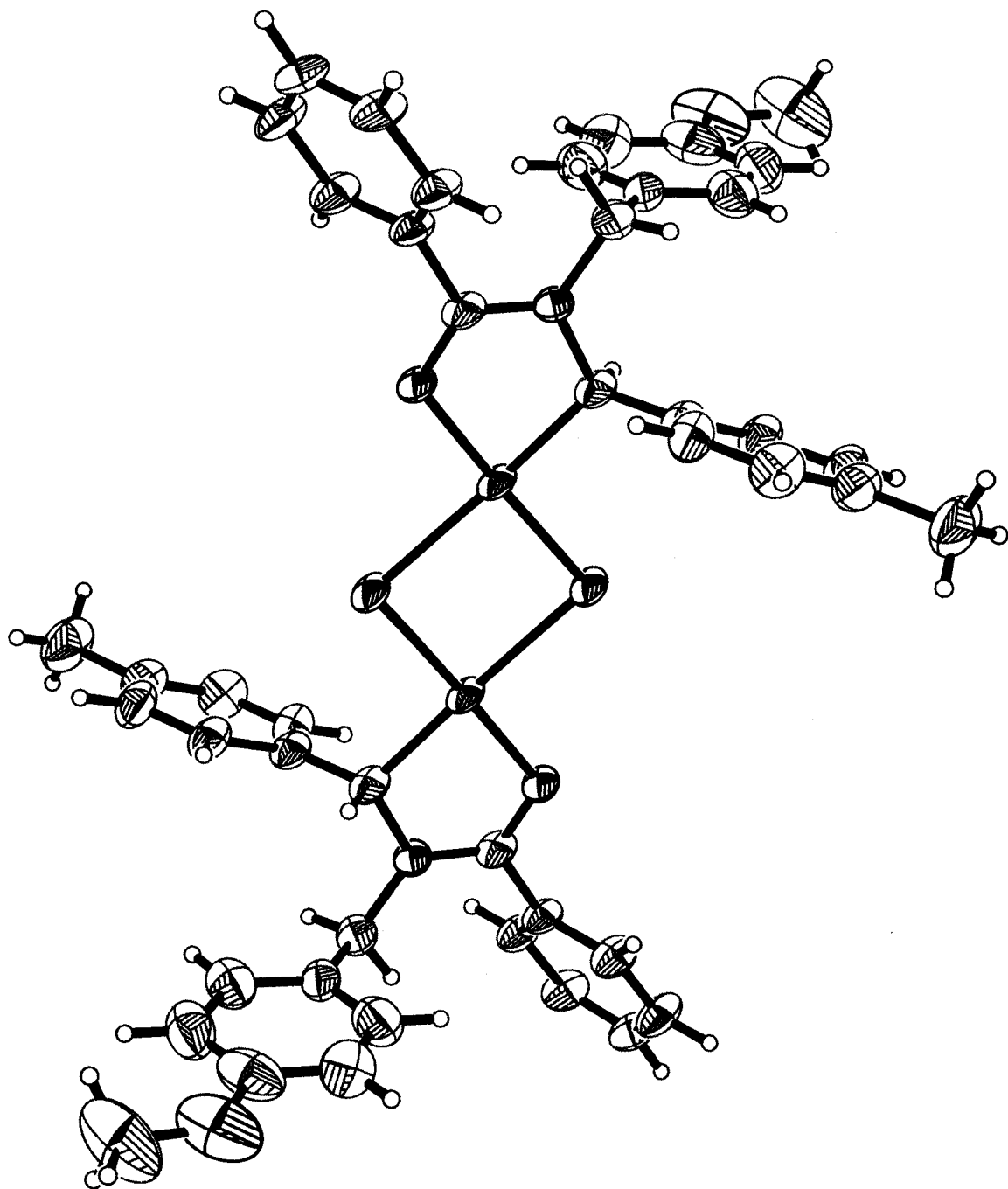
Appendix C

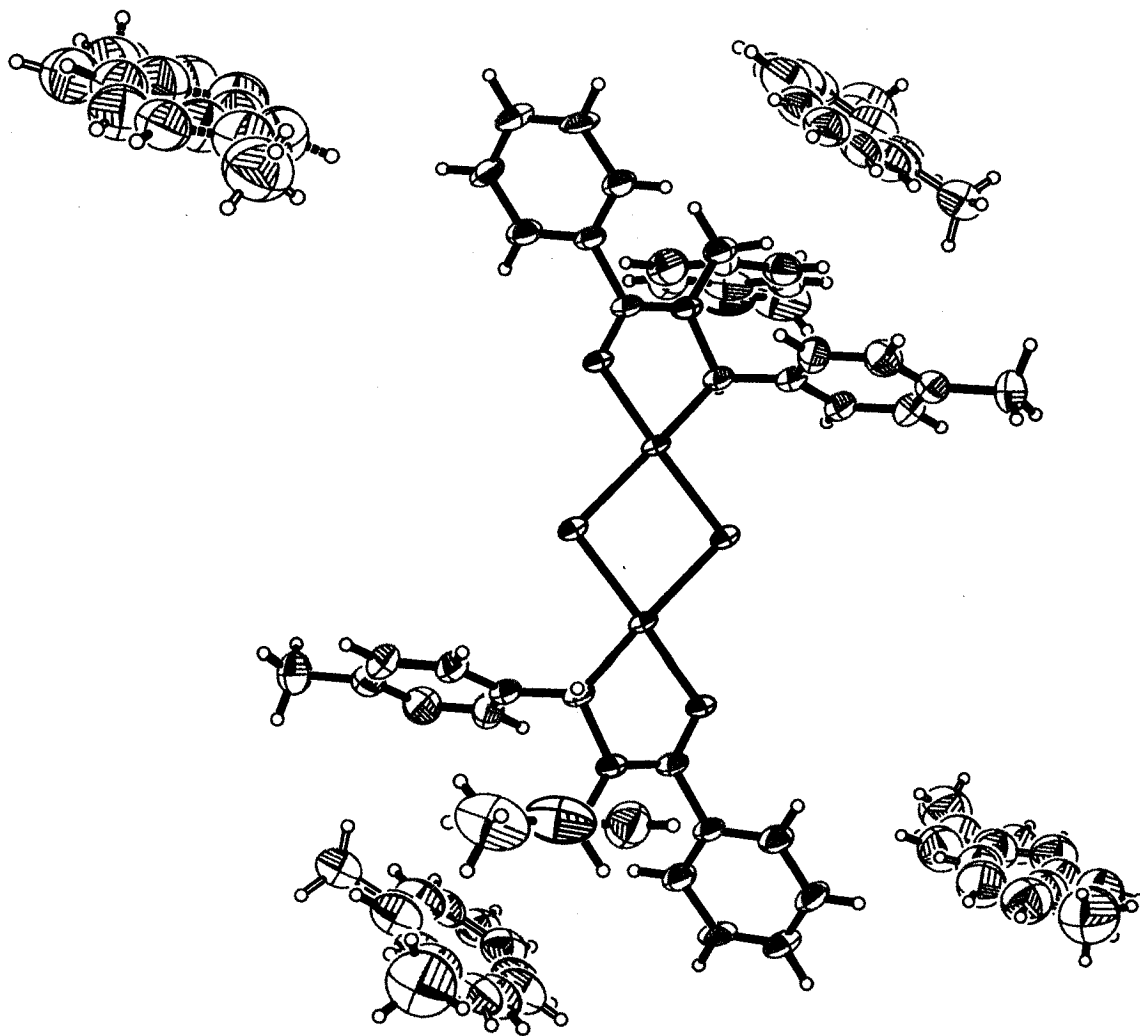
X-ray Structural Data for Complex 6.6b



PMB = p-C₆H₄-OCH₃
Tol = p-C₆H₄-CH₃







CRYSTAL AND MOLECULAR STRUCTURE OF
C74 H76 Cl2 N2 O4 Pd2 COMPOUND (arst29)

Saturday, August 21, 2004

Equipe Dr Arndtsen

Department of Chemistry, Otto Maass Chemistry Building
McGill University, Montréal, Québec (Canada) H3A 2K6

Structure solved and refined in the laboratory of X-ray diffraction
Université de Montréal by Francine Bélanger-Gariépy.

Table 1. Crystal data and structure refinement for C₇₄ H₇₆ Cl₂ N₂ O₄ Pd₂.

Identification code	arst29
Empirical formula	C ₇₄ H ₇₆ Cl ₂ N ₂ O ₄ Pd ₂
Formula weight	1341.07
Temperature	220(2)K
Wavelength	1.54178 Å
Crystal system	Monoclinic
Space group	P21/n
Unit cell dimensions	a = 17.5028(11) Å $\alpha = 90^\circ$ b = 9.7001(6) Å $\beta = 103.052(3)^\circ$ c = 20.2231(13) Å $\gamma = 90^\circ$
Volume	3344.8(4)Å ³
Z	2
Density (calculated)	1.332 Mg/m ³
Absorption coefficient	5.450 mm ⁻¹
F(000)	1384
Crystal size	0.24 x 0.17 x 0.07 mm
Theta range for data collection	3.02 to 55.29°
Index ranges	-18 ≤ h ≤ 18, -10 ≤ k ≤ 10, -21 ≤ l ≤ 21
Reflections collected	42029
Independent reflections	4165 [R _{int} = 0.064]
Absorption correction	Semi-empirical from equivalents
Max. and min. transmission	0.7600 and 0.4800
Refinement method	Full-matrix least-squares on F ²
Data / restraints / parameters	4165 / 613 / 499
Goodness-of-fit on F ²	1.031
Final R indices [I > 2σ(I)]	R ₁ = 0.0689, wR ₂ = 0.1657
R indices (all data)	R ₁ = 0.1121, wR ₂ = 0.1822

Largest diff. peak and hole 2.063 and -1.216 e/Å³

Table 2. Atomic coordinates ($\times 10^4$) and equivalent isotropic displacement parameters ($\text{Å}^2 \times 10^3$) for C74 H76 Cl2 N2 O4 Pd2.

U_{eq} is defined as one third of the trace of the orthogonalized U_{ij} tensor.

	Occ.	x	y	z	U_{eq}
Pd	1	5906(1)	732(1)	355(1)	60(1)
Cl	1	4959(1)	-845(2)	698(1)	72(1)
C(1)	1	6692(4)	1951(6)	92(3)	58(2)
N(2)	1	7351(3)	2115(5)	720(3)	63(2)
C(3)	1	7275(4)	1442(7)	1264(3)	60(2)
O(4)	1	6682(3)	702(4)	1267(2)	63(1)
C(11)	1	6396(4)	3318(7)	-191(3)	62(2)
C(12)	1	6299(4)	3550(8)	-883(4)	73(2)
C(13)	1	6004(4)	4804(8)	-1169(4)	87(3)
C(14)	1	5793(5)	5826(7)	-777(5)	84(3)
C(15)	1	5896(5)	5597(8)	-84(5)	89(3)
C(16)	1	6192(5)	4357(8)	196(4)	80(2)
C(17)	1	5456(6)	7195(8)	-1097(5)	127(4)
C(21)	1	8054(4)	2870(8)	628(3)	73(2)
C(22)	1	8402(4)	2266(8)	113(4)	70(2)
C(23)	1	8707(5)	976(10)	201(5)	105(3)
C(24)	1	9036(5)	348(13)	-264(5)	126(4)
C(25)	1	9069(5)	1015(11)	-865(5)	115(4)
C(26)	1	8760(5)	2357(10)	-965(5)	112(3)
C(27)	1	8420(5)	2927(9)	-467(4)	92(3)
O(28)	1	9419(5)	320(9)	-1325(4)	168(3)
C(29)	1	9505(8)	970(13)	-1898(6)	192(6)
C(31)	1	7902(4)	1514(7)	1905(3)	59(2)
C(32)	1	8239(4)	309(7)	2183(3)	73(2)
C(33)	1	8787(4)	333(8)	2792(4)	83(3)
C(34)	1	9002(4)	1539(9)	3121(4)	78(2)
C(35)	1	8655(4)	2738(8)	2866(3)	77(2)
C(36)	1	8100(4)	2752(7)	2244(3)	70(2)
C(41)	0.50	8101(6)	7047(11)	544(5)	105(5)
C(42)	0.50	8830(6)	6539(14)	498(6)	129(6)
C(43)	0.50	9323(6)	5951(16)	1063(7)	125(6)
C(44)	0.50	9088(8)	5870(15)	1674(6)	138(7)
C(45)	0.50	8359(9)	6379(15)	1720(5)	117(6)
C(46)	0.50	7865(6)	6967(13)	1154(5)	107(6)
C(47)	0.50	7601(9)	7693(18)	-60(7)	138(7)
C(51)	0.50	9007(8)	6310(20)	619(7)	137(7)
C(52)	0.50	9295(10)	5880(30)	1279(7)	149(7)
C(53)	0.50	8844(9)	6140(30)	1761(8)	147(7)
C(54)	0.50	8109(10)	6640(20)	1479(8)	123(6)
C(55)	0.50	7835(10)	7120(20)	837(8)	140(7)
C(56)	0.50	8288(9)	6910(20)	360(8)	139(7)
C(57)	0.50	9518(13)	5920(30)	152(12)	280(14)
C(61)	0.50	6086(9)	1219(19)	7299(8)	152(6)
C(62)	0.50	6566(9)	1130(20)	6834(9)	163(7)
C(63)	0.50	7224(11)	280(20)	7042(9)	186(8)
C(64)	0.50	7315(11)	-400(20)	7653(9)	181(8)
C(65)	0.50	6844(10)	-430(20)	8091(10)	178(8)
C(66)	0.50	6179(11)	390(20)	7868(9)	165(7)

C(67)	0.50	5374 (12)	2050 (30)	7006 (13)	223 (12)
C(71)	0.50	7008 (10)	210 (20)	7352 (9)	190 (7)
C(72)	0.50	6873 (11)	1050 (20)	6772 (10)	184 (8)
C(73)	0.50	6187 (10)	1830 (20)	6630 (9)	172 (7)
C(74)	0.50	5771 (13)	1900 (20)	7126 (10)	186 (8)
C(75)	0.50	5896 (10)	1060 (20)	7670 (10)	141 (7)
C(76)	0.50	6588 (11)	290 (20)	7850 (10)	155 (7)
C(77)	0.50	7608 (17)	-860 (30)	7364 (17)	290 (14)

Table 3. Hydrogen coordinates ($\times 10^4$) and isotropic displacement parameters ($\text{\AA}^2 \times 10^3$) for C74 H76 Cl2 N2 O4 Pd2.

	Occ.	x	y	z	U_{eq}
H(1)	1	6907	1464	-256	70
H(12)	1	6433	2856	-1161	87
H(13)	1	5948	4950	-1637	104
H(15)	1	5764	6291	195	107
H(16)	1	6255	4221	665	96
H(17A)	1	5406	7157	-1585	191
H(17B)	1	5805	7944	-908	191
H(17C)	1	4944	7349	-1002	191
H(21A)	1	7908	3826	503	88
H(21B)	1	8444	2884	1060	88
H(23)	1	8690	498	602	126
H(24)	1	9244	-545	-179	151
H(26)	1	8782	2858	-1359	134
H(27)	1	8195	3810	-540	110
H(29A)	1	9000	1309	-2145	288
H(29B)	1	9714	328	-2180	288
H(29C)	1	9865	1738	-1777	288
H(32)	1	8097	-533	1958	87
H(33)	1	9013	-497	2982	99
H(34)	1	9391	1545	3526	94
H(35)	1	8787	3564	3107	92
H(36)	1	7868	3583	2062	84
H(42)	0.50	8990	6593	85	155
H(43)	0.50	9816	5607	1033	150
H(44)	0.50	9421	5473	2057	166
H(45)	0.50	8199	6324	2133	140
H(46)	0.50	7373	7311	1185	129
H(47A)	0.50	7925	8223	-299	206
H(47B)	0.50	7225	8299	78	206
H(47C)	0.50	7324	6983	-359	206
H(52)	0.50	9779	5416	1403	179
H(53)	0.50	9027	5984	2229	177
H(54)	0.50	7752	6659	1764	148
H(55)	0.50	7351	7576	717	168
H(56)	0.50	8118	7161	-99	167
H(57A)	0.50	9201	5511	-256	420
H(57B)	0.50	9911	5269	375	420
H(57C)	0.50	9775	6743	31	420
H(62)	0.50	6458	1608	6418	195
H(63)	0.50	7592	174	6771	223
H(64)	0.50	7776	-926	7782	218
H(65)	0.50	6949	-933	8498	214
H(66)	0.50	5782	379	8113	197
H(67A)	0.50	4919	1627	7123	334
H(67B)	0.50	5299	2085	6516	334
H(67C)	0.50	5440	2978	7189	334
H(72)	0.50	7232	1082	6490	221
H(73)	0.50	6018	2286	6212	206
H(74)	0.50	5377	2574	7085	223
H(75)	0.50	5516	986	7930	170
H(76)	0.50	6752	-144	8275	186

H(77A)	0.50	7537	-1589	7671	434
H(77B)	0.50	8125	-456	7518	434
H(77C)	0.50	7556	-1229	6911	434

Table 4. Anisotropic parameters ($\text{\AA}^2 \times 10^3$) for C74 H76 Cl2 N2 O4 Pd2.

The anisotropic displacement factor exponent takes the form:

$$-2 \pi^2 [h^2 a^{*2} U_{11} + \dots + 2 h k a^* b^* U_{12}]$$

	U11	U22	U33	U23	U13	U12
Pd	52(1)	62(1)	48(1)	6(1)	-25(1)	-13(1)
Cl	64(1)	79(1)	53(1)	16(1)	-26(1)	-21(1)
C(1)	58(4)	61(4)	44(4)	-8(3)	-13(3)	-8(3)
N(2)	51(3)	77(4)	49(4)	7(3)	-13(3)	-22(3)
C(3)	57(4)	62(4)	47(4)	-9(4)	-16(4)	-12(4)
O(4)	53(3)	74(3)	49(3)	9(2)	-20(2)	-23(2)
C(11)	57(4)	64(5)	54(5)	-4(4)	-11(4)	-8(4)
C(12)	75(5)	70(5)	60(5)	1(4)	-9(4)	-2(4)
C(13)	89(6)	90(6)	67(5)	17(5)	-12(5)	-4(5)
C(14)	81(5)	63(5)	96(6)	1(5)	-3(5)	-4(4)
C(15)	102(6)	70(6)	91(7)	-17(5)	14(5)	2(5)
C(16)	89(5)	71(6)	74(5)	7(4)	7(5)	5(4)
C(17)	130(8)	72(6)	159(9)	33(6)	-11(7)	8(6)
C(21)	65(5)	92(5)	53(5)	4(4)	-6(4)	-19(4)
C(22)	63(5)	76(5)	62(5)	10(4)	-4(4)	-16(4)
C(23)	89(6)	142(9)	85(7)	8(6)	22(5)	-17(6)
C(24)	116(9)	144(9)	116(9)	17(7)	25(8)	5(7)
C(25)	88(6)	155(9)	106(8)	-47(7)	31(6)	-42(6)
C(26)	117(7)	124(8)	89(7)	10(6)	15(6)	-39(6)
C(27)	93(6)	105(6)	77(6)	-10(5)	16(5)	-25(5)
O(28)	142(6)	221(8)	155(7)	-83(6)	61(5)	-51(6)
C(29)	224(13)	265(15)	117(8)	-87(9)	103(9)	-89(11)
C(31)	49(4)	61(4)	54(4)	-6(4)	-13(4)	-4(4)
C(32)	70(5)	68(5)	65(5)	-14(4)	-15(4)	-4(4)
C(33)	76(5)	83(6)	67(5)	2(4)	-29(5)	6(4)
C(34)	61(5)	101(6)	56(5)	-9(5)	-19(4)	1(5)
C(35)	67(5)	90(6)	55(5)	-25(4)	-22(4)	-17(4)
C(36)	62(5)	67(5)	68(5)	-7(4)	-13(4)	0(4)
C(41)	112(9)	105(9)	124(10)	-37(9)	77(8)	-43(8)
C(42)	123(11)	117(10)	155(11)	-31(9)	46(9)	-29(9)
C(43)	133(10)	119(10)	132(11)	-9(9)	48(9)	-50(9)
C(44)	141(11)	115(11)	168(11)	-24(10)	53(10)	-26(9)
C(45)	112(10)	88(9)	150(11)	-29(9)	26(9)	-7(9)
C(46)	127(10)	80(9)	115(10)	-10(9)	29(9)	-33(8)
C(47)	130(12)	123(12)	152(13)	2(11)	14(11)	-37(10)
C(51)	138(11)	128(10)	152(11)	-21(10)	46(10)	-44(10)
C(52)	153(11)	133(11)	166(12)	-16(10)	43(10)	-49(10)
C(53)	146(12)	121(11)	179(12)	-16(10)	43(10)	-25(10)
C(54)	120(11)	93(10)	147(11)	-26(9)	11(10)	-10(9)
C(55)	151(11)	121(10)	152(12)	-35(10)	40(10)	-40(10)
C(56)	138(11)	125(11)	160(11)	-27(10)	42(10)	-29(10)
C(57)	276(19)	269(19)	290(20)	-16(14)	59(15)	-26(14)
C(61)	148(10)	141(10)	164(11)	-14(9)	31(9)	-11(9)
C(62)	161(11)	159(11)	163(11)	-8(10)	24(10)	-5(10)
C(63)	181(12)	179(12)	189(12)	-27(11)	26(10)	1(11)
C(64)	173(12)	163(12)	193(12)	-20(11)	9(11)	15(10)
C(65)	165(13)	170(13)	194(13)	-7(11)	27(11)	-17(11)
C(66)	156(12)	163(12)	174(12)	-21(10)	37(10)	-5(11)

C(67)	218(17)	192(16)	251(18)	-22(14)	39(14)	-10(14)
C(71)	182(12)	178(11)	200(12)	-18(11)	24(10)	-2(10)
C(72)	192(12)	178(12)	177(12)	-13(11)	28(11)	-9(11)
C(73)	184(12)	165(12)	166(12)	5(11)	39(10)	-13(11)
C(74)	182(13)	172(13)	193(13)	-8(11)	22(11)	-21(11)
C(75)	152(11)	145(11)	131(11)	-16(10)	42(10)	-33(10)
C(76)	157(11)	154(11)	155(11)	-8(10)	36(10)	-13(10)
C(77)	287(19)	277(19)	288(19)	-8(14)	30(14)	-8(14)

Table 5. Bond lengths [Å] and angles [°] for C74 H76 Cl2 N2 O4 Pd2

Pd-C(1)	1.976(6)	C(72)-C(73)	1.394(15)
Pd-O(4)	2.028(4)	C(73)-C(74)	1.367(16)
Pd-Cl#1	2.3198(16)	C(74)-C(75)	1.350(15)
Pd-Cl	2.4655(18)	C(75)-C(76)	1.400(15)
Cl-Pd#1	2.3198(16)		
C(1)-C(11)	1.490(8)	C(1)-Pd-O(4)	83.6(2)
C(1)-N(2)	1.519(7)	C(1)-Pd-Cl#1	94.29(17)
N(2)-C(3)	1.312(8)	O(4)-Pd-Cl#1	177.77(13)
N(2)-C(21)	1.479(8)	C(1)-Pd-Cl	178.11(18)
C(3)-O(4)	1.264(7)	O(4)-Pd-Cl	95.19(13)
C(3)-C(31)	1.498(8)	Cl#1-Pd-Cl	86.92(6)
C(11)-C(16)	1.372(10)	Pd#1-Cl-Pd	93.08(6)
C(11)-C(12)	1.389(9)	C(11)-C(1)-N(2)	111.1(5)
C(12)-C(13)	1.395(10)	C(11)-C(1)-Pd	115.7(5)
C(13)-C(14)	1.371(11)	N(2)-C(1)-Pd	106.4(4)
C(14)-C(15)	1.389(11)	C(3)-N(2)-C(21)	126.6(5)
C(14)-C(17)	1.536(10)	C(3)-N(2)-C(1)	116.6(5)
C(15)-C(16)	1.380(9)	C(21)-N(2)-C(1)	116.3(5)
C(21)-C(22)	1.444(10)	O(4)-C(3)-N(2)	121.6(5)
C(22)-C(27)	1.343(10)	O(4)-C(3)-C(31)	117.7(6)
C(22)-C(23)	1.357(10)	N(2)-C(3)-C(31)	120.7(6)
C(23)-C(24)	1.353(12)	C(3)-O(4)-Pd	111.8(4)
C(24)-C(25)	1.391(14)	C(16)-C(11)-C(12)	117.8(7)
C(25)-O(28)	1.397(12)	C(16)-C(11)-C(1)	123.2(6)
C(25)-C(26)	1.406(12)	C(12)-C(11)-C(1)	119.0(6)
C(26)-C(27)	1.395(12)	C(11)-C(12)-C(13)	120.6(7)
O(28)-C(29)	1.356(12)	C(14)-C(13)-C(12)	120.9(7)
C(31)-C(32)	1.372(9)	C(13)-C(14)-C(15)	118.5(7)
C(31)-C(36)	1.387(9)	C(13)-C(14)-C(17)	120.6(8)
C(32)-C(33)	1.380(9)	C(15)-C(14)-C(17)	120.9(8)
C(33)-C(34)	1.356(10)	C(16)-C(15)-C(14)	120.3(8)
C(34)-C(35)	1.359(9)	C(11)-C(16)-C(15)	121.9(8)
C(35)-C(36)	1.404(8)	C(22)-C(21)-N(2)	112.9(6)
C(41)-C(42)	1.39	C(27)-C(22)-C(23)	117.9(9)
C(41)-C(46)	1.39	C(27)-C(22)-C(21)	122.2(8)
C(41)-C(47)	1.472(14)	C(23)-C(22)-C(21)	119.8(8)
C(42)-C(43)	1.39	C(24)-C(23)-C(22)	122.7(1)
C(43)-C(44)	1.39	C(23)-C(24)-C(25)	120.40(11)
C(44)-C(45)	1.39	C(24)-C(25)-O(28)	118.00(11)
C(45)-C(46)	1.39	C(24)-C(25)-C(26)	117.7(1)
C(51)-C(56)	1.379(14)	O(28)-C(25)-C(26)	124.3(1)
C(51)-C(52)	1.381(14)	C(27)-C(26)-C(25)	118.4(9)
C(51)-C(57)	1.488(18)	C(22)-C(27)-C(26)	122.6(9)
C(52)-C(53)	1.410(15)	C(29)-O(28)-C(25)	119.6(1)
C(53)-C(54)	1.374(15)	C(32)-C(31)-C(36)	119.9(6)
C(54)-C(55)	1.359(15)	C(32)-C(31)-C(3)	118.5(6)
C(55)-C(56)	1.394(15)	C(36)-C(31)-C(3)	121.4(6)
C(61)-C(66)	1.383(15)	C(31)-C(32)-C(33)	119.9(6)
C(61)-C(62)	1.398(15)	C(34)-C(33)-C(32)	120.8(7)
C(61)-C(67)	1.490(17)	C(33)-C(34)-C(35)	120.1(6)
C(62)-C(63)	1.404(15)	C(34)-C(35)-C(36)	120.5(7)
C(63)-C(64)	1.379(15)	C(31)-C(36)-C(35)	118.6(6)
C(64)-C(65)	1.340(15)	C(42)-C(41)-C(46)	120
C(65)-C(66)	1.398(15)	C(42)-C(41)-C(47)	118.6(6)
C(71)-C(76)	1.376(15)	C(46)-C(41)-C(47)	121.4(6)
C(71)-C(72)	1.402(15)	C(41)-C(42)-C(43)	120
C(71)-C(77)	1.472(18)	C(42)-C(43)-C(44)	120

C(45)-C(44)-C(43)	120	C(64)-C(63)-C(62)	118.10(15)
C(44)-C(45)-C(46)	120	C(65)-C(64)-C(63)	129.70(16)
C(45)-C(46)-C(41)	120	C(64)-C(65)-C(66)	111.60(15)
C(56)-C(51)-C(52)	126.80(13)	C(61)-C(66)-C(65)	122.10(16)
C(56)-C(51)-C(57)	119.50(14)	C(76)-C(71)-C(72)	124.40(15)
C(52)-C(51)-C(57)	113.40(15)	C(76)-C(71)-C(77)	121.40(17)
C(51)-C(52)-C(53)	118.20(14)	C(72)-C(71)-C(77)	114.00(17)
C(54)-C(53)-C(52)	113.30(14)	C(73)-C(72)-C(71)	117.50(15)
C(55)-C(54)-C(53)	127.70(15)	C(74)-C(73)-C(72)	116.90(15)
C(54)-C(55)-C(56)	118.70(15)	C(75)-C(74)-C(73)	123.50(17)
C(51)-C(56)-C(55)	114.20(14)	C(74)-C(75)-C(76)	120.50(16)
C(66)-C(61)-C(62)	123.40(14)	C(71)-C(76)-C(75)	114.30(15)
C(66)-C(61)-C(67)	125.10(16)		
C(62)-C(61)-C(67)	109.90(14)		
C(61)-C(62)-C(63)	114.30(14)		

Symmetry transformations used to generate equivalent atoms:

#1 -x+1,-y,-z

Table 6. Torsion angles [$^{\circ}$] for C74 H76 Cl2 N2 O4 Pd2.

C(1)-PD-CL-PD#1	-129(5)	C(3)-C(31)-C(32)-C(33)	-176.5(7)
O(4)-PD-CL-PD#1	179.29(13)	C(31)-C(32)-C(33)-C(34)	-0.40(12)
CL#1-PD-CL-PD#1	0	C(32)-C(33)-C(34)-C(35)	2.70(12)
O(4)-PD-C(1)-C(11)	-125.0(5)	C(33)-C(34)-C(35)-C(36)	-3.20(12)
CL#1-PD-C(1)-C(11)	54.2(5)	C(32)-C(31)-C(36)-C(35)	0.80(11)
CL-PD-C(1)-C(11)	-176(100)	C(3)-C(31)-C(36)-C(35)	175.8(7)
O(4)-PD-C(1)-N(2)	-1.1(4)	C(34)-C(35)-C(36)-C(31)	1.40(11)
CL#1-PD-C(1)-N(2)	178.1(4)	C(46)-C(41)-C(42)-C(43)	0
CL-PD-C(1)-N(2)	-52(6)	C(47)-C(41)-C(42)-C(43)	178.60(11)
C(11)-C(1)-N(2)-C(3)	127.9(6)	C(41)-C(42)-C(43)-C(44)	0
PD-C(1)-N(2)-C(3)	1.2(7)	C(42)-C(43)-C(44)-C(45)	0
C(11)-C(1)-N(2)-C(21)	-59.7(8)	C(43)-C(44)-C(45)-C(46)	0
PD-C(1)-N(2)-C(21)	173.6(5)	C(44)-C(45)-C(46)-C(41)	0
C(21)-N(2)-C(3)-O(4)	-172.0(6)	C(42)-C(41)-C(46)-C(45)	0
C(1)-N(2)-C(3)-O(4)	-0.4(1)	C(47)-C(41)-C(46)-C(45)	-178.50(11)
C(21)-N(2)-C(3)-C(31)	7.20(11)	C(56)-C(51)-C(52)-C(53)	-5(4)
C(1)-N(2)-C(3)-C(31)	178.8(6)	C(57)-C(51)-C(52)-C(53)	-178(2)
N(2)-C(3)-O(4)-PD	-0.6(8)	C(51)-C(52)-C(53)-C(54)	9(3)
C(31)-C(3)-O(4)-PD	-179.8(5)	C(52)-C(53)-C(54)-C(55)	-12(4)
C(1)-PD-O(4)-C(3)	1.0(5)	C(53)-C(54)-C(55)-C(56)	10(4)
CL#1-PD-O(4)-C(3)	-19(4)	C(52)-C(51)-C(56)-C(55)	2(4)
CL-PD-O(4)-C(3)	179.5(4)	C(57)-C(51)-C(56)-C(55)	175(2)
N(2)-C(1)-C(11)-C(16)	-49.7(9)	C(54)-C(55)-C(56)-C(51)	-4(3)
PD-C(1)-C(11)-C(16)	71.6(7)	C(66)-C(61)-C(62)-C(63)	-9(3)
N(2)-C(1)-C(11)-C(12)	132.1(6)	C(67)-C(61)-C(62)-C(63)	-175(2)
PD-C(1)-C(11)-C(12)	-106.5(6)	C(61)-C(62)-C(63)-C(64)	2(3)
C(16)-C(11)-C(12)-C(13)	0.1(1)	C(62)-C(63)-C(64)-C(65)	3(4)
C(1)-C(11)-C(12)-C(13)	178.3(6)	C(63)-C(64)-C(65)-C(66)	-1(4)
C(11)-C(12)-C(13)-C(14)	-0.90(11)	C(62)-C(61)-C(66)-C(65)	12(3)
C(12)-C(13)-C(14)-C(15)	1.40(12)	C(67)-C(61)-C(66)-C(65)	176(2)
C(12)-C(13)-C(14)-C(17)	-179.0(7)	C(64)-C(65)-C(66)-C(61)	-6(3)
C(13)-C(14)-C(15)-C(16)	-1.10(13)	C(76)-C(71)-C(72)-C(73)	-12(4)
C(17)-C(14)-C(15)-C(16)	179.3(8)	C(77)-C(71)-C(72)-C(73)	163(2)
C(12)-C(11)-C(16)-C(15)	0.20(11)	C(71)-C(72)-C(73)-C(74)	11(3)
C(1)-C(11)-C(16)-C(15)	-177.9(7)	C(72)-C(73)-C(74)-C(75)	-14(4)
C(14)-C(15)-C(16)-C(11)	0.30(13)	C(73)-C(74)-C(75)-C(76)	16(4)
C(3)-N(2)-C(21)-C(22)	114.8(8)	C(72)-C(71)-C(76)-C(75)	13(4)
C(1)-N(2)-C(21)-C(22)	-56.8(8)	C(77)-C(71)-C(76)-C(75)	-162(2)
N(2)-C(21)-C(22)-C(27)	114.6(8)	C(74)-C(75)-C(76)-C(71)	-15(3)
N(2)-C(21)-C(22)-C(23)	-63.9(9)		
C(27)-C(22)-C(23)-C(24)	1.00(13)		
C(21)-C(22)-C(23)-C(24)	179.5(8)		
C(22)-C(23)-C(24)-C(25)	-0.50(14)		
C(23)-C(24)-C(25)-O(28)	179.8(8)		
C(23)-C(24)-C(25)-C(26)	0.80(14)		
C(24)-C(25)-C(26)-C(27)	-1.70(13)		
O(28)-C(25)-C(26)-C(27)	179.4(8)		
C(23)-C(22)-C(27)-C(26)	-2.00(12)		
C(21)-C(22)-C(27)-C(26)	179.5(7)		
C(25)-C(26)-C(27)-C(22)	2.40(13)		
C(24)-C(25)-O(28)-C(29)	-175.9(1)		
C(26)-C(25)-O(28)-C(29)	3.00(14)		
O(4)-C(3)-C(31)-C(32)	56.5(9)		
N(2)-C(3)-C(31)-C(32)	-122.7(8)		
O(4)-C(3)-C(31)-C(36)	-118.6(8)		
N(2)-C(3)-C(31)-C(36)	62.2(1)		
C(36)-C(31)-C(32)-C(33)	-1.30(11)		

Symmetry transformations used to generate equivalent atoms:

#1 $-x+1, -y, -z$

ORTEP view of the C₇₄ H₇₆ Cl₂ N₂ O₄ Pd₂ compound with the numbering scheme adopted. Ellipsoids drawn at 30% probability level. Hydrogens represented by sphere of arbitrary size.

REFERENCES

International Tables for Crystallography (1992). Vol. C. Tables 4.2.6.8 and 6.1.1.4, Dordrecht: Kluwer Academic Publishers.

SAINT (1999) Release 6.06; Integration Software for Single Crystal Data. Bruker AXS Inc., Madison, WI 53719-1173.

Sheldrick, G.M. (1996). SADABS, Bruker Area Detector Absorption Corrections. Bruker AXS Inc., Madison, WI 53719-1173.

Sheldrick, G.M. (1997). SHELXS97, Program for the Solution of Crystal Structures. Univ. of Gottingen, Germany.

Sheldrick, G.M. (1997). SHELXL97, Program for the Refinement of Crystal Structures. Univ. of Gottingen, Germany.

SHELXTL (1997) Release 5.10; The Complete Software Package for Single Crystal Structure Determination. Bruker AXS Inc., Madison, WI 53719-1173.

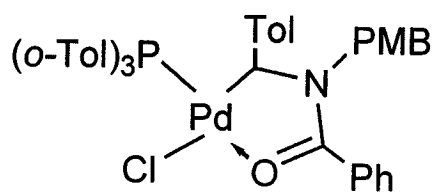
SMART (1999) Release 5.059; Bruker Molecular Analysis Research Tool. Bruker AXS Inc., Madison, WI 53719-1173.

Spek, A.L. (2000). PLATON, Molecular Geometry Program, 2000 version. University of Utrecht, Utrecht, Holland.

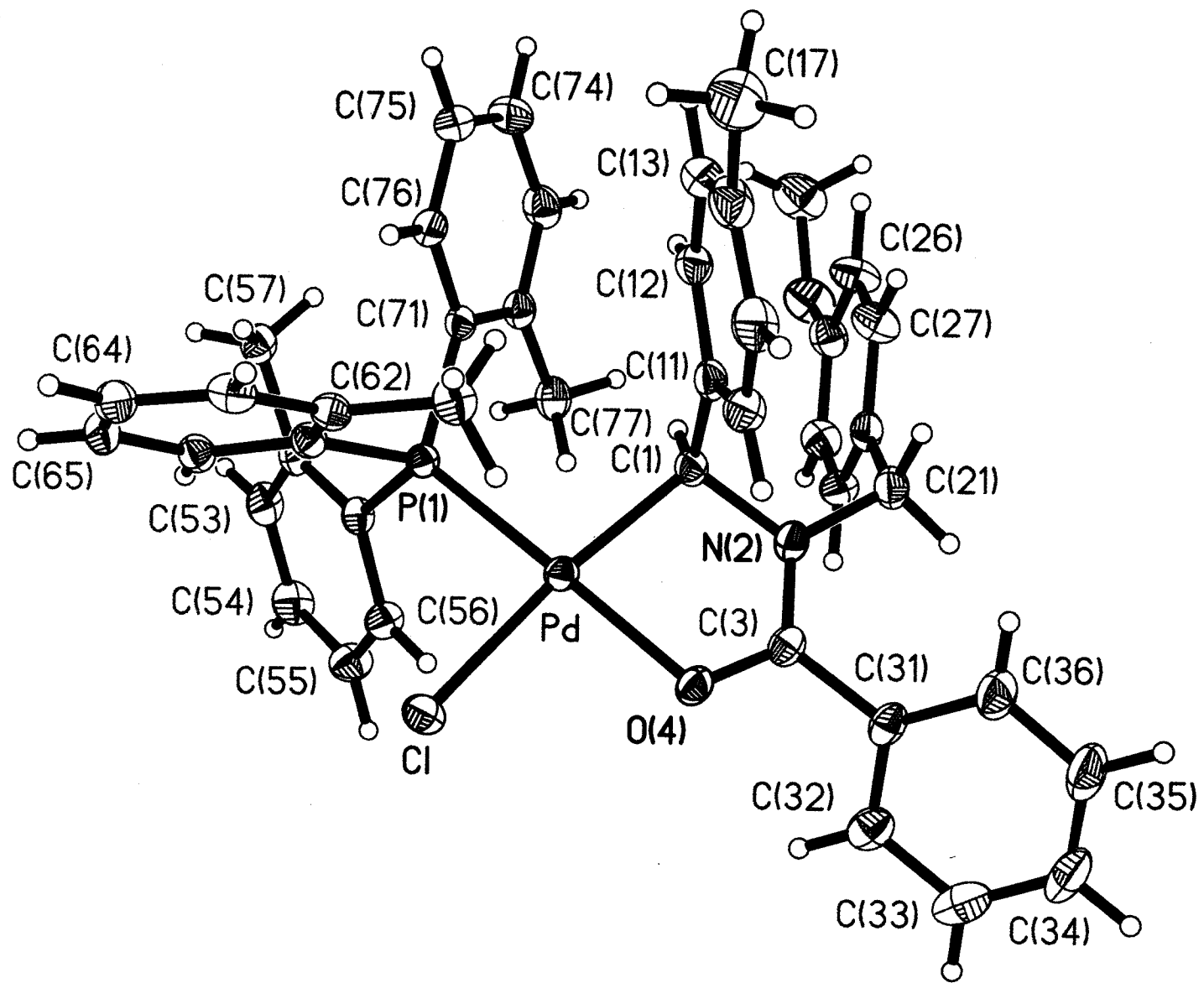
XPREP (1997) Release 5.10; X-ray data Preparation and Reciprocal space Exploration Program. Bruker AXS Inc., Madison, WI 53719-1173.

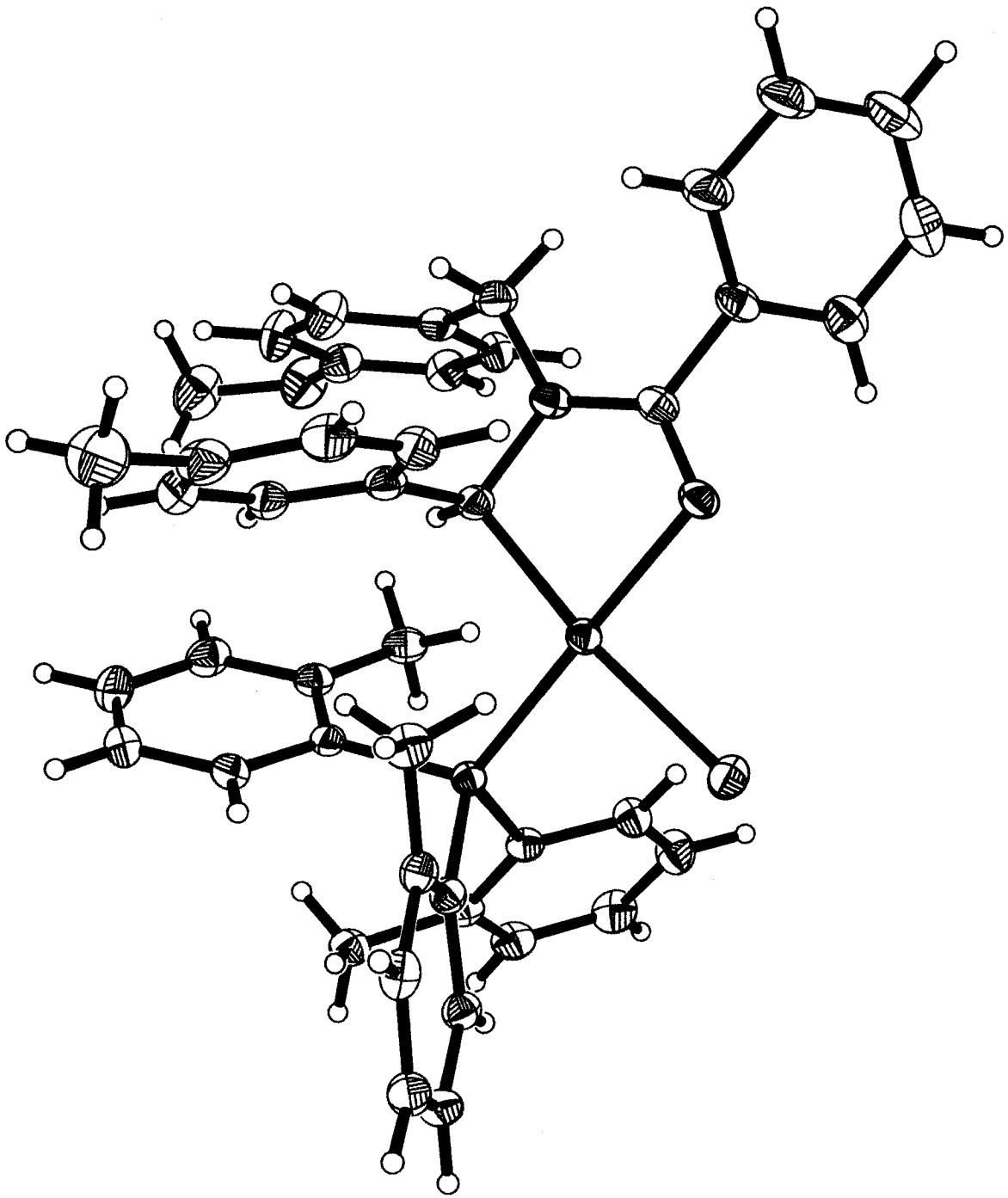
Appendix D

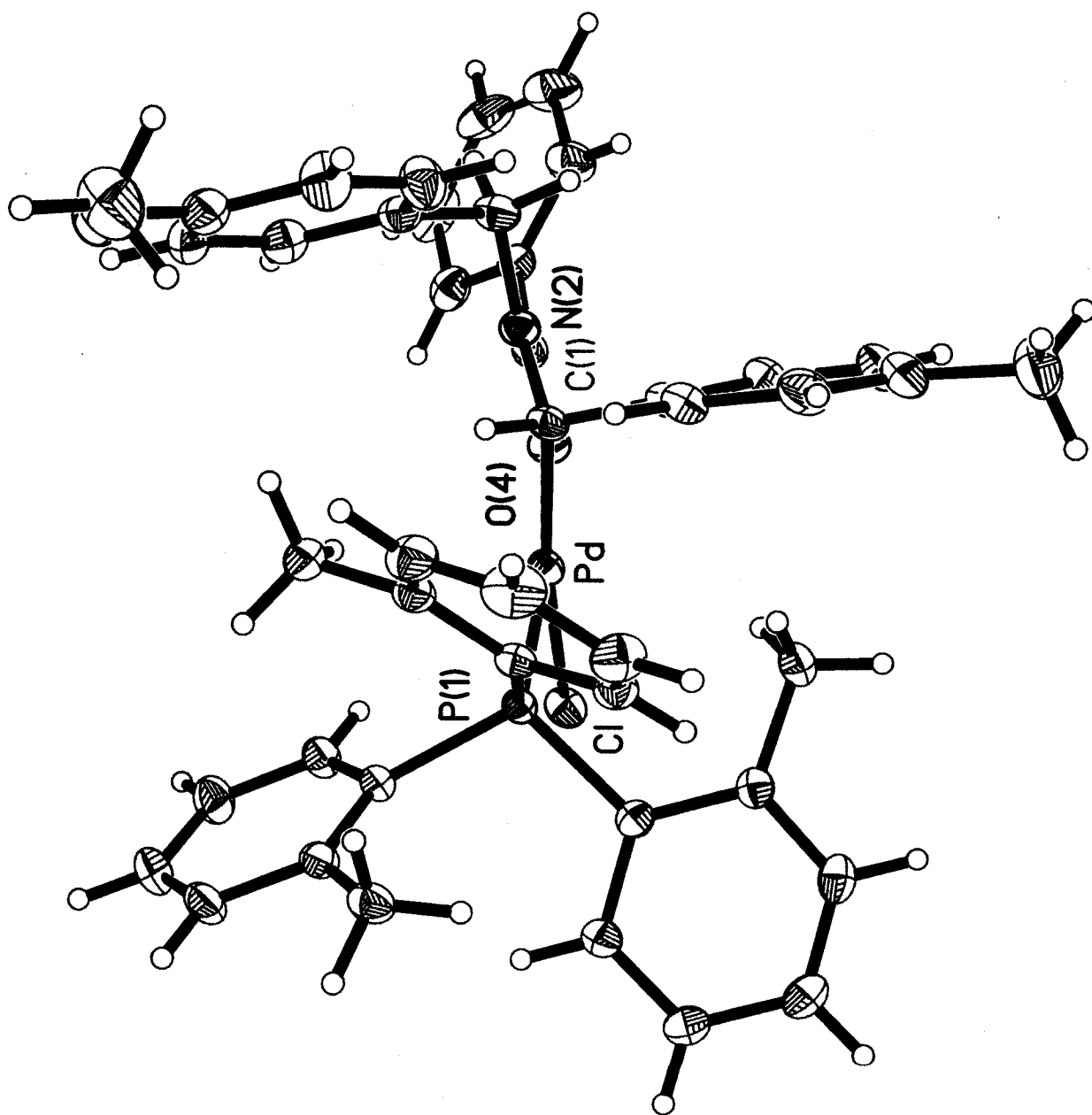
X-ray Structural Data for Complex 6.14b

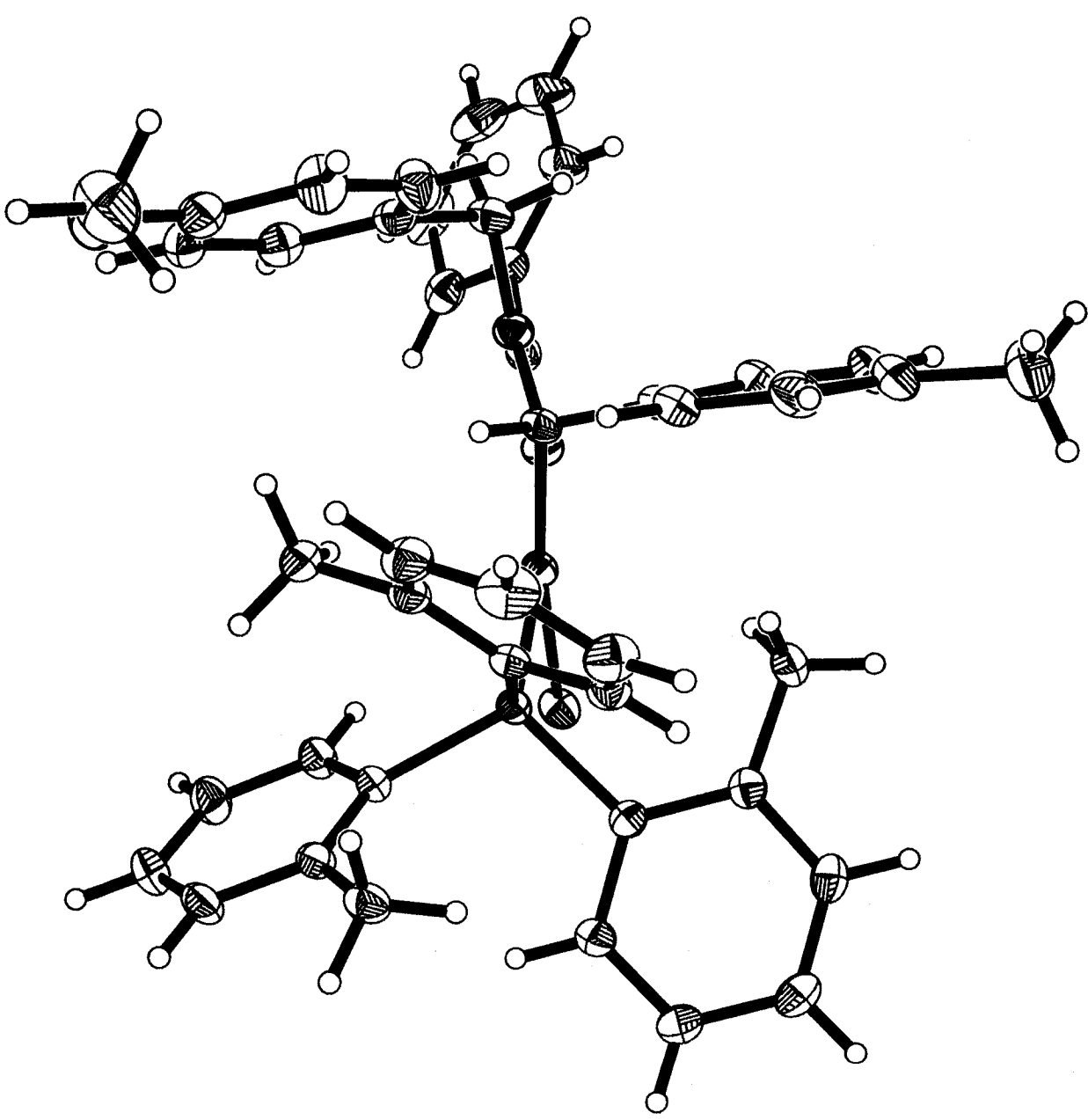


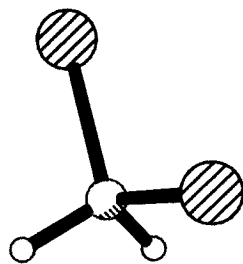
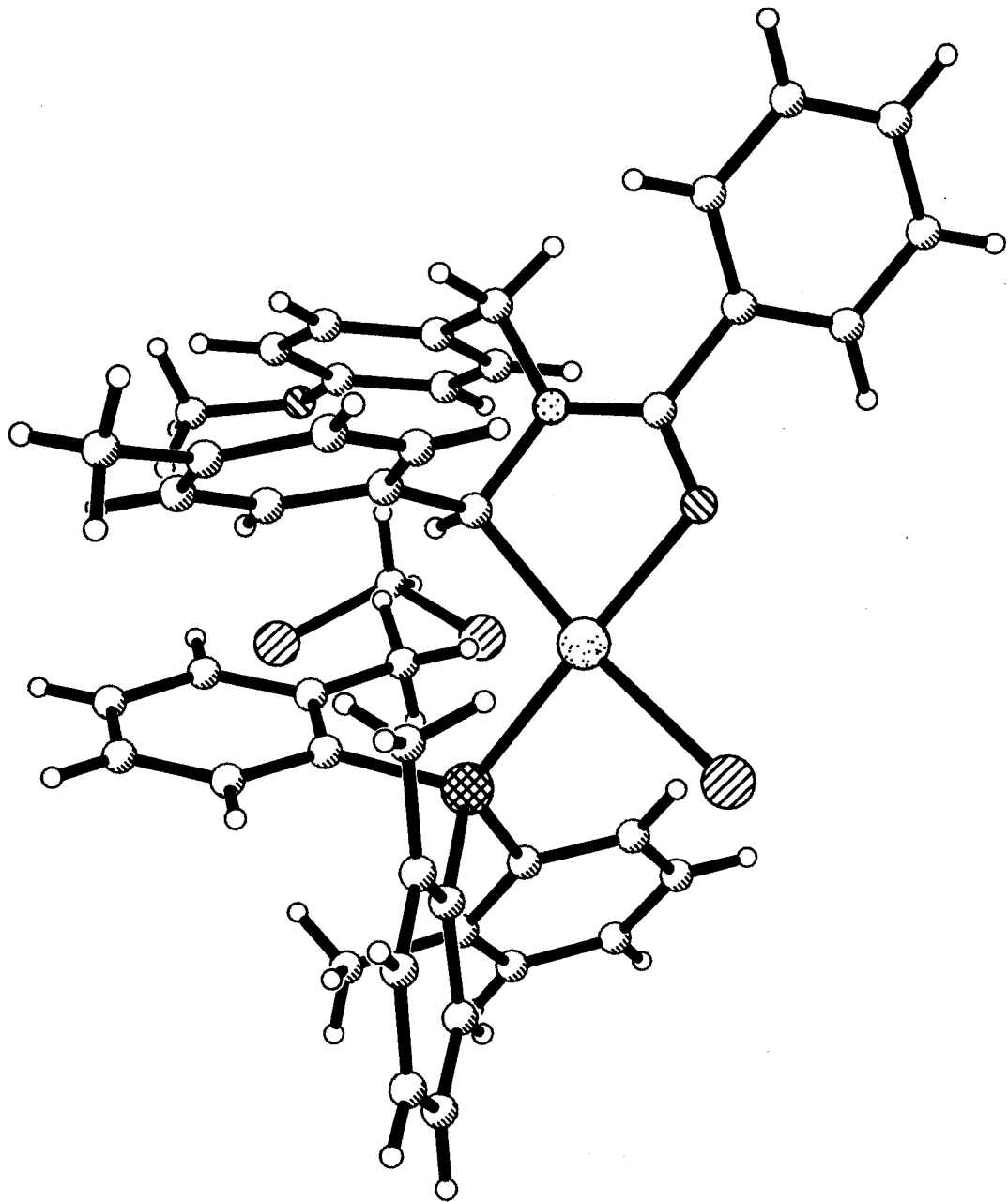
PMB = p-C₆H₄-OCH₃
Tol = p-C₆H₄-CH₃











CRYSTAL AND MOLECULAR STRUCTURE OF
C46 H47 Cl5 N O2 P Pd COMPOUND (arst30)

Saturday, August 21, 2004

Equipe Dr Arndtsen

Department of Chemistry, Otto Maass Chemistry Building
McGill University, Montréal, Québec (Canada) H3A 2K6

Structure solved and refined in the laboratory of X-ray diffraction
Université de Montréal by Francine Bélanger-Gariépy.

Table 1. Crystal data and structure refinement for C₄₆ H₄₇ Cl₅ N O₂ P Pd.

Identification code	arst30
Empirical formula	C ₄₆ H ₄₇ Cl ₅ N O ₂ P Pd
Formula weight	960.47
Temperature	220(2)K
Wavelength	1.54178 Å
Crystal system	Monoclinic
Space group	P21/n
Unit cell dimensions	a = 16.1433(3) Å $\alpha = 90^\circ$ b = 16.4443(4) Å $\beta = 96.4340(10)^\circ$ c = 16.6678(4) Å $\gamma = 90^\circ$
Volume	4396.85(17) Å ³
Z	4
Density (calculated)	1.451 Mg/m ³
Absorption coefficient	6.844 mm ⁻¹
F(000)	1968
Crystal size	0.50 x 0.28 x 0.28 mm
Theta range for data collection	3.61 to 72.98°
Index ranges	-19 ≤ h ≤ 19, -20 ≤ k ≤ 18, -20 ≤ l ≤ 20
Reflections collected	35618
Independent reflections	8663 [R _{int} = 0.034]
Absorption correction	Semi-empirical from equivalents
Max. and min. transmission	0.3400 and 0.1400
Refinement method	Full-matrix least-squares on F ²
Data / restraints / parameters	8663 / 0 / 510
Goodness-of-fit on F ²	1.041
Final R indices [I > 2σ(I)]	R ₁ = 0.0448, wR ₂ = 0.1149
R indices (all data)	R ₁ = 0.0518, wR ₂ = 0.1184

Largest diff. peak and hole

1.268 and $-0.580 \text{ e}/\text{\AA}^3$

Table 2. Atomic coordinates ($\times 10^4$) and equivalent isotropic displacement parameters ($\text{\AA}^2 \times 10^3$) for C46 H47 Cl5 N O2 P Pd.

U_{eq} is defined as one third of the trace of the orthogonalized U_{ij} tensor.

	x	y	z	U_{eq}
Pd	6219(1)	6265(1)	3715(1)	29(1)
Cl	6452(1)	6568(1)	5133(1)	41(1)
C(1)	5817(2)	6061(2)	2521(2)	33(1)
N(2)	5379(2)	6826(2)	2232(2)	36(1)
C(3)	5157(2)	7343(2)	2779(2)	36(1)
O(4)	5390(1)	7230(1)	3519(1)	37(1)
C(11)	5227(2)	5351(2)	2402(2)	35(1)
C(12)	5444(2)	4655(2)	2000(2)	39(1)
C(13)	4932(2)	3972(2)	1948(2)	49(1)
C(14)	4182(2)	3967(3)	2284(3)	54(1)
C(15)	3948(2)	4678(2)	2653(2)	52(1)
C(16)	4454(2)	5353(2)	2707(2)	43(1)
C(17)	3647(3)	3210(3)	2257(3)	77(1)
C(21)	5144(2)	6883(2)	1352(2)	42(1)
C(22)	5871(2)	6748(2)	877(2)	38(1)
C(23)	6521(2)	7300(2)	916(2)	42(1)
C(24)	7180(2)	7190(2)	465(2)	46(1)
C(25)	7204(2)	6526(2)	-27(2)	46(1)
C(26)	6561(3)	5965(3)	-82(2)	54(1)
C(27)	5894(2)	6090(2)	372(2)	52(1)
O(28)	7885(2)	6465(2)	-440(2)	62(1)
C(29)	8006(3)	5726(3)	-852(3)	77(1)
C(31)	4643(2)	8084(2)	2553(2)	38(1)
C(32)	4924(2)	8810(2)	2894(2)	47(1)
C(33)	4477(3)	9523(2)	2688(3)	64(1)
C(34)	3752(3)	9486(3)	2164(3)	68(1)
C(35)	3466(3)	8763(3)	1844(3)	67(1)
C(36)	3901(2)	8052(3)	2034(2)	54(1)
P(1)	7232(1)	5315(1)	3875(1)	27(1)
C(51)	8280(2)	5767(2)	4101(2)	31(1)
C(52)	9034(2)	5346(2)	4037(2)	35(1)
C(53)	9774(2)	5794(2)	4152(2)	44(1)
C(54)	9789(2)	6620(2)	4315(2)	49(1)
C(55)	9053(2)	7024(2)	4392(2)	47(1)
C(56)	8307(2)	6598(2)	4282(2)	39(1)
C(57)	9105(2)	4457(2)	3859(2)	41(1)
C(61)	7095(2)	4618(2)	4715(2)	31(1)
C(62)	6316(2)	4267(2)	4804(2)	34(1)
C(63)	6267(2)	3734(2)	5447(2)	40(1)
C(64)	6946(2)	3536(2)	5985(2)	43(1)
C(65)	7704(2)	3899(2)	5904(2)	41(1)
C(66)	7777(2)	4447(2)	5284(2)	35(1)
C(67)	5542(2)	4450(2)	4248(2)	42(1)
C(71)	7349(2)	4658(2)	3011(2)	30(1)
C(72)	7669(2)	4960(2)	2315(2)	35(1)
C(73)	7759(2)	4422(2)	1685(2)	46(1)
C(74)	7538(3)	3609(2)	1725(2)	55(1)
C(75)	7210(2)	3322(2)	2397(2)	48(1)

C(76)	7113(2)	3840(2)	3027(2)	37(1)
C(77)	7952(2)	5825(2)	2223(2)	43(1)
C1(81)	7038(1)	3660(1)	9553(1)	99(1)
C1(82)	7733(1)	3717(1)	8043(1)	97(1)
C(80)	7873(4)	3388(4)	9033(4)	93(2)
C1(91)	9576(1)	7225(1)	1357(1)	120(1)
C1(92)	10046(1)	5949(1)	304(1)	128(1)
C(90)	9756(3)	6969(3)	374(4)	86(2)

Table 3. Hydrogen coordinates ($\times 10^4$) and isotropic displacement parameters ($\text{\AA}^2 \times 10^3$) for C46 H47 Cl5 N O2 P Pd.

	x	y	z	U_{eq}
H(1)	6302	5968	2218	40
H(12)	5943	4647	1759	47
H(13)	5097	3506	1681	59
H(15)	3434	4697	2868	62
H(16)	4277	5826	2954	51
H(17A)	3771	2908	2756	115
H(17B)	3764	2873	1805	115
H(17C)	3063	3364	2192	115
H(21A)	4906	7421	1223	51
H(21B)	4713	6477	1190	51
H(23)	6515	7756	1254	51
H(24)	7614	7574	497	55
H(26)	6572	5507	-419	64
H(27)	5452	5715	332	62
H(29A)	8050	5280	-469	116
H(29B)	8514	5761	-1111	116
H(29C)	7536	5633	-1258	116
H(32)	5411	8827	3261	56
H(33)	4669	10025	2904	77
H(34)	3452	9966	2027	81
H(35)	2969	8747	1492	80
H(36)	3701	7553	1815	65
H(53)	10282	5524	4117	53
H(54)	10297	6904	4373	59
H(55)	9057	7582	4517	56
H(56)	7806	6876	4331	46
H(57A)	9025	4372	3280	61
H(57B)	8683	4160	4109	61
H(57C)	9654	4264	4074	61
H(63)	5748	3500	5517	48
H(64)	6896	3159	6400	52
H(65)	8172	3775	6271	49
H(66)	8290	4707	5245	42
H(67A)	5421	5027	4266	63
H(67B)	5078	4144	4417	63
H(67C)	5626	4297	3701	63
H(73)	7975	4615	1220	55
H(74)	7613	3256	1295	65
H(75)	7053	2773	2426	57
H(76)	6881	3640	3481	44
H(77A)	8539	5870	2420	64
H(77B)	7631	6183	2532	64
H(77C)	7869	5978	1658	64
H(80A)	8387	3625	9304	111
H(80B)	7935	2796	9043	111
H(90A)	10199	7316	206	104
H(90B)	9249	7069	6	104

Table 4. Anisotropic parameters ($\text{\AA}^2 \times 10^3$) for C46 H47 Cl5 N O2 P Pd.

The anisotropic displacement factor exponent takes the form:

$$-2 \pi^2 [h^2 a^{*2} U_{11} + \dots + 2 h k a^* b^* U_{12}]$$

	U11	U22	U33	U23	U13	U12
Pd	25(1)	30(1)	33(1)	-2(1)	3(1)	3(1)
Cl	38(1)	48(1)	38(1)	-9(1)	4(1)	0(1)
C(1)	27(1)	40(2)	32(1)	-3(1)	1(1)	6(1)
N(2)	31(1)	38(1)	37(1)	4(1)	2(1)	6(1)
C(3)	25(1)	37(2)	44(2)	3(1)	6(1)	4(1)
O(4)	36(1)	37(1)	40(1)	1(1)	5(1)	11(1)
C(11)	28(2)	43(2)	34(2)	1(1)	-2(1)	4(1)
C(12)	33(2)	43(2)	41(2)	-4(1)	-1(1)	3(1)
C(13)	49(2)	45(2)	51(2)	-7(2)	-6(2)	1(2)
C(14)	41(2)	56(2)	60(2)	4(2)	-9(2)	-10(2)
C(15)	30(2)	64(2)	61(2)	2(2)	2(2)	-4(2)
C(16)	30(2)	50(2)	48(2)	-4(2)	4(1)	4(1)
C(17)	60(3)	65(3)	103(4)	7(3)	-6(3)	-21(2)
C(21)	37(2)	52(2)	36(2)	0(1)	-2(1)	9(1)
C(22)	37(2)	42(2)	33(2)	5(1)	0(1)	6(1)
C(23)	50(2)	34(2)	43(2)	-1(1)	3(1)	2(1)
C(24)	46(2)	45(2)	46(2)	2(2)	5(2)	-8(2)
C(25)	46(2)	57(2)	36(2)	2(2)	6(1)	0(2)
C(26)	59(2)	56(2)	47(2)	-21(2)	15(2)	-8(2)
C(27)	49(2)	57(2)	49(2)	-11(2)	7(2)	-13(2)
O(28)	53(2)	79(2)	58(2)	-12(2)	21(1)	-7(1)
C(29)	61(3)	102(4)	71(3)	-28(3)	20(2)	5(3)
C(31)	32(2)	42(2)	43(2)	7(1)	13(1)	11(1)
C(32)	49(2)	46(2)	49(2)	4(2)	19(2)	6(2)
C(33)	91(3)	42(2)	66(3)	6(2)	38(3)	12(2)
C(34)	82(3)	67(3)	58(2)	25(2)	25(2)	44(2)
C(35)	53(2)	87(3)	60(3)	9(2)	7(2)	36(2)
C(36)	40(2)	63(2)	59(2)	1(2)	2(2)	16(2)
P(1)	24(1)	28(1)	30(1)	0(1)	2(1)	0(1)
C(51)	25(1)	36(2)	33(1)	2(1)	2(1)	-2(1)
C(52)	28(2)	45(2)	31(1)	3(1)	2(1)	2(1)
C(53)	24(2)	59(2)	48(2)	2(2)	2(1)	2(1)
C(54)	32(2)	57(2)	59(2)	-1(2)	1(2)	-12(2)
C(55)	41(2)	39(2)	61(2)	-5(2)	4(2)	-8(1)
C(56)	31(2)	37(2)	48(2)	-2(1)	4(1)	0(1)
C(57)	32(2)	47(2)	42(2)	0(1)	3(1)	8(1)
C(61)	33(2)	31(1)	29(1)	-1(1)	5(1)	1(1)
C(62)	34(2)	35(2)	32(1)	-3(1)	7(1)	-1(1)
C(63)	45(2)	38(2)	39(2)	-5(1)	15(1)	-9(1)
C(64)	59(2)	38(2)	33(2)	4(1)	10(2)	1(2)
C(65)	47(2)	44(2)	32(2)	3(1)	2(1)	3(1)
C(66)	33(2)	39(2)	33(2)	-2(1)	2(1)	2(1)
C(67)	30(2)	50(2)	47(2)	2(2)	5(1)	-6(1)
C(71)	27(1)	33(1)	30(1)	-1(1)	0(1)	5(1)
C(72)	30(2)	41(2)	34(2)	3(1)	1(1)	5(1)
C(73)	46(2)	59(2)	33(2)	0(2)	8(1)	6(2)
C(74)	66(3)	54(2)	43(2)	-16(2)	4(2)	11(2)
C(75)	61(2)	33(2)	48(2)	-4(2)	-2(2)	3(2)

C(76)	37(2)	34(2)	39(2)	2(1)	-1(1)	3(1)
C(77)	39(2)	51(2)	38(2)	9(1)	6(1)	0(1)
C1(81)	107(1)	121(1)	69(1)	3(1)	15(1)	-40(1)
C1(82)	142(2)	79(1)	74(1)	12(1)	28(1)	10(1)
C(80)	78(4)	94(4)	101(4)	38(3)	-14(3)	13(3)
C1(91)	105(1)	115(1)	138(2)	3(1)	4(1)	-20(1)
C1(92)	120(1)	62(1)	184(2)	0(1)	-59(1)	10(1)
C(90)	64(3)	59(3)	132(5)	17(3)	-11(3)	-8(2)

Table 5. Bond lengths [\AA] and angles [$^\circ$] for C46 H47 Cl5 N O2 P Pd

Pd-C(1)	2.050(3)	Cl(82)-C(80)	1.728(6)
Pd-O(4)	2.078(2)	Cl(91)-C(90)	1.747(7)
Pd-P(1)	2.2563(7)	Cl(92)-C(90)	1.748(5)
Pd-Cl	2.4030(8)		
C(1)-N(2)	1.495(4)	C(1)-PD-O(4)	81.01(10)
C(1)-C(11)	1.506(4)	C(1)-PD-P(1)	98.50(8)
N(2)-C(3)	1.324(4)	O(4)-PD-P(1)	173.29(6)
N(2)-C(21)	1.476(4)	C(1)-PD-Cl	170.36(8)
C(3)-O(4)	1.262(4)	O(4)-PD-Cl	91.37(6)
C(3)-C(31)	1.498(4)	P(1)-PD-Cl	89.76(3)
C(11)-C(12)	1.390(4)	N(2)-C(1)-C(11)	109.9(2)
C(11)-C(16)	1.398(4)	N(2)-C(1)-PD	105.17(19)
C(12)-C(13)	1.391(5)	C(11)-C(1)-PD	112.5(2)
C(13)-C(14)	1.390(6)	C(3)-N(2)-C(21)	125.7(3)
C(14)-C(15)	1.394(6)	C(3)-N(2)-C(1)	118.2(3)
C(14)-C(17)	1.513(5)	C(21)-N(2)-C(1)	115.7(2)
C(15)-C(16)	1.375(5)	O(4)-C(3)-N(2)	120.3(3)
C(21)-C(22)	1.506(4)	O(4)-C(3)-C(31)	117.4(3)
C(22)-C(27)	1.374(5)	N(2)-C(3)-C(31)	122.3(3)
C(22)-C(23)	1.383(5)	C(3)-O(4)-PD	112.45(18)
C(23)-C(24)	1.380(5)	C(12)-C(11)-C(16)	117.4(3)
C(24)-C(25)	1.370(5)	C(12)-C(11)-C(1)	120.8(3)
C(25)-O(28)	1.365(4)	C(16)-C(11)-C(1)	121.8(3)
C(25)-C(26)	1.385(5)	C(11)-C(12)-C(13)	121.0(3)
C(26)-C(27)	1.399(5)	C(14)-C(13)-C(12)	121.2(3)
O(28)-C(29)	1.420(5)	C(13)-C(14)-C(15)	117.7(3)
C(31)-C(32)	1.377(5)	C(13)-C(14)-C(17)	120.9(4)
C(31)-C(36)	1.398(5)	C(15)-C(14)-C(17)	121.4(4)
C(32)-C(33)	1.399(5)	C(16)-C(15)-C(14)	121.1(3)
C(33)-C(34)	1.381(7)	C(15)-C(16)-C(11)	121.5(3)
C(34)-C(35)	1.363(7)	N(2)-C(21)-C(22)	112.6(3)
C(35)-C(36)	1.383(5)	C(27)-C(22)-C(23)	118.3(3)
P(1)-C(71)	1.827(3)	C(27)-C(22)-C(21)	120.9(3)
P(1)-C(61)	1.842(3)	C(23)-C(22)-C(21)	120.8(3)
P(1)-C(51)	1.847(3)	C(24)-C(23)-C(22)	121.0(3)
C(51)-C(56)	1.399(4)	C(25)-C(24)-C(23)	120.4(3)
C(51)-C(52)	1.416(4)	O(28)-C(25)-C(24)	116.1(3)
C(52)-C(53)	1.398(4)	O(28)-C(25)-C(26)	123.9(3)
C(52)-C(57)	1.499(4)	C(24)-C(25)-C(26)	120.0(3)
C(53)-C(54)	1.385(5)	C(25)-C(26)-C(27)	118.9(3)
C(54)-C(55)	1.379(5)	C(22)-C(27)-C(26)	121.4(3)
C(55)-C(56)	1.388(4)	C(25)-O(28)-C(29)	117.9(3)
C(61)-C(66)	1.398(4)	C(32)-C(31)-C(36)	120.5(3)
C(61)-C(62)	1.407(4)	C(32)-C(31)-C(3)	117.0(3)
C(62)-C(63)	1.395(4)	C(36)-C(31)-C(3)	122.4(3)
C(62)-C(67)	1.501(4)	C(31)-C(32)-C(33)	119.2(4)
C(63)-C(64)	1.375(5)	C(34)-C(33)-C(32)	119.8(4)
C(64)-C(65)	1.382(5)	C(35)-C(34)-C(33)	120.7(4)
C(65)-C(66)	1.386(4)	C(34)-C(35)-C(36)	120.5(4)
C(71)-C(76)	1.399(4)	C(35)-C(36)-C(31)	119.2(4)
C(71)-C(72)	1.412(4)	C(71)-P(1)-C(61)	105.29(13)
C(72)-C(73)	1.394(4)	C(71)-P(1)-C(51)	103.09(13)
C(72)-C(77)	1.506(5)	C(61)-P(1)-C(51)	106.26(13)
C(73)-C(74)	1.387(5)	C(71)-P(1)-PD	116.99(9)
C(74)-C(75)	1.377(6)	C(61)-P(1)-PD	111.93(10)
C(75)-C(76)	1.375(5)	C(51)-P(1)-PD	112.33(10)
Cl(81)-C(80)	1.741(6)	C(56)-C(51)-C(52)	119.1(3)

C(56)-C(51)-P(1)	116.4(2)	C(64)-C(65)-C(66)	120.2(3)
C(52)-C(51)-P(1)	124.3(2)	C(65)-C(66)-C(61)	120.7(3)
C(53)-C(52)-C(51)	117.5(3)	C(76)-C(71)-C(72)	118.7(3)
C(53)-C(52)-C(57)	117.2(3)	C(76)-C(71)-P(1)	120.0(2)
C(51)-C(52)-C(57)	125.3(3)	C(72)-C(71)-P(1)	121.3(2)
C(54)-C(53)-C(52)	122.6(3)	C(73)-C(72)-C(71)	118.3(3)
C(55)-C(54)-C(53)	119.7(3)	C(73)-C(72)-C(77)	117.7(3)
C(54)-C(55)-C(56)	119.2(3)	C(71)-C(72)-C(77)	124.0(3)
C(55)-C(56)-C(51)	121.9(3)	C(74)-C(73)-C(72)	121.9(3)
C(66)-C(61)-C(62)	119.4(3)	C(75)-C(74)-C(73)	119.6(3)
C(66)-C(61)-P(1)	119.2(2)	C(76)-C(75)-C(74)	119.8(3)
C(62)-C(61)-P(1)	121.3(2)	C(75)-C(76)-C(71)	121.8(3)
C(63)-C(62)-C(61)	117.9(3)	CL82-C(80)-CL81	111.7(3)
C(63)-C(62)-C(67)	119.1(3)	CL91-C(90)-CL92	111.6(3)
C(61)-C(62)-C(67)	123.0(3)		
C(64)-C(63)-C(62)	122.7(3)		
C(63)-C(64)-C(65)	119.0(3)		

Table 6. Torsion angles [$^{\circ}$] for C46 H47 Cl5 N O2 P Pd.

O(4)-PD-C(1)-N(2)	14.11(18)	C(33)-C(34)-C(35)-C(36)	-0.5(7)
P(1)-PD-C(1)-N(2)	-159.12(17)	C(34)-C(35)-C(36)-C(31)	-0.5(6)
CL-PD-C(1)-N(2)	52.2(6)	C(32)-C(31)-C(36)-C(35)	2.1(5)
O(4)-PD-C(1)-C(11)	-105.5(2)	C(3)-C(31)-C(36)-C(35)	-179.2(3)
P(1)-PD-C(1)-C(11)	81.3(2)	C(1)-PD-P(1)-C(71)	-3.59(14)
CL-PD-C(1)-C(11)	-67.4(6)	O(4)-PD-P(1)-C(71)	-88.9(5)
C(11)-C(1)-N(2)-C(3)	104.8(3)	CL-PD-P(1)-C(71)	171.41(11)
PD-C(1)-N(2)-C(3)	-16.6(3)	C(1)-PD-P(1)-C(61)	-125.20(14)
C(11)-C(1)-N(2)-C(21)	-67.9(3)	O(4)-PD-P(1)-C(61)	149.5(5)
PD-C(1)-N(2)-C(21)	170.8(2)	CL-PD-P(1)-C(61)	49.8(1)
C(21)-N(2)-C(3)-O(4)	179.4(3)	C(1)-PD-P(1)-C(51)	115.35(13)
C(1)-N(2)-C(3)-O(4)	7.5(4)	O(4)-PD-P(1)-C(51)	30.1(6)
C(21)-N(2)-C(3)-C(31)	-2.0(5)	CL-PD-P(1)-C(51)	-69.65(10)
C(1)-N(2)-C(3)-C(31)	-173.9(3)	C(71)-P(1)-C(51)-C(56)	137.5(2)
N(2)-C(3)-O(4)-PD	6.2(4)	C(61)-P(1)-C(51)-C(56)	-112.0(2)
C(31)-C(3)-O(4)-PD	-172.5(2)	PD-P(1)-C(51)-C(56)	10.7(3)
C(1)-PD-O(4)-C(3)	-12.3(2)	C(71)-P(1)-C(51)-C(52)	-37.1(3)
P(1)-PD-O(4)-C(3)	74.0(6)	C(61)-P(1)-C(51)-C(52)	73.4(3)
CL-PD-O(4)-C(3)	173.7(2)	PD-P(1)-C(51)-C(52)	-163.9(2)
N(2)-C(1)-C(11)-C(12)	128.0(3)	C(56)-C(51)-C(52)-C(53)	-0.7(4)
PD-C(1)-C(11)-C(12)	-115.1(3)	P(1)-C(51)-C(52)-C(53)	173.8(2)
N(2)-C(1)-C(11)-C(16)	-53.7(4)	C(56)-C(51)-C(52)-C(57)	179.1(3)
PD-C(1)-C(11)-C(16)	63.1(3)	P(1)-C(51)-C(52)-C(57)	-6.5(4)
C(16)-C(11)-C(12)-C(13)	-3.8(5)	C(51)-C(52)-C(53)-C(54)	-0.6(5)
C(1)-C(11)-C(12)-C(13)	174.5(3)	C(57)-C(52)-C(53)-C(54)	179.6(3)
C(11)-C(12)-C(13)-C(14)	1.1(5)	C(52)-C(53)-C(54)-C(55)	1.8(6)
C(12)-C(13)-C(14)-C(15)	2.0(6)	C(53)-C(54)-C(55)-C(56)	-1.7(6)
C(12)-C(13)-C(14)-C(17)	-177.4(4)	C(54)-C(55)-C(56)-C(51)	0.4(6)
C(13)-C(14)-C(15)-C(16)	-2.2(6)	C(52)-C(51)-C(56)-C(55)	0.8(5)
C(17)-C(14)-C(15)-C(16)	177.1(4)	P(1)-C(51)-C(56)-C(55)	-174.1(3)
C(14)-C(15)-C(16)-C(11)	-0.6(6)	C(71)-P(1)-C(61)-C(66)	99.9(2)
C(12)-C(11)-C(16)-C(15)	3.6(5)	C(51)-P(1)-C(61)-C(66)	-9.1(3)
C(1)-C(11)-C(16)-C(15)	-174.7(3)	PD-P(1)-C(61)-C(66)	-132.0(2)
C(3)-N(2)-C(21)-C(22)	133.9(3)	C(71)-P(1)-C(61)-C(62)	-81.3(3)
C(1)-N(2)-C(21)-C(22)	-54.0(4)	C(51)-P(1)-C(61)-C(62)	169.8(2)
N(2)-C(21)-C(22)-C(27)	115.3(4)	PD-P(1)-C(61)-C(62)	46.8(3)
N(2)-C(21)-C(22)-C(23)	-66.9(4)	C(66)-C(61)-C(62)-C(63)	-2.4(4)
C(27)-C(22)-C(23)-C(24)	-0.4(5)	P(1)-C(61)-C(62)-C(63)	178.8(2)
C(21)-C(22)-C(23)-C(24)	-178.3(3)	C(66)-C(61)-C(62)-C(67)	176.8(3)
C(22)-C(23)-C(24)-C(25)	-0.5(5)	P(1)-C(61)-C(62)-C(67)	-2.1(4)
C(23)-C(24)-C(25)-O(28)	-179.1(3)	C(61)-C(62)-C(63)-C(64)	-0.7(5)
C(23)-C(24)-C(25)-C(26)	0.7(6)	C(67)-C(62)-C(63)-C(64)	-179.9(3)
O(28)-C(25)-C(26)-C(27)	179.8(4)	C(62)-C(63)-C(64)-C(65)	2.3(5)
C(24)-C(25)-C(26)-C(27)	0.0(6)	C(63)-C(64)-C(65)-C(66)	-0.8(5)
C(23)-C(22)-C(27)-C(26)	1.1(6)	C(64)-C(65)-C(66)-C(61)	-2.3(5)
C(21)-C(22)-C(27)-C(26)	179.0(4)	C(62)-C(61)-C(66)-C(65)	3.9(5)
C(25)-C(26)-C(27)-C(22)	-0.9(6)	P(1)-C(61)-C(66)-C(65)	-177.2(2)
C(24)-C(25)-O(28)-C(29)	169.9(4)	C(61)-P(1)-C(71)-C(76)	16.4(3)
C(26)-C(25)-O(28)-C(29)	-9.9(6)	C(51)-P(1)-C(71)-C(76)	127.6(2)
O(4)-C(3)-C(31)-C(32)	47.5(4)	PD-P(1)-C(71)-C(76)	-108.6(2)
N(2)-C(3)-C(31)-C(32)	-131.1(3)	C(61)-P(1)-C(71)-C(72)	-164.1(2)
O(4)-C(3)-C(31)-C(36)	-131.2(3)	C(51)-P(1)-C(71)-C(72)	-52.9(3)
N(2)-C(3)-C(31)-C(36)	50.1(5)	PD-P(1)-C(71)-C(72)	70.9(3)
C(36)-C(31)-C(32)-C(33)	-2.7(5)	C(76)-C(71)-C(72)-C(73)	-1.9(4)
C(3)-C(31)-C(32)-C(33)	178.5(3)	P(1)-C(71)-C(72)-C(73)	178.6(2)
C(31)-C(32)-C(33)-C(34)	1.7(6)	C(76)-C(71)-C(72)-C(77)	-179.4(3)
C(32)-C(33)-C(34)-C(35)	-0.1(6)	P(1)-C(71)-C(72)-C(77)	1.1(4)

C(71)-C(72)-C(73)-C(74)	0.4(5)
C(77)-C(72)-C(73)-C(74)	178.1(3)
C(72)-C(73)-C(74)-C(75)	1.0(6)
C(73)-C(74)-C(75)-C(76)	-0.8(6)
C(74)-C(75)-C(76)-C(71)	-0.8(6)
C(72)-C(71)-C(76)-C(75)	2.2(5)
P(1)-C(71)-C(76)-C(75)	-178.3(3)

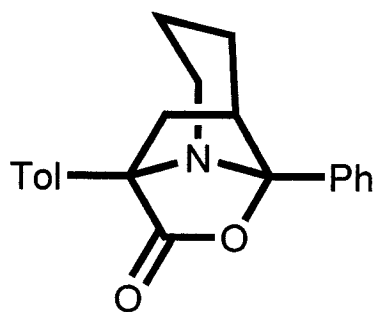
ORTEP view of the C₄₆ H₄₇ Cl₅ N O₂ P Pd compound with the numbering scheme adopted. Ellipsoids drawn at 30% probability level. Hydrogens represented by sphere of arbitrary size.

REFERENCES

- International Tables for Crystallography (1992). Vol. C. Tables 4.2.6.8 and 6.1.1.4, Dordrecht: Kluwer Academic Publishers.
- SAINT (1999) Release 6.06; Integration Software for Single Crystal Data. Bruker AXS Inc., Madison, WI 53719-1173.
- Sheldrick, G.M. (1996). SADABS, Bruker Area Detector Absorption Corrections. Bruker AXS Inc., Madison, WI 53719-1173.
- Sheldrick, G.M. (1997). SHELXS97, Program for the Solution of Crystal Structures. Univ. of Gottingen, Germany.
- Sheldrick, G.M. (1997). SHELXL97, Program for the Refinement of Crystal Structures. Univ. of Gottingen, Germany.
- SHELXTL (1997) Release 5.10; The Complete Software Package for Single Crystal Structure Determination. Bruker AXS Inc., Madison, WI 53719-1173.
- SMART (1999) Release 5.059; Bruker Molecular Analysis Research Tool. Bruker AXS Inc., Madison, WI 53719-1173.
- Spek, A.L. (2000). PLATON, Molecular Geometry Program, 2000 version. University of Utrecht, Utrecht, Holland.
- XPREP (1997) Release 5.10; X-ray data Preparation and Reciprocal space Exploration Program. Bruker AXS Inc., Madison, WI 53719-1173.

Appendix E

2D-NMR and X-ray Structural Data for Complex A.24



Tol = p-C₆H₄-CH₃

CRYSTAL AND MOLECULAR STRUCTURE OF

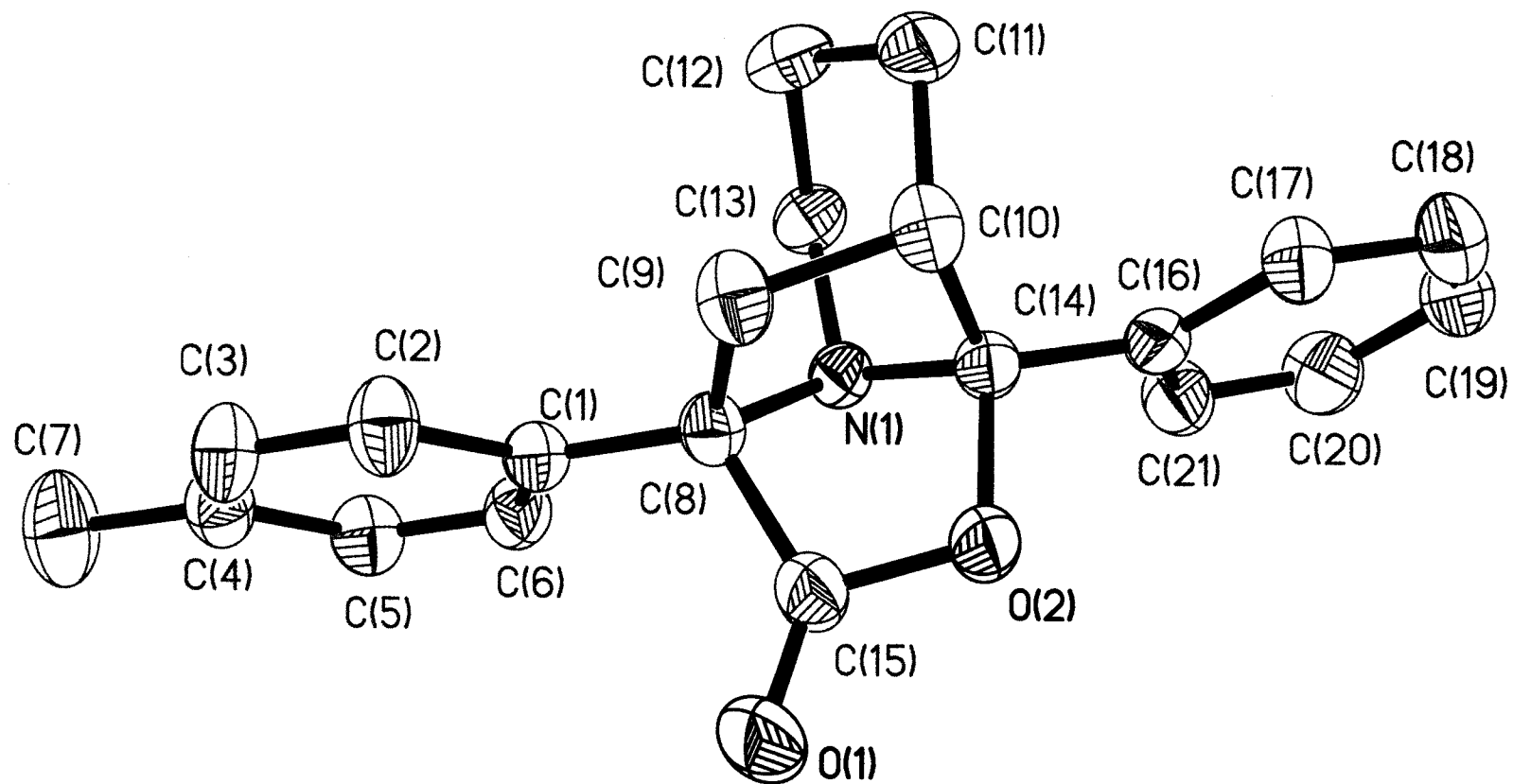
C21 H21 N O2 (arst27)

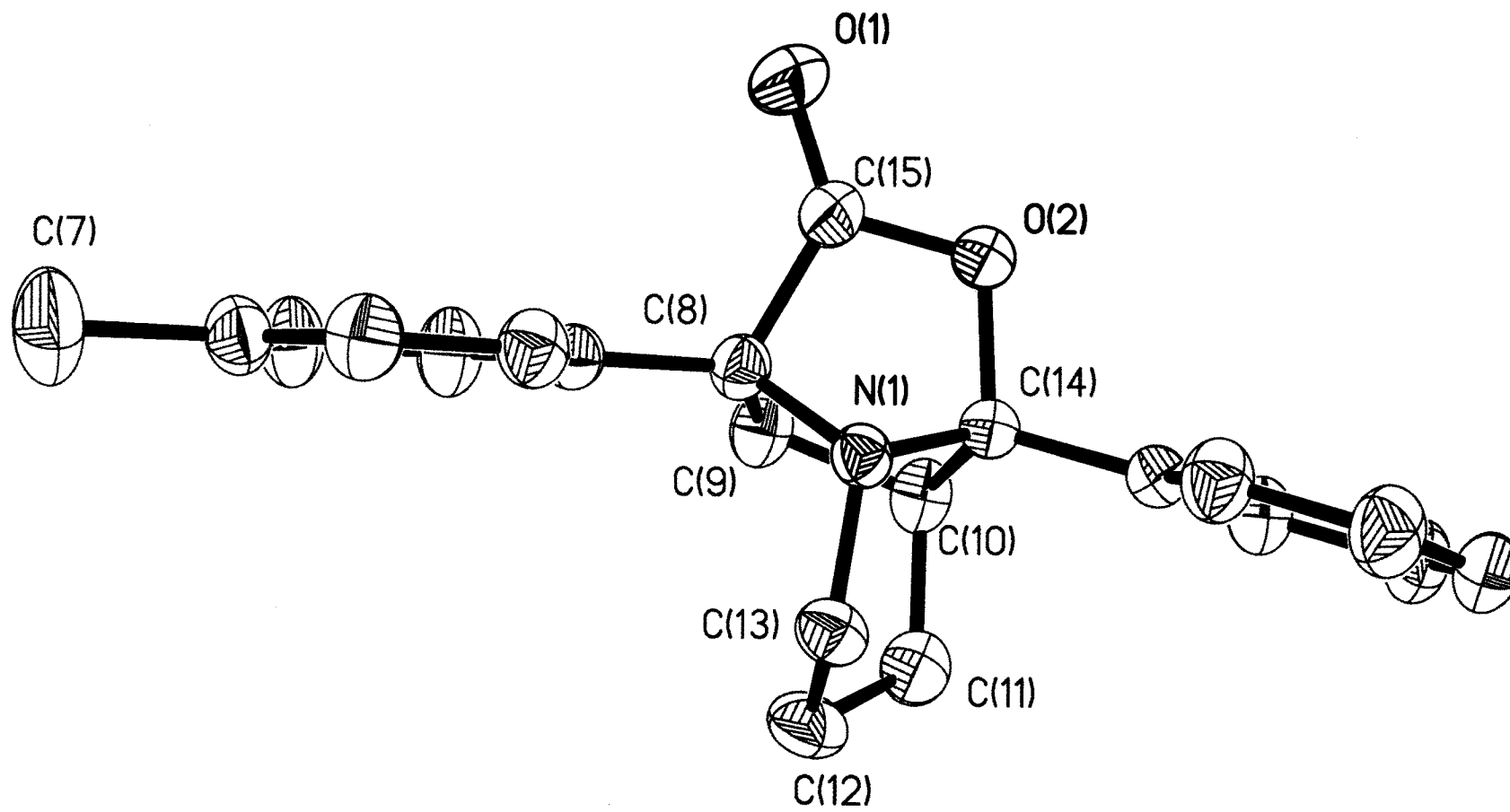
Rajiv Dhawan (Bruce Arndtsen)

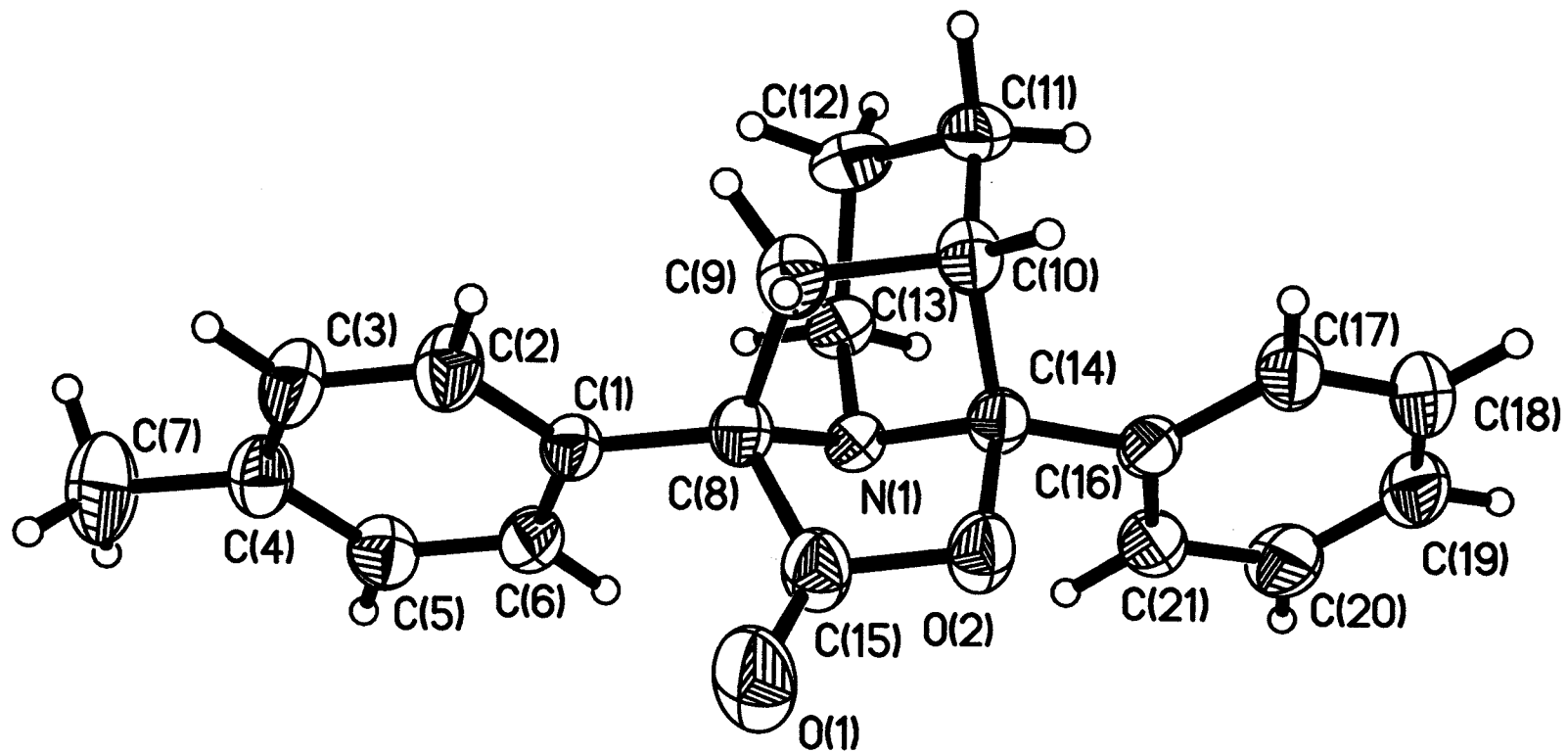
Departement of chemistry, McGill University,

Otto Maass Chemistry Bldg, 801 Sherbrooke St. W. Montreal, Canada, H3A 2K6

Structure solved by X-Ray crystallography laboratory, chemistry department,
McGill University by Dr Anne-Marie Lebuis, November 2001







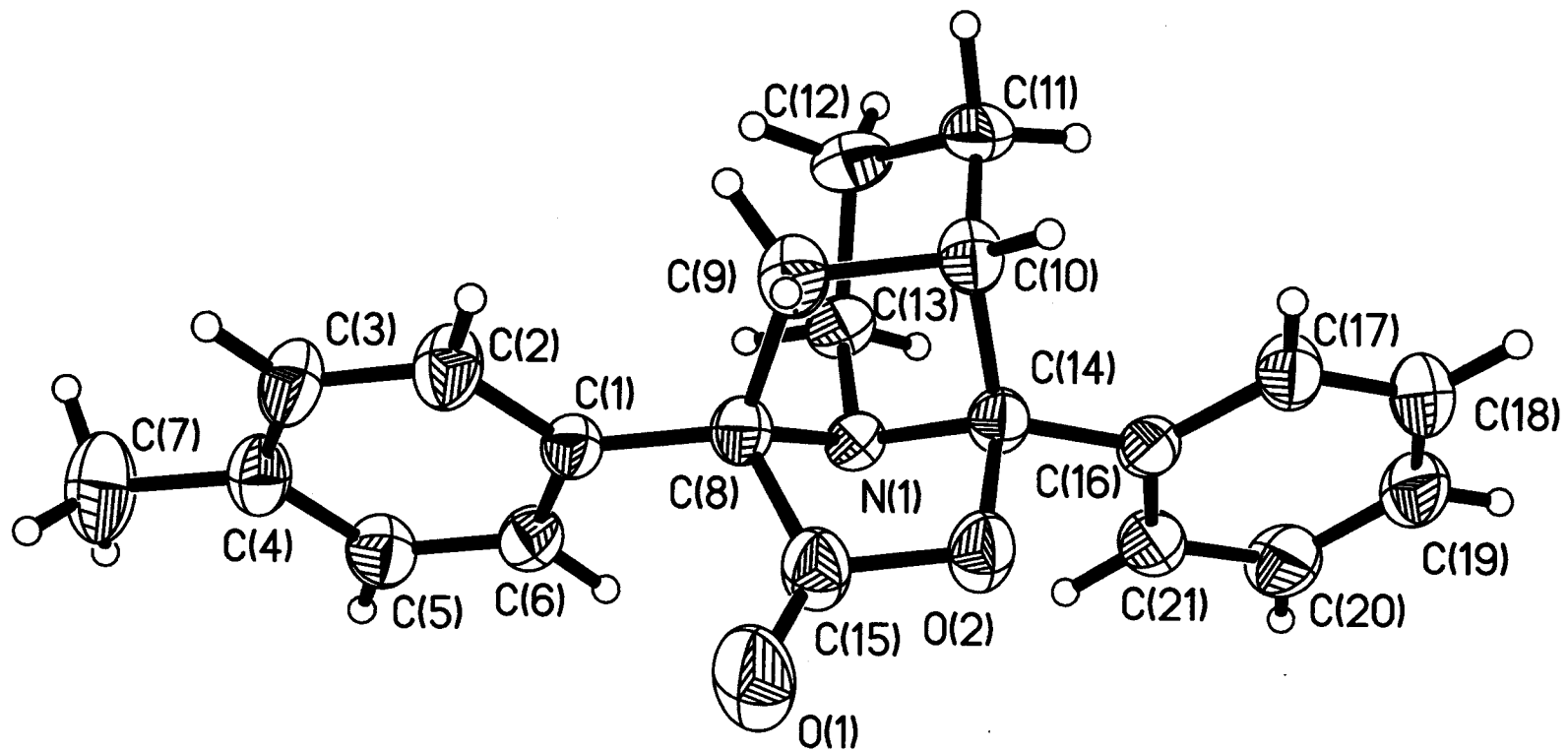


Table 1. Crystal data and structure refinement for C₂₁ H₂₁ N O₂.

Identification code	arst27	
Empirical formula	C ₂₁ H ₂₁ N O ₂	
Formula weight, Mr	319.39	
Cell setting	Orthorhombic	
Space group	Pbca	
Unit cell dimensions (A, deg)	a = 12.317(3) b = 15.858(3) c = 17.287(4)	alpha = 90 beta = 90 gamma = 90
Volume of unit cell, V (A ³)	3376.5(12)	
Formula units per cell, Z	8	
Formula units per asymmetric unit, Z'	1	
Density calculated from formula and cell, Dx (Mg/m ³)	1.257	
F(000)	1360	
Radiation type	CuK α	
Wavelength, lambda (A)	1.54178	
No. of reflections for cell measurement	25	
Theta range (deg)	20 to 25	
Linear absorption coefficient, mu (mm ⁻¹)	0.636	
Measurement temperature (K)	293(2)	
Crystal shape	prism	
Colour	colourless	
Size (mm)	0.608 x 0.516 x 0.460	
Data collection		
Diffractionmeter type	Nonius CAD-4	
Data-collection method	omega/2theta scans	
Absorption correction type	None	

Max and min transmission values	0.88 and 0.71
No. of reflections measured	26142
No. of independent reflections	3200
Completeness of data to Theta max	1.000
No. of observed reflections	2329
Criterion for observed reflections	>2sigma(I)
Rint	0.051
Theta range for data collection	5.12 to 69.92 deg.
Ranges of h,k,l	-15<=h<=15, -19<=k<=19, -21<=l<=21
No. of standard reflections	5
Intensity decay (%)	none
Refinement	
Refinement method	Full-matrix on F ²
Final R indices, I>2sigma(I)	R1 = 0.0358, wR2 = 0.1003
R indices, all data	R1 = 0.0513, wR2 = 0.1003
Goodness-of-fit on F ² , S	0.977
$R1 = \frac{\sum (\text{absabs } Foabs - \text{abs } Fcabsabs)}{\sum (\text{abs } Foabs)}$ $wR2 = \frac{[\sum [w(Fo^{2^{\wedge}} - Fc^{2^{\wedge}})^{2^{\wedge}}] / \sum [w(Fo^{2^{\wedge}})^{2^{\wedge}}]}{^1 * 2^{\wedge}}$ $GoF = \frac{[\sum [w(Fo^{2^{\wedge}} - Fc^{2^{\wedge}})^{2^{\wedge}}]}{(\text{No. of reflns} - \text{No. of params.})} ^1 * 2^{\wedge}$	
Data / restraints / parameters	3200 / 0 / 218
Method of refining and locating H atoms	mixed
Weighting scheme	based on measured s.u.'s
Function minimized	sum w(Fo ² -Fc ²)
calc w=1/[s ² (Fo ²)+(0.0552P) ²] where P=(Fo ² +2Fc ²)/3	
Maximum shift/sigma	0.000
Largest diff. peak and hole	0.145 and -0.158 e.A ³
Secondary extinction value	0.00125(13)

Table 2. Atomic coordinates and equivalent isotropic displacement parameters ($\text{\AA}^2 \times 10^{-2}$) for C₂₁H₂₁N₂O₂.

$$U_{eq} = (1/3) \sum_i \sum_j U_{ij} a_i^* a_j^* \cos \alpha_{ij}$$

	x	y	z	U(eq)
O(1)	0.87710 (12)	0.31591 (8)	0.44645 (8)	8.47 (5)
O(2)	0.76576 (9)	0.25568 (6)	0.36001 (6)	5.21 (3)
N(1)	0.77521 (9)	0.12443 (7)	0.40998 (6)	3.55 (3)
C(1)	0.83997 (11)	0.16078 (9)	0.54571 (8)	3.91 (3)
C(2)	0.80937 (13)	0.18542 (11)	0.61912 (9)	5.34 (4)
C(3)	0.86903 (14)	0.16293 (11)	0.68360 (9)	5.57 (4)
C(4)	0.96141 (14)	0.11499 (9)	0.67748 (9)	5.03 (4)
C(5)	0.99350 (13)	0.09094 (10)	0.60349 (9)	5.08 (4)
C(6)	0.93421 (12)	0.11307 (9)	0.53921 (8)	4.55 (4)
C(7)	1.02508 (19)	0.08909 (13)	0.74785 (11)	8.11 (6)
C(8)	0.77528 (11)	0.18536 (9)	0.47582 (8)	3.92 (3)
C(9)	0.65336 (12)	0.21101 (10)	0.48832 (8)	4.85 (4)
C(10)	0.60219 (12)	0.18764 (9)	0.40997 (8)	4.37 (3)
C(14)	0.70484 (11)	0.17607 (8)	0.36023 (8)	3.80 (3)
C(15)	0.81681 (14)	0.26005 (10)	0.42965 (9)	5.16 (4)
C(13)	0.72948 (11)	0.04001 (8)	0.42475 (9)	4.23 (3)
C(12)	0.61371 (13)	0.03757 (10)	0.45486 (10)	5.39 (4)
C(11)	0.54262 (12)	0.10358 (10)	0.41539 (9)	5.10 (4)
C(16)	0.69141 (11)	0.14815 (8)	0.27794 (8)	4.00 (3)
C(17)	0.59851 (13)	0.16833 (10)	0.23682 (9)	5.06 (4)
C(18)	0.58547 (15)	0.14224 (11)	0.16121 (9)	5.96 (5)
C(19)	0.66471 (15)	0.09543 (11)	0.12565 (9)	5.94 (4)
C(20)	0.75816 (15)	0.07550 (12)	0.16535 (10)	6.10 (5)
C(21)	0.77205 (12)	0.10229 (10)	0.24110 (9)	5.14 (4)

Table 3. Bond lengths (Å) and angles (deg) for C21 H21 N O2.

O(1)-C(15)	1.1918(18)	O(2)-C(15)	1.3599(18)
O(2)-C(14)	1.4686(16)	N(1)-C(14)	1.4702(17)
N(1)-C(13)	1.4747(17)	N(1)-C(8)	1.4931(17)
C(1)-C(2)	1.3803(19)	C(1)-C(6)	1.390(2)
C(1)-C(8)	1.4988(19)	C(2)-C(3)	1.382(2)
C(2)-H(2)	0.9300	C(3)-C(4)	1.373(2)
C(3)-H(3)	0.9300	C(4)-C(5)	1.392(2)
C(4)-C(7)	1.505(2)	C(5)-C(6)	1.375(2)
C(5)-H(5)	0.9300	C(6)-H(6)	0.9300
C(7)-H(7A)	0.9600	C(7)-H(7B)	0.9600
C(7)-H(7C)	0.9600	C(7)-H(7D)	0.9600
C(7)-H(7E)	0.9600	C(7)-H(7F)	0.9600
C(8)-C(15)	1.517(2)	C(8)-C(9)	1.571(2)
C(9)-C(10)	1.5391(19)	C(9)-H(9A)	0.9700
C(9)-H(9B)	0.9700	C(10)-C(11)	1.525(2)
C(10)-C(14)	1.5400(19)	C(10)-H(10)	0.9800
C(14)-C(16)	1.4991(19)	C(13)-C(12)	1.5184(19)
C(13)-H(13A)	0.9700	C(13)-H(13B)	0.9700
C(12)-C(11)	1.526(2)	C(12)-H(12A)	0.9700
C(12)-H(12B)	0.9700	C(11)-H(11A)	0.9700
C(11)-H(11B)	0.9700	C(16)-C(17)	1.385(2)
C(16)-C(21)	1.386(2)	C(17)-C(18)	1.380(2)
C(17)-H(17)	0.9300	C(18)-C(19)	1.372(2)
C(18)-H(18)	0.9300	C(19)-C(20)	1.377(2)
C(19)-H(19)	0.9300	C(20)-C(21)	1.387(2)
C(20)-H(20)	0.9300	C(21)-H(21)	0.9300
C(15)-O(2)-C(14)	106.13(10)	C(14)-N(1)-C(13)	112.44(10)
C(14)-N(1)-C(8)	94.91(10)	C(13)-N(1)-C(8)	117.11(10)
C(2)-C(1)-C(6)	117.15(13)	C(2)-C(1)-C(8)	121.48(13)
C(6)-C(1)-C(8)	121.36(12)	C(1)-C(2)-C(3)	121.56(14)
C(1)-C(2)-H(2)	119.2	C(3)-C(2)-H(2)	119.2
C(4)-C(3)-C(2)	121.44(14)	C(4)-C(3)-H(3)	119.3
C(2)-C(3)-H(3)	119.3	C(3)-C(4)-C(5)	117.26(14)
C(3)-C(4)-C(7)	121.40(15)	C(5)-C(4)-C(7)	121.35(15)
C(6)-C(5)-C(4)	121.45(15)	C(6)-C(5)-H(5)	119.3
C(4)-C(5)-H(5)	119.3	C(5)-C(6)-C(1)	121.13(13)
C(5)-C(6)-H(6)	119.4	C(1)-C(6)-H(6)	119.4
C(4)-C(7)-H(7A)	109.5	C(4)-C(7)-H(7B)	109.5
H(7A)-C(7)-H(7B)	109.5	C(4)-C(7)-H(7C)	109.5
H(7A)-C(7)-H(7C)	109.5	H(7B)-C(7)-H(7C)	109.5
C(4)-C(7)-H(7D)	109.5	H(7A)-C(7)-H(7D)	141.1
H(7B)-C(7)-H(7D)	56.3	H(7C)-C(7)-H(7D)	56.3
C(4)-C(7)-H(7E)	109.5	H(7A)-C(7)-H(7E)	56.3
H(7B)-C(7)-H(7E)	141.1	H(7C)-C(7)-H(7E)	56.3
H(7D)-C(7)-H(7E)	109.5	C(4)-C(7)-H(7F)	109.5
H(7A)-C(7)-H(7F)	56.3	H(7B)-C(7)-H(7F)	56.3
H(7C)-C(7)-H(7F)	141.1	H(7D)-C(7)-H(7F)	109.5
H(7E)-C(7)-H(7F)	109.5	N(1)-C(8)-C(1)	116.51(11)
N(1)-C(8)-C(15)	95.99(11)	C(1)-C(8)-C(15)	116.61(12)
N(1)-C(8)-C(9)	105.78(11)	C(1)-C(8)-C(9)	117.69(12)
C(15)-C(8)-C(9)	101.11(12)	C(10)-C(9)-C(8)	102.01(11)

C(10)-C(9)-H(9A)	111.4	C(8)-C(9)-H(9A)	111.4
C(10)-C(9)-H(9B)	111.4	C(8)-C(9)-H(9B)	111.4
H(9A)-C(9)-H(9B)	109.2	C(11)-C(10)-C(9)	110.71(12)
C(11)-C(10)-C(14)	108.98(11)	C(9)-C(10)-C(14)	100.60(11)
C(11)-C(10)-H(10)	112.0	C(9)-C(10)-H(10)	112.0
C(14)-C(10)-H(10)	112.0	O(2)-C(14)-N(1)	100.32(10)
O(2)-C(14)-C(16)	107.93(11)	N(1)-C(14)-C(16)	117.11(11)
O(2)-C(14)-C(10)	108.57(11)	N(1)-C(14)-C(10)	102.93(10)
C(16)-C(14)-C(10)	118.32(12)	O(1)-C(15)-O(2)	122.80(15)
O(1)-C(15)-C(8)	131.46(14)	O(2)-C(15)-C(8)	105.66(12)
N(1)-C(13)-C(12)	116.18(12)	N(1)-C(13)-H(13A)	108.2
C(12)-C(13)-H(13A)	108.2	N(1)-C(13)-H(13B)	108.2
C(12)-C(13)-H(13B)	108.2	H(13A)-C(13)-H(13B)	107.4
C(13)-C(12)-C(11)	111.60(12)	C(13)-C(12)-H(12A)	109.3
C(11)-C(12)-H(12A)	109.3	C(13)-C(12)-H(12B)	109.3
C(11)-C(12)-H(12B)	109.3	H(12A)-C(12)-H(12B)	108.0
C(100)-C(11)-C(12)	110.55(12)	C(10)-C(11)-H(11A)	109.5
C(12)-C(11)-H(11A)	109.5	C(10)-C(11)-H(11B)	109.5
C(12)-C(11)-H(11B)	109.5	H(11A)-C(11)-H(11B)	108.1
C(17)-C(16)-C(21)	118.53(14)	C(17)-C(16)-C(14)	120.68(13)
C(21)-C(16)-C(14)	120.79(13)	C(18)-C(17)-C(16)	120.86(15)
C(18)-C(17)-H(17)	119.6	C(16)-C(17)-H(17)	119.6
C(19)-C(18)-C(17)	120.25(16)	C(19)-C(18)-H(18)	119.9
C(17)-C(18)-H(18)	119.9	C(18)-C(19)-C(20)	119.72(15)
C(18)-C(19)-H(19)	120.1	C(20)-C(19)-H(19)	120.1
C(19)-C(20)-C(21)	120.22(16)	C(19)-C(20)-H(20)	119.9
C(21)-C(20)-H(20)	119.9	C(16)-C(21)-C(20)	120.40(15)
C(16)-C(21)-H(21)	119.8	C(20)-C(21)-H(21)	119.8

Table 4. Torsion angles (deg) for C21 H21 N O2.

C(6)-C(1)-C(2)-C(3)	-0.7(2)	C(8)-C(1)-C(2)-C(3)	-179.89(15)
C(1)-C(2)-C(3)-C(4)	0.0(3)	C(2)-C(3)-C(4)-C(5)	0.9(3)
C(2)-C(3)-C(4)-C(7)	-178.77(17)	C(3)-C(4)-C(5)-C(6)	-1.0(2)
C(7)-C(4)-C(5)-C(6)	178.64(16)	C(4)-C(5)-C(6)-C(1)	0.3(2)
C(2)-C(1)-C(6)-C(5)	0.6(2)	C(8)-C(1)-C(6)-C(5)	179.75(14)
C(14)-N(1)-C(8)-C(1)	-179.85(11)	C(13)-N(1)-C(8)-C(1)	61.83(15)
C(14)-N(1)-C(8)-C(15)	-56.09(12)	C(13)-N(1)-C(8)-C(15)	-174.42(11)
C(14)-N(1)-C(8)-C(9)	47.26(12)	C(13)-N(1)-C(8)-C(9)	-71.07(14)
C(2)-C(1)-C(8)-N(1)	-148.53(14)	C(6)-C(1)-C(8)-N(1)	32.33(19)
C(2)-C(1)-C(8)-C(15)	99.12(17)	C(6)-C(1)-C(8)-C(15)	-80.02(17)
C(2)-C(1)-C(8)-C(9)	-21.3(2)	C(6)-C(1)-C(8)-C(9)	159.56(13)
N(1)-C(8)-C(9)-C(10)	-20.18(14)	C(1)-C(8)-C(9)-C(10)	-152.42(12)
C(15)-C(8)-C(9)-C(10)	79.37(13)	C(8)-C(9)-C(10)-C(11)	100.62(13)
C(8)-C(9)-C(10)-C(14)	-14.50(14)	C(15)-O(2)-C(14)-N(1)	-30.80(14)
C(15)-O(2)-C(14)-C(16)	-153.88(13)	C(15)-O(2)-C(14)-C(10)	76.72(14)
C(13)-N(1)-C(14)-O(2)	176.47(10)	C(8)-N(1)-C(14)-O(2)	54.44(11)
C(13)-N(1)-C(14)-C(16)	-67.12(15)	C(8)-N(1)-C(14)-C(16)	170.85(11)
C(13)-N(1)-C(14)-C(10)	64.51(13)	C(8)-N(1)-C(14)-C(10)	-57.52(11)
C(11)-C(10)-C(14)-O(2)	-175.94(11)	C(9)-C(10)-C(14)-O(2)	-59.53(13)
C(11)-C(10)-C(14)-N(1)	-70.21(13)	C(9)-C(10)-C(14)-N(1)	46.20(13)
C(11)-C(10)-C(14)-C(16)	60.70(16)	C(9)-C(10)-C(14)-C(16)	177.10(12)
C(14)-O(2)-C(15)-O(1)	176.69(17)	C(14)-O(2)-C(15)-C(8)	-6.09(15)
N(1)-C(8)-C(15)-O(1)	-143.4(2)	C(1)-C(8)-C(15)-O(1)	-19.7(3)
C(9)-C(8)-C(15)-O(1)	109.2(2)	N(1)-C(8)-C(15)-O(2)	39.76(14)
C(1)-C(8)-C(15)-O(2)	163.44(12)	C(9)-C(8)-C(15)-O(2)	-67.66(14)
C(14)-N(1)-C(13)-C(12)	-52.29(16)	C(8)-N(1)-C(13)-C(12)	56.11(17)
N(1)-C(13)-C(12)-C(11)	39.55(18)	C(9)-C(10)-C(11)-C(12)	-47.87(16)
C(14)-C(10)-C(11)-C(12)	61.88(15)	C(13)-C(12)-C(11)-C(10)	-44.16(18)
O(2)-C(14)-C(16)-C(17)	-94.56(15)	N(1)-C(14)-C(16)-C(17)	153.28(13)
C(10)-C(14)-C(16)-C(17)	29.12(19)	O(2)-C(14)-C(16)-C(21)	84.82(15)
N(1)-C(14)-C(16)-C(21)	-27.34(19)	C(10)-C(14)-C(16)-C(21)	-151.50(14)
C(21)-C(16)-C(17)-C(18)	1.1(2)	C(14)-C(16)-C(17)-C(18)	-179.54(14)
C(16)-C(17)-C(18)-C(19)	0.2(3)	C(17)-C(18)-C(19)-C(20)	-0.9(3)
C(18)-C(19)-C(20)-C(21)	0.3(3)	C(17)-C(16)-C(21)-C(20)	-1.7(2)
C(14)-C(16)-C(21)-C(20)	178.91(14)	C(19)-C(20)-C(21)-C(16)	1.0(3)

Table 5. Hydrogen coordinates and isotropic displacement parameters ($\text{\AA}^2 \times 10^4$) for C21 H21 N O2.

	x	y	z	U~iso~
H(2)	0.7471	0.2179	0.6253	6.4
H(3)	0.8461	0.1807	0.7322	6.7
H(5)	1.0564	0.0592	0.5974	6.1
H(6)	0.9576	0.0958	0.4906	5.5
H(7A)	1.0866	0.0561	0.7323	12.2
H(7B)	0.9797	0.0562	0.7814	12.2
H(7C)	1.0496	0.1385	0.7748	12.2
H(7D)	0.9906	0.1111	0.7934	12.2
H(7E)	1.0976	0.1110	0.7442	12.2
H(7F)	1.0277	0.0287	0.7508	12.2
H(9A)	0.6208	0.1793	0.5303	5.8
H(9B)	0.6463	0.2708	0.4989	5.8
H(10)	0.5553	0.2326	0.3901	5.2
H(13A)	0.7757	0.0115	0.4619	5.1
H(13B)	0.7324	0.0080	0.3770	5.1
H(12A)	0.6140	0.0476	0.5102	6.5
H(12B)	0.5833	-0.0180	0.4459	6.5
H(11A)	0.5235	0.0844	0.3639	6.1
H(11B)	0.4760	0.1109	0.4446	6.1
H(17)	0.5442	0.1999	0.2604	6.1
H(18)	0.5227	0.1565	0.1343	7.2
H(19)	0.6553	0.0772	0.0749	7.1
H(20)	0.8121	0.0440	0.1413	7.3
H(21)	0.8359	0.0894	0.2673	6.2

Table 6. Anisotropic parameters ($\text{\AA}^2 \times 10^2$) for C21 H21 N O2.

The anisotropic displacement factor exponent takes the form:

$$-2 \pi^2 [h^2 a^{*2} U_{11} + \dots + 2 h k a^* b^* U_{12}]$$

	U11	U22	U33	U23	U13	U12
O(1)	11.78(12)	6.38(8)	7.24(9)	0.86(7)	-3.40(8)	-4.35(8)
O(2)	7.04(7)	4.27(5)	4.32(6)	0.72(4)	-1.22(5)	-1.57(5)
N(1)	3.64(6)	3.84(6)	3.16(5)	-0.03(5)	0.30(5)	0.00(5)
C(1)	4.15(7)	4.11(7)	3.47(7)	-0.20(6)	0.03(6)	-0.14(6)
C(2)	5.63(10)	6.33(10)	4.05(8)	-0.71(7)	-0.05(7)	1.86(8)
C(3)	6.78(11)	6.51(10)	3.42(8)	-0.53(7)	-0.03(7)	1.25(9)
C(4)	6.31(10)	4.47(8)	4.32(8)	0.33(7)	-0.88(7)	0.31(7)
C(5)	4.74(8)	5.34(9)	5.17(9)	-0.15(7)	-0.18(7)	0.95(7)
C(6)	4.38(8)	5.49(9)	3.77(7)	-0.30(6)	0.45(6)	0.19(7)
C(7)	10.40(16)	8.19(13)	5.75(11)	0.50(10)	-2.43(11)	2.61(12)
C(8)	4.30(8)	3.98(7)	3.47(7)	-0.33(6)	-0.13(6)	0.10(6)
C(9)	5.17(9)	5.20(9)	4.16(8)	-0.93(7)	-0.20(7)	1.37(7)
C(10)	4.29(8)	4.87(8)	3.96(8)	-0.65(6)	-0.23(6)	1.29(7)
C(14)	4.28(8)	3.52(7)	3.59(7)	0.12(5)	-0.26(6)	-0.36(6)
C(15)	6.56(10)	4.43(8)	4.49(9)	0.09(7)	-1.22(8)	-1.10(8)
C(13)	4.56(8)	3.65(7)	4.48(8)	0.22(6)	0.57(6)	0.14(6)
C(12)	5.28(9)	5.11(9)	5.77(9)	0.59(8)	1.39(8)	-1.08(7)
C(11)	3.53(7)	6.98(10)	4.78(8)	-0.41(8)	0.86(6)	-0.39(7)
C(16)	4.29(7)	4.29(7)	3.42(7)	0.08(6)	0.13(6)	-0.69(6)
C(17)	5.27(9)	5.75(9)	4.15(8)	-0.01(7)	-0.41(7)	0.50(7)
C(18)	6.41(11)	7.13(11)	4.34(9)	-0.24(8)	-1.28(8)	-0.18(9)
C(19)	6.94(11)	7.03(11)	3.84(8)	-0.73(8)	-0.27(8)	-1.56(9)
C(20)	6.15(10)	7.52(11)	4.62(9)	-1.22(8)	1.13(8)	-0.09(9)
C(21)	4.37(8)	6.78(10)	4.28(8)	-0.45(7)	0.20(7)	0.09(8)

Table 7. Least-squares planes (x,y,z in crystal coordinates) and deviations from them for C21 H21 N O2.

(* indicates atom used to define plane)

PLANE 1

$$5.2702 (0.0076) x + 13.3887 (0.0064) y - 5.5777 (0.0107) z = 4.0855 (0.0056)$$

* -0.0083 (0.0011) C16
* 0.0017 (0.0011) C17
* 0.0053 (0.0012) C18
* -0.0055 (0.0012) C19
* -0.0013 (0.0012) C20
* 0.0082 (0.0011) C21

Rms deviation of fitted atoms = 0.0058

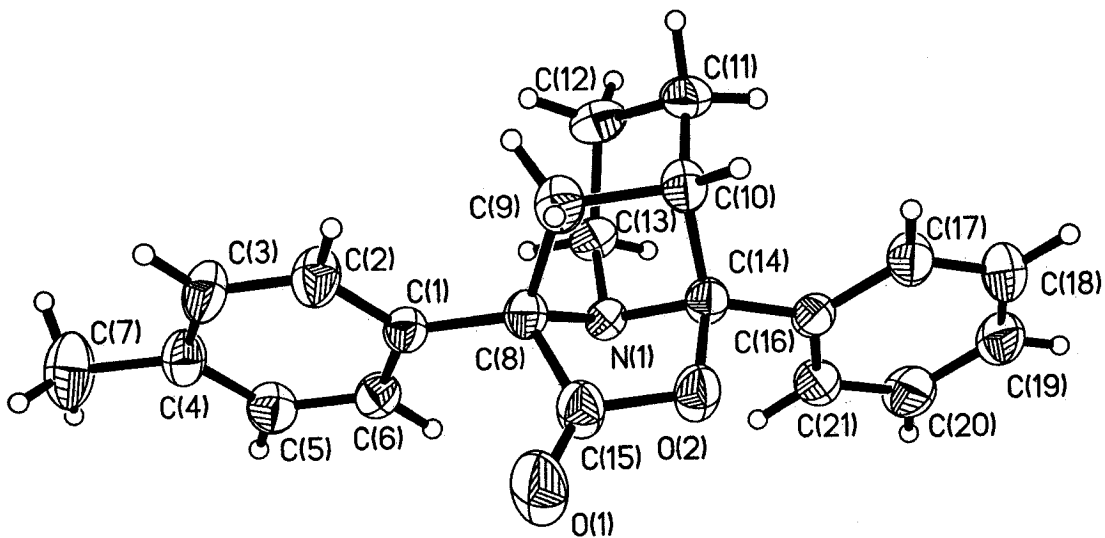
PLANE 2

$$6.6741 (0.0070) x + 13.2516 (0.0064) y - 1.5551 (0.0109) z = 6.8932 (0.0086)$$

Angle to previous plane (with approximate esd) = 14.90 (0.08)

* -0.0052 (0.0011) C1
* 0.0030 (0.0012) C2
* 0.0028 (0.0012) C3
* -0.0064 (0.0012) C4
* 0.0041 (0.0012) C5
* 0.0016 (0.0011) C6
-0.0341 (0.0029) C7

Rms deviation of fitted atoms = 0.0042



ORTEP view of C₂₁ H₂₁ N O₂

with the numbering scheme adopted. Ellipsoids drawn at 40% probability level. Hydrogens represented by spheres of arbitrary size. Only one orientation of the disordered Hydrogens in CH₃ group are shown

Discussion data collection, structure determination and refinement procedure

X-ray crystallographic data for I were collected from a single crystal sample, which was mounted on a glass fiber

Space group confirmed by PLATON program (Spek, 1995). Data reduction performed using a locally modified version of the NRC-2 program (Ahmed et al, 1973). The structure was solved by direct method using SHELXS97 (Sheldrick, 1997) and difmap synthesis using SHELXTL (Sheldrick, 1997) and SHELXL96 (Sheldrick, 1996). All non-hydrogen atoms anisotropic, hydrogen atoms isotropic. Hydrogen atoms constrained to the parent site using a riding model; SHELXL96 defaults; C-H 0.93 to 0.97\%A. The isotropic factors, Uiso, were adjusted to a value 20% higher than that of the parent site (50% for methyl). The hydrogens of the methyl group are disordered over two orientations related by a 180 degree rotation. A final verification for possibly missed symmetry and of possible voids was performed using the ADDSYM and VOID routines of the PLATON program (Spek, 1995).

REFERENCES

- Ahmed, F.R., Hall, S.R., Pippy, M.E. and Huber, C.P. (1973).
NRC Crystallographic Computer Programs for the IBM/360.
Accession Nos. 133-147 in J. Appl. Cryst. 6, 309-346.
- Enraf-Nonius (1989). CAD-4 Software, Version 5.0. Enraf-Nonius, Delft, Holland.
- Flack, H.D. (1983). Acta Cryst. A39, 876-881.
- Flack, H.D. and Schwarzenbach, D. (1988). Acta Cryst. A44, 499-506.
- Gabe, E.J., Le Page, Y., Charland, J.-P., Lee, F.L. and White, P.S. (1989). J. Appl. Cryst. 22, 384-387.
- International Tables for Crystallography (1992). Vol. C. Tables 4.2.6.8 and 6.1.1.4, Dordrecht: Kluwer Academic Publishers.
- Sheldrick, G.M. (1997). SHELXS97, Program for the Solution of Crystal Structures Univ. of Gottingen, Germany.
- Sheldrick, G.M. (1996). SHELXL96, Program for the Refinement of Crystal Structures. Univ. of Gottingen, Germany.
- SHELXTL (1997) Release 5.10; The Complete Software Package for Single Crystal Structure Determination. Bruker AXS Inc., Madison, WI 53719-1173.
- Spek, A.L. (1995). PLATON, Molecular Geometry Program, July 1995 version. University of Utrecht, Utrecht, Holland.